



Publicly Accessible Penn Dissertations


Fall 12-22-2009

Biochemical and Biomechanical Modulation of Nucleus Pulposus Cells Encapsulated in Novel Cellulose-Based Hydrogels

Anna T. Reza

University of Pennsylvania, areza@seas.upenn.edu

Follow this and additional works at: <http://repository.upenn.edu/edissertations>

 Part of the [Biomaterials Commons](#), and the [Molecular, Cellular, and Tissue Engineering Commons](#)

Recommended Citation

Reza, Anna T., "Biochemical and Biomechanical Modulation of Nucleus Pulposus Cells Encapsulated in Novel Cellulose-Based Hydrogels" (2009). *Publicly Accessible Penn Dissertations*. 78.
<http://repository.upenn.edu/edissertations/78>

This paper is posted at ScholarlyCommons. <http://repository.upenn.edu/edissertations/78>
For more information, please contact libraryrepository@pobox.upenn.edu.

Biochemical and Biomechanical Modulation of Nucleus Pulposus Cells Encapsulated in Novel Cellulose-Based Hydrogels

Abstract

Low back pain may be caused by a direct, acute injury or degeneration of the intervertebral disc (IVD). Intradiscal replacement of the nucleus pulposus (NP) with a tissue engineered hydrogel scaffold may provide a biologic therapy capable of restoring the structure and mechanical function of the IVD. Therefore, the global objective of this dissertation was to develop and optimize a novel, cell-laden, covalently crosslinkable carboxymethylcellulose (CMC) hydrogel construct as a functional tissue engineered NP replacement. The versatility of the photocrosslinkable CMC system was explored by examining the resultant differences in material and mechanical properties due to varying the macromer concentration and molecular weight of the starting material. These biomaterials were shown to support NP cell viability and exhibited tunable material properties that may be easily tailored for specific applications. Culture conditions (medium formulation and TGF-beta3 supplementation) were also investigated in order to enhance matrix deposition and improve construct material and mechanical properties. Scaffolds cultured in serum-free medium supplemented with TGF-beta3 showed approximately a ten-fold increase in glycosaminoglycan (GAG) accumulation and a five-fold increase in mechanical properties (E_y). Given the load-bearing function of the NP, biomechanical stimulation, via hydrostatic pressurization, was utilized in conjunction with biochemical mediators to further augment tissue formation by engineered CMC constructs. However, TGF-beta3 supplementation alone was shown to have a more profound effect on the functional development of NP-seeded CMC constructs. Finally, the long-term effects of in vitro pre-conditioning with TGF-beta3 were examined in vitro, as well as in vivo, using a subcutaneous murine pouch model. Constructs maintained without TGF-beta3 exhibited no quantifiable changes in matrix content or mechanical properties over time. In contrast, TGF-beta3-treated scaffolds experienced a significant increase in matrix accumulation and E_y during the in vitro pre-conditioning period. TGF-beta3-treated scaffolds cultured in vitro following the pre-culture period were able to sustain these properties, while TGF-beta3-treated scaffolds maintained in vivo exhibited a significant loss in matrix accumulation and E_y, possibly due to scaffold stiffness and diffusion limitations. Although TGF-beta3 pre-conditioning produced long-term effects in vitro, the degradative properties of the CMC scaffold must be tailored for in vivo conditions. Taken together, cell-laden, covalently crosslinkable CMC hydrogel constructs may serve as potential NP tissue engineered replacements but will require further optimization prior to use in regenerative therapies.

Degree Type

Dissertation

Degree Name

Doctor of Philosophy (PhD)

Graduate Group

Bioengineering

First Advisor

Steven B. Nicoll

Keywords

disc, spine, hydrogel, carboxymethylcellulose, biomaterial

Subject Categories

Biomaterials | Molecular, Cellular, and Tissue Engineering

**BIOCHEMICAL AND BIOMECHANICAL MODULATION OF NUCLEUS
PULPOSUS CELLS ENCAPSULATED IN NOVEL CELLULOSE-BASED
HYDROGELS**

Anna T. Reza

A DISSERTATION

in

Bioengineering

Presented to the Faculties of the University of Pennsylvania

in

Partial Fulfillment of the Requirements for the

Degree of Doctor of Philosophy

2009

Steven B. Nicoll, Ph.D. – Dissertation Supervisor

Susan S. Margulies, Ph.D. – Graduate Group Chair

Dissertation Committee

Jason A. Burdick, Ph.D. – Committee Chair

Robert L. Mauck, Ph.D.

Dawn Elliott, Ph.D.

ACKNOWLEDGMENTS

First of all, I'd like to thank my parents and family for teaching me that I can do anything I put my mind to and for giving me the strength to tackle grad school. And, I'd like to thank my grandma who was always a role model and blessed us with her unique combination of humor and strength. Without the love and support of my family, I would not be who I am today. And, in particular, I would like to thank my friends – Julie, Jeanne, Cathy, and Steph – who have been there through the ups and downs of grad school and really helped make this experience so much more fun and enjoyable.

I would especially like to acknowledge the prior members of the Nicoll Lab – Alice, Simone, Charlie, Hallie, and Greg. I've gained an even greater appreciation for them all over the past year and a half and have missed having them around. I'd also like to thank the members of the Burdick lab, especially Cindy, Darren, and Jamie, who have adopted me this past year once my own lab mates moved on and were always there to answer questions or just talk when my own lab was too quiet.

I would like to thank my thesis committee members, Dr. Jason Burdick, Dr. Dawn Elliott, and Dr. Rob Mauck, for their comments and insight which helped develop and fine tune my thesis project. I would also like to acknowledge our collaborators, Dr. Sunday Akintoye and Dr. Demin Wen, for all their help with our animal studies. And, of course, I would like to thank my advisor, Dr. Steve Nicoll who has provided guidance, advice, and support throughout this whole process of grad school. With his help, I have grown as a scientist, learning to think independently, and his encouragement has helped me accomplish more than I thought possible with this work.

ABSTRACT

BIOCHEMICAL AND BIOMECHANICAL MODULATION OF NUCLEUS PULPOSUS CELLS ENCAPSULATED IN NOVEL CELLULOSE-BASED HYDROGELS

Anna T. Reza

Advisor: Steven B. Nicoll, Ph.D.

Low back pain may be caused by a direct, acute injury or degeneration of the intervertebral disc (IVD). Intradiscal replacement of the nucleus pulposus (NP) with a tissue engineered hydrogel scaffold may provide a biologic therapy capable of restoring the structure and mechanical function of the IVD. Therefore, the global objective of this dissertation was to develop and optimize a novel, cell-laden, covalently crosslinkable carboxymethylcellulose (CMC) hydrogel construct as a functional tissue engineered NP replacement. The versatility of the photocrosslinkable CMC system was explored by examining the resultant differences in material and mechanical properties due to varying the macromer concentration and molecular weight of the starting material. These biomaterials were shown to support NP cell viability and exhibited tunable material properties that may be easily tailored for specific applications. Culture conditions (medium formulation and TGF- β_3 supplementation) were also investigated in order to

enhance matrix deposition and improve construct material and mechanical properties. Scaffolds cultured in serum-free medium supplemented with TGF- β_3 showed approximately a ten-fold increase in glycosaminoglycan (GAG) accumulation and a five-fold increase in mechanical properties (E_y). Given the load-bearing function of the NP, biomechanical stimulation, via hydrostatic pressurization, was utilized in conjunction with biochemical mediators to further augment tissue formation by engineered CMC constructs. However, TGF- β_3 supplementation alone was shown to have a more profound effect on the functional development of NP-seeded CMC constructs. Finally, the long-term effects of *in vitro* pre-conditioning with TGF- β_3 were examined *in vitro*, as well as *in vivo*, using a subcutaneous murine pouch model. Constructs maintained without TGF- β_3 exhibited no quantifiable changes in matrix content or mechanical properties over time. In contrast, TGF- β_3 -treated scaffolds experienced a significant increase in matrix accumulation and E_y during the *in vitro* pre-conditioning period. TGF- β_3 -treated scaffolds cultured *in vitro* following the pre-culture period were able to sustain these properties, while TGF- β_3 -treated scaffolds maintained *in vivo* exhibited a significant loss in matrix accumulation and E_y , possibly due to scaffold stiffness and diffusion limitations. Although TGF- β_3 pre-conditioning produced long-term effects *in vitro*, the degradative properties of the CMC scaffold must be tailored for *in vivo* conditions. Taken together, cell-laden, covalently crosslinkable CMC hydrogel constructs may serve as potential NP tissue engineered replacements but will require further optimization prior to use in regenerative therapies.

TABLE OF CONTENTS

Chapter 1: An Introduction to the Intervertebral Disc and Tissue Engineering	1
1.1. Intervertebral Disc Anatomy and Composition	1
1.2. Intervertebral Disc Mechanical Function	5
1.3. Intervertebral Disc Aging and Degeneration	6
1.4. Current Treatments for Disc Degeneration and Low Back Pain	9
1.5. Intervertebral Disc Tissue Engineering	12
1.6. Cell Sources for Intervertebral Disc Tissue Engineering	13
1.7. Biomaterial Scaffolds for Intervertebral Disc Tissue Engineering.....	14
<i>1.7.1. Fibrous Scaffolds for Annulus Fibrosus Tissue Engineering</i>	<i>15</i>
<i>1.7.2 Hydrogels for Nucleus Pulposus Tissue Engineering.....</i>	<i>15</i>
<i>1.7.3. Photocrosslinkable Hydrogels for Tissue Engineering</i>	<i>17</i>
<i>1.7.4. Cellulose-based Materials for Tissue Engineering Applications</i>	<i>18</i>
1.8. Biochemical Signals for Intervertebral Disc Tissue Engineering.....	21
<i>1.8.1. Exogenous Growth Factor Delivery</i>	<i>22</i>
<i>1.8.2. Gene Therapy.....</i>	<i>23</i>
1.9. Biomechanical Stimulation in Intervertebral Disc Tissue Engineering.....	24
<i>1.9.1. Deformational Loading.....</i>	<i>25</i>
<i>1.9.2. Hydrostatic Pressure</i>	<i>26</i>
1.10. Motivation and Research Overview	27
1.11. Overview of Present Investigation.....	30
1.12. References.....	32

Chapter 2: Characterization of Novel Photocrosslinked Carboxymethylcellulose Hydrogels for Encapsulation of Nucleus Pulposus Cells..... 50

2.1. Introduction.....	50
2.2. Materials and Methods.....	53
2.2.1. <i>Macromer Synthesis</i>	53
2.2.2. <i>Cell Isolation</i>	55
2.2.3. <i>Cell Encapsulation in Photocrosslinked Hydrogels</i>	55
2.2.4. <i>Cell Viability and Dynamic Mechanical Testing</i>	56
2.2.5. <i>Swelling Ratio</i>	58
2.2.6. <i>Characterization of Equilibrium Mechanical Properties</i>	58
2.2.7. <i>Histology and Immunohistochemistry</i>	59
2.2.8. <i>Statistical Analysis</i>	60
2.3. Results.....	60
2.4. Discussion.....	67
2.5. References.....	73

Chapter 3: Serum-Free, Chemically-Defined Medium with TGF- β_3 Enhances Functional Properties of Nucleus Pulposus Cell-laden Carboxymethylcellulose Hydrogel Constructs..... 82

3.1. Introduction.....	82
3.2. Materials and Methods.....	85
3.2.1. <i>Macromer Synthesis</i>	85
3.2.2. <i>Primary Cell Culture and Isolation</i>	86
3.2.3. <i>Cell Encapsulation in Photocrosslinked Hydrogels</i>	87

3.2.4. Swelling Ratio	89
3.2.5. Biochemistry	89
3.2.6. Histology and Immunohistochemistry.....	90
3.2.7. Mechanical Testing.....	91
3.2.8. Statistical Analysis	91
3.3. Results.....	92
3.4. Discussion.....	100
3.5. References.....	107

Chapter 4: Hydrostatic Pressure Modulates Collagen Production but Does Not Affect the Functional Properties of Nucleus Pulposus Cell-laden Carboxymethylcellulose Hydrogel Constructs..... 117

4.1. Introduction.....	117
4.2. Materials and Methods.....	120
4.2.1. Macromer Synthesis.....	120
4.2.2. Primary Cell Culture and Isolation	121
4.2.3. Cell Encapsulation in Photocrosslinked Hydrogels	122
4.2.4. Dynamic Hydrostatic Pressurization.....	123
4.2.5. Swelling Ratio	125
4.2.6. Biochemistry	125
4.2.7. Histology and Immunohistochemistry.....	126
4.2.8. Mechanical Testing.....	127
4.2.9. Statistical Analysis	127
4.3. Results.....	128

4.4. Discussion.....	138
4.5. References.....	146
Chapter 5: Response of Nucleus Pulposus Cells Encapsulated in Photocrosslinked Carboxymethylcellulose Hydrogels Following Pretreatment with TGF-β_3: Differential Maturation <i>in vitro</i> and <i>in vivo</i>.....	155
5.1. Introduction.....	155
5.2. Materials and Methods.....	158
5.2.1. <i>Macromer Synthesis</i>	158
5.2.2. <i>Primary Cell Culture and Isolation</i>	158
5.2.3. <i>Cell Encapsulation in Photocrosslinked Hydrogels</i>	159
5.2.4. <i>in vivo Subcutaneous Pouch Model</i>	160
5.2.5. <i>Swelling Ratio</i>	162
5.2.6. <i>Biochemistry</i>	162
5.2.7. <i>Histology and Immunohistochemistry</i>	163
5.2.8. <i>Mechanical Testing</i>	164
5.2.9. <i>Statistical Analysis</i>	165
5.3. Results.....	165
5.4. Discussion.....	176
5.5. References.....	183
Chapter 6: Conclusions, Limitations, and Future Directions.....	192
6.1. Overview.....	192
6.2. Characterization of Photocrosslinked CMC for NP Cell Encapsulation (Chapter 2)	193

6.3. Biochemical Stimulation of Cell-laden CMC Constructs (Chapter 3)	194
6.4. Biomechanical and Biochemical Stimulation of Cell-laden CMC Constructs (Chapter 4)	195
6.5. Long-term Assessment of <i>in vitro</i> Pre-Conditioning with TGF- β_3 (Chapter 5). 198	
6.6. Limitations and Future Directions	202
6.7. Final Conclusions	208
6.8. References.....	209

LIST OF TABLES

Table 3.1. Physical properties and DNA content of CMC constructs as a function of medium formulation.....	93
Table 3.2. Diameter and thickness measurements of CMC constructs as a function of medium formulation.....	97
Table 4.1. Material properties and DNA content of unloaded controls and constructs pressurized at 2 MPa.....	129
Table 4.2. Material properties and DNA content of unloaded controls and constructs pressurized at 5 MPa.....	133
Table 4.3. Day 28 pressure magnitude comparison for mechanically stimulated constructs	138
Table 4.4. Effects of hydrostatic pressure on NP tissue engineered constructs.....	142
Table 5.1. Diameter and thickness measurements of constructs cultured <i>in vitro</i> and <i>in vivo</i> with and without TGF- β_3	175

LIST OF FIGURES

Figure 1.1. Anatomy of the intervertebral disc	1
Figure 1.2. Extracellular matrix of the nucleus pulposus	3
Figure 1.3. Gross image and transverse histological section of a rat IVD.....	4
Figure 1.4. Tissue engineering triad.....	13
Figure 1.5. Chemical structure of alginate.....	16
Figure 1.6. Chemical structure of cellulose	19
Figure 1.7. Chemical structure of methylcellulose	19
Figure 1.8. NP cell viability in methylcellulose hydrogels.....	20
Figure 1.9. Chemical structure of carboxymethylcellulose	21
Figure 2.1. Synthesis schematic for methacrylated carboxymethylcellulose	54
Figure 2.2. ¹ H-NMR spectra of unmodified and methacrylated CMC	61
Figure 2.3. Viability data for 90 kDa and 250 kDa CMC constructs	62
Figure 2.4. Elastic modulus of 90 and 250 kDa CMC constructs.....	64
Figure 2.5. Equilibrium Young's modulus for 90 and 250 kDa CMC constructs.....	65
Figure 2.6. Equilibrium Young's modulus for 3% 250 kDa CMC constructs	66
Figure 2.7. Histological staining of 3% 250 kDa CMC constructs.....	67
Figure 3.1. Schematic of the synthesis of methacrylated CMC and NP cell encapsulation	86
Figure 3.2. GAG content of CMC constructs as a function of medium formulation.....	94
Figure 3.3. CSPG immunohistochemical staining for CMC constructs as a function of medium formulation.....	95
Figure 3.4. Type II collagen content and immunohistochemical staining of CMC constructs as a function of medium formulation.....	96
Figure 3.5. Type I collagen content and immunohistochemical staining of CMC constructs as a function of medium formulation.....	97
Figure 3.6. Mechanical properties and stress vs. time curves for CMC constructs as a function of medium formulation.....	98
Figure 3.7. Equilibrium Young's modulus and stereoscope images for CMC constructs as a function of medium formulation	100
Figure 4.1. Hydrostatic pressure device and representative 2 MPa and 5 MPa dynamic loading cycles.....	124
Figure 4.2. GAG quantification and CSPG deposition of unloaded controls and constructs pressurized at 2 MPa.....	130
Figure 4.3. Type II collagen quantification and deposition of unloaded controls and constructs pressurized at 2 MPa.....	131
Figure 4.4. Equilibrium Young's modulus of unloaded controls and constructs pressurized at 2 MPa.....	132
Figure 4.5. Correlation analyses of matrix content and the functional properties of 2 MPa constructs	132
Figure 4.6. GAG quantification and CSPG deposition of unloaded controls and constructs pressurized at 5 MPa.....	134

Figure 4.7. Type II collagen quantification and deposition of unloaded controls and constructs pressurized at 5 MPa.....	135
Figure 4.8. Equilibrium Young's modulus of unloaded controls and constructs pressurized at 5 MPa.....	136
Figure 4.9. Correlation analyses of matrix content and the functional properties of 5 MPa constructs	137
Figure 5.1. Timeline for the investigation of the long-term effects of TGF- β_3 pre-treatment	161
Figure 5.3. Q_w for <i>in vivo</i> and <i>in vitro</i> constructs cultured with or without TGF- β_3	166
Figure 5.3. H&E staining of constructs cultured <i>in vitro</i> and <i>in vivo</i> with and without TGF- β_3	167
Figure 5.4. Fibrous capsule formation for <i>in vivo</i> constructs cultured with and without TGF- β_3	168
Figure 5.5. CSPG localization and GAG accumulation in constructs cultured <i>in vitro</i> and <i>in vivo</i> with and without TGF- β_3	169
Figure 5.6. Type II collagen localization and accumulation in constructs cultured <i>in vitro</i> and <i>in vivo</i> with and without TGF- β_3	170
Figure 5.7. Type I collagen localization and accumulation in constructs cultured <i>in vitro</i> and <i>in vivo</i> with and without TGF- β_3	171
Figure 5.8. DNA content of constructs cultured <i>in vitro</i> and <i>in vivo</i> with and without TGF- β_3	172
Figure 5.9. Gross images of constructs cultured <i>in vitro</i> and <i>in vivo</i> (following excision and fibrous capsule removal) with and without TGF- β_3	173
Figure 5.10. Equilibrium Young's modulus of constructs cultured <i>in vitro</i> and <i>in vivo</i> with and without TGF- β_3	176
Figure 6.1. Elastic modulus of 2% and 2.5% CMC hydrogels formed via redox-initiated polymerization	206
Figure 6.2. Live/Dead image of 2.5% 10mM CMC construct at day 1	206

Chapter 1: An Introduction to the Intervertebral Disc and Tissue Engineering

1.1. Intervertebral Disc Anatomy and Composition

The intervertebral disc (IVD) is a heterogeneous, fibrocartilaginous tissue that is located between the vertebral bodies of the spine and confers motion and flexibility to this otherwise bony structure¹. The IVD is a complex composite, comprised of the central, gelatinous nucleus pulposus (NP) and the fibrous, lamellar annulus fibrosus, which surrounds the NP laterally (Figure 1.1). The IVD is bordered inferiorly and superiorly by the cartilaginous endplates of the vertebral bodies that serve as the source of diffusion-based nutrient delivery for the avascular, aneural IVD.

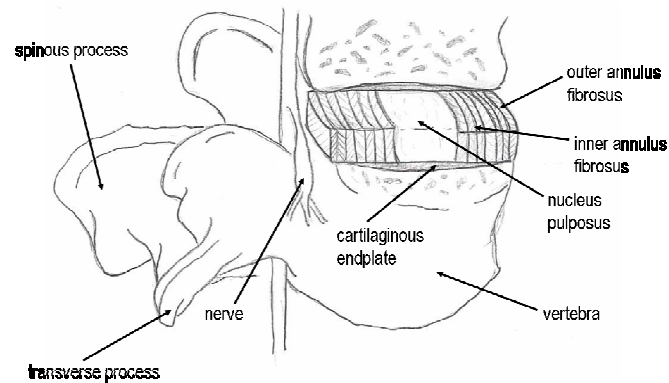


Figure 1.1. Anatomy of the spine and the intervertebral disc (in cross-section).

The NP is a hydrated tissue, characterized biochemically by a high content of negatively charged, water-retaining proteoglycans, such as aggrecan, and randomly oriented collagen fibers (mainly type II collagen)² which allow the IVD to resist

compressive forces through the generation of a hydrostatic swelling pressure, similar to other cartilaginous tissues. Aggrecan, the primary proteoglycan in the IVD, consists of a core protein chain to which the glycosaminoglycans (GAGs) chondroitin sulfate and the shorter, keratin sulfate bind. With age, the proportion of chondroitin sulfate to keratin sulfate decreases, and the ability of the disc to retain water correspondingly decreases as these shorter keratin sulfate GAGs are less effective at maintaining a strong interaction with water². The aggrecan monomer interacts with hyaluronic acid present in the extracellular matrix (ECM) through a link protein to form large proteoglycan aggregates, capable of efficiently trapping water² (Figure 1.2). The number of proteoglycan aggregates, however, decreases with age in relation to the total number of proteoglycans in the disc³, as the increased population of non-aggregating proteoglycans are thought to be a consequence of proteolytic degradation. These fragments are retained within the disc due to their size, structure, and charge, but lack the amino terminal globular region of aggrecan that is necessary for interaction with hyaluronic acid². The proteoglycan and water content of the NP (14% and 77% of tissue wet weight, respectively) greatly exceed that in the annulus (5% and 70%, respectively)⁴. In contrast, collagen accounts for only 4% of NP wet weight in comparison to 15% in the annulus⁴.

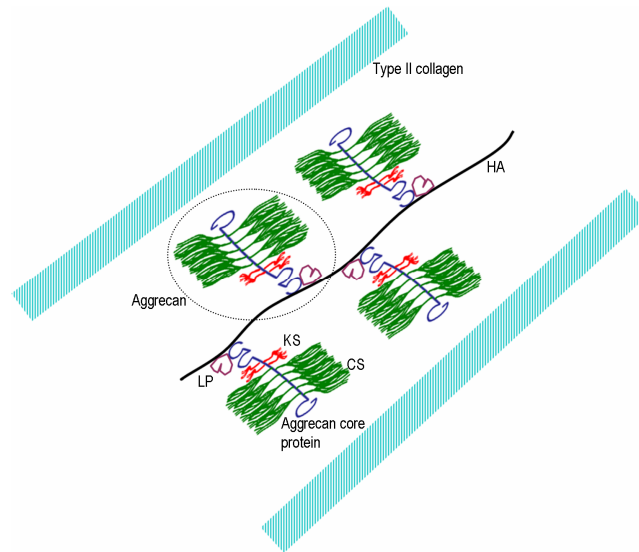


Figure 1.2. Extracellular matrix of the NP, consisting of aggrecan, chondroitin sulfate (CS), keratin sulfate (KS), link protein (LP), hyaluronic acid (HA), and type II collagen.

The annulus fibrosus is comprised of a series of concentric lamellae which contain collagen fibers arranged in parallel within each lamellar sheet that alternate in angles from 28° - 44° with respect to the transverse plane⁵. The annulus fibrosus can be further subdivided into the outer annulus (OA) and inner annulus (IA) based on the biochemical composition and structure of each tissue (Figure 1.3). The OA is a highly organized, densely packed, lamellar tissue rich in type I collagen, with minimal proteoglycan content. The IA serves as a transition zone between the lamellar organization of the OA and the random orientation of the NP. As such, the IA contains a less dense matrix in comparison to the OA, composed of both type I and type II collagen and proteoglycans which reside between layers of collagen fibrils. Progressing radially from the OA to the NP, there is an increase in proteoglycan and type II collagen content and a decrease in type I collagen¹.

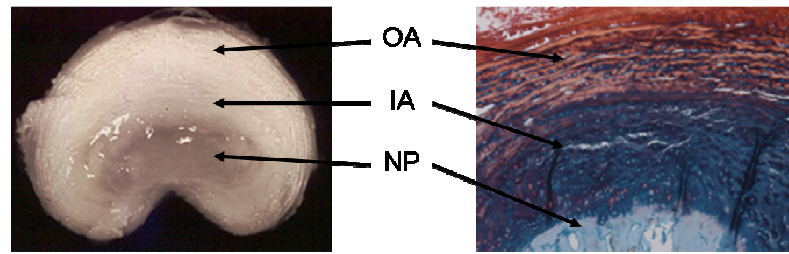


Figure 1.3. Gross image (left) and alcian blue/picrosirius red histological staining of a transverse section of a rat IVD with anatomical regions identified by arrows. Proteoglycans are indicated in blue, while collagens are stained red.

The IVD has a low cell density, even in comparison to other cartilaginous tissues. The cell density in the human annulus fibrosus of a mature adult is about 9×10^6 cells/mL while that in the NP is less than half that, at a density of about 4×10^6 cells/mL⁶. These values fall well below that seen in hyaline cartilage (14×10^6 cells/mL).

Cells isolated from the OA, IA, and NP show distinct differences in morphology and ECM production. When examined *in vitro* in monolayer culture, OA cells display an elongated, fibroblast-like shape and are positioned in parallel with collagen fibril orientation⁷. Consistent with fibroblastic tissues typically loaded in tension, OA cells exhibit high levels of type I collagen gene expression⁸. Morphologically, IA cells are more polygonal and produce a fibrocartilaginous ECM that includes both type I and type II collagen, while NP cells display a rounded, chondrocyte-like morphology and secrete the largest amounts of type II collagen amongst these three cell populations⁸. These morphological and biochemical differences are retained in monolayer culture through passage two in bovine caudal IVD cells. However, similar to articular chondrocytes, IVD cells may lose characteristic phenotypic differentiation markers after this point, and three-dimensional culture systems must be used in order to prevent cell de-differentiation⁹.

1.2. Intervertebral Disc Mechanical Function

As a whole, the IVD serves to stabilize and align the spine by functionally connecting neighboring vertebral bodies. The IVD is a soft tissue which allows for movement between the vertebrae, giving the spine flexibility, while also absorbing and distributing loads¹. These complex mechanical functions are possible due to the composite, heterogeneous structure of the disc. The high proteoglycan and water content of the NP allow this tissue to effectively support approximately 70% of the compressive axial loads placed upon the spine⁷ through the generation of a hydrostatic swelling pressure. However, this results in a bulging of the tissue, which is minimized and contained by the dense cross-ply of the circumferential collagenous lamellae of the OA. These lamellae additionally resist annular strains created during more complex motions, such as bending and torsional loading¹⁰. Under cases of extreme compressive load, the less dense, semi-hydrated matrix of the IA also aids in load absorption by creating fluid flow to dissipate energy¹. Disc height is a function of disc hydration and fluid flow. As loads are placed upon the spine, interstitial water is forced out, resulting in a diurnal decrease in height over the course of the day. Disc height is recovered during sleep, when the body is in a recumbent position, largely due to the Donnan osmotic pressure generated by the negatively charged proteoglycans in the disc¹.

1.3. Intervertebral Disc Aging and Degeneration

The structure and biochemical composition of the IVD continually change from birth through old age¹⁰. Nutrient transport and waste removal are most efficient just after birth due to small blood vessels located at the disc periphery and extending between lamellae of the OA; these vessels may even penetrate into the IA. Anatomically, the NP occupies almost half of the disc just after birth and is populated by notochordal cells, derived from the notochord in embryonic development. These cells elaborate large proteoglycan aggregates (i.e., many aggrecan molecules bound to a central hyaluronic acid filament) similar to that seen in healthy articular cartilage¹⁰. Notochordal cells disappear with skeletal maturity and chondrocyte-like cells of mesenchymal origin which reside in the cartilaginous endplate or IA migrate into the NP¹¹⁻¹⁵.

In adulthood, the vascular supply becomes more limited and is largely restricted to capillaries originating in the vertebral bodies, as peripheral blood vessels once present at birth and persisting through adolescence disappear with age⁴. The avascular, aneural nature of the IVD limits the capacity for self-repair. Calcification of the cartilaginous endplates also occurs over time, which decreases endplate permeability and further limits the diffusion- and bulk fluid flow-based nutrient supply and waste transport of the disc, resulting in a perpetuating cycle of decline in disc health¹⁶. The decreased oxygen supply causes cells to rely on anaerobic metabolism, resulting in the production and accumulation of lactic acid due to impaired waste removal. This lowers the local pH, which compromises cell metabolism and may precipitate cell death, as up to 50% of cells in adult discs have been reported necrotic¹³. Additionally, the acidic environment favors

the activation of matrix proteinases that are normally inactive at the neutral pH found in healthy connective tissues².

In conjunction with an overall decline in the cell population and an increase in matrix proteinases, the percentage of aggregating proteoglycans in the NP decreases from around 30% at 6 months to as low as 10% in the adult¹⁷. Additionally, the concentration of chondroitin sulfate present in the disc decreases with age, while that of keratin sulfate increases². Keratin sulfate is a shorter GAG, which reduces the capacity to retain water in comparison to chondroitin sulfate. Moreover, proteolytic processing, instigated due to decreased pH and activation of proteinases, can degrade aggrecan molecules such that these fragments are able to leach from the tissue, producing a significant alteration in the biochemical composition of the disc. The loss of these negatively charged GAG molecules decreases the osmotic pressure of the disc and thus precipitates a loss of hydration⁴. The NP is subsequently rendered more fibrous in content, resulting in an altered distribution of loads and further impairment of nutrient transport and waste removal¹⁸. In addition, type II collagen fibrils undergo proteolytic processing² and are often replaced by type I collagen as the annulus begins to encroach on the NP¹⁶, contributing to the fibrotic nature of the aged disc. However, the reduced capability for matrix turnover (due to impaired diffusion), allows collagen molecules to become crosslinked as a result of interaction effects which, in the short term, enables the disc to entrap fragmented proteoglycans and thereby retain water¹⁶. Unfortunately, the increased crosslinking further inhibits matrix turnover and disc repair, compounding the damage to the disc.

While all discs undergo changes with age, not all discs degenerate. To clarify this ambiguity, Adams and Roughley proposed to define a degenerate disc as one with cell-mediated structural failure combined with accelerated or advanced signs of aging in conjunction with pain¹⁶. Approximately 80% of Americans will experience at least one episode of significant back pain during their lifetime¹⁹, and annual related medical expenses attributed to back pain alone total over \$80 billion²⁰.

While any of the factors described above in relation to aging of the disc may contribute to disc degeneration, it is unclear what serves as the trigger to progress into degeneration. Environmental and lifestyle factors such as an occupation requiring heavy and repetitive mechanical loading^{21, 22} or an occupation involving high frequency vibration (driving, flying), smoking²³, vascular disease, diabetes, or immobilization¹⁸ may all increase the rate and severity of age-related changes in the disc to precipitate degeneration. As seen in older discs, degenerated discs display decreased proteoglycan and water content and an increased collagen concentration, which all contribute to a decreased ability to maintain disc height and distribute loads. The degenerated NP exhibits an increased shear modulus, as the loss of water increases tissue stiffness, and the disc becomes more elastic, likely due to the increased collagen content from the encroaching annulus¹⁰.

Late stage disc degeneration may be associated with osteophyte formation in the vertebral bodies or facet joint arthritis¹⁰. Additionally, small blood vessels may extend from the vertebral bodies and grow into the periphery of degenerated discs^{24, 25} accompanied by the ingrowth of nerves to the inner part of the disc^{24, 26, 27}. Given the loss of disc structure and mechanical properties and the release of potential inflammatory

factors which sensitize newly established nerve endings, degenerated discs may give rise to back pain. Cell necrosis may further contribute to back pain by sensitizing nociceptive nerve endings due to cytokine release, free radicals, and matrix debris from degradation¹⁸.

1.4. Current Treatments for Disc Degeneration and Low Back Pain

Traditionally, clinical interventions for disc degeneration have largely focused on alleviation of the pain associated with this pathological condition, rather than repair of the disc itself to restore the essential mechanical functions which this tissue provides. Although up to 80% of adults will experience at least one episode of severe back pain, most will improve without any formal treatment²⁸. Because of this, discogenic pain is often treated initially with a conservative, nonsurgical approach, which includes administration of analgesics, muscle relaxants, or corticosteroid injections⁴. Other therapies may include lifestyle modifications, such as weight reduction, smoking cessation, and exercise²⁹. Up to 90% of patients with disc degeneration obtain satisfactory pain relief by conservative treatment methods, though this may take many months to achieve⁴. More severe cases may require surgical intervention, and recently developed techniques provide a minimally invasive option to major surgery. These options include various forms of discectomy, such as chemonucleolysis, to remove a portion of the NP to reduce impingement on spinal nerves in cases of herniation, and annuloplasty, which seals fissures and burns nociceptors (thereby reducing sensitivity to pain) in the annulus via electrothermal or radiofrequency thermal energy⁴.

The most severe cases of late-stage disc degeneration may necessitate major surgery and total disc excision. Disc excision is typically followed by spinal fusion, and approximately 200,000 of these procedures were performed in the United States in 2002²⁸. However, the outcome of this procedure is often unpredictable and many adverse effects have been reported, such as posterior muscular atrophy and a limited range of motion and associated stiffness. Fusion results in an altered distribution of loads along the spine, increasing stress on adjacent spinal levels, which may result in facet hypertrophy, spinal stenosis, and accelerate degeneration in neighboring discs³⁰⁻³².

One option to spinal fusion following total disc excision is the placement of a prosthetic disc. The most popular disc prosthesis is the SB Charité III (DePuy, Johnson & Johnson), with over 5,000 implants worldwide from 1987 to 2003. The Charité is a three-piece articulating device which attempts to mimic normal disc biomechanics by allowing translation and rotation within the artificial disc³³. The Charité disc consists of a sliding polyethylene core placed between two cobalt-chromium alloy endplates which are anchored to the adjacent vertebral bodies by small teeth on the metal surfaces. In over ten years of clinical use, there have been no published reports of device failure or spinal displacement and no data to indicate the formation of wear debris from the polyethylene core³³. However, as with all major spinal surgeries there are possible complications, including immune reactions to the implant, spinal cord or nerve damage, and leakage of spinal fluid.

Although spinal fusion and disc prosthetics are options for the treatment of late-stage disc degeneration, if the patient presents with an intact annulus, nucleus pulposus augmentation, following a partial or full nucleotomy, may serve as an alternative to

restore biomechanical function of the diseased disc and slow degeneration of adjacent level discs³⁴. The main goal of nucleus pulposus replacement procedures is to rehydrate the central portion of the disc via minimally invasive methods, which subsequently restores annular tension, thereby re-establishing the biomechanical function of the disc. The mechanical properties of the NP replacement material should closely match that of the native tissue to prevent a modulus mismatch and any associated abnormalities of load distribution or implant extrusion²⁸. Current NP replacement materials can be categorized as intradiscal implants, which are placed into the disc in a dehydrated, semi-solid state, or *in situ* curing polymers, which are injected in liquid form and polymerize in the nuclear cavity. Examples of intradiscal implants include the Prosthetic Disc Nucleus (Raymedica, Inc.), a polyacrylamide/polyacrylonitrile copolymer hydrogel encased in an ultrahigh molecular weight polyethylene jacket, the Aquarelle (Stryker Spine), a semi-hydrated polyvinyl alcohol hydrogel, and the NeuDisc (Replication Medical, Inc.), a hydrolyzed polyacrylonitrile polymer reinforced by a Dacron mesh. Additionally, the Newcleus (Zimmer, Spine) is a polycarbonate urethane elastomer inserted as a curled, preformed spiral which absorbs water and expands upon implantation, similar to the above described materials^{28, 34, 35}. Some *in situ* curing implants include the Injectable Disc Nucleus (Spine Wave), a synthetic silk-elastin copolymer created through DNA bacterial synthesis fermentation, the Dascor nuclear replacement (Disc Dynamics), an injectable polyurethane, and the Biodisc (Cryolife), a bovine albumin/glutaraldehyde hydrogel^{28, 34, 35}. Although some of these prosthetics have shown promise in pre-clinical and clinical studies, further data are required to examine their long-term ability to maintain the viscoelastic properties of the disc and sustain multidirectional loads.

While these more recent techniques for the treatment of disc degeneration not only alleviate the pain associated with this disease but also attempt to restore mechanical function of the disc, tissue engineering strategies may be able to additionally address the biological facet of disc degeneration to create a truly functional disc replacement.

1.5. Intervertebral Disc Tissue Engineering

Tissue engineering presents an alternative to current clinical treatment modalities, with the objective of developing a biological substitute that restores, maintains, or improves tissue function through the combination of cells, signaling factors, and/or biocompatible scaffolds³⁶ (Figure 1.4). The degree of disc degeneration will ultimately dictate what combination of the above stated components must be utilized for a tissue engineered solution³⁷. Ideally, clinical intervention will occur in the early stages of degeneration, and growth factor therapy alone may stimulate matrix production by resident NP cells⁷. However, patients often do not present with lower back pain until the later stages of degeneration, so improved detection methods must be developed. Middle-stage disc degeneration may still be addressed by tissue engineering techniques if the annulus is intact. Treatment options at this stage may include growth factor treatment (as in early stages), placement of a cell-seeded scaffold in the NP following a nucleotomy, or placement of a cell-seeded scaffold in the NP in the presence of growth factors⁷. However, if the patient presents with a compromised annulus that would be unable to retain a repaired NP, a complete *in vitro*-developed disc composite which recapitulates both the annulus and nucleus may be required.

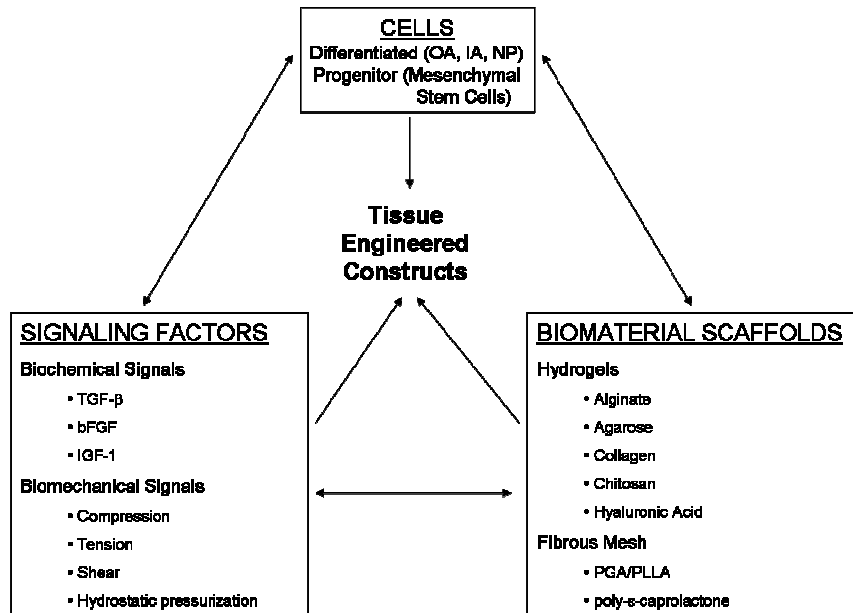


Figure 1.4. Tissue engineering strategies utilize cells, signaling factors, and biomaterial scaffolds alone or in conjunction to develop constructs for tissue repair or regeneration.

1.6. Cell Sources for Intervertebral Disc Tissue Engineering

The IVD is less characterized at the cellular and tissue levels in comparison to other orthopaedic tissues, such as cartilage. As a result, most IVD tissue engineering research has utilized cells derived from the native tissue in order to determine benchmarks for the behavior of these primary cells. Studies have incorporated human cells from both healthy and degenerate discs³⁸⁻⁴² and cells isolated from a wide variety of animal sources, including rat⁴³, bovine^{8, 44-49}, rabbit^{50, 51}, ovine⁵²⁻⁵⁴, canine^{11, 55}, and swine⁵⁶⁻⁵⁹. However, as research in the field has progressed, interest has turned to more clinically relevant cell sources, such as autologous mesenchymal stem cells (MSCs), since allogeneic and xenogeneic cells carry the potential to illicit an immune response. Multipotent MSCs are present in various adult tissues, such as bone marrow, trabecular bone, cartilage, muscle, adipose⁶⁰, and have been recently identified within the disc⁶¹. These cells have the ability to differentiate along various lineages of mesenchymal origin,

such as those found in the IVD, given the proper biochemical environment. Recent studies examined the effects of MSCs embedded in an atelocollagen matrix which was injected into rabbit IVDs following nucleotomy. This therapy resulted in a partial restoration of disc height and disc hydration, as injected cells were found to have differentiated along a cartilaginous lineage and expressed type II collagen, keratin sulfate, and chondroitin-4-sulfate⁶²⁻⁶⁴.

1.7. Biomaterial Scaffolds for Intervertebral Disc Tissue Engineering

Biomaterial scaffolds used in tissue engineering applications often attempt to mimic the multi-dimensional structure of the given native tissue. However, the disparity in phenotype observed when comparing the fibroblastic cell population found in the OA and the chondrocyte-like cells of the NP prevents the use of a singular scaffold for IVD cell culture. Cells from highly oriented, collagenous tissues, such as tendons, ligaments, and the annulus fibrosus, are routinely cultured on fibrous scaffolds which may be fabricated in an aligned or random orientation using synthetic or natural polymers, such as resorbable polyesters or collagen⁶⁵⁻⁶⁹. In contrast, cells from highly hydrated, load-bearing tissues, such as cartilage and the NP, are often encapsulated within a hydrogel scaffold in order to maintain the rounded cell morphology and expression of characteristic ECM components, such as type II collagen and aggrecan, observed *in vivo*^{32, 70}. Various natural and synthetic polymers, including alginate^{8, 45, 46, 50, 52, 55, 58, 71-74}, agarose⁵⁷, chitosan⁷⁵⁻⁷⁷, hyaluronic acid⁷⁸⁻⁸⁰, and poly(ethylene glycol)⁸¹, have been investigated for use in the repair of cartilaginous tissues.

1.7.1. Fibrous Scaffolds for Annulus Fibrosus Tissue Engineering

Early work in annulus fibrosus tissue engineering utilized commercially available scaffolds, such as poly(glycolic acid) (PGA) meshes, which were then reinforced with a poly(L-lactic acid) (PLLA) solution to slow degradation of the polymer^{8, 47, 53, 54}. However, these materials possess a random fiber orientation, in contrast to the circumferential lamellae observed in the native disc. Additionally, the fiber size of these scaffolds is on the macroscale, while the collagen fibers in the ECM measure on the nanoscale. Electrospinning has emerged as a technique that can recapitulate the scale and unique architecture of highly organized tissues, such as the annulus. Nanofibrous electrospun poly(ϵ -caprolactone) scaffolds seeded with bovine annulus fibrosus cells have recently been shown to allow for GAG and collagen accumulation, and these constructs exhibited tensile properties comparable to that of the native annulus⁵. Other polymers used to create electrospun scaffolds for annulus fibrosus tissue engineering include PLLA and polycarbonate polyurethane^{78, 82}.

1.7.2 Hydrogels for Nucleus Pulposus Tissue Engineering

The highly hydrated nature of the NP is similar to that of hydrogel networks, making such polymeric structures prime candidates to serve as scaffolds for NP regeneration. A wide variety of polymers have been used to create such hydrogels, including hyaluronic acid⁷⁸⁻⁸⁰, collagen^{40, 41, 63, 64}, and agarose⁵⁷. Chitosan, derived from the shells of crustaceans, has also been recently investigated as a potential hydrogel scaffold as its cationic charge theoretically allows the gel to trap anionic proteoglycans produced by encapsulated cells⁷⁵⁻⁷⁷. Additionally, chitosan is a thermosensitive polymer

which transitions from a liquid to a viscoelastic solid at 37°C and could potentially serve as an injectable scaffold^{83, 84}. A thermogelling chitosan/glycerophosphate system has been developed for drug delivery⁸⁵ and studied for use as a tissue engineering scaffold, but was found to lack a firm structure⁷⁶, which would prove deleterious for a load bearing structure, such as the NP.

The prevailing mode of NP cell culture has been cell encapsulation within alginate, a naturally-derived polysaccharide originating from brown algae^{8, 45, 46, 50, 52, 55, 58, 71-74} (Figure 1.5).

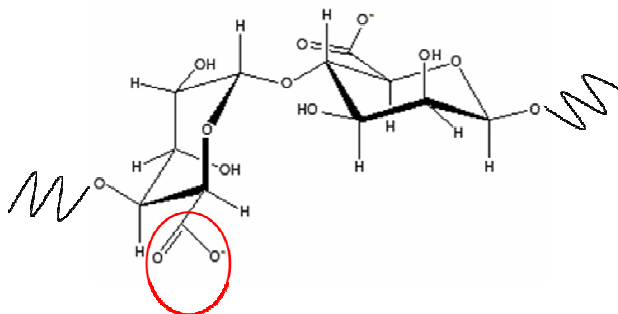


Figure 1.5. Alginate chemical structure, with a representative carboxylic acid moiety circled in red.

The traditional method of alginate gelation is through ionic crosslinking, achieved via diffusion of divalent cations, such as calcium, to carboxylic acid moieties on the polymer to produce a crosslinked network. Although this initially produces stable gels, studies have shown that cell-seeded, ionically crosslinked alginate hydrogels lose mechanical integrity over time in long-term static *in vitro* and *in vivo* culture^{9, 45}, possibly due to a loss of crosslinking ions through diffusion into the culture medium or depletion by encapsulated cells.

1.7.3. Photocrosslinkable Hydrogels for Tissue Engineering

The reversible nature of conventional ionic crosslinking techniques has led to the investigation of more stable, covalent crosslinking methods. Photopolymerization is a well-established method used in dental applications for the *in situ* crosslinking of polymer networks^{86, 87}. This technique employs biocompatible, light-sensitive photoinitiators which produce covalently crosslinked 3-D networks via radical polymerization⁸⁷. Photopolymerization provides spatial and temporal control of gelation and can be performed *in situ* using a liquid cell-polymer solution to completely fill irregularly shaped defect sites while maintaining good contact with the surrounding tissue.

Elisseff et al. first described use of a modified, methacrylated poly(ethylene oxide) (PEO) polymer for cartilage tissue engineering applications^{86, 88}. Radicals produced by the photoinitiator react with methacrylate groups along the polymer backbone to polymerize the cell-laden mixture and form a crosslinked hydrogel network. This scaffold was able to retain GAGs and collagen elaborated by encapsulated chondrocytes. This technique was modified by Bryant et al. to incorporate degradable lactic acid units into poly(ethylene glycol)-based (PEG) hydrogels to enhance the spatial distribution of ECM components in these otherwise inert polymers⁸¹. Smeds et al. utilized these same principles to investigate natural polymers and created photocrosslinked polysaccharide-based hydrogels from modified alginate and hyaluronic acid macromers⁸⁹. Methacrylated hyaluronic acid was used as a scaffold in cartilage tissue engineering applications by Burdick et al. and Nettles et al. who confirmed accumulation of GAGs and type II collagen elaborated by encapsulated chondrocytes⁹⁰.

⁹¹. These constructs were shown to allow for functional matrix production following *in vivo* implantation in a subcutaneous murine pouch model⁹². Additionally, studies conducted by Burdick et al. and Chung et al. have demonstrated that hyaluronic acid hydrogels can be fabricated with tunable material properties by altering the macromer concentration (weight/volume) and molecular weight^{90, 93}.

This approach has recently been applied to NP tissue engineering using methacrylated alginate to produce photocrosslinkable, mechanically stable hydrogel constructs capable of supporting NP cell growth and viability⁴⁵. Similar to results observed for hyaluronic acid constructs, alginate hydrogel material properties increased with increasing macromer concentration and methacrylation. Nevertheless, raw alginate has been shown to stimulate an immune response *in vivo* in mice and requires additional processing to remove impurities for biomedical applications⁹⁴. Similar purification procedures are required for animal-derived products, such as hyaluronic acid, chitosan, and chondroitin sulfate, which have also been used to engineer cartilaginous tissues^{76, 84, 89-92, 95, 96}. However, the results observed for these photocrosslinkable hydrogels indicate the potential of comparable polysaccharide-based systems for use in additional orthopaedic tissue engineering applications.

1.7.4. Cellulose-based Materials for Tissue Engineering Applications

Cellulose, the major structural component of plant cell walls, is a naturally-occurring polysaccharide that is FDA-approved, biocompatible, and commercially available. In addition, as a plant-derived polysaccharide, cellulose and its derivatives represent a class of renewable, environmentally-friendly biomaterials. Although

cellulose has been studied in limited biomedical applications, the rigid, symmetric molecular structure of the polymer backbone minimizes flexibility, and hydrogen bonding of hydroxyl groups, both within the molecule and across cellulose chains, forms non-soluble crystalline structures⁹⁷ (Figure 1.6). However, modification of these hydroxyl groups with more hydrophobic groups, such as methyl or carboxymethyl groups, reduces hydrogen bonding and improves water affinity⁹⁸.

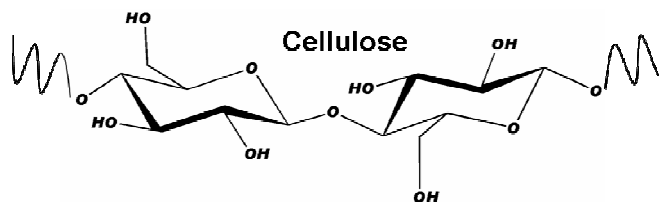


Figure 1.6. Chemical structure of cellulose

Methylcellulose, a water-soluble derivative of cellulose which substitutes methyl groups in place of some hydroxyl hydrogen atoms, is similarly a non-toxic, biocompatible, FDA-approved material that is commercially available at low-cost⁹⁹ (Figure 1.7).

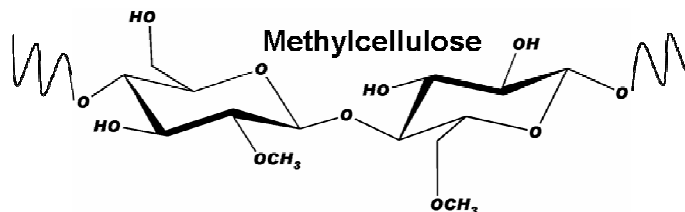


Figure 1.7. Chemical structure of methylcellulose

Although methacrylated methylcellulose has recently been shown to form stable, photocrosslinkable cell-free hydrogels for dermal filler applications¹⁰⁰, these gels were not able to support the viability of encapsulated NP cells when examined *in vitro*. NP cells encapsulated at 10×10^6 cells/mL experienced ~70% reduction in viability over 21

days (Figure 1.8). This may be due, in part, to the hydrophobic methyl groups which prevent any significant degree of swelling and result in a stiffer environment.

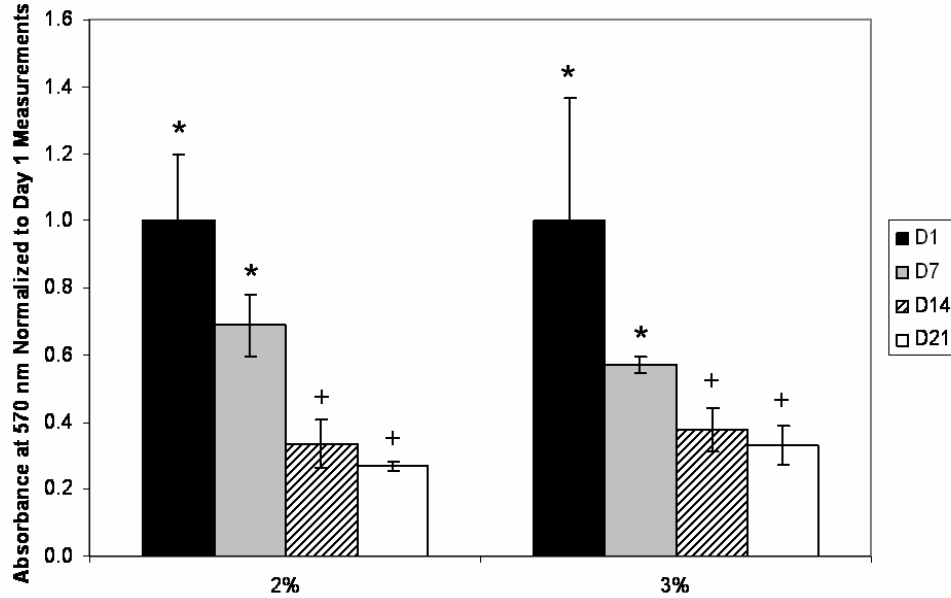


Figure 1.8. Viability data for NP cells encapsulated in 2% and 3% methacrylated methylcellulose hydrogels at a density of 10×10^6 cells/mL. *: significant vs. all other time points. +: Significant vs. D1 and D7.

Carboxymethylcellulose (CMC) is also a biocompatible, water-soluble derivative of cellulose that is likewise low-cost, FDA-approved, and commercially available in high purity forms. At physiological pH, the carboxylic acid of the carboxymethyl group is deprotonated, resulting in a negatively-charged polymer network, which is similar to that provided by the GAGs in the ECM of cartilaginous tissues (Figure 1.9).

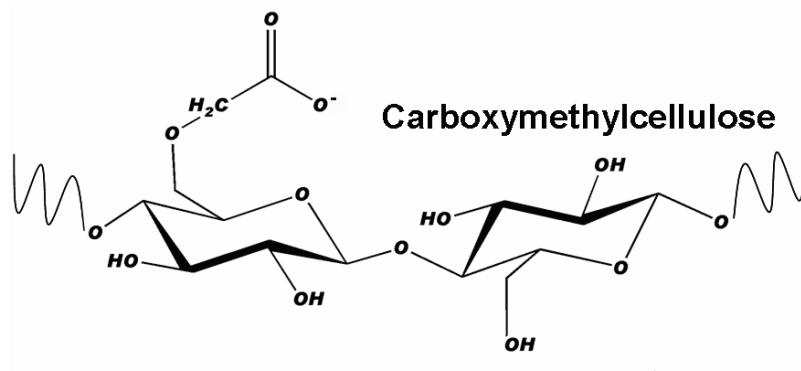


Figure 1.9 Chemical structure of carboxymethylcellulose

This negative charge alters the properties of the biomaterial, allowing for a greater degree of swelling in comparison to cellulose and methylcellulose. Similar to methylcellulose, CMC has been studied for use in dermal filler applications, and when combined with PEO, produces an easily injectable solution without necessitating chemical crosslinking agents¹⁰¹. CMC-based hydrogels have also been investigated for tissue engineering applications, applying various crosslinking chemistries¹⁰²⁻¹⁰⁵. Cytotoxicity has been tested in these investigations using multiple cell lines with positive results. **These studies, combined with the work by Stalling et al. to develop a photocrosslinkable methylcellulose platform¹⁰⁰, demonstrate the potential of a similar photocrosslinkable CMC-based hydrogel for NP cell encapsulation.**

1.8. Biochemical Signals for Intervertebral Disc Tissue Engineering

Growth factors, found circulating in body fluids such as blood and the synovium, bind to cell transmembrane receptors and initiate an intracellular signaling cascade that can affect cell proliferation, differentiation, migration, apoptosis, matrix production, and repair via the endocrine, paracrine, or autocrine systems¹⁰⁶. Growth factor

supplementation is a biologic approach to address disc degeneration, possibly preventing, ceasing, or reversing its effects by increasing ECM synthesis¹⁰⁷. A variety of growth factors have been identified within the native disc tissue, including insulin-like growth factor-1 (IGF-1)¹⁰⁸, basic fibroblast growth factor (bFGF)¹⁰⁹, platelet-derived growth factor (PDGF)¹¹⁰, transforming growth factor- β (TGF- β)¹¹¹, and members of the bone morphogenetic protein (BMP) family^{112, 113}. These growth factors have thus served as a starting point for investigations into the effects of *in vitro* biochemical stimulation of tissue engineered constructs.

1.8.1. Exogenous Growth Factor Delivery

The exogenous delivery of growth factors, also called protein therapy, is accomplished *in vitro* as an additive to cell culture medium. However, it is important to note that several variables can affect the efficacy and outcome of growth factor supplementation, including concentration and timing of delivery, culture conditions (i.e., 3-D vs. monolayer culture, serum-containing medium vs. serum-free medium, etc.), and cell source¹¹⁴. Although this makes it difficult to compare between studies, exogenous growth factor delivery has been shown, to varying degrees, to stimulate matrix production and cell proliferation.

A wide range of growth factors, including IGF-1^{44, 115}, TGF- β isoforms^{44, 72, 115-117}, and members of the BMP family^{14, 118} have been investigated in IVD tissue engineering. An early study by Thompson et al. examined the effects of multiple growth factors on proteoglycan synthesis and cell proliferation by mature canine disc tissues and found the greatest response with TGF- β_1 and epidermal growth factor (EGF) supplementation, while the effects of IGF-1 supplementation were marginal¹¹⁵. However, a study by

Gruber et al. showed a decrease in the apoptosis of monolayer human annulus fibrosus cells cultured in low serum conditions when supplemented with IGF-1¹¹⁹.

A systematic study by Alini et al. examined the independent and combinatorial effects of TGF- β_1 , IGF-1, and bFGF on annulus fibrosus and NP cells cultured on a 3-D collagen/hyaluronic acid scaffold under serum-free conditions⁴⁴. This investigation found that the combination of TGF- β_1 and bFGF resulted in the greatest increase in retained proteoglycans, although this value never exceeded 10% of the native NP, even after 60 days of culture. Work by Risbud et al. compared two commonly used isoforms of TGF- β , TGF- β_1 and TGF- β_3 ¹¹⁷. Using whole disc organ culture maintained in serum-containing medium, Risbud et al. reported that TGF- β_3 produced a differential increase in the expression of critical matrix genes and elevated proteoglycan synthesis. Kim et al. studied the effect of BMP-2 on monolayer IVD cells (mixed population of annulus and NP cells) and found increased proteoglycan synthesis along with an upregulation of aggrecan, type I collagen, and type II collagen gene expression without increasing the expression of the bone-associated gene, osteocalcin¹⁴. Taken together, these studies highlight the beneficial effect of exogenous growth factor supplementation on *in vitro* IVD cell culture systems.

1.8.2. Gene Therapy

While exogenous growth factor delivery is a feasible option for *in vitro* studies, the short half-life of these proteins serves as a limitation for their clinical applicability. Gene therapy is an alternative approach in which cells are genetically modified in order to induce sustained synthesis of such growth factors endogenously. The goal of *ex vivo*

gene therapy is to transduce cells *in vitro* using viral (i.e., adenoviral, retroviral, baculoviral) vector or non-viral (i.e., plasmids, liposomes, polymers) techniques and then deliver these transduced cells *in vivo*. Although viral vectors carry greater safety concerns, such as induction of viral protein production that may stimulate a host immune reaction, these vectors have high transfection efficiency, whereas non-viral delivery methods carry fewer safety concerns but also exhibit lower transfection efficiencies.

Gilbertson et al. examined the effect of adenoviral BMP-12 on matrix synthesis by human annulus fibrosus and NP cells in pellet culture maintained in serum-free medium over six days¹²⁰. This study showed an increase in matrix protein synthesis and cell proliferation by both populations, supporting its use as a potential therapy for the disc. Lee et al. utilized adenoviral TGF- β_1 to transfect IVD cells and compared the effects of alginate bead culture to pellet culture. After three weeks *in vitro*, both culture systems displayed increased proteoglycan synthesis, with the most pronounced results observed in pellet culture, indicating the importance of both growth factor delivery and cell culture environment¹²¹.

1.9. Biomechanical Stimulation in Intervertebral Disc Tissue Engineering

The unique structure and function of each tissue within the IVD allows this integral load-bearing tissue to absorb and distribute the daily forces to which it is exposed. Gravity and muscle tension produced during movement result in a wide variety of mechanical stimuli applied to the disc, such as compression, hydrostatic pressure, shear, torsion, and flexion¹²². These forces induce a biologic response at the cellular level and are thought to be key regulators of IVD matrix content¹²². It is hypothesized

that such forces, applied within physiologic levels, act as anabolic factors and stimulate the synthesis of matrix proteins, while forces that fall below or exceed this range may inhibit matrix synthesis^{123, 124}. These principals serve as the general guidelines in applying mechanical loads which mimic those experienced *in vivo* in order to modulate the matrix production and functional properties of tissue engineered constructs.

1.9.1. Deformational Loading

As with many other forms of mechanical loading, the effect of compressive loading is highly dependent upon the magnitude and frequency at which it is applied. Static compression applied to intact disc tissue over eight hours *in vitro* was shown to increase proteoglycan and collagen synthesis at low magnitudes (5-10 kg load) and decrease synthesis at higher magnitudes (15 kg)¹²⁵. However, dynamic compression applied at low frequency (0.01 Hz) and/or high stress (1.3 MPa) was found to increase proteoglycan content and anabolic matrix gene expression, while also increasing cell death when applied *in vivo* using a mouse tail model¹²⁶. A study by MacLean et al. reported a similar dependence on frequency, as 1 MPa dynamic compression applied at 0.01 Hz increased anabolic gene expression in the NP, while 1 MPa compression applied at 1 Hz increased the expression of catabolic factors in the same tissue¹²⁷. Dynamic compression has also been applied *in vitro* by Korecki et al. to NP cell-laden alginate hydrogels to compare the effects of frequency (0.1, 1, and 3 Hz) and donor age. They demonstrated that maturation was a significant factor in the cellular response to mechanical loading, though the impact of loading frequency was minimal¹²⁸.

Cyclic tensile strain (1-8% applied at 1 Hz) has also been shown to produce beneficial effects, increasing type II collagen and aggrecan gene expression while decreasing MMP-3 expression in annulus fibrosus cells encapsulated in collagen gels⁴⁰. Additionally, a study by Iatridis et al. found that permanent deformation, induced by cyclic tensile strain, was dependent on the magnitude of the strain and the number of cycles, as the most damage occurred in samples undergoing a fatigue loading protocol¹²⁹.

1.9.2. Hydrostatic Pressure

The IVD responds to axial compression with a radial, bulging deformation that loads the annulus fibrosus in tension, while the NP responds predominantly as a fluid and generates a large hydrostatic pressure¹. As such, hydrostatic pressure has been studied as a method to modulate NP construct development *in vitro*, with investigations primarily focusing within the range of pressure observed *in vivo*, 0.1 – 3 MPa^{40, 41, 55, 74}. An early study by Ishihara et al. determined that hydrostatic pressure applied at 2.5 MPa stimulated proteoglycan synthesis in human NP tissue fractions, while 10 MPa pressure inhibited synthesis¹²⁴. Similarly, Handa et al. concluded that physiologic levels (0.3 MPa) of hydrostatic pressure increased proteoglycan synthesis in NP tissue fractions and increased the production of TIMP-1, an inhibitor of matrix metalloproteinases (MMPs), while excessive (3 MPa) or insufficient (0.1 MPa) pressures decreased proteoglycan synthesis and increased MMP-3 production¹²³.

More recent work has examined the effects of pressure on tissue engineered constructs. Hutton et al. examined the effects of static hydrostatic pressure (1 MPa continuously applied for 9 days) applied to NP cells encapsulated in alginate and found

increased collagen and proteoglycan synthesis, along with increased aggrecan, type I collagen, and type II collagen gene expression in comparison to unloaded controls⁵⁵. Kasra et al. examined a wide range of frequencies (1-20 Hz) and magnitudes (0-3 MPa) and surprisingly found that high magnitude, high frequency (3 MPa, 20 Hz) loading resulted in the largest increases in collagen production and the greatest reduction in collagen degradation by NP cells encapsulated in alginate⁵⁰. In contrast, a study by Neidlinger-Wilke observed a decrease in aggrecan and type II collagen gene expression in response to 2.5 MPa pressure, accompanied by an increase in MMP-3 expression by NP cells cultured in a collagen gel⁴¹.

While there have been many studies examining the effects of hydrostatic pressure on tissue engineered constructs, there is yet no consensus on the most physiologically relevant loading regimen. Furthermore, though many studies have concluded a beneficial effect of hydrostatic pressurization, previous experiments have only examined the short-term impact of mechanical stimulation, characterizing gene expression and matrix biosynthesis without determining if this form of loading was effectively translated into altered functional properties for these engineered constructs. As such, future studies should examine both the biochemical and biomechanical properties of tissue engineered constructs which have been subjected to hydrostatic pressurization.

1.10. Motivation and Research Overview

Low back pain, experienced by as much as 80% of the American population¹⁹, may be caused by a direct, acute injury or degeneration of the IVD. Intradiscal replacement of the NP with a synthetic hydrogel presents a less invasive alternative to

conventional surgery techniques to mechanically re-establish structure and function to the IVD. However, most hydrogels currently investigated for this use are non-degrading polymers which do not support cell growth, and thus do not address the biological component of the IVD structure and function³⁴. Tissue engineering strategies may provide a biologic alternative capable of restoring both the structure and mechanical function of the IVD through the use of a cell-laden scaffold. As such, **the governing hypothesis of this thesis is that CMC may be chemically modified to form a stable, photocrosslinkable hydrogel capable of supporting the viability and matrix production of encapsulated NP cells.** In addition, we hypothesized that the functional properties of these cell-laden constructs could be modulated biochemically, through growth factor supplementation, and biomechanically, through the application of dynamic hydrostatic pressure to enhance the development of this tissue engineered scaffold.

To test these hypotheses, the following specific aims were proposed:

Specific Aim 1. Modify CMC with photopolymerizable methacrylate groups to form covalently crosslinked hydrogels capable of supporting NP cell viability and matrix production. CMC will be chemically modified with functional methacrylate groups which may be crosslinked using photoinitiated radical polymerization to create a three-dimensional network. Hydrogels will be formed at various macromer concentrations (weight/volume) using CMC of various molecular weights and these gels will be characterized by determining the swelling and mechanical properties. In addition, the viability of encapsulated NP cells and the associated matrix elaboration will be assessed to determine a mechanically stable hydrogel formulation.

Specific Aim 2. Identify a cell culture medium to enhance the development of NP tissue engineered constructs by comparing the effects of medium formulation and TGF- β_3 on functional matrix development. A standard serum-containing medium will be compared to a serum-free formulation commonly used in cartilage tissue engineering applications and both media will be additionally supplemented with TGF- β_3 . NP cell-laden CMC hydrogels maintained under these conditions will be examined to assess swelling properties, cell viability, matrix production, and construct mechanical properties in order to optimize *in vitro* culture conditions.

Specific Aim 3. Examine the effects of hydrostatic pressurization and growth factor supplementation on the matrix production and functional properties of NP cells encapsulated in photocrosslinked CMC hydrogels. NP cell-laden hydrogels will be cultured with and without TGF- β_3 and will be subjected to dynamic hydrostatic pressure or maintained at atmospheric pressure to determine the effects of these biochemical and biomechanical stimuli. Swelling properties, cell viability, matrix production, and mechanical properties will be measured to determine if the external stimuli enhance the functional and material properties of these constructs in an independent, additive, or synergistic manner.

Specific Aim 4. Evaluate the tissue formation and functional properties of subcutaneously implanted NP cell-laden CMC hydrogels that have been pre-cultured *in vitro* in the presence of TGF- β_3 . Constructs will be pre-cultured for 14 days *in vitro* with and without TGF- β_3 prior to subcutaneous implantation *in vivo* for up to 8 weeks using a murine pouch model. Corresponding controls will be maintained to additionally compare long-term *in vitro* and *in vivo* culture conditions by assessing the

swelling properties, cell viability, matrix production, and mechanical properties of these constructs.

Taken together, these studies will establish a novel scaffold for IVD tissue engineering and will provide insight into the effects of biochemical and biomechanical stimulation on matrix elaboration by NP cells encapsulated in these hydrogels.

1.11. Overview of Present Investigation

The objective of this thesis project was to develop and optimize a novel, cell-laden CMC hydrogel able to support NP cell viability and matrix accumulation in order to create a functional tissue engineered replacement. To accomplish this, the versatility of the photocrosslinkable CMC system was explored by examining the resultant differences in material and mechanical properties due to varying the macromer concentration and molecular weight of the starting material, as is presented in Chapter 2. This study demonstrated the utility of photocrosslinkable CMC hydrogels for NP cell encapsulation, as these biomaterials were shown to support NP cell viability and may be easily tailored for specific applications.

Although the system described in Chapter 2 produced stable hydrogels which supported NP cell viability and promoted phenotypic matrix deposition capable of maintaining initial mechanical properties *in vitro*, in order to create a truly functional tissue engineered NP replacement, culture conditions were examined to enhance matrix deposition and improve construct material and mechanical properties. Chapter 3 compared the effects of medium formulation and TGF- β_3 supplementation on the *in vitro* culture of cell-laden CMC constructs in an effort to improve matrix deposition and

functional material properties. This work showed approximately a ten-fold increase in GAG accumulation and a five-fold increase in mechanical properties when specimens were cultured in serum-free medium supplemented with TGF- β_3 .

Building upon the investigation of biochemical stimuli described in Chapter 3, Chapter 4 examined biochemical and biomechanical stimulation, via hydrostatic pressurization, utilized in conjunction to further develop tissue formation by engineered CMC constructs. This work assessed the effect of each stimulus, when applied independently and in concert, and determined a more pronounced impact of growth factor supplementation alone on the functional development of NP-seeded CMC constructs in support of the results from Chapter 3. Chapter 5 evaluated the long-term effect of TGF- β_3 supplementation applied over a two-week *in vitro* pre-culture period prior to subcutaneous implantation in a murine pouch model for up to eight weeks. This investigation also examined the mechanical, biochemical, and material properties of subcutaneous constructs following excision and compared these values to those measured prior to implantation and those of samples maintained under *in vitro* culture conditions. Constructs maintained without TGF- β_3 exhibited no quantifiable changes in matrix content or mechanical properties over time under both *in vitro* and *in vivo* conditions. In contrast, scaffolds pre-treated with TGF- β_3 and maintained *in vitro* demonstrated a long-term enhancement in matrix accumulation and mechanical properties. However, samples which were exposed to TGF- β_3 and subsequently implanted *in vivo* experienced a significant decrease in matrix content and mechanical properties, indicating a differential effect on construct maturation in response to TGF- β_3 supplementation, which is dependent upon culture condition.

Chapter 6 details the overall conclusions of this thesis and future directions for related work. This section has outlined limitations to the studies presented and describes pilot studies investigating a redox initiation system which would further improve the versatility of this system for use as an injectable NP replacement.

1.12. References

1. Buckwalter JA, Mow VC, Boden SD, Eyre DR and Weidenbaum M. 2000. "Intervertebral disk structure, composition, and mechanical function." In: Orthopaedic Basic Science. Edited by Buckwalter JA, Einhorn TA and Simon SR. 2nd ed. Rosemont, IL: American Academy of Orthopaedic Surgeons. p 547-556.
2. Roughley PJ. 2004. Biology of intervertebral disc aging and degeneration: involvement of the extracellular matrix. *Spine* **29(23)**: 2691-2699.
3. Buckwalter JA, Pedrini-Mille A, Pedrini V and Tudisco C. 1985. Proteoglycans of human infant intervertebral disc. Electron microscopic and biochemical studies. *J Bone Joint Surg Am* **67(2)**: 284-294.
4. Raj PP. 2008. Intervertebral disc: anatomy-physiology-pathophysiology-treatment. *Pain Pract* **8(1)**: 18-44.
5. Nerurkar NL, Elliott DM and Mauck RL. 2007. Mechanics of oriented electrospun nanofibrous scaffolds for annulus fibrosus tissue engineering. *J Orthop Res* **25(8)**: 1018-1028.
6. Oegema TR. 1993. Biochemistry of the intervertebral disc. *Clin Sports Med* **12(3)**: 419-439.

7. O'Halloran DM and Pandit AS. 2007. Tissue-engineering approach to regenerating the intervertebral disc. *Tissue Eng* **13(8)**: 1927-1954.
8. Chou AI, Reza AT and Nicoll SB. 2008. Distinct intervertebral disc cell populations adopt similar phenotypes in three-dimensional culture. *Tissue Eng Part A* **14(12)**: 2079-2087.
9. Wang JY, Baer AE, Kraus VB and Setton LA. 2001. Intervertebral disc cells exhibit differences in gene expression in alginate and monolayer culture. *Spine* **26(16)**: 1747-1751.
10. Buckwalter J. 1998. Do intervertebral discs deserve their bad reputation? *Iowa Orthop J* **18**: 1-11.
11. Hunter CJ, Matyas JR and Duncan NA. 2003. The three-dimensional architecture of the notochordal nucleus pulposus: novel observations on cell structures in the canine intervertebral disc. *J Anat* **202(3)**: 279-291.
12. Trout JJ, Buckwalter JA, Moore KC and Landas SK. 1982. Ultrastructure of the human intervertebral disc. I. Changes in notochordal cells with age. *Tissue Cell* **14(2)**: 359-369.
13. Trout JJ, Buckwalter JA and Moore KC. 1982. Ultrastructure of the human intervertebral disc: II. Cells of the nucleus pulposus. *Anat Rec* **204(4)**: 307-314.
14. Kim K-W, Lim T-H, Kim JG, Jeong S-T, Masuda K and An HS. 2003. The origin of chondrocytes in the nucleus pulposus and histologic findings associated with the transition of a notochordal nucleus pulposus to a fibrocartilaginous nucleus pulposus in intact rabbit intervertebral discs. *Spine* **28(10)**: 982-990.

15. Rufai A, Benjamin M and Ralphs J. 1995. The development of fibrocartilage in the rat intervertebral disc. *Anat Embryol* **192(1)**: 53-62.
16. Adams MA and Roughley PJ. 2006. What is intervertebral disc degeneration, and what causes it? *Spine* **31(18)**: 2151-2161.
17. Bushell GR, Ghosh P, Taylor TF and Akeson WH. 1977. Proteoglycan chemistry of the intervertebral disks. *Clin Orthop Relat Res* **129**: 115-123.
18. Buckwalter JA, Boden SD, Eyre DR, Mow VC and Weidenbaum M. 2000. "Intervertebral disk aging, degeneration, and herniation." In: Orthopaedic Basic Science. Edited by Buckwalter JA, Einhorn TA and Simon SR. 2nd ed. Rosemont, IL: American Academy of Orthopaedic Surgeons. p 557-566.
19. Frymoyer JW and Cats-Baril WL. 1991. An overview of the incidences and costs of low back pain. *Orthop Clin North Am* **22(2)**: 263-271.
20. Martin BI, Deyo RA, Mirza SK, Turner JA, Comstock BA, Hollingworth W and Sullivan SD. 2008. Expenditures and health status among adults with back and neck problems. *JAMA* **299(6)**: 656-664.
21. Battié MC, Videman T and Parent E. 2004. Lumbar disc degeneration: epidemiology and genetic influences. *Spine* **29(23)**: 2679-2690.
22. Videman T, Sarna S, Battié MC, Koskinen S, Gill K, Paananen H and Gibbons L. 1995. The long-term effects of physical loading and exercise lifestyles on back-related symptoms, disability, and spinal pathology among men. *Spine* **20(6)**: 699-709.
23. Battié MC, Videman T, Gill K, Moneta GB, Nyman R, Kaprio J and Koskenvuo M. 1991. 1991 Volvo Award in clinical sciences. Smoking and lumbar

- intervertebral disc degeneration: an MRI study of identical twins. *Spine* **16(9)**: 1015-1021.
24. Brown MF, Hukkanen MV, McCarthy ID, Redfern DR, Batten JJ, Crock HV, Hughes SP and Polak JM. 1997. Sensory and sympathetic innervation of the vertebral endplate in patients with degenerative disc disease. *J Bone Joint Surg Br* **79(1)**: 147-153.
 25. Kauppila LI. 1995. Ingrowth of blood vessels in disc degeneration. Angiographic and histological studies of cadaveric spines. *J Bone Joint Surg Am* **77(1)**: 26-31.
 26. Freemont AJ, Peacock TE, Goupille P, Hoyland JA, O'Brien J and Jayson MI. 1997. Nerve ingrowth into diseased intervertebral disc in chronic back pain. *Lancet* **350(9072)**: 178-181.
 27. Stähler A, Weiss M, Scheidler J, Krödel A, Seiderer M and Reiser M. 1996. Degenerative disk vascularization on MRI: correlation with clinical and histopathologic findings. *Skeletal Radiol* **25(2)**: 119-126.
 28. Goins ML, Wimberley DW, Yuan PS, Fitzhenry LN and Vaccaro AR. 2005. Nucleus pulposus replacement: an emerging technology. *Spine J* **5(6 Suppl)**: 317S-324S.
 29. Yang X and Li X. 2009. Nucleus pulposus tissue engineering: a brief review. *Eur Spine J* doi: 10.1007/s00586-00009-01092-00588.
 30. Lee CK and Langrana NA. 1984. Lumbosacral spinal fusion. A biomechanical study. *Spine* **9(6)**: 574-581.

31. Rolander SD. 1966. Motion of the lumbar spine with special reference to the stabilizing effect of posterior fusion. An experimental study on autopsy specimens. *Acta Orthop Scand* **90**: 1-143 (translated by P. Hart).
32. Yang SW, Langrana NA and Lee CK. 1986. Biomechanics of lumbosacral spinal fusion in combined compression-torsion loads. *Spine* **11(9)**: 937-941.
33. Guyer RD and Ohnmeiss DD. 2003. Intervertebral disc prostheses. *Spine* **28(15 Suppl)**: S15-S23.
34. Di Martino A, Vaccaro AR, Lee JY, Denaro V and Lim MR. 2005. Nucleus pulposus replacement: Basic science and indications for clinical use. *Spine* **30 (16 Suppl)**: S16-S22.
35. Carl A, Ledet E, Yuan H and Sharan A. 2004. New developments in nucleus pulposus replacement technology. *Spine J* **4(6 Suppl)**: 325S-329S.
36. Langer R and Vacanti JP. 1993. Tissue engineering. *Science* **260(5110)**: 920-926.
37. An HS, Thonar E and Masuda K. 2003. Biological repair of intervertebral disc. *Spine* **28(15 Suppl)**: S86-S92.
38. Gruber HE, Stasky AA and Hanley Jr EN. 1997. Characterization and phenotypic stability of human disc cells *in vitro*. *Matrix Biol* **16(5)**: 285-288.
39. Le Maitre CL, Frain J, Fotheringham AP, Freemont AJ and Hoyland JA. 2008. Human cells derived from degenerate intervertebral discs respond differently to those derived from non-degenerate intervertebral discs following application of dynamic hydrostatic pressure. *Biorheology* **45(5)**: 563-575.
40. Neidlinger-Wilke C, Würtz K, Liedert A, Schmidt C, Börm W, Ignatius A, Wilke H-J and Claes L. 2005. A three-dimensional collagen matrix as a suitable culture

- system for the comparison of cyclic strain and hydrostatic pressure effects on intervertebral disc cells. *J Neurosurg Spine* **2(4)**: 457-465.
41. Neidlinger-Wilke C, Würtz K, Urban JPG, Börm W, Arand M, Ignatius A, Wilke H-J and Claes LE. 2006. Regulation of gene expression in intervertebral disc cells by low and high hydrostatic pressure. *Eur Spine J* **15 (Suppl 3)**: S372-378.
 42. Wuertz K, Urban JPG, Klasen J, Ignatius A, Wilke H-J, Claes L and Neidlinger-Wilke C. 2007. Influence of extracellular osmolarity and mechanical stimulation on gene expression of intervertebral disc cells. *J Orthop Res* **25(11)**: 1513-1522.
 43. Gruber HE, Johnson TL, Leslie K, Ingram JA, Martin D, Hoelscher G, Banks D, Phieffer L, Coldham G and Hanley Jr EN. 2002. Autologous intervertebral disc cell implantation: a model using *Psammomys obesus*, the sand rat. *Spine* **27(15)**: 1626-1633.
 44. Alini M, Li W, Markovic P, Aebi M, Spiro RC and Roughley PJ. 2003. The potential and limitations of a cell-seeded collagen/hyaluronan scaffold to engineer an intervertebral disc-like matrix. *Spine* **28(5)**: 446-454.
 45. Chou AI and Nicoll SB. 2009. Characterization of photocrosslinked alginate hydrogels for nucleus pulposus cell encapsulation. *J Biomed Mater Res A* **91A(1)**: 187-194.
 46. Chou AI, Akintoye SO and Nicoll SB. 2009. Photo-crosslinked alginate hydrogels support enhanced matrix accumulation by nucleus pulposus cells *in vivo*. *Osteoarthritis Cartilage* **17(10)**: 1377-1384.

47. Reza AT and Nicoll SB. 2008. Hydrostatic pressure differentially regulates outer and inner annulus fibrosus cell matrix production in 3D scaffolds. *Ann Biomed Eng* **36(2)**: 204-213.
48. Reza AT and Nicoll SB. 2009. Characterization of novel photocrosslinked carboxymethylcellulose hydrogels for encapsulation of nucleus pulposus cells. *Acta Biomater* doi:10.1016/j.actbio.2009.1006.1004.
49. Reza AT and Nicoll SB. 2009. Serum-free, chemically defined medium with TGF-beta(3) enhances functional properties of nucleus pulposus cell-laden carboxymethylcellulose hydrogel constructs. *Biotechnol Bioeng* doi: 10.1002/bit.22545.
50. Kasra M, Goel V, Martin J, Wang ST, Choi W and Buckwalter J. 2003. Effect of dynamic hydrostatic pressure on rabbit intervertebral disc cells. *J Orthop Res* **21(4)**: 597-603.
51. Sato M, Kikuchi M, Ishihara M, Ishihara M, Asazuma T, Kikuchi T, Masuoka K, Hattori H and Fujikawa K. 2003. Tissue engineering of the intervertebral disc with cultured annulus fibrosus cells using atelocollagen honeycomb-shaped scaffold with a membrane seal (ACHMS scaffold). *Med Biol Eng Comput* **41(3)**: 365-371.
52. Chou AI, Bansal A, Miller GJ and Nicoll SB. 2006. The effect of serial monolayer passaging on the collagen expression profile of outer and inner annulus fibrosus cells. *Spine* **31(17)**: 1875-1881.

53. Mizuno H, Roy AK, Vacanti CA, Kojima K, Ueda M and Bonassar LJ. 2004. Tissue-engineered composites of anulus fibrosus and nucleus pulposus for intervertebral disc replacement. *Spine* **29(12)**: 1290-1297.
54. Mizuno H, Roy AK, Zaporozhan V, Vacanti CA, Ueda M and Bonassar LJ. 2006. Biomechanical and biochemical characterization of composite tissue-engineered intervertebral discs. *Biomaterials* **27(3)**: 362-370.
55. Hutton WC, Elmer WA, Boden SD, Hyon S, Toribatake Y, Tomita K and Hair GA. 1999. The effect of hydrostatic pressure on intervertebral disc metabolism. *Spine* **24(15)**: 1507-1515.
56. Baer AE, Wang JY, Kraus VB and Setton LA. 2001. Collagen gene expression and mechanical properties of intervertebral disc cell-alginate cultures. *J Orthop Res* **19(1)**: 2-10.
57. Gokorsch S, Nehringm D, Grottke C and Czermak P. 2004. Hydrodynamic stimulation and long term cultivation of nucleus pulposus cells: a new bioreactor system to induce extracellular matrix synthesis by nucleus pulposus cells dependent on intermittent hydrostatic pressure. *Int J Artif Organs* **27(11)**: 962-970.
58. Kasra M, Merryman WD, Loveless KN, Goel VK, Martin JD and Buckwalter JA. 2006. Frequency response of pig intervertebral disc cells subjected to dynamic hydrostatic pressure. *J Orthop Res* **24(10)**: 1967-1973.
59. Wenger KH, Woods JA, Holecek A, Eckstein EC, Robertson JT and Hasty KA. 2005. Matrix Remodeling Expression in Anulus Cells Subjected to Increased Compressive Load. *Spine* **30**: 1122-1126.

60. Chen FH and Tuan RS. 2008. Mesenchymal stem cells in arthritic diseases. *Arthritis Res Ther* **10(5)**: 223-234.
61. Risbud MV, Guttapalli A, Tsai T-T, Lee JY, Danielson KG, Vaccaro AR, Albert TJ, Gazit Z, Gazit D and Shapiro IM. 2007. Evidence for skeletal progenitor cells in the degenerate human intervertebral disc. *Spine* **32(23)**: 2537-2544.
62. Sakai D, Mochida J, Yamamoto Y, Nomura T, Okuma M, Nishimura K, Nakai T, Ando K and Hotta T. 2003. Transplantation of mesenchymal stem cells embedded in Atelocollagen gel to the intervertebral disc: a potential therapeutic model for disc degeneration. *Biomaterials* **24(20)**: 3531-3541.
63. Sakai D, Mochida J, Iwashina T, Watanabe T, Nakai T, Ando K and Hotta T. 2005. Differentiation of mesenchymal stem cells transplanted to a rabbit degenerative disc model: potential and limitations for stem cell therapy in disc regeneration. *Spine* **30(21)**: 2379-2387.
64. Sakai D, Mochida J, Iwashina T, Hiyama A, Omi H, Imai M, Nakai T, Ando K and Hotta T. 2006. Regenerative effects of transplanting mesenchymal stem cells embedded in atelocollagen to the degenerated intervertebral disc. *Biomaterials* **27(3)**: 335-345.
65. Cao Y, Vacanti JP, Ma X, Paige KT, Upton J, Chowanski Z, Schloo B, Langer R and Vacanti CA. 1994. Generation of neo-tendon using synthetic polymers seeded with tenocytes. *Transplant Proc* **26(6)**: 3390-3392.
66. Aoki M, Miyamoto S, Okamura K, Yamashita T, Ikada Y and Matsuda S. 2004. Tensile properties and biological response of poly(L-lactic acid) felt graft: an

- experimental trial for rotator-cuff reconstruction. *J Biomed Mater Res B Appl Biomater* **71(2)**: 252-259.
67. Cao D, Liu W, Wei X, Xu F, Cui L and Cao Y. 2006. *In vitro* tendon engineering with avian tenocytes and polyglycolic acids: a preliminary report. *Tissue Eng* **12(5)**: 1369-1377.
68. Caruso AB and Dunn MG. 2005. Changes in mechanical properties and cellularity during long-term culture of collagen fiber ACL reconstruction scaffolds. *J Biomed Mater Res A* **73(4)**: 388-397.
69. Lee CH, Shin HJ, Cho IH, Kang Y-M, Kim IA, Park K-D and Shin J-W. 2005. Nanofiber alignment and direction of mechanical strain affect the ECM production of human ACL fibroblast. *Biomaterials* **26(11)**: 1261-1270.
70. Maldonado BA and Oegema TRJ. 1992. Initial characterization of the metabolism of intervertebral disc cells encapsulated in microspheres. *J Orthop Res* **10(5)**: 677-690.
71. Chiba K, Andersson GBJ, Masuda K, Momohara S, Williams JM and Thonar EJ-MA. 1998. A new culture system to study the metabolism of the intervertebral disc *in vitro*. *Spine* **23(17)**: 1821-1827.
72. Gruber HE, Fisher Jr. EC, Desai B, Stasky AA, Hoelscher G and Hanley Jr. EN. 1997. Human intervertebral disc cells from the annulus: three-dimensional culture in agarose or alginate and responsiveness to TGF- β_1 . *Exp Cell Res* **235(1)**: 13-21.
73. Thonar E, An H and Masuda K. 2002. Compartmentalization of the matrix formed by nucleus pulposus and annulus fibrosus cells in alginate gel. *Biochem Soc Trans* **30(6)**: 874-888.

74. Hutton WC, Elmer WA, Bryce LM, Kozłowska EE, Boden SD and Kozłowski M. 2001. Do the intervertebral disc cells respond to different levels of hydrostatic pressure? *Clin Biomech* **16(9)**: 728-734.
75. Alini M, Roughley PJ, Antoniou J, Stoll T and Aebi M. 2002. A biological approach to treating disc degeneration: not for today, but maybe for tomorrow. *Eur Spine J* **11(Suppl 2)**: S215-S220.
76. Roughley P, Hoemann C, DesRosiers E, Mwale F, Antoniou J and Alini M. 2006. The potential of chitosan-based gels containing intervertebral disc cells for nucleus pulposus supplementation. *Biomaterials* **27(3)**: 388-396.
77. Cheng Y-H, Lin F-H and Yang KC. 2009. Thermosensitive chitosan-gelatin-glycerol phosphate hydrogels as a cell carrier for nucleus pulposus regeneration: an *in-vitro* study. *Tissue Eng Part A* doi:10.1089/ten.TEA.2009.0229.
78. Nesti LJ, Li W-J, Shanti RM, Jiang YJ, Jackson W, Freedman BA, Kuklo TR, Giuliani JR and Tuan RS. 2008. Intervertebral disc tissue engineering using a novel hyaluronic acid-nanofibrous scaffold (HANFS) amalgam. *Tissue Eng Part A* **14(9)**: 1527-1537.
79. Cloyd JM, Malhotra NR, Weng L, Chen W, Mauck RL and Elliott DM. 2007. Material properties in unconfined compression of human nucleus pulposus, injectable hyaluronic acid-based hydrogels and tissue engineering scaffolds. *Eur Spine J* **16(11)**: 1892-1898.
80. Crevensten G, Walsh AJL, Ananthakrishnan D, Page P, Wahba GM, Lotz JC and Berven S. 2004. Intervertebral disc cell therapy for regeneration: mesenchymal stem cell implantation in rat intervertebral discs. *Ann Biomed Eng* **32(3)**: 430-434.

81. Bryant SJ, Durand KL and Anseth KS. 2003. Manipulations in hydrogel chemistry control photoencapsulated chondrocyte behavior and their extracellular matrix production. *J Biomed Mater Res A* **67(4)**: 1430-1436.
82. Yang L, Kandel RA, Chang G and Santerre JP. 2008. Polar surface chemistry of nanofibrous polyurethane scaffold affects annulus fibrosus cell attachment and early matrix accumulation. *J Biomed Mater Res A* doi: 10.1002/jbm.a.32331.
83. Khor E and Lim LY. 2003. Implantable applications of chitin and chitosan. *Biomaterials* **24(13)**: 2339-2349.
84. Di Martino A, Sittinger M and Risbud MV. 2005. Chitosan: a versatile biopolymer for orthopaedic tissue-engineering. *Biomaterials* **26(30)**: 5983-5990.
85. Chenite A, Chaput C, Wang D, Combes C, Buschmann MD, Hoemann CD, Leroux JC, Atkinson BL, Binette F and Selmani A. 2000. Novel injectable neutral solutions of chitosan form biodegradable gels *in situ*. *Biomaterials* **21(21)**: 2155-2161.
86. Elisseff JH, Anseth K, Sims D, McIntosh W, Randolph M and Langer R. 1999. Transdermal photopolymerization for minimally invasive implantation. *Proc Natl Acad Sci USA* **96(6)**: 3104–3107.
87. Nguyen KT and West JL. 2002. Photopolymerizable hydrogels for tissue engineering applications. *Biomaterials* **23(22)**: 4307-4314.
88. Elisseff J, Anseth K, Sims D, McIntosh W, Randolph M, Yaremchuk M and Langer R. 1999. Transdermal photopolymerization of poly(ethylene oxide)-based injectable hydrogels for tissue-engineered cartilage. *Plast Reconstr Surg* **104(4)**: 1014-1022.

89. Smeds KA, Pfister-Serres A, Miki D, Dastgheib K, Inoue M, Hatchell DL and Grinstaff MW. 2001. Photocrosslinkable polysaccharides for *in situ* hydrogel formation. *J Biomed Mater Res* **54(1)**: 115-121.
90. Burdick JA, Chung C, Jia X, Randolph MA and Langer R. 2005. Controlled degradation and mechanical behavior of photopolymerized hyaluronic acid networks. *Biomacromolecules* **6(1)**: 386 -391.
91. Nettles DL, Vail TP, Morgan MT, Grinstaff MW and Setton LA. 2004. Photocrosslinkable hyaluronan as a scaffold for articular cartilage repair. *Ann Biomed Eng* **32(3)**: 391-397.
92. Chung C, Mesa J, Miller GJ, Randolph MA, Gill TJ and Burdick JA. 2006. Effects of auricular chondrocyte expansion on neocartilage formation in photocrosslinked hyaluronic acid networks. *Tissue Eng* **12(9)**: 2665-2673.
93. Chung C, Mesa J, Randolph MA, Yaremchuk M and Burdick JA. 2006. Influence of gel properties on neocartilage formation by auricular chondrocytes photoencapsulated in hyaluronic acid networks. *J Biomed Mater Res A* **77(3)**: 518-525.
94. Orive G, Ponce S, Hernández RM, Gascón AR, Igartua M and Pedraz JL. 2002. Biocompatibility of microcapsules for cell immobilization elaborated with different type of alginates. *Biomaterials* **23(18)**: 3825-3831.
95. Liu Y, Shu XZ and Prestwich GD. 2006. Osteochondral defect repair with autologous bone marrow-derived mesenchymal stem cells in an injectable, *in situ*, cross-linked synthetic extracellular matrix. *Tissue Eng* **12(12)**: 3405-3416.

96. Li Q, Williams CG, Sun DDN, Wang J, Leong K and Elisseeff JH. 2004. Photocrosslinkable polysaccharides based on chondroitin sulfate. *J Bio Mat Res A* **68(1)**: 28-33.
97. Li L, Thangamathesvaran PM, Yue CY, Tam KC, Hu X and Lam YC. 2001. Gel network structure of methylcellulose in water. *Langmuir* **17**: 8062-8068.
98. Sarkar N and Walker LC. 1995. Hydration-dehydration properties of methylcellulose and hydroxypropylmethylcellulose. *Carbohydr Polymers* **27(3)**: 177-185.
99. Miyamoto T, Takahashi S, Ito H, Inagaki H and Noishiki Y. 1989. Tissue biocompatibility of cellulose and its derivatives. *J Biomed Mater Res* **23(1)**: 125-133.
100. Stalling SS, Akintoye SO and Nicoll SB. 2009. Development of photocrosslinked methylcellulose hydrogels for soft tissue reconstruction. *Acta Biomater* **5(6)**: 1911-1918.
101. Falcone SJ, Doerfler AM and Berg RA. 2007. Novel synthetic dermal fillers based on sodium carboxymethylcellulose: comparison with crosslinked hyaluronic acid-based dermal fillers. *Dermatol Surg* **33(Suppl 2)**: S136-S143.
102. Ogushi Y, Sakai S and Kawakami K. 2007. Synthesis of enzymatically-gellable carboxymethylcellulose for biomedical applications. *J Biosci Bioeng* **104(1)**: 30-33.
103. Sakai S, Ogushi Y and Kawakami K. 2009. Enzymatically crosslinked carboxymethylcellulose-tyramine conjugate hydrogel: cellular adhesiveness and feasibility for cell sheet technology. *Acta Biomater* **5(2)**: 554-559.

104. Pal K, Banthia AK and Majumdar DK. 2006. Development of carboxymethyl cellulose acrylate for various biomedical applications. *Biomed Mater* **1(2)**: 85-91.
105. Leone G, Fini M, Torricelli P, Giardino R and Barbucci R. 2008. An amidated carboxymethylcellulose hydrogel for cartilage regeneration. *J Mater Sci Mater Med* **19(8)**: 2873-2880.
106. Reddi AH. 2001. Bone morphogenetic proteins: from basic science to clinical applications. *J Bone Joint Surg Am* **83(Suppl 1)**: S1-S6.
107. Evans C. 2006. Potential biologic therapies for the intervertebral disc. *J Bone Joint Surg Am* **88(Suppl 2)**: 95-98.
108. Osada R, Ohshima H, Ishihara H, Yudoh K, Sakai K, Matsui H and Tsuji H. 1996. Autocrine/paracrine mechanism of insulin-like growth factor-1 secretion, and the effect of insulin-like growth factor-1 on proteoglycan synthesis in bovine intervertebral discs. *J Orthop Res* **14(5)**: 690-699.
109. Tolonen J, Grönblad M, Virri J, Seitsalo S, Rytömaa T and Karaharju E. 1995. Basic fibroblast growth factor immunoreactivity in blood vessels and cells of disc herniations. *Spine* **20(3)**: 271-276.
110. Tolonen J, Grönblad M, Virri J, Seitsalo S, Rytömaa T and Karaharju EO. 1997. Platelet-derived growth factor and vascular endothelial growth factor expression in disc herniation tissue: and immunohistochemical study. *Eur Spine J* **6(1)**: 63-69.
111. Konttinen YT, Kempainen P, Li TF, Waris E, Pihlajamäki H, Sorsa T, Takagi M, Santavirta S, Schultz GS and Humphreys-Beher MG. 1999. Transforming and

- epidermal growth factors in degenerated intervertebral discs. *J Bone Joint Surg Br* **81(6)**: 1058-1063.
112. Takae R, Matsunaga S, Origuchi N, Yamamoto T, Morimoto N, Suzuki S and Sakou T. 1999. Immunolocalization of bone morphogenetic protein and its receptors in degeneration of intervertebral disc. *Spine* **24(14)**: 1397-1401.
113. Nakase T, Ariga K, Miyamoto S, Okuda S, Tomita T, Iwasaki M, Yonenobu K and Yoshikawa H. 2001. Distribution of genes for bone morphogenetic protein-4, -6, growth differentiation factor-5, and bone morphogenetic protein receptors in the process of experimental spondylosis in mice. *J Neurosurg* **94(1 Suppl)**: 68-75.
114. Masuda K, Oegema Jr TR and An HS. 2004. Growth factors and treatment of intervertebral disc degeneration. *Spine* **29(23)**: 2757-2769.
115. Thompson JP, Oegema Jr TR and Bradford DS. 1991. Stimulation of mature canine intervertebral disc by growth factors. *Spine* **16(3)**: 253-260.
116. Risbud MV, Izzo MW, Adams CS, Arnold WW, Hillibrand AS, Vresilovic EJ, Vaccaro AR, Albert TJ and Shapiro IM. 2003. An organ culture system for the study of the nucleus pulposus: description of the system and evaluation of the cells. *Spine* **28(24)**: 2652-2658.
117. Risbud MV, Di Martino A, Guttapalli A, Seghatoleslami R, Denaro V, Vaccaro AR, Albert TJ and Shapiro IM. 2006. Toward an optimum system for intervertebral disc organ culture: TGF-beta 3 enhances nucleus pulposus and annulus fibrosus survival and function through modulation of TGF-beta-R expression and ERK signaling. *Spine* **31(8)**: 884-890.

118. Yoon S, Li J, Kim KS, Park JS and Hutton W. 2003. BMP-2 stimulates disc cell matrix production and other BMPs. *Spine J* **3(5)**: 144-145.
119. Gruber HE, Norton HJ and Hanley Jr EN. 2000. Anti-apoptotic effects of IGF-1 and PDGF on human intervertebral disc cells *in vitro*. *Spine* **25(17)**: 2153-2157.
120. Gilbertson L, Ahn S-H, Teng P-N, Studer RK, Niyibizi C and Kang JD. 2008. The effects of recombinant human bone morphogenetic protein-2, recombinant human bone morphogenetic protein-12, and adenoviral bone morphogenetic protein-12 on matrix synthesis in human annulus fibrosis and nucleus pulposus cells. *Spine J* **8(3)**: 449-456.
121. Lee JY, Hall R, Pelinkovic D, Cassinelli E, Usas A, Gilbertson L, Huard J and Kang J. 2001. New use of a three-dimensional pellet culture system for human intervertebral disc cells: initial characterization and potential use for tissue engineering. *Spine* **26(21)**: 2316-2322.
122. Holm S and Nachemson A. 1983. Variations in the nutrition of the canine intervertebral disc induced by motion. *Spine* **8(8)**: 866-874.
123. Handa T, Ishihara H, Ohshima H, Osada R, Tsuji H and Obata Ki. 1997. Effects of hydrostatic pressure on matrix synthesis and matrix metalloproteinase production in the human lumbar intervertebral disc. *Spine* **22(10)**: 1085-1091.
124. Ishihara H, McNally DS, Urban JPG and Hall AC. 1996. Effects of hydrostatic pressure on matrix synthesis in different regions of the intervertebral disk. *J Appl Physiol* **80**: 839-846.

125. Ohshima H, Urban JP and Bergel DH. 1995. Effect of static load on matrix synthesis rates in the intervertebral disc measured *in vitro* by a new perfusion technique. *J Orthop Res* **13(1)**: 22-29.
126. Walsh AJL and Lotz JC. 2004. Biological response of the intervertebral disc to dynamic loading. *J Biomech* **37(3)**: 329-337.
127. MacLean JJ, Lee CR, Alini M and Iatridis JC. 2004. Anabolic and catabolic mRNA levels of the intervertebral disc vary with the magnitude and frequency of *in vivo* dynamic compression. *J Orthop Res* **22(6)**: 1193-1200.
128. Korecki CL, Kuo CK, Tuan RS and Iatridis JC. 2009. Intervertebral disc cell response to dynamic compression is age and frequency dependent. *J Orthop Res* **27(6)**: 800-806.
129. Iatridis JC, MacLean JJ and Ryan DA. 2005. Mechanical damage to the intervertebral disc annulus fibrosus subjected to tensile loading. *J Biomech* **38(3)**: 557-565.

Chapter 2: Characterization of Novel Photocrosslinked Carboxymethylcellulose Hydrogels for Encapsulation of Nucleus Pulposus Cells

2.1. Introduction

The intervertebral disc (IVD) is a heterogeneous tissue that permits motion and flexibility, supports and distributes loads, and dissipates energy in the spine¹. The IVD is comprised of the collagenous, lamellar annulus fibrosus, which maintains disc shape and allows the spine to resist tensile loads², and the gelatinous nucleus pulposus (NP). The NP is a hydrated tissue, characterized by high proteoglycan (i.e., aggrecan) and type II collagen content¹. This region functions to resist compressive loads through the generation of a hydrostatic swelling pressure.

Degeneration of the IVD is strongly associated with back pain, a significant healthcare problem, afflicting approximately 80% of Americans during their lifetime³ and costing over \$80 billion in annual related medical expenses⁴. Disc degeneration often results from traumatic injury or occurs naturally with aging. This pathological condition is commonly attributed to increased degradation of aggrecan molecules, giving rise to significant alterations in disc biochemical composition and a loss of hydration⁵. The NP is thus rendered more fibrous in structure and content, which reduces nutrient diffusion and waste removal⁶. The resulting increase in lactate concentration within the tissue lowers the local pH⁷. The increased acidity compromises cell metabolism and may

precipitate cell death, as up to 50% of cells in adult discs have been reported as necrotic⁸. Disc degeneration may be asymptomatic, or the change in extracellular matrix (ECM) content may contribute to increased disc stiffness and low back pain from the altered distribution of loads⁹. Current clinical treatments focus on alleviation of pain rather than restoring the structure and function of the disc. Tissue engineering strategies may provide a biologic alternative capable of restoring both the structure and mechanical function of the IVD.

Biomaterial scaffolds used in tissue engineering applications often attempt to mimic the native structure of the respective tissue. The highly hydrated nature of the NP is similar to that of hydrogel networks, making such materials prime candidates to serve as scaffolds for NP regeneration. Hydrogels are hydrophilic, crosslinked polymers which absorb large volumes of water and swell without dissolution of the polymer¹⁰. Nucleus pulposus cells are routinely cultured by encapsulation in hydrogels made from alginate, a naturally-derived polysaccharide originating from brown algae¹¹⁻¹⁵. Alginate cell encapsulation promotes a rounded, chondrocyte-like morphology in contrast to the elongated, fibroblast-like morphology seen in monolayer cultures. The predominant method of alginate gelation is through ionic crosslinking, achieved via diffusion of divalent cations to carboxylic acid moieties on the polymer, resulting in a crosslinked network. Although this initially produces stable gels, mechanical integrity has been found to decrease over time, possibly due to a loss of ions through diffusion¹¹ or depletion by the encapsulated cells.

Photopolymerization has been widely used *in situ* to covalently crosslink polymer networks in dental applications^{10, 16}. This method employs biocompatible, light-sensitive

photoinitiators that absorb light, creating free radicals that can initiate polymerization to covalently crosslink functional groups along the polymer backbone¹⁰. Elisseff et al. developed a photopolymerization method to successfully encapsulate chondrocytes in poly(ethylene oxide)-based (PEO) hydrogels for tissue engineering applications¹⁶. This technique was modified by Bryant et al. to incorporate degradable lactic acid units into poly(ethylene glycol)-based (PEG) hydrogels to enhance the spatial distribution of ECM components in these otherwise inert polymers¹⁷. Photopolymerization has also been employed to create polysaccharide-based hydrogels using alginate and hyaluronic acid macromers modified with functional methacrylate groups¹⁸. In an extension of this work, methacrylated hyaluronic acid was used to engineer hydrogels for cartilage cell encapsulation^{19, 20}. These constructs were shown to allow for functional matrix production following *in vivo* implantation in a subcutaneous murine pouch model²¹. Although hyaluronic acid-based hydrogels have shown promising results, these biomaterials are often derived from an animal source, which presents the risk of batch-to-batch variations and the need for additional purification steps to reduce the possibility of stimulating an immune response upon implantation. Nevertheless, the results observed for hyaluronic acid-based hydrogels indicate the potential of similar polysaccharide-based systems for use in orthopaedic tissue engineering applications.

One such candidate polysaccharide is carboxymethylcellulose (CMC), a water-soluble derivative of cellulose, the primary structural component of plant cell walls. CMC is a biocompatible, low-cost, FDA-approved material that is commercially available in high purity forms, making this polymer a highly attractive option for

biomedical applications²². However, CMC-based materials have not been used previously for IVD repair.

Therefore, the objective of this study was to create photocrosslinked CMC hydrogels with tunable material properties for NP cell encapsulation. We hypothesized that CMC macromers could be synthesized with methacrylate groups that would allow for photopolymerization. Moreover, an increase in CMC molecular weight and weight percent would be expected to give rise to an inverse relationship between the equilibrium Young's modulus and the swelling ratio of the resulting hydrogels.

2.2. Materials and Methods

2.2.1. Macromer Synthesis

Methacrylated carboxymethylcellulose (Me-CMC) was synthesized through esterification of hydroxyl groups based on previously described protocols^{18, 19} (Figure 2.1). Briefly, 1 gram of 90 kDa or 250 kDa CMC (Sigma, St. Louis, MO) was dissolved in 100 mL of RNase/DNase-free water at 50°C and stirred for 30 minutes. The mixture was then stirred at room temperature for one hour and finally, placed on an orbital shaker for 48 hours at 4°C to yield a 1 wt % solution. Methacrylic anhydride (Sigma) at 20-fold excess was reacted with 1% CMC over 24 hours at 4°C with 12 periodic adjustments to pH 8.0 using 3N NaOH to modify hydroxyl groups of the polymer with functional methacrylate groups. The modified CMC solution was purified via dialysis for 96 hours against RNase/DNase-free water (Spectra/Por1, MW 5-8 kDa, Rancho Dominguez, CA) to remove excess, unreacted methacrylic anhydride. Purified Me-CMC was recovered by lyophilization and stored at -20°C. The degree of substitution was confirmed using ¹H-

NMR (360 MHz, DMX360, Bruker, Madison, WI) following acid hydrolysis of purified Me-CMC. Briefly, a 20 mg sample of lyophilized Me-CMC was dissolved in 20 mL of RNase/DNase-free water and hydrolyzed at a pH of 2.0 at 80°C for 2.3 hours. The pH of the hydrolyzed solution was readjusted to 7.0, recovered via lyophilization, and resuspended in deuterium oxide. Molar percent of methacrylation was determined by the relative integrations of methacrylate proton peaks (methylene, $\delta = 6.2$ ppm and 5.8 ppm and the methyl peak, $\delta = 2.0$ ppm) to carbohydrate protons.

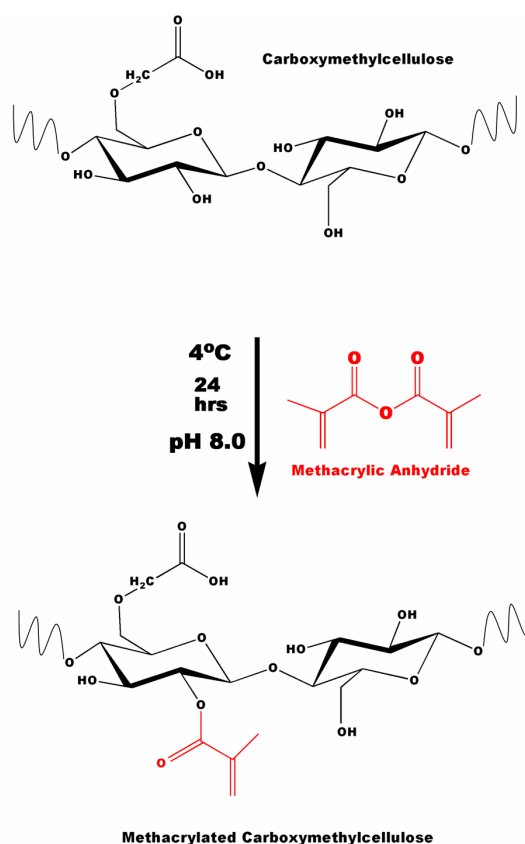


Figure 2.1. Schematic of the synthesis of methacrylated carboxymethylcellulose.

2.2.2. Cell Isolation

All cell culture supplies, including media, antibiotics, and buffering agents, were purchased from Invitrogen (Carlsbad, CA) unless otherwise noted. Discs C2-C4 were isolated from bovine caudal IVDs obtained from a local abattoir, and the NP was separated through gross visual inspection based on previous protocols^{23, 24}. Tissue was maintained in Dulbecco's Modified Eagle Medium (DMEM) supplemented with 20% fetal bovine serum (FBS) (Hyclone, Logan, UT), 0.075% sodium bicarbonate, 100 U/mL penicillin, 100 µg/mL streptomycin, and 0.25 µg/mL Fungizone reagent at 37°C, 5% CO₂ for two days prior to digestion to ensure no contamination occurred during harvesting. A single serum lot was used for all experiments to reduce potential variability in the cellular response.

Tissue was diced and NP cells were released by collagenase (Type IV, Sigma) digestion at an activity of 7000 U collagenase per gram of tissue. Following incubation in collagenase, undigested tissue was removed using a 40 µm mesh filter. Cells from multiple levels (C2-C4) were pooled and rinsed in sterile Dulbecco's Phosphate Buffered Saline (DPBS). These primary cells were plated onto tissue culture flasks, designated as passage 0, and maintained in DMEM with 10% FBS, 0.075% sodium bicarbonate, 100 U/mL penicillin, and 100 µg/mL streptomycin (growth medium). Cells were subcultured twice to obtain the necessary number of cells, and passage 2 cells were used in all experiments²³.

2.2.3. Cell Encapsulation in Photocrosslinked Hydrogels

Cell-encapsulated photocrosslinked constructs were prepared at various weight percents. Prior to dissolution, lyophilized Me-CMC was sterilized by a 30-minute

exposure to germicidal UV light. The sterilized product was then dissolved in filter-sterilized 0.05 wt% photoinitiator, 2-hydroxy-1-[4-(2-hydroxyethoxy)phenyl]-2-methyl-1-propanone (Irgacure 2959, I2959, Ciba Specialty Chemicals, Basel, Switzerland), in sterile DPBS at 4°C to various weight percents (90 kDa Me-CMC: 3.2, 4.2, and 5.2%; 250 kDa: 1.2, 2.2, and 3.2%). Passage 2 NP cells were resuspended in a small volume of 0.05% photoinitiator and then homogeneously mixed with dissolved Me-CMC at 30×10^6 cells/mL. The seeding density was selected based on previous studies using cell-seeded constructs for engineering of cartilaginous tissues²⁵⁻²⁹. Solutions were cast at final concentrations of 3, 4, and 5% (90 kDa Me-CMC) and 1, 2, and 3% (250 kDa Me-CMC) in a custom-made glass casting device. The mixtures were exposed to long-wave UV light (EIKO, Shawnee, KS, peak 368 nm, 1.2W) for 10 minutes to produce covalently crosslinked hydrogel disks of 8-mm diameter x 2-mm thickness. Each hydrogel was incubated in 3 mL of growth medium at 37°C, 5% CO₂. At day 1, the medium was fully exchanged with L-ascorbic acid supplemented medium (growth medium with 50 µg/mL L-ascorbic acid), which was used for the remainder of the study and replaced every 2-3 days. Initial viability studies (described below) were performed using gels cast at 5-mm diameter x 2-mm thickness, incubated in 1.5 mL of L-ascorbic acid supplemented growth medium.

2.2.4. Cell Viability and Dynamic Mechanical Testing

Preliminary screening studies examined the effects of weight percent and molecular weight on cell viability and the elastic mechanical properties of 3, 4, and 5% 90 kDa Me-CMC and 1, 2, and 3% 250 kDa Me-CMC. Cell viability was assessed at days 1 and 7 using the MTT (3-(4, 5-dimethylthiazolyl-2)-2, 5-diphenyltetrazolium

bromide) proliferation assay kit (ATCC, Manassas, VA). Photocrosslinked Me-CMC hydrogels (n=4) were incubated in 1 mL of growth medium supplemented with 100 μ L of yellow tetrazolium MTT for 4 hours at 37°C, 5% CO₂, shielded from light. Hydrogels were then homogenized and formazan crystals were extracted using the MTT detergent solution (MTT cell proliferation assay kit, ATCC), incubating for an additional 4 hours at room temperature, shielded from light. Total absorbance of the solubilized product was quantified at 570 nm using a Bio-Tek Synergy-HT microplate reader (Winooski, VA). MTT absorbance values were compared between samples and to cell-free control gels to quantify relative viability. Day 7 measurements were also evaluated against day 1 values to determine loss of viability over time.

Cell viability of 2% 250 kDa Me-CMC constructs was visually assessed at day 0 (one hour after casting) and day 1 using the Live/Dead kit (Invitrogen). Samples were rinsed in DPBS and then incubated in Live/Dead solution (1 mM calcein AM, 1 mM ethidium homodimer-2) for 45 minutes. Images were captured using a Zeiss Axiovert 200 microscope with fluorescent capabilities at excitation/emission wavelengths of 494/517 nm (calcein) and 528/617 nm (ethidium homodimer-2/DNA complex). Live and dead cells were counted using Image J software (National Institutes of Health).

At day 7, a Dynamic Mechanical Analyzer (DMA) 8000 (PerkinElmer, Inc., Waltham, MA) testing apparatus was used to determine the elastic modulus of Me-CMC hydrogels at the weight percents described above. Samples (n=5) were rinsed in DPBS and loaded into the DMA. Unconfined compression testing was performed at 25°C at a strain rate of 10%/minute. The modulus was determined from the linear region of the stress versus strain curves at strains between 5% and 20%.

2.2.5. Swelling Ratio

Following the initial studies examining cell viability and elastic mechanical properties, 4% 90 kDa, 2% 250 kDa, and 3% 250 kDa Me-CMC hydrogels were chosen for further characterization. The equilibrium weight swelling ratio, Q_w , was determined for these formulations at days 1, 7, and 14 for cell-laden and cell-free control samples (n=4). Constructs were weighed to determine the wet weight (W_s), lyophilized, and then weighed again to determine the dry weight (W_d). Q_w was calculated using the following equation:

$$Q_w = W_s/W_d$$

2.2.6. Characterization of Equilibrium Mechanical Properties

Based on the early screening studies, unconfined compression testing was conducted on 4% 90 kDa, 2% 250 kDa, and 3% 250 kDa Me-CMC cell-laden and cell-free control samples (n=5) at days 1, 7, and 14 to measure the equilibrium Young's modulus (E_y). The mechanical testing device is based on a similar setup described by Soltz and Ateshian³⁰. The device consists of a computer-controlled stepper motor (Oriental Motor Corp., Model 18515, Stratford, CT) that prescribed a displacement on the specimen using a steel indenter with glass platen attachment. A data card and LabVIEW software (National Instruments, Austin, TX) were used for controlling the stepper motor and data acquisition. Displacement was measured using a linear variable differential transformer (Schaeffler, Model PR812, Hampton, VA), and the load applied was measured using a 250 g load cell (Sensotec, Model 31, Columbus, OH). Samples were compressed between two impermeable glass platens in a DPBS bath. The unconfined compression testing protocol was comprised of a creep test followed by a multi-ramp stress-relaxation

test. The creep test consisted of a 1 g tare load applied at a 10 $\mu\text{m/s}$ ramp velocity for 1800 seconds until equilibrium was reached (equilibrium criteria: $<10 \mu\text{m}$ change in 10 minutes). The multi-ramp stress-relaxation test consisted of three 5% strain ramps at a 10 $\mu\text{m/s}$ ramp velocity, each followed by a 2000 second relaxation period (equilibrium criteria: $<0.5 \text{ g}$ change in 10 minutes). Equilibrium stress was calculated at the end of each ramp using surface area measurements and plotted against the applied strain. An average equilibrium Young's modulus was calculated from the stress versus strain curves and reported for each sample.

2.2.7. Histology and Immunohistochemistry

Cell-laden hydrogels were fixed for 45 minutes in acid formalin at room temperature and processed for paraffin embedding after graded serial ethanol dehydration. Samples were sectioned at a thickness of 8 μm , and hematoxylin and eosin staining was conducted to visualize cellular distribution throughout the hydrogel. Immunohistochemical analyses were performed to assess extracellular matrix accumulation of chondroitin sulfate proteoglycan (CSPG). Samples were treated with 0.5N acetic acid for two hours at 4°C. Non-specific binding was blocked using 10% goat serum (Invitrogen) in DPBS. A monoclonal antibody to CSPG (1:100 dilution in blocking solution) (Sigma) was used, followed by incubation in biotinylated goat/anti-mouse IgM secondary antibody (1:50 dilution in blocking solution) (Vector Labs, Burlingame, CA). A peroxidase-based detection system (Vectastain Elite ABC, Vector Labs) and 3,3' diaminobenzidine (Vector Labs) as the chromagen were used according to the manufacturer's protocols to detect ECM localization. Non-immune controls were processed in blocking solution without primary antibody. Samples were viewed with a

Zeiss Axioskop 40 optical microscope and images were captured using AxioVision software.

2.2.8. *Statistical Analysis*

A one-way analysis of variance (ANOVA) was performed on MTT viability measurements to determine the effect of weight percent and the effect of time. A two-way ANOVA was conducted on elastic modulus data to determine the effects of weight percent and cells (cell-laden vs. cell-free control constructs). A three-way ANOVA was conducted on swelling and E_y data for 4% 90 kDa, 2% 250 kDa, and 3% 250 kDa Me-CMC constructs to determine the effects of time, cells, and starting material. A two-way ANOVA was performed on equilibrium Young's modulus measurements for 3% 250 kDa Me-CMC constructs to examine the effects of time and cells. A Tukey's post-hoc test was performed on all ANOVA calculations to detect significant differences between groups. All results are presented as mean \pm standard deviation with statistical significance defined as $p < 0.05$. Statistical analyses were completed using JMP software (SAS Institute, Cary, NC).

2.3. Results

CMC was successfully modified (90 kDa CMC: 3.29% methacrylation; 250 kDa CMC: 2.87% methacrylation), as verified by $^1\text{H-NMR}$ (Figure 2.2). Initial studies examined the effects of weight percent and molecular weight on cell viability and elastic mechanical properties. Weight percent ranges were selected based on ease of handling (a function of pre-crosslinked polymer solution viscosity) and stable hydrogel formation.

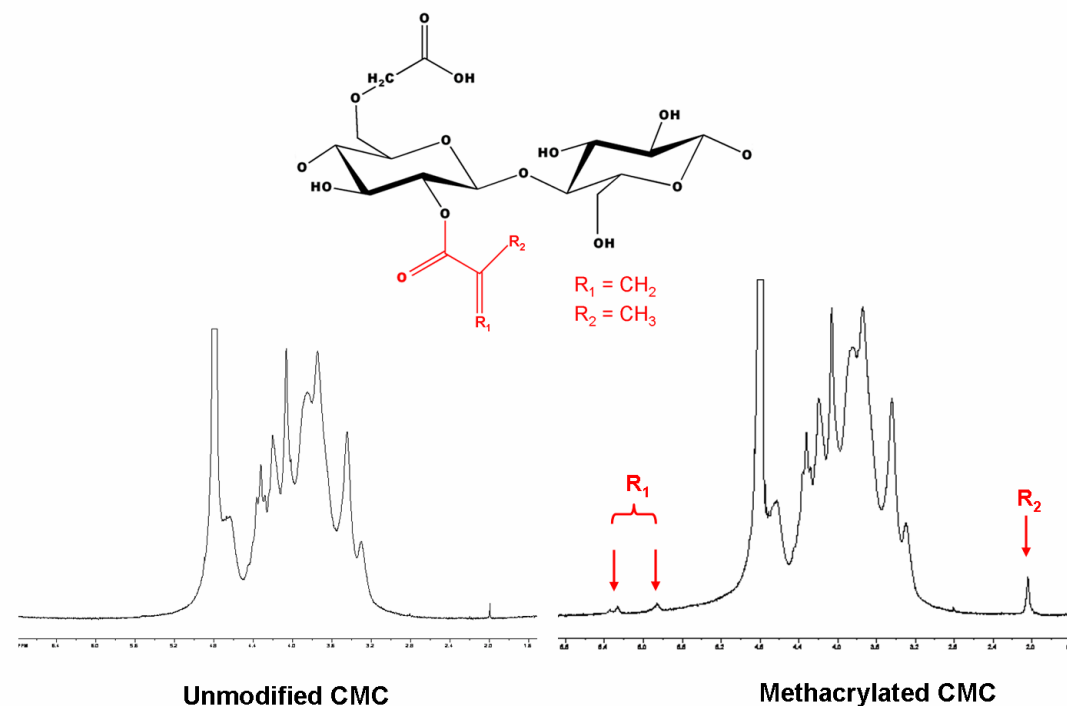


Figure 2.2. Representative $^1\text{H-NMR}$ spectra of unmodified and methacrylated carboxymethylcellulose, with methacrylate peaks indicated by arrows.

The formulations selected for initial analysis were 3, 4, and 5% 90 kDa CMC and 1, 2, and 3% 250 kDa CMC. Bovine NP cells were encapsulated in these gel formulations and samples were isolated at days 1 and 7 to assess cell viability using the MTT assay. Overall, evenly distributed, viable cells were observed for all groups at both time points (Figure 2.3 B-G). There were no significant differences in viability based on weight percent for 90 kDa CMC constructs at either time point (Figure 2.3A). Day 1 viability in 3% 250 kDa CMC hydrogels was significantly lower than 1% 250 kDa CMC samples; however, this was not significant in comparison to 2% 250 kDa CMC constructs. By day 7, viability in 2% 250 kDa CMC samples was significantly higher than that for 1 and 3% counterparts (Figure 2.3A). There was no significant loss in viability over time for any group except 1% 250 kDa CMC constructs, as measured using the MTT assay (Figure

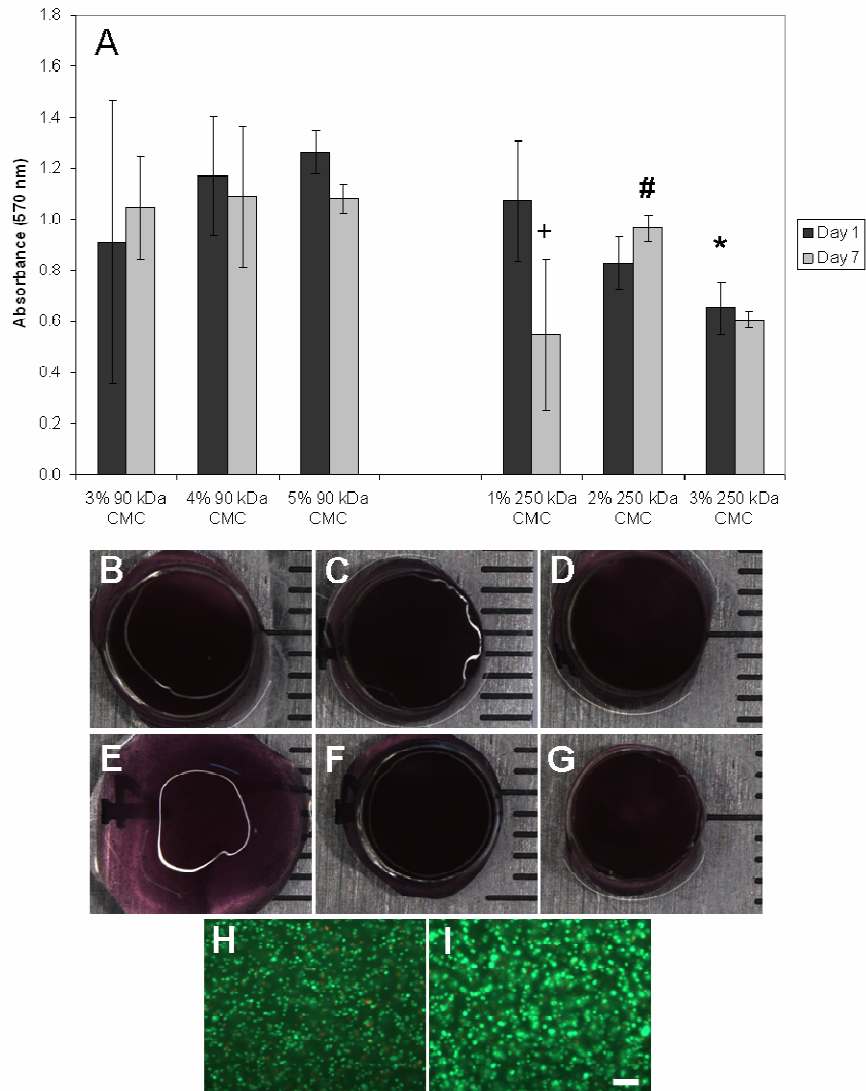


Figure 2.3. Mitochondrial activity measurements (MTT) at days 1 and 7 for (A) photocrosslinked 90 kDa and 250 kDa CMC hydrogels (n=4) at various weight percents encapsulated with bovine nucleus pulposus cells at 30×10^6 cells/mL. Representative day 7 MTT stereomicrograph images of 3% 90kDa (B), 4% 90 kDa (C), 5% 90 kDa (D), 1% 250 kDa (E), 2% 250 kDa (F), and 3% 250 kDa (G) CMC cell-laden hydrogels (scale in mm). Live/Dead images of 2% 250 kDa CMC samples at days 0 (H) and 1 (I) with live cells stained green and dead cells shown in red (bar = 100 μ m). Significance set at $p < 0.05$. *: Significant vs. 1% 250 kDa CMC within time point. #: Significant vs. 1 and 3% 250 kDa CMC within time point. +: Significant effect of time within group.

2.3A). Stable disks were formed for all groups at both molecular weights, with the exception of 1% 250 kDa CMC, which was not able to retain structural integrity (Figure 2.3E).

Viability was also visually assessed early on at days 0 and 1 for 2% 250 kDa CMC constructs. A highly viable cell population (~83%, indicated in green) was observed on day 0 (one hour after casting) (Figure 2.3H) and at day 1 (~76%) (Figure 2.3I), with some dead cells present (red).

Elastic mechanical properties of cell-laden and cell-free control gels at these six formulations were also quantified at day 7. Although 3% 90 kDa CMC formed stable constructs, these samples were too weak to be mechanically tested and were excluded, as were the amorphous 1% 250 kDa CMC gels. Quantification of the elastic modulus determined no significant differences between cell-laden and cell-free hydrogels at day 7 in any group (Figure 2.4). There was a significant overall effect of weight percent, as samples at higher concentrations exhibited a higher modulus (4% vs. 5% 90 kDa CMC and 2% vs. 3% 250 kDa CMC). From these preliminary studies, 4% 90 kDa CMC and 2% 250 kDa CMC were selected for further characterization.

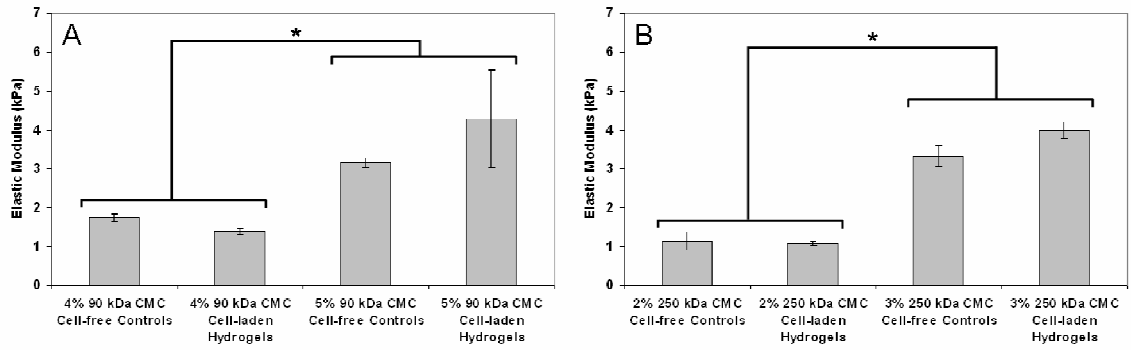


Figure 2.4. Elastic modulus of day 7 photocrosslinked 90 kDa (A) and 250 kDa (B) CMC hydrogels encapsulated with bovine nucleus pulposus cells at 30×10^6 cells/mL and corresponding cell-free control gels (n=5) at various weight percents. Significance set at $p < 0.05$. *: Significant effect of weight percent.

Cell-laden and cell-free hydrogels composed of 4% 90 kDa CMC and 2% 250 kDa CMC were cast and analyzed at days 1, 7, and 14 to determine the swelling ratio and the equilibrium Young's modulus. Overall, there were no significant differences in swelling between cell-laden and cell-free hydrogels at either molecular weight at any time point (Q_w : 46.45 ± 3.15 and 48.55 ± 2.91 for 90 kDa and 250 kDa CMC, respectively). In addition, there was no significant effect of molecular weight (90 kDa vs. 250 kDa) at any time point, nor was there a significant effect of time, as Q_w was stable over the 14-day study for all groups.

Unconfined compression testing of 4% 90 kDa CMC and 2% 250 kDa CMC constructs revealed a significant loss in mechanical properties over time for all groups (Figure 2.5). Cell-laden and cell-free control hydrogels at both 4% 90 kDa CMC and 2% 250 kDa CMC exhibited a significant decrease in E_y by day 14. Overall, there was no

significant effect of CMC molecular weight (90 kDa vs. 250 kDa) nor of cells (cell-laden samples vs. cell-free controls) for any group, except 4% 90 kDa CMC at day 1.

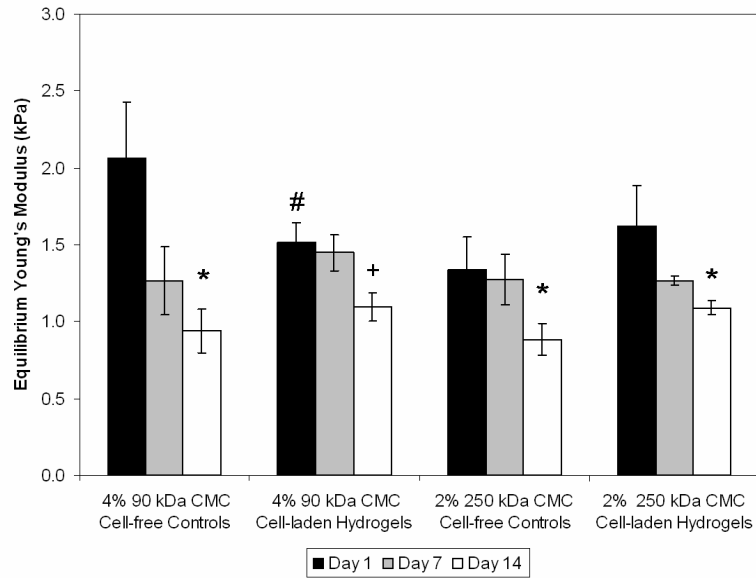


Figure 2.5. Equilibrium Young's modulus for 4% 90 kDa and 2% 250 kDa CMC cell-free control and cell-laden hydrogels (n=5) over 14 days of *in vitro* culture. Significance set at $p < 0.05$. *: Significant vs. day 1 within group. +: Significant vs. days 1 and 7 within group. #: Significant vs. corresponding cell-free control.

Based on the steady decrease in mechanical properties observed for both 4% 90 kDa CMC and 2% 250 kDa CMC constructs, a higher weight percent gel was chosen to provide a stiffer initial environment. Cell-laden and cell-free 3% 250 kDa CMC hydrogels were cast and again analyzed at days 1, 7, and 14 to determine the swelling ratio, mechanical properties, and ECM accumulation. In contrast to 2% 250 kDa CMC constructs, the presence of cells in 3% 250 kDa CMC gels resulted in a significantly lower degree of swelling than was observed for cell-free controls (Q_w : 40.14 ± 1.80 vs. 44.67 ± 2.27 , respectively). However, as for 2% 250 kDa CMC constructs, Q_w for 3%

250 kDa CMC samples was stable over the 14-day study, with no effect of time observed for either cell-laden or cell-free control gels. Overall, Q_w was significantly lower for 3% 250 kDa samples in comparison to both 4% 90 kDa and 2% 250 kDa CMC hydrogels (42.41 ± 3.06 vs. 46.45 ± 3.14 and 48.55 ± 2.91 , respectively).

3% 250 kDa CMC samples were tested in unconfined compression to determine the equilibrium Young's modulus. A significant temporal decrease in mechanical properties was again observed for cell-free control gels (Figure 2.6). In contrast, there was no significant effect of time observed for cell-laden constructs. By day 14, cell-free control gels were significantly weaker than their cell-laden counterparts. Overall, the average equilibrium Young's modulus for 3% 250 kDa CMC samples was significantly higher in comparison to both 4% 90 kDa and 2% 250 kDa CMC hydrogels (3.53 ± 0.87 kPa vs. 1.37 ± 0.44 kPa and 1.27 ± 0.35 kPa, respectively).

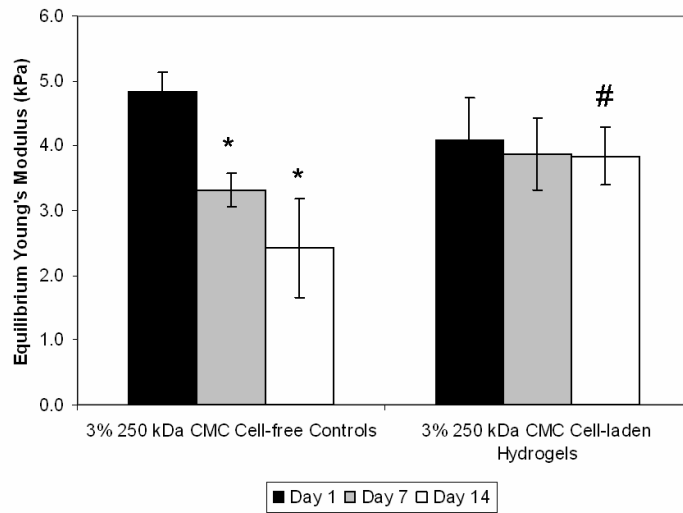


Figure 2.6. Equilibrium Young's modulus for 3% 250 kDa CMC cell-free control and cell-laden hydrogels (n=5) over 14 days of *in vitro* culture. Significance set at $p < 0.05$. *: Significant vs. day 1 within group. #: Significant vs. corresponding cell-free control.

Histological analyses conducted on 3% 250 kDa CMC constructs at day 14 confirmed a phenotypic rounded cellular morphology within the hydrogel, as determined by hematoxylin and eosin staining (Figure 2.7A). By day 14, cells were localized in limited lacunae at the center of the construct and well-developed, extensive lacunae at the scaffold periphery. Immunohistochemical staining verified pericellular deposition of CSPG throughout the construct, with more pronounced interterritorial staining present at the periphery (Figure 2.7B). Non-immune control samples exhibited no positive staining.

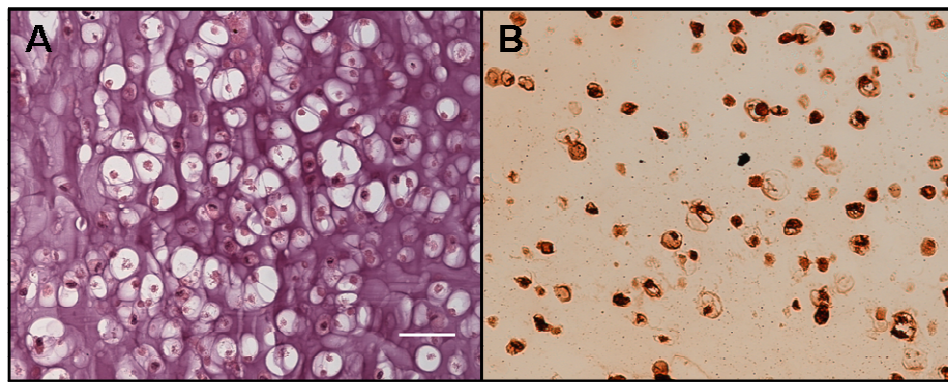


Figure 2.7. Hematoxylin and eosin staining (A) and chondroitin sulfate proteoglycan immunohistochemical staining (B) of cell-laden 3% 250 kDa CMC constructs at day 14. Bar = 50 μ m.

2.4. Discussion

In this study, CMC was successfully modified with methacrylate groups to produce photocrosslinked hydrogels with tunable properties. In addition, this is the first investigation to demonstrate successful encapsulation of NP cells in photocrosslinked CMC hydrogels, suggesting that these materials may serve as alternate scaffolds for IVD replacement therapies.

Alginate is the most widely used biomaterial in NP tissue engineering applications¹¹⁻¹⁵. However, the reversible nature of conventional ionic crosslinking techniques has led to investigation of photopolymerization methods. This approach has recently been applied to alginate to produce mechanically stable hydrogel constructs capable of supporting NP cell growth and viability³¹. Nevertheless, raw alginate has been shown to stimulate an immune response *in vivo* in mice and requires additional processing to remove impurities for biomedical applications³². Similar purification procedures are required for animal-derived products, such as hyaluronic acid, chitosan, and chondroitin sulfate, which have also been used to engineer cartilaginous tissues^{18-21, 33-36}.

CMC is a well-established derivative of cellulose, which is rendered water-soluble through the introduction of carboxymethyl groups along the polymer backbone. At physiological pH, the carboxylic acid of the carboxymethyl group is deprotonated, resulting in a negatively-charged polymer network, which is similar to that provided by the glycosaminoglycans in the ECM of cartilaginous tissues. CMC is commercially available in high-purity forms, making it an appealing low-cost alternative to other natural polysaccharides and inert polymers currently used in tissue engineering applications. Additionally, as a derivative of the plant-based polysaccharide, cellulose, CMC represents a renewable, environmentally-friendly biomaterial.

Recent work has examined the efficacy of CMC-based hydrogels for cell encapsulation^{22, 37-39}. These studies have successfully utilized various chemistries for CMC crosslinking, including phenol modification of CMC carboxylic acid (COOH) groups^{22, 37}, acrylation of CMC³⁸, amidation of CMC COOH groups³⁹, and electrostatic

interactions⁴⁰, highlighting the versatility of the CMC polymer. Cytotoxicity has been tested using multiple cell lines with positive results. However, some studies have examined CMC hydrogels in sheet or membrane form, which may not be ideal for orthopaedic applications. Additionally, modification of CMC COOH groups limits the availability of charged moieties, thereby reducing the swelling capability of the hydrogel and neutralizing the negatively-charged polymer network. Moreover, gels formed through electrostatic interactions may not be as stable as covalently crosslinked hydrogels – an important feature of an orthopaedic scaffold for load-bearing tissues.

Our early screening studies examined the effects of molecular weight and macromer concentration on cell viability and elastic modulus. Metabolic activity measurements using the MTT assay showed no significant decrease over time for any group except for the amorphous 1% 250 kDa CMC constructs. The lack of structural integrity in these samples resulted in a significant loss of material during transfer and may have contributed to the lower than expected activity/viability measurements. Although the MTT assay is routinely used to assess cell viability^{16, 31, 41-43}, this assay measures the activity of the mitochondrial enzyme, succinate dehydrogenase. Since the number of mitochondria can vary between cells, the MTT assay may not accurately reflect cell viability⁴⁴. Live/Dead fluorescent staining was used as a more direct evaluation of cell viability. Contrary to the MTT results, the staining demonstrated a noticeable loss of viability over time. However, decreased cell viability in such hydrogel systems is not surprising, as this trend has also been observed for bovine articular chondrocytes encapsulated in PEO hydrogels and bovine NP cells encapsulated in alginate, suggesting that additional environmental factors may influence cell growth in

photopolymerized hydrogels^{31, 41}. Although cell-interactive signals (i.e., growth factors, adhesive peptides) have been shown to play an important role in modulating cellular viability and function in engineered constructs^{45, 46}, the objective of this first study was to investigate cell-polymer interactions in these novel photocrosslinkable CMC hydrogels, excluding the influence of any exogenous factors.

Our initial screening study demonstrated the effects of CMC molecular weight (90 and 250 kDa) and macromer concentration on hydrogel properties. These studies underscore the influence of crosslinking density on hydrogel material properties. Crosslinking density is increased at higher macromer concentrations due to a greater number of methacrylate functional groups available for photoinitiated crosslinking. The theory of rubber elasticity predicts that an increase in crosslinking density gives rise to an increase in hydrogel stiffness and a concomitant decrease in swelling ratio⁴⁷. The significant increases in elastic modulus associated with increasing CMC molecular weight (as determined in our initial studies), combined with the marked differences in swelling ratio and equilibrium modulus of 2 versus 3% 250 kDa CMC are consistent with the theory and with our original hypothesis.

Based on the results from our initial screening, the swelling ratio was characterized in cell culture medium for three formulations of CMC: 4% 90 kDa CMC and 2 and 3% 250 kDa CMC. Q_w remained steady over time for all groups. Additional studies demonstrated similar results in physiological saline and simulated body fluid. A stable swelling ratio is important for potential IVD clinical applications as an intradiscal replacement material in order to prevent bulging and extrusion into the annulus fibrosus. Although Q_w remained unchanged, the mechanical properties (E_y) of 4% 90 kDa CMC

and 2% 250 kDa CMC constructs experienced a significant decrease over time for both cell-laden and cell-free constructs (Figure 2.4). These two formulations were originally chosen for more extensive characterization based on a study by Chou and Nicoll in which bovine NP cells were encapsulated in photocrosslinked methacrylated alginate hydrogels and implanted subcutaneously in nude mice for 8 weeks⁴⁸. The equilibrium Young's modulus of these alginate constructs was ~1.25 kPa at day 1 and increased to ~4.31 kPa at 8 weeks, which indicated the elaboration of a functional matrix that closely approximates values of the native NP (~5 kPa) reported by Cloyd et al⁴⁹. The results of our initial study showed that the elastic modulus for 4% 90 kDa CMC and 2% 250 kDa CMC constructs was ~1 kPa at day 7 (Figure 2.4). As such, these formulations were selected for a more detailed analysis with the belief that the starting mechanical properties of the scaffold would allow for matrix accumulation, resulting in a temporal increase in modulus. However, E_y exhibited a continual decrease over time for both groups. Because CMC is a derivative of cellulose, the polymer backbone is degraded by the plant-derived enzyme, cellulase. As this enzyme was not introduced into the system, the loss in mechanical properties was surprising. The decrease in modulus was observed for both cell-laden and cell-free constructs, indicating a non-cellular mediator of hydrogel weakening. Although the schematic in Figure 2.1 indicates methacrylation of the hydroxyl group off of the C2 carbon, theoretically, this could also occur at a hydroxyl bonded to the C6 carbon. This arm would be more susceptible to ester hydrolysis as the longer chain is less sterically hindered, thereby resulting in the cleavage of periodic interchain crosslinks without a significant loss in mass. Future analyses may evaluate

CMC modification using higher resolution $^1\text{H-NMR}$ (i.e., 900 MHz vs. 360 MHz) in order to distinguish between modification sites.

Due to the decrease in mechanical properties observed for 4% 90 kDa CMC and 2% 250 kDa CMC, a higher weight percent formulation was chosen to provide a higher crosslinking density. Although viability was robust in all concentrations of 90 kDa CMC (Figure 2.3A), a higher weight percent at this molecular weight was not selected due to the large amount of starting material necessary and the increased concentration of free radicals during polymerization. Therefore, the 3% 250 kDa CMC formulation was selected. Similar to 4% 90 kDa and 2% 250 kDa hydrogels, 3% 250 kDa cell-free control samples also experienced a temporal decrease in mechanical properties (Figure 2.6). However, the stiffer initial environment (~ 4 kPa) was on par with native NP tissue (~ 5 kPa)⁴⁹ and cell-laden constructs elaborated a matrix that was able to overcome the decrease in mechanics and maintain the original modulus. Unlike the softer 4% 90 kDa and 2% 250 kDa CMC hydrogels, the partial hydrolysis of the stiffer 3% 250 kDa CMC constructs provided void space for the accumulation of secreted matrix macromolecules while maintaining sufficient structural integrity. Histological analyses showed cells localized in lacunae throughout the scaffold, as is typical of cartilaginous tissues (Figure 2.7A), and the pericellular deposition of CSPG was observed with pronounced interterritorial staining at the periphery of the construct (Figure 2.7B).

Although this study concentrated on characterizing the material properties (degree of swelling and modulus) of cell-free and cell-laden hydrogels, histological analyses confirmed the phenotypic rounded morphology and elaboration of characteristic proteoglycans (i.e., CSPG) by encapsulated NP cells at 14 days *in vitro*. While robust

viability was verified at 7 days for all formulations, future work will investigate the effects of time and environmental stimuli, such as growth factor supplementation (i.e., TGF- β_3)⁵⁰⁻⁵³ and mechanical loading (i.e., hydrostatic pressurization)⁵⁴⁻⁵⁹, on cell viability and the functional assembly of phenotypic ECM components.

Taken together, these findings indicate the utility of photocrosslinkable CMC hydrogels for NP cell encapsulation, as these biomaterials support NP cell viability and may be easily tailored for specific applications. Moreover, photocrosslinkable CMC may serve as a cost-effective, biocompatible alternative to inert polymers, including PEO and PEG, and expensive bacterial- and animal-derived polysaccharides, such as hyaluronic acid and chondroitin sulfate, for use in the engineering of hydrated cartilaginous tissues.

2.5. References

1. Buckwalter JA, Mow VC, Boden SD, Eyre DR and Weidenbaum M. 2000. "Intervertebral disk structure, composition, and mechanical function." In: Orthopaedic Basic Science. Edited by Buckwalter JA, Einhorn TA and Simon SR. 2nd ed. Rosemont, IL: American Academy of Orthopaedic Surgeons. p 547-556.
2. Hall SJ. 2003. In: Basic Biomechanics. Boston: McGraw-Hill. p 276-282.
3. Frymoyer JW and Cats-Baril WL. 1991. An overview of the incidences and costs of low back pain. *Orthop Clinics N Am* **22(2)**: 263-271.
4. Martin BI, Deyo RA, Mirza SK, Turner JA, Comstock BA, Hollingworth W and Sullivan SD. 2008. Expenditures and health status among adults with back and neck problems. *JAMA* **299(6)**: 656-664.

5. Larson JW, Levicoff EA, Gilbertson LG and Kang JD. 2006. Biologic modification of animal models of intervertebral disc degeneration. *J Bone Joint Surg Am* **88 (Suppl 2)**: 83-87.
6. Raj PP. 2008. Intervertebral disc: anatomy-physiology-pathophysiology-treatment. *Pain Pract* **8(1)**: 18-44.
7. Buckwalter J. 1998. Do intervertebral discs deserve their bad reputation? *Iowa Orthop J* **18**: 1-11.
8. Trout JJ, Buckwalter JA and Moore KC. 1982. Ultrastructure of the human intervertebral disc: II. Cells of the nucleus pulposus. *Anat Rec* **204(4)**: 307-314.
9. Buckwalter JA, Boden SD, Eyre DR, Mow VC and Weidenbaum M. 2000. "Intervertebral disk aging, degeneration, and herniation." In: Orthopaedic Basic Science. Edited by Buckwalter JA, Einhorn TA and Simon SR. 2nd ed. Rosemont, IL: American Academy of Orthopaedic Surgeons. p 557-566.
10. Nguyen KT and West JL. 2002. Photopolymerizable hydrogels for tissue engineering applications. *Biomaterials* **23(22)**: 4307-4314.
11. Baer AE, Wang JY, Kraus VB and Setton LA. 2001. Collagen gene expression and mechanical properties of intervertebral disc cell-alginate cultures. *J Orthop Res* **19(1)**: 2-10.
12. Gruber HE, Fisher EC, Desai B, Stasky AA, Hoelscher G and Hanley EN. 1997. Human intervertebral disc cells from the annulus: three-dimensional culture in agarose or alginate and responsiveness to TGF- β_1 . *Exp Cell Res* **235(1)**: 13-21.

13. Maldonado BA and Oegema TRJ. 1992. Initial characterization of the metabolism of intervertebral disc cells encapsulated in microspheres. *J Orthop Res* **10(5)**: 677-690.
14. Melrose J, Smith S, Ghosh P and Taylor TKF. 2001. Differential expression of proteoglycan epitopes and growth characteristics of intervertebral disc cells grown in alginate bead culture. *Cells Tissues Organs* **168(3)**: 137-146.
15. Wang JY, Baer AE, Kraus VB and Setton LA. 2001. Intervertebral disc cells exhibit differences in gene expression in alginate and monolayer culture. *Spine* **26(16)**: 1747-1751.
16. Elisseeff JH, Anseth K, Sims D, McIntosh W, Randolph M and Langer R. 1999. Transdermal photopolymerization for minimally invasive implantation. *Proc Natl Acad Sci USA* **96(6)**: 3104–3107.
17. Bryant SJ, Durand KL and Anseth KS. 2003. Manipulations in hydrogel chemistry control photoencapsulated chondrocyte behavior and their extracellular matrix production. *J Biomed Mater Res A* **67(4)**: 1430-1436.
18. Smeds KA, Pfister-Serres A, Miki D, Dastgheib K, Inoue M, Hatchell DL and Grinstaff MW. 2001. Photocrosslinkable polysaccharides for *in situ* hydrogel formation. *J Biomed Mater Res* **54(1)**: 115-121.
19. Burdick JA, Chung C, Jia X, Randolph MA and Langer R. 2005. Controlled degradation and mechanical behavior of photopolymerized hyaluronic acid networks. *Biomacromolecules* **6(1)**: 386 -391.

20. Nettles DL, Vail TP, Morgan MT, Grinstaff MW and Setton LA. 2004. Photocrosslinkable hyaluronan as a scaffold for articular cartilage repair. *Ann Biomed Eng* **32(3)**: 391-397.
21. Chung C, Mesa J, Miller GJ, Randolph MA, Gill TJ and Burdick JA. 2006. Effects of auricular chondrocyte expansion on neocartilage formation in photocrosslinked hyaluronic acid networks. *Tissue Eng* **12(9)**: 2665-2673.
22. Ogushi Y, Sakai S and Kawakami K. 2007. Synthesis of enzymatically-gellable carboxymethylcellulose for biomedical applications. *J Biosci Bioeng* **104(1)**: 30-33.
23. Chou AI, Bansal A, Miller GJ and Nicoll SB. 2006. The effect of serial monolayer passaging on the collagen expression profile of outer and inner anulus fibrosus cells. *Spine* **31(17)**: 1875-1881.
24. Chou AI, Reza AT and Nicoll SB. 2008. Distinct intervertebral disc cell populations adopt similar phenotypes in three-dimensional culture. *Tissue Eng Part A* **14(12)**: 2079-2087.
25. Iwasa J, Ochi M, Uchio Y, Katsube K, Adachi N and Kawasaki K. 2003. Effects of cell density on proliferation and matrix synthesis of chondrocytes embedded in atelocollagen gel. *Artif Organs* **27(3)**: 249-255.
26. Mauck RL, Seyhan SL, Ateshian GA and Hung CT. 2002. Influence of seeding density and dynamic deformational loading on the developing structure/function relationships of chondrocyte-seeded agarose hydrogels. *Ann Biomed Eng* **30(8)**: 1046-1056.

27. Chang SCN, Rowley JA, Tobias G, Genes NG, Roy AK, Mooney DJ, Vacanti CA and Bonassar LJ. 2001. Injection molding of chondrocyte/alginate constructs in the shape of facial implants. *J Biomed Mater Res* **55(4)**: 503-511.
28. Puelacher WC, Kim SW, Vacanti JP, Schloo B, Mooney D and Vacanti CA. 1994. Tissue-engineered growth of cartilage: the effect of varying the concentration of chondrocytes seeded onto synthetic polymer matrices. *Int J Oral Maxillofac Surg* **23(1)**: 49-53.
29. Vunjak-Novakovic G, Obradovic B, Martin I, Bursac PM, Langer R and Freed LE. 1998. Dynamic cell seeding of polymer scaffolds for cartilage tissue engineering. *Biotechnol Prog* **14(2)**: 193-202.
30. Soltz MA and Ateshian GA. 1998. Experimental verification and theoretical prediction of cartilage interstitial fluid pressurization at an impermeable contact interface in confined compression. *J Biomech* **31(10)**: 927-934.
31. Chou AI and Nicoll SB. 2009. Characterization of photocrosslinked alginate hydrogels for nucleus pulposus cell encapsulation. *J Biomed Mater Res A* **91A(1)**: 187-194.
32. Orive G, Ponce S, Hernández RM, Gascón AR, Igartua M and Pedraz JL. 2002. Biocompatibility of microcapsules for cell immobilization elaborated with different type of alginates. *Biomaterials* **23(18)**: 3825-3831.
33. Roughley P, Hoemann C, DesRosiers E, Mwale F, Antoniou J and Alini M. 2006. The potential of chitosan-based gels containing intervertebral disc cells for nucleus pulposus supplementation. *Biomaterials* **27(3)**: 388-396.

34. Di Martino A, Sittinger M and Risbud MV. 2005. Chitosan: a versatile biopolymer for orthopaedic tissue-engineering. *Biomaterials* **26(30)**: 5983-5990.
35. Liu Y, Shu XZ and Prestwich GD. 2006. Osteochondral defect repair with autologous bone marrow-derived mesenchymal stem cells in an injectable, *in situ*, cross-linked synthetic extracellular matrix. *Tissue Eng* **12(12)**: 3405-3416.
36. Li Q, Williams CG, Sun DDN, Wang J, Leong K and Elisseeff JH. 2004. Photocrosslinkable polysaccharides based on chondroitin sulfate. *J Bio Mat Res A* **68(1)**: 28-33.
37. Sakai S, Ogushi Y and Kawakami K. 2009. Enzymatically crosslinked carboxymethylcellulose-tyramine conjugate hydrogel: cellular adhesiveness and feasibility for cell sheet technology. *Acta Biomater* **5(2)**: 554-559.
38. Pal K, Banthia AK and Majumdar DK. 2006. Development of carboxymethyl cellulose acrylate for various biomedical applications. *Biomed Mater* **1(2)**: 85-91.
39. Leone G, Fini M, Torricelli P, Giardino R and Barbucci R. 2008. An amidated carboxymethylcellulose hydrogel for cartilage regeneration. *J Mater Sci Mater Med* **19(8)**: 2873-2880.
40. Kim KS, Lee JY, Kang YM, Kim ES, Lee B, Chun HJ, Kim JH, Min BH, Lee HB and kim MS. 2009. Electrostatic crosslinked *in situ*-forming *in vivo* scaffold for rat bone marrow mesenchymal stem cells. *Tissue Eng Part A* **15(10)**: 3201-3209.
41. Elisseeff J, McIntosh W, Anseth K, Riley S, Ragan P and Langer R. 2000. Photoencapsulation of chondrocytes in poly(ethylene oxide)-based semi-interpenetrating networks. *J Biomed Mater Res* **51(2)**: 164-171.

42. Chung C, Erickson IE, Mauck RL and Burdick JA. 2008. Differential behavior of auricular and articular chondrocytes in hyaluronic acid hydrogels. *Tissue Eng Part A* **14(7)**: 1121-1131.
43. Bryant SJ, Nuttelman CR and Anseth KS. 2000. Cytocompatibility of UV and visible light photoinitiating systems on cultured NIH/3T3 fibroblasts *in vitro*. *J Biomater Sci Polym Ed* **11(5)**: 439-457.
44. Vistica DT, Skehan P, Scudiero D, Monks A, Pittman A and Boyd MR. 1991. Tetrazolium-based assays for cellular viability: a critical examination of selected parameters affecting formazan production. *Cancer Res* **51(10)**: 2515-2520.
45. Nuttelman CR, Tripodi MC and Anseth KS. 2005. Synthetic hydrogel niches that promote hMSC viability. *Matrix Biol* **24(3)**: 208-218.
46. Mann BK, Schmedlen RH and West JL. 2001. Tethered-TGF- β increases extracellular matrix production of vascular smooth muscle cells. *Biomaterials* **22(5)**: 439-444.
47. Anseth KS, Bowman CN and Brannon-Peppas L. 1996. Mechanical properties of hydrogels and their experimental determination. *Biomaterials* **17(17)**: 1647-1657.
48. Chou AI, Akintoye SO and Nicoll SB. 2009. Photo-crosslinked alginate hydrogels support enhanced matrix accumulation by nucleus pulposus cells *in vivo*. *Osteoarthritis Cartilage* **17(10)**: 1377-1384.
49. Cloyd JM, Malhotra NR, Weng L, Chen W, Mauck RL and Elliott DM. 2007. Material properties in unconfined compression of human nucleus pulposus, injectable hyaluronic acid-based hydrogels and tissue engineering scaffolds. *Eur Spine J* **16(11)**: 1892-1898.

50. Miyanishi K, Trindade MCD, Lindsey DP, Beaupré GS, Carter DR, Goodman SB, Schurman DJ and Smith RL. 2006. Effects of hydrostatic pressure and transforming growth factor-beta 3 on adult human mesenchymal stem cell chondrogenesis *in vitro*. *Tissue Eng* **12(6)**: 1419-1428.
51. Mauck RL, Nicoll SB, Seyhan SL, Ateshian GA and Hung CT. 2003. Synergistic action of growth factors and dynamic loading for articular cartilage tissue engineering. *Tissue Eng* **9(4)**: 597-611.
52. Byers BA, Mauck RL, Chiang IE and Tuan RS. 2008. Transient exposure to transforming growth factor beta 3 under serum-free conditions enhances the biomechanical and biochemical maturation of tissue-engineered cartilage. *Tissue Eng Part A* **14(11)**: 1821-1834.
53. Risbud MV, Di Martino A, Guttapalli A, Seghatoleslami R, Denaro V, Vaccaro AR, Albert TJ and Shapiro IM. 2006. Toward an optimum system for intervertebral disc organ culture: TGF-beta 3 enhances nucleus pulposus and annulus fibrosus survival and function through modulation of TGF-beta-R expression and ERK signaling. *Spine* **31(8)**: 884-890.
54. Reza AT and Nicoll SB. 2008. Hydrostatic pressure differentially regulates outer and inner annulus fibrosus cell matrix production in 3D scaffolds. *Ann Biomed Eng* **36(2)**: 204-213.
55. Hutton WC, Elmer WA, Boden SD, Hyon S, Toribatake Y, Tomita K and Hair GA. 1999. The effect of hydrostatic pressure on intervertebral disc metabolism. *Spine* **24(15)**: 1507-1515.

56. Hutton WC, Elmer WA, Bryce LM, Kozłowska EE, Boden SD and Kozłowski M. 2001. Do the intervertebral disc cells respond to different levels of hydrostatic pressure? *Clin Biomech* **16(9)**: 728-734.
57. Kasra M, Goel V, Martin J, Wang S-T, Choi W and Buckwalter J. 2003. Effect of dynamic hydrostatic pressure on rabbit intervertebral disc cells. *J Orthop Res* **21(4)**: 597-603.
58. Neidlinger-Wilke C, Würtz K, Liedert A, Schmidt C, Börm W, Ignatius A, Wilke H-J and Claes L. 2005. A three-dimensional collagen matrix as a suitable culture system for the comparison of cyclic strain and hydrostatic pressure effects on intervertebral disc cells. *J Neurosurg Spine* **2(4)**: 457-465.
59. Neidlinger-Wilke C, Würtz K, Urban JPG, Börm W, Arand M, Ignatius A, Wilke H-J and Claes LE. 2006. Regulation of gene expression in intervertebral disc cells by low and high hydrostatic pressure. *Eur Spine J* **15 (Suppl 3)**: S372-378.

Chapter 3: Serum-Free, Chemically-Defined Medium with TGF- β_3 Enhances Functional Properties of Nucleus Pulposus Cell-laden Carboxymethylcellulose Hydrogel Constructs

3.1. Introduction

The intervertebral disc (IVD) is a heterogeneous tissue that functions to permit motion and flexibility, support and distribute loads, and dissipate energy in the spine¹. The IVD is comprised of the collagenous, lamellar annulus fibrosus, which maintains disc shape and allows the spine to resist tensile loads², and the gelatinous nucleus pulposus (NP). The NP is a hydrated tissue located at the center of the disc, characterized by high proteoglycan (i.e., aggrecan) and type II collagen content¹. This region functions to resist compressive loads through the generation of a hydrostatic swelling pressure. Similar to articular cartilage, the IVD is a largely avascular, aneural tissue, dependent upon bulk diffusion for nutrient transport, which thus limits its capacity for self-repair³.

Intervertebral disc degeneration occurs naturally with aging or may be accelerated by injury. This pathological condition is commonly attributed to increased degradation of aggrecan molecules, giving rise to significant alterations in disc biochemical composition and a subsequent loss of hydration⁴. The NP is thus rendered more fibrous in structure and content, which reduces nutrient diffusion and waste removal⁵. The accompanied increase in lactate concentration lowers the local pH⁶ and may precipitate cell death⁷. Disc degeneration may be asymptomatic, or the associated change in

extracellular matrix (ECM) composition and altered loading pattern may contribute to increased disc stiffness and low back pain⁸.

Tissue engineering strategies may provide a viable NP replacement therapy as an alternative to current surgical procedures for alleviating back pain. Growth factor supplementation can affect the maturation of such tissue engineered constructs⁹. For example, transforming growth factor- β_3 (TGF- β_3), a member of the TGF- β superfamily which is known to affect proliferation, differentiation, and gene expression of ECM components¹⁰, has been shown to enhance cell survival and matrix deposition in rat lumbar IVD organ culture¹¹. Furthermore, TGF- β_3 is known to improve the functional properties of tissue engineered cartilage constructs, as chondrocyte-seeded agarose gels achieved compressive moduli and proteoglycan content comparable to native tissue levels^{9,12}.

Although tissue engineered nucleus pulposus constructs are typically cultured in serum-containing medium¹³⁻¹⁸, animal-derived sera, such as fetal bovine serum (FBS), are not well-characterized and may present batch-to-batch variations in constituent composition^{19, 20}. Moreover, medium formulations utilizing animal-derived serum may face regulatory barriers for any human clinical applications. Related work in cartilage tissue engineering has demonstrated the additional benefit of serum-free medium, as these formulations typically resulted in improved construct maturation in comparison to serum-containing medium^{9, 21}. Therefore, identifying a chemically-defined medium formulation that supports NP construct maturation without the use of serum may not only improve clinical applicability, but may also enhance construct development.

Scaffold selection is another major factor impacting the success of any tissue engineered implant. The highly hydrated nature of the NP is similar to that of hydrogel networks, making such polymeric structures prime candidates to serve as scaffolds for NP regeneration. Although NP cells are routinely cultured by encapsulation in ionically crosslinked alginate hydrogels²²⁻²⁶, these materials have been found to lose mechanical integrity over time, possibly due to a loss of crosslinking calcium ions through diffusion²² or depletion by the encapsulated cells. Moreover, raw alginate has been shown to stimulate an immune response *in vivo* in mice and requires additional processing to remove impurities for biomedical applications²⁷. Similar purification procedures are required for animal-derived products, such as hyaluronic acid, chitosan, and chondroitin sulfate, which have also been used to engineer cartilaginous tissues²⁸⁻³⁵, thus motivating the investigation of alternative natural biomaterials.

One potential candidate material is carboxymethylcellulose (CMC), a water-soluble polysaccharide derivative of cellulose, the primary structural component of plant cell walls. CMC is a biocompatible, low-cost, FDA-approved material that is commercially available in high purity forms, making this polymer a highly attractive option for biomedical applications³⁶. Photocrosslinked CMC has been recently shown to produce stable hydrogels, support NP cell viability, and promote phenotypic matrix deposition capable of maintaining initial mechanical properties *in vitro*³⁷. However, in order to further enhance the development of CMC constructs, culture conditions must be optimized.

Therefore, the objective of this study was to identify an optimal cell culture medium for NP tissue engineering by comparing the effects of medium formulation and

TGF- β_3 on the *in vitro* culture of cell-laden CMC constructs. We hypothesized that a chemically-defined, serum-free medium would support stability of the NP cellular phenotype, as evidenced by proteoglycan accumulation and type II collagen retention, and growth factor supplementation would further improve matrix deposition and functional material properties.

3.2. Materials and Methods

3.2.1. Macromer Synthesis

Methacrylated carboxymethylcellulose was synthesized through esterification of hydroxyl groups based on previously described protocols^{13, 28, 29, 37} (Figure 3.1). Briefly, a 20-fold excess of methacrylic anhydride (Sigma, St. Louis, MO) was reacted with a 1 wt% solution of 250 kDa CMC (Sigma) in RNase/DNase-free water over 24 hours at 4°C. The pH was periodically adjusted to 8.0 using 3N NaOH to modify hydroxyl groups of the polymer with functional methacrylate groups. The modified CMC solution was purified via dialysis for 96 hours against RNase/DNase-free water (Spectra/Por1, MW 5-8 kDa, Rancho Dominguez, CA) to remove excess, unreacted methacrylic anhydride. Purified methacrylated CMC was recovered by lyophilization and stored at -20°C. The degree of substitution was confirmed using ¹H-NMR (360 MHz, DMX360, Bruker, Madison, WI) following acid hydrolysis of purified methacrylated CMC³⁷. Molar percent of methacrylation was determined by the relative integrations of methacrylate proton peaks (methylene, $\delta = 6.2$ ppm and 5.8 ppm and the methyl peak, $\delta = 2.0$ ppm) to carbohydrate protons.

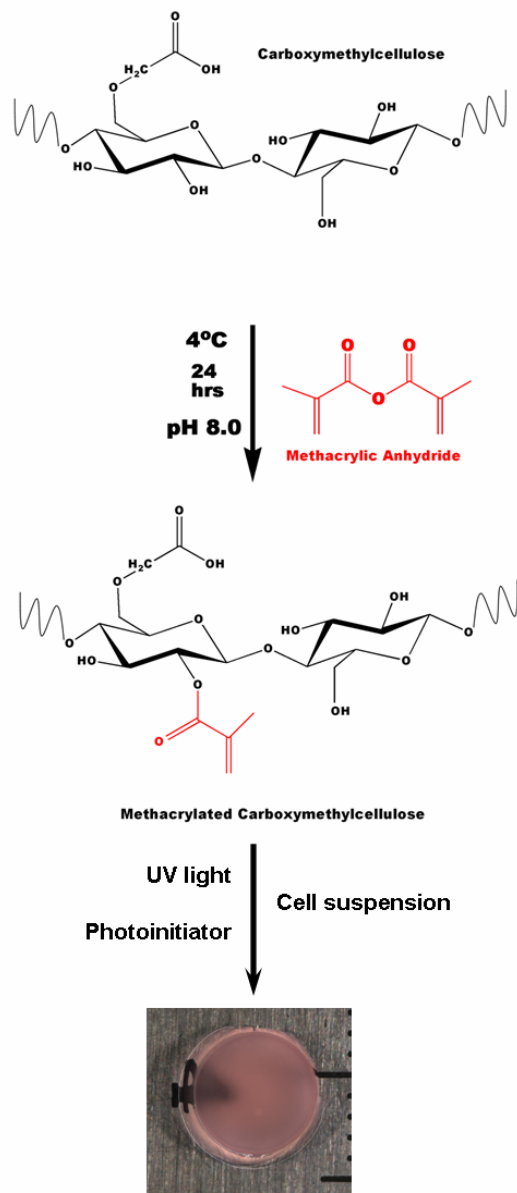


Figure 3.1. Schematic of the synthesis of methacrylated CMC and nucleus pulposus cell encapsulation.

3.2.2. Primary Cell Culture and Isolation

All cell culture supplies, including media, antibiotics, and buffering agents, were purchased from Invitrogen (Carlsbad, CA) unless otherwise noted. Discs C2-C4 were

isolated from bovine caudal IVDs obtained from a local abattoir, and the NP was separated through gross visual inspection based on previous protocols^{38, 39}. Tissue was maintained in Dulbecco's Modified Eagle Medium (DMEM) supplemented with 20% FBS (Hyclone, Logan, UT), 0.075% sodium bicarbonate, 100 U/mL penicillin, 100 µg/mL streptomycin, and 0.25 µg/mL Fungizone reagent at 37°C, 5% CO₂ for two days prior to digestion to ensure no contamination occurred during harvesting. A single serum lot was used for all experiments to reduce potential variability in the cellular response.

Tissue was diced and NP cells were released by collagenase (Type IV, Sigma) digestion at an activity of 7000 U collagenase per gram of tissue. Following incubation in collagenase, undigested tissue was removed using a 40 µm mesh filter. Cells from multiple levels (C2-C4) were pooled and rinsed in sterile Dulbecco's Phosphate Buffered Saline (DPBS). These primary cells were plated onto tissue culture flasks, designated as passage 0, and maintained in DMEM with 10% FBS, 0.075% sodium bicarbonate, 100 U/mL penicillin, and 100 µg/mL streptomycin (growth medium). Cells were subcultured twice to obtain the necessary number of cells, and passage 2 cells³⁸ were used in all experiments, as these cells have been shown to retain phenotypic differences observed *in vivo* up to the second passage³⁹. Medium was changed three times per week.

3.2.3. Cell Encapsulation in Photocrosslinked Hydrogels

Prior to dissolution, lyophilized methacrylated CMC was sterilized by a 30-minute exposure to germicidal UV light. The sterilized product was then dissolved to 2.75% in filter-sterilized 0.05 wt% photoinitiator, 2-hydroxy-1-[4-(2-hydroxyethoxy)phenyl]-2-methyl-1-propanone (Irgacure 2959, I2959, Ciba Specialty Chemicals, Basel, Switzerland), in sterile DPBS at 4°C. Passage 2 NP cells were

resuspended in a small volume of 0.05% I2959 and then homogeneously mixed with dissolved methacrylated CMC at 30×10^6 cells/mL for a final concentration of 2.5%. The seeding density was selected based on previous studies using cell-seeded constructs for engineering of cartilaginous tissues⁴⁰⁻⁴⁵. The 2.5% CMC solution was cast in a custom-made glass casting device and exposed to long-wave UV light (EIKO, Shawnee, KS, peak 368 nm, 1.2W) for 10 minutes to produce covalently crosslinked hydrogel disks of 5-mm diameter x 2-mm thickness. Each hydrogel was incubated in 1.5 mL of growth medium at 37°C, 5% CO₂. At day 1, growth medium was fully exchanged with the respective media formulations utilized for the remainder of the study. Two base formulations of media were compared. Growth medium, described above, was supplemented with 50 µg/mL L-ascorbic acid as previously described³⁷ and is designated as DMEM. Chemically defined medium (CDM) was comprised of Dulbecco's Modified Eagle Medium with 1% insulin-transferrin-selenium + universal culture supplement (BD Biosciences, San Jose, CA), 100 U/mL penicillin, 100 µg/mL streptomycin, 40 µg/mL L-proline (Sigma), 1 mM sodium pyruvate (Mediatech, Inc., Manassas, VA), 50 µg/mL ascorbic acid 2-phosphate (Sigma), and 100 nM dexamethasone (Sigma)⁴⁶. Both base formulations (DMEM and CDM) were further supplemented with 10 ng/mL rhTGF-β₃ (R&D Systems, Minneapolis, MN). These formulations are referred to as DMEM+ and CDM+, respectively. The TGF-β₃ concentration utilized was chosen based on previous IVD and cartilage tissue engineering studies^{9, 11, 12, 46, 47}. Media were changed three times per week.

3.2.4. Swelling Ratio

The equilibrium weight swelling ratio, Q_w , was calculated at days 3, 14, and 28 (n=4). Constructs were weighed to determine the wet weight (W_s), lyophilized, and then weighed again to measure the dry weight (W_d). Q_w was calculated using the following equation:

$$Q_w = W_s/W_d$$

3.2.5. Biochemistry

Following lyophilization, total protein and DNA (n=4) were extracted at days 3, 14, and 28 by pepsin digestion based on previous studies³⁹. Briefly, lyophilized samples were homogenized and treated with pepsin (Sigma) in 0.05N acetic acid (1.9 mg/mL) for 48 hrs at 4°C. Afterwards, pepsin was neutralized by the addition of 10X tris buffered saline. Cell-free hydrogels (n=3) were maintained for all groups to serve as negative controls. Total DNA content was measured using the PicoGreen DNA assay⁴⁸ (Molecular Probes, Eugene, OR) with calf thymus DNA (Sigma) as the standard³⁹. Samples were analyzed at 480 nm excitation and 520 nm emission using a Bio-Tek Instruments microplate reader (Synergy HTTM, Winooski, VT).

Total sulfated glycosaminoglycan (GAG) content was measured at days 3, 14, and 28 using the 1,9 dimethylmethylene blue (DMMB) assay⁴⁹. The DMMB dye was reduced to pH 1.5 to minimize the formation of CMC carboxyl group-DMMB dye complexes⁵⁰ and absorbance was determined at 595 nm using a chondroitin-6 sulfate standard curve (Sigma).

Collagen production was quantified at day 28 via an indirect enzyme-linked immunosorbent assay using monoclonal antibodies to type I collagen (COL I, Sigma) and

type II collagen (COL II) (II-II6B3, Developmental Studies Hybridoma Bank, University of Iowa, Iowa City, IA) based on previous protocols³⁹. Protein values for each sample were determined using a standard curve generated from bovine COL I and COL II (Rockland Immunochemicals, Gilbertsville, PA). Absorbance was measured at 450 nm. DNA, GAG, and collagen content are presented normalized to wet weight.

3.2.6. *Histology and Immunohistochemistry*

Constructs were fixed for 45 minutes in acid formalin at room temperature and processed for paraffin embedding after graded serial ethanol dehydration. Samples were sectioned at a thickness of 8 μm using a Leica microtome (Model 2030, Nussloch, Germany), and hematoxylin and eosin staining was conducted to visualize cellular distribution throughout the hydrogel. Immunohistochemical analyses were performed to assess extracellular matrix accumulation according to previous studies³⁹. Briefly, monoclonal antibodies to COL I (1:200 dilution in blocking solution, comprised of 10% horse serum diluted in DPBS), COL II (1:3 dilution in blocking solution, composed of 10% horse serum diluted in DPBS), and chondroitin sulfate proteoglycan (1:100 dilution in blocking solution, consisting of 10% goat serum diluted in DPBS) (CSPG, Sigma) were used. A peroxidase-based system (Vectastain Elite ABC, Vector Labs) and 3,3'-diaminobenzidine (Vector Labs) as the chromagen were employed to visualize ECM localization. Non-immune controls were processed without primary antibody. Samples were viewed with a Zeiss Axioskop 40 optical microscope and images were captured using AxioVision software (Carl Zeiss, Inc., Thornwood, NY).

3.2.7. Mechanical Testing

Unconfined compression testing was conducted on CMC hydrogels (n=5) at day 28 using a custom-built apparatus, as previously described^{13, 37, 51}. Briefly, the unconfined compression testing protocol was comprised of a creep test followed by a multi-ramp stress-relaxation test. The creep test consisted of a 1 g tare load applied at a 10 $\mu\text{m/s}$ ramp velocity for 1800 seconds until equilibrium was reached (equilibrium criteria: <10 μm change in 10 minutes). Transient creep strain at 30 seconds after the onset of the tare load ($\varepsilon_{t=30s}$) and the equilibrium creep strain (ε_{eq}) in the axial direction were determined by measuring the change in specimen thickness at the respective time point divided by the initial, unloaded thickness. Following creep, the multi-ramp stress-relaxation test consisted of three 5% strain ramps at a 10 $\mu\text{m/s}$ ramp velocity, each followed by a 2000 second relaxation period (equilibrium criteria: <0.5 g change in 10 minutes). Peak stress (σ_{pk}) and equilibrium stress (σ_{eq}) were measured at the third ramp, corresponding to 15% strain, and were used to calculate % relaxation:

$$\% \text{ Relaxation} = \left(1 - \frac{\sigma_{eq}}{\sigma_{pk}} \right) \times 100\%$$

Equilibrium stress was calculated at each ramp using surface area measurements and plotted against the applied strain. An average equilibrium Young's modulus, E_y , was calculated from the slope of the stress versus strain curves and reported for each sample.

3.2.8. Statistical Analysis

A three-way ANOVA was used to determine the effects of time, medium, and TGF- β_3 on wet weight, dry weight, Q_w , DNA content, and GAG accumulation (n=4). A Tukey's post-hoc test was performed on the three-factor interaction. A two-way

ANOVA was used to determine the effects of medium and TGF- β_3 on collagen content (n=4), thickness, diameter, and mechanical properties (n=5) at day 28. A Tukey's post-hoc test was performed on the two-factor interaction. Significance was set at $p < 0.05$. Data represent the mean \pm standard deviation. All statistical analyses were performed using JMP software (SAS Institute, Cary, NC).

3.3. Results

250 kDa CMC was methacrylated at a 5.63% modification, as verified by $^1\text{H-NMR}$. Constructs were isolated at days 3, 14, and 28 to determine swelling ratio measurements, DNA content, and GAG accumulation. TGF- β_3 -treated groups (DMEM+ and CDM+) experienced significant increases in both wet weight and dry weight at each time point, while measurements for untreated groups (DMEM and CDM) remained unchanged from day 3 values and significantly lower in comparison (Table 3.1). A significant temporal decrease in Q_w was measured for DMEM+ and CDM+ groups, whereas the swelling ratio of corresponding untreated samples stayed constant and markedly higher. DNA content significantly decreased in DMEM constructs but increased in both TGF- β_3 supplemented groups and was highest in DMEM+ samples.

		Wet Weight (mg)	Dry Weight (mg)	Q _w	DNA/Wet Weight (ng/mg)
DMEM	D3	64.54 ± 3.23	1.68 ± 0.35	39.4 ± 6.1	67.6 ± 3.7 * +
	D14	67.99 ± 2.36 +	1.76 ± 0.09 +	38.8 ± 2.8 +	31.7 ± 4.9 + #
	D28	67.84 ± 0.91 +	1.94 ± 0.24 +	35.5 ± 4.6 +	28.9 ± 3.2 + #
DMEM+	D3	63.65 ± 4.79 *	1.65 ± 0.20 *	38.8 ± 2.4 *	130.6 ± 7.9 *
	D14	80.14 ± 1.21 * #	3.03 ± 0.16 * #	26.5 ± 1.7	277.1 ± 12.2 #
	D28	92.60 ± 2.76 * #	4.08 ± 0.09 * #	22.7 ± 0.9	272.0 ± 14.2 #
CDM	D3	64.30 ± 3.19	1.73 ± 0.08	37.3 ± 3.3	83.4 ± 3.5 †
	D14	66.52 ± 6.88 +	1.75 ± 0.23 +	38.1 ± 2.3 +	59.2 ± 8.8 + #
	D28	71.41 ± 1.17 +	1.80 ± 0.04 +	39.8 ± 1.5 +	71.0 ± 2.3 + #
CDM+	D3	67.84 ± 4.22 *	1.96 ± 0.06 *	34.7 ± 1.7 *	108.8 ± 18.6
	D14	108.74 ± 0.96 * #	4.19 ± 0.20 * #	26.0 ± 1.2	97.0 ± 4.6 #
	D28	127.18 ± 4.11 * #	5.73 ± 0.13 * #	22.2 ± 0.5	155.3 ± 4.9 * #

Table 3.1. Physical properties and normalized DNA content of CMC constructs (n=4) at days 3, 14, and 28 as a function of medium formulation. * Significant vs. all other time points within group. + Significant vs. corresponding TGF-β₃-treated group (i.e., DMEM vs. DMEM+) within time point. # Significant vs. opposing media type (i.e., DMEM+ vs. CDM+) within time point. † Significant vs. D14 within group.

GAG accumulation significantly increased over time in both TGF-β₃-treated groups and was highest in CDM+ constructs (Figure 3.2). There was no quantifiable GAG content in untreated DMEM hydrogels and no effect of medium formulation when comparing untreated groups (DMEM versus CDM).

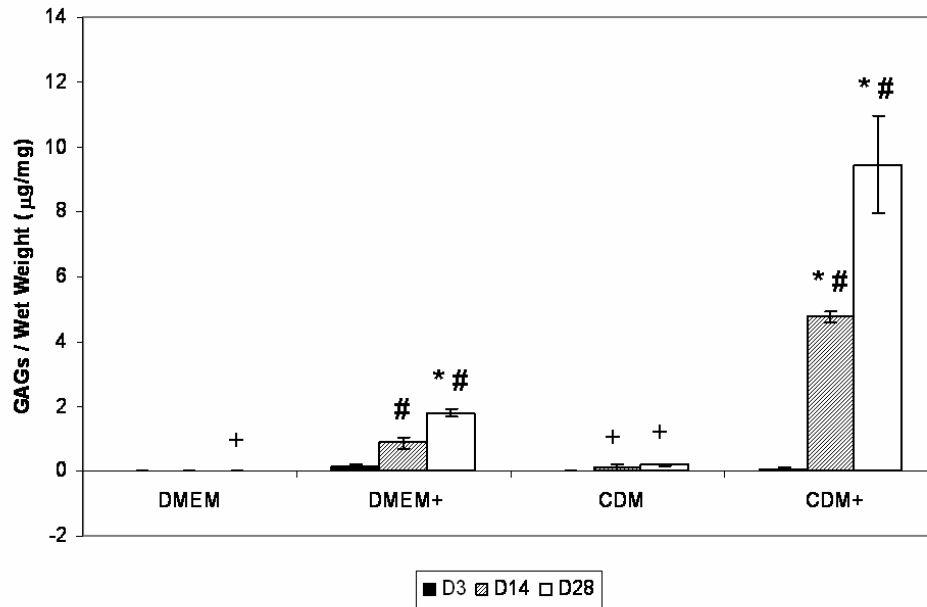


Figure 3.2. Normalized GAG content (n=4) at days 3, 14, and 28 as a function of medium formulation. * Significant vs. all other time points within group. + Significant vs. corresponding TGF- β_3 -treated group (i.e., DMEM vs. DMEM+) within time point. # Significant vs. opposing media type (i.e., DMEM+ vs. CDM+) within time point.

Immunohistochemical analyses conducted at day 28 revealed limited pericellular deposition of CSPG in untreated DMEM samples with enhanced interterritorial staining for DMEM+ constructs (Figure 3.3 A, B). Although staining was more intense in CDM samples, CSPG deposition remained highly concentrated in lacunae whereas CDM+ groups exhibited uniform interterritorial CSPG accumulation throughout the construct (Figure 3.3D). Non-immune control samples exhibited no positive staining.

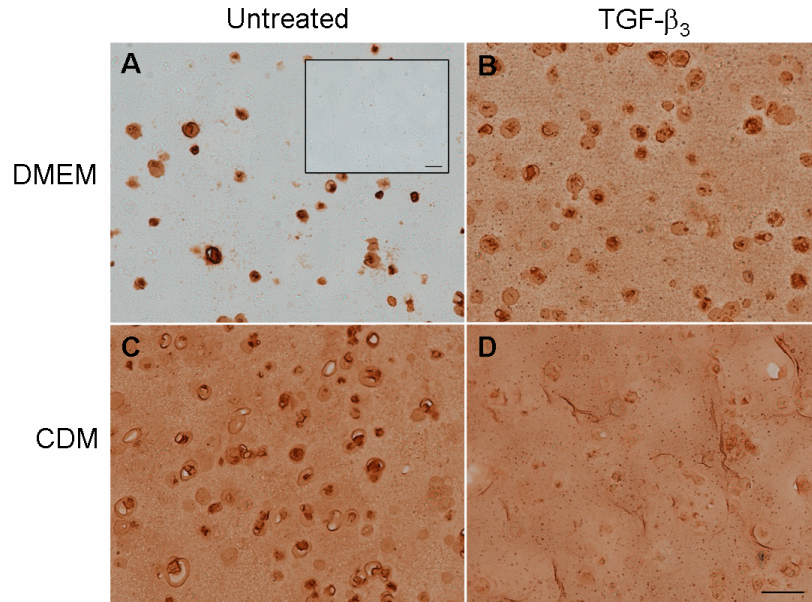


Figure 3.3. Immunohistochemical staining for CSPG content of CMC constructs at day 28 cultured in DMEM (A, B) and CDM (C, D) with (B, D) and without (A, C) TGF- β_3 , with representative non-immune control inlayed in Panel A. Bar = 50 μ m.

At 28 days, quantification of COL II accumulation was significantly greater in both CDM groups in comparison to corresponding DMEM samples and was highest in CDM+ constructs (Figure 3.4A). There was no detectable COL II in untreated DMEM samples. These measurements were verified by COL II immunohistochemistry. By day 28, there was still no detectable COL II staining in untreated DMEM samples and light, pericellular staining at the periphery of DMEM+ samples (Figure 3.4 B, C). Both CDM groups were positive for pericellular COL II throughout the construct, with the most intense staining observed for CDM+ samples (Figure 3.4E). Non-immune controls exhibited no positive staining.

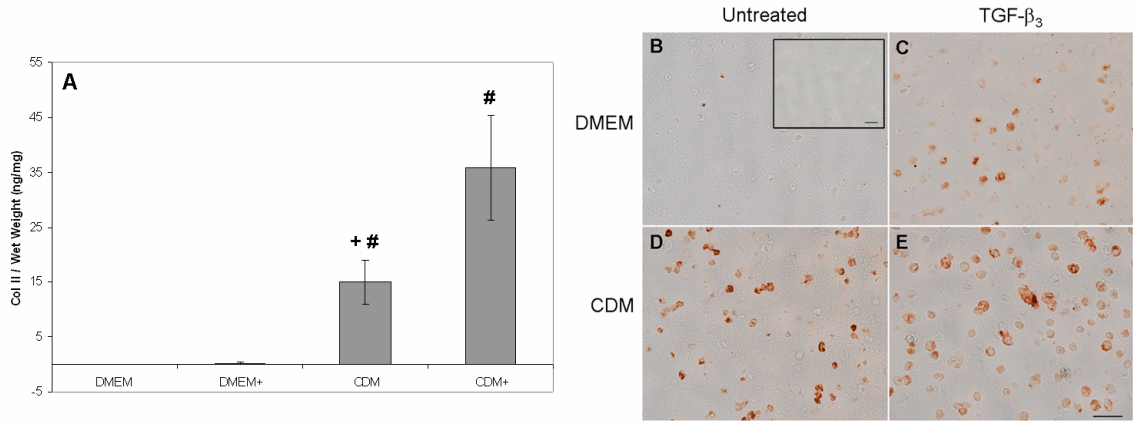


Figure 3.4. Normalized COL II content (n=4) (A) and immunohistochemical staining at day 28 for CMC constructs cultured in DMEM (B, C) and CDM (D, E) with (C, E) and without (B, D) TGF- β_3 , with representative non-immune control inlayed in Panel B. Bar = 50 μm . + Significant vs. corresponding TGF- β_3 -treated group (i.e., DMEM vs. DMEM+). # Significant vs. opposing media type (i.e., DMEM+ vs. CDM+).

Type I collagen content was highest in DMEM+ samples after 28 days, while there was no detectable COL I in either CDM group (Figure 3.5A). Immunohistochemical analyses revealed light COL I deposition at the periphery of DMEM and DMEM+ samples (Figure 3.5 B, C). In addition, DMEM+ constructs possessed a thick (100-200 μm) outer ring of fibroblastic cells, which stained positive for COL I (Figure 3.5C), while there was minimal COL I staining observed in either CDM group. As with CSPG and COL II, non-immune control samples exhibited no positive staining.

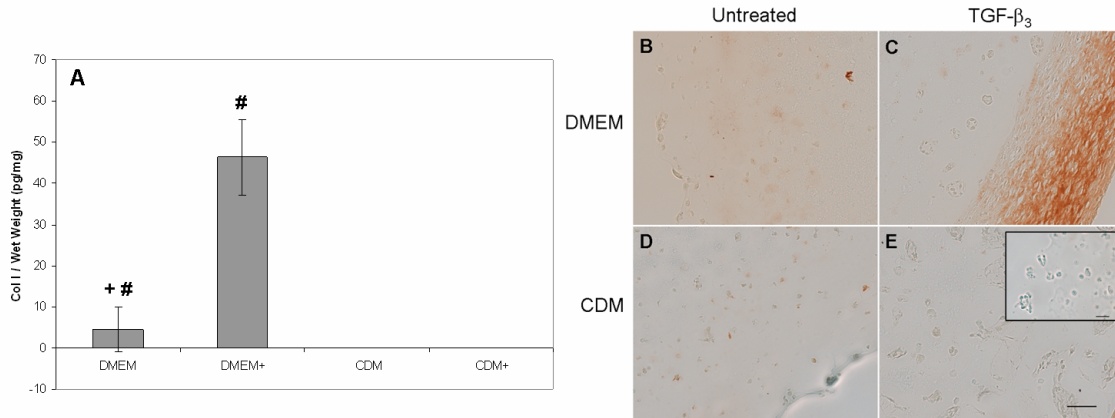


Figure 3.5. Normalized COL I content (n=4) (A) and immunohistochemical staining of the scaffold periphery at day 28 for CMC constructs cultured in DMEM (B, C) and CDM (D, E) with (C, E) and without (B, D) TGF- β_3 , with representative non-immune control inlayed in Panel E. Bar = 50 μ m. + Significant vs. corresponding TGF- β_3 -treated group (i.e., DMEM vs. DMEM+). # Significant vs. opposing media type (i.e., DMEM+ vs. CDM+).

Constructs were tested in unconfined compression at day 28 to determine the mechanical properties. Hydrogel diameter and thickness measurements in both TGF- β_3 -treated groups (DMEM+ and CDM+) were significantly greater than those for corresponding untreated groups and were largest in CDM+ constructs, as TGF- β_3 -treated constructs grew in both the radial and axial directions (Table 3.2).

	Diameter (mm)	Thickness (mm)
DMEM	5.53 \pm 0.09 +	2.44 \pm 0.06 +
DMEM+	6.39 \pm 0.07 #	2.89 \pm 0.07 #
CDM	5.65 \pm 0.09 +	2.48 \pm 0.04 +
CDM+	6.62 \pm 0.05 #	3.48 \pm 0.10 #

Table 3.2. Diameter and thickness measurements of mechanical testing samples (n=5) at day 28 as a function of medium formulation. + Significant vs. corresponding TGF- β_3 -treated group (i.e., DMEM vs. DMEM+). # Significant vs. opposing media type (i.e., DMEM+ vs. CDM+).

Sample thickness was assessed thirty seconds after the application of a one gram tare load in the creep test to determine the transient strain in the axial direction, $\epsilon_{t=30s}$ (Figure 3.6A). Untreated DMEM constructs experienced the most deformation shortly after loading ($\epsilon_{t=30s}$: $13.074 \pm 0.958\%$) while there was no significant difference between TGF- β_3 -treated groups (DMEM+ vs. CDM+, $3.642 \pm 0.623\%$). The equilibrium creep strain, ϵ_{eq} , followed the same trend (Figure 3.6A), with untreated DMEM samples displaying the greatest deformation ($13.91 \pm 0.494\%$), with no significant difference between TGF- β_3 supplemented groups (average deformation = $4.46 \pm 0.80\%$).

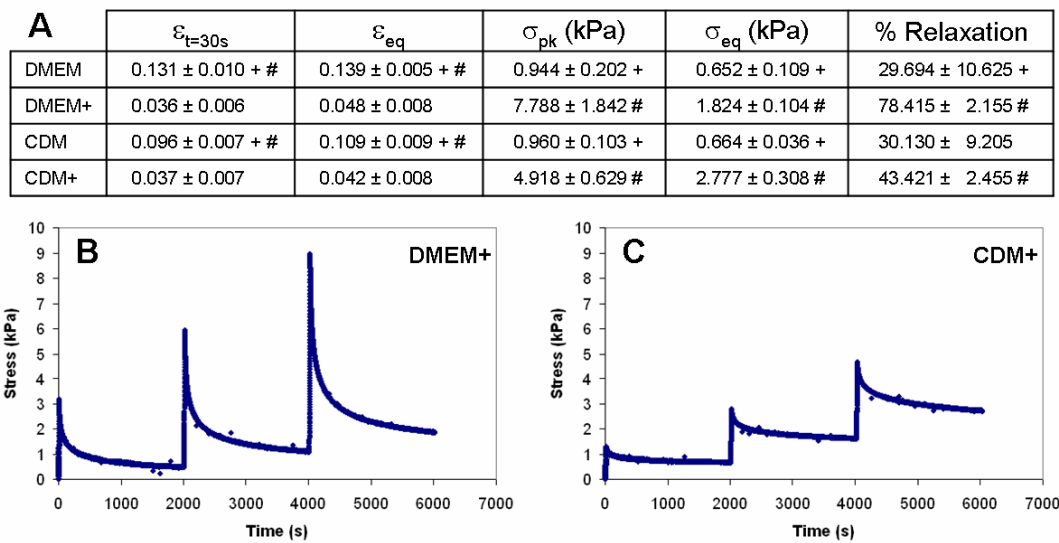


Figure 3.6. Mechanical properties (A) of CMC constructs (n=5) at day 28, as demonstrated by the transient (30s after loading) and equilibrium creep strain ($\epsilon_{t=30s}$ and ϵ_{eq} , respectively), and peak stress (σ_{pk}), equilibrium stress (σ_{eq}), and percent relaxation at 15% strain. Representative stress vs. time curves for DMEM+ (B) and CDM+ (C) samples. + Significant vs. corresponding TGF- β_3 -treated group (i.e., DMEM vs. DMEM+). # Significant vs. opposing media type (i.e., DMEM+ vs. CDM+).

After creep, samples were subjected to a multi-ramp stress-relaxation test. DMEM+ constructs exhibited the highest σ_{pk} (7.788 ± 1.842 kPa), almost a full order of magnitude greater than untreated groups (Figure 3.6A). However, DMEM+ constructs were unable to sustain this stress and displayed a rapid relaxation (Figure 3.6B) which corresponded to the highest % relaxation among all groups. Conversely, CDM+ samples maintained a higher σ_{eq} to σ_{pk} ratio (Figure 3.6C), with a % relaxation significantly less than DMEM+ scaffolds. The equilibrium Young's modulus was significantly greater in both TGF- β_3 -treated groups and was highest for CDM+ (CDM+: 18.54 ± 1.92 kPa; DMEM+: 11.82 ± 0.92 kPa) (Figure 3.7). TGF- β_3 -treated constructs were most opaque in gross appearance, with the highest degree of opacity observed for CDM+ constructs (Figure 3.7). There was no effect of medium formulation on diameter, thickness, σ_{eq} , σ_{pk} , % relaxation, or E_y values when comparing untreated groups (DMEM versus CDM).

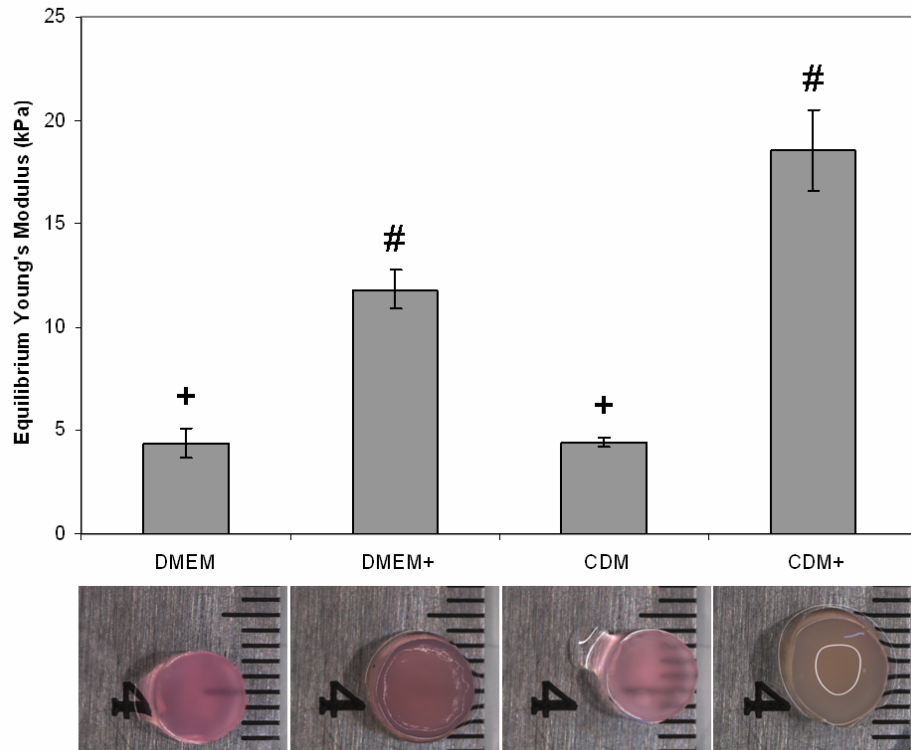


Figure 3.7. Equilibrium Young's modulus of CMC constructs (n=5) at day 28 as a function of medium formulation with representative corresponding stereomicrograph images shown below. Scale in mm. + Significant vs. corresponding TGF- β_3 -treated group (i.e., DMEM vs. DMEM+). # Significant vs. opposing media type (i.e., DMEM+ vs. CDM+).

3.4. Discussion

This study is the first to examine the effects of medium formulation and growth factor supplementation on NP cells encapsulated in CMC hydrogels. Although serum-free, chemically-defined medium alone produced increased COL II accumulation and improved CSPG distribution, there were no significant differences in GAG quantification or mechanical properties when comparing CDM and DMEM constructs. However, COL II elaboration is a key distinguishing characteristic when comparing cartilaginous tissue,

such as the NP, to fibrous tissue, thereby indicating a trend in support of our first hypothesis. Consistent with our second hypothesis, we demonstrated that serum-free, chemically-defined medium supplemented with TGF- β_3 resulted in increased GAG and COL II accumulation and maintenance of the NP cellular phenotype, as well as enhanced functional properties (i.e., E_y). These findings underscore the importance of medium formulation on the development of engineered NP constructs.

CMC is a well-established derivative of cellulose, which is rendered water-soluble through the introduction of carboxymethyl groups along the polymer backbone. CMC is commercially available in high-purity forms, making it an appealing low-cost alternative to other natural polysaccharides (i.e., hyaluronic acid and chondroitin sulfate) and inert polymers, such as poly(ethylene glycol), currently used in tissue engineering applications. Additionally, as a derivative of the plant-based polysaccharide, cellulose, CMC represents a renewable, environmentally-friendly biomaterial. At physiological pH, the carboxylic acid of the carboxymethyl group is deprotonated, resulting in a negatively-charged polymer network, similar to that provided by the GAGs in the ECM of cartilaginous tissues, such as the NP. In addition, the hydrolysis of periodic ester crosslinks between methacrylated CMC chains under physiologic conditions provides void space for the accumulation of secreted matrix macromolecules while maintaining sufficient structural integrity³⁷. Furthermore, photocrosslinked CMC hydrogels have been shown to support NP cell viability and promote phenotypic matrix production³⁷.

In this study, the effects of two variables, medium formulation and supplementation with TGF- β_3 , were examined by comparing a standard serum-containing medium to a chemically-defined, serum-free medium first described by Mackay et al.⁴⁶.

In general, the addition of TGF- β_3 resulted in enhanced matrix deposition by both groups (DMEM+ and CDM+), in support of our hypothesis. As a result of the marked temporal increases in wet and dry weight, Q_w for both TGF- β_3 -treated groups at day 28 was 22.44 ± 0.71 , closely approaching the Q_w for the native NP tissue (19.94 ± 3.09 , unpublished data).

Although similar overall trends were observed in comparison to corresponding untreated controls for both DMEM+ and CDM+ samples, the effect of base medium (DMEM versus CDM) was clearest when measuring ECM components most often associated with the NP phenotype. The combination of CDM and TGF- β_3 resulted in dramatic increases in GAG accumulation. By day 28, CDM+ samples retained 9.46 ± 1.51 μg GAG/mg wet weight, while DMEM+ constructs retained less than five times this amount (1.80 ± 0.11 $\mu\text{g}/\text{mg}$) (Figure 3.2). This 28-day value for CDM+ samples is ~40% of that obtained after 16 weeks of *in vivo* culture (24.14 ± 0.71 $\mu\text{g}/\text{mg}$) using a subcutaneous murine pouch model for NP cells encapsulated in alginate at a similar initial seeding density¹⁷. In addition, when normalized to dry weight, CDM+ GAG content approaches 210 $\mu\text{g}/\text{mg}$, also ~40% of that measured in the native NP (~550 $\mu\text{g}/\text{mg}$)⁵².

The distinct effects of CDM media were also evident when examining collagen production. There was no quantifiable COL II present in either untreated or TGF- β_3 -treated DMEM groups, while both CDM groups displayed significant accumulation, in support of our first hypothesis. COL II accumulation was highest in CDM+ samples, though limited to pericellular deposition. In addition, TGF- β_3 supplementation of DMEM resulted in a multilayered ring of fibroblastic cells encapsulating the CMC

hydrogel which stained positive for COL I, contrary to the native NP phenotype (Figure 3.5C). The peripheral cell layer, not observed in any serum-free constructs, may have contributed to the significant increase in DNA content observed for DMEM+ samples. This phenomenon was also reported by Byers et al. when evaluating the effect of TGF- β_3 supplemented DMEM on the development of engineered cartilage. The authors postulated that the external cell layer may have been due to the presence of serum proteins and adhesion molecules which then promoted cell outgrowth and proliferation at the construct periphery⁹.

The increased GAG and COL II deposition observed as a result of TGF- β_3 supplementation also translated into enhanced functional mechanical properties for cell-laden constructs. Consistent with greater matrix deposition, DMEM+ and CDM+ constructs displayed the lowest axial deformation in creep. In examining the transient mechanical response, DMEM+ constructs exhibited the highest σ_{pk} among all groups, although σ_{pk} differed greatly from σ_{eq} for these samples. This disparity in the transient versus equilibrium response may be due to the fibrous ring encircling DMEM+ constructs, as this extra reinforcing layer may have restricted radial distension in compression, thereby requiring a greater force to achieve the given displacement for a prescribed 15% strain. However, the fibrous outer layer was comprised primarily of type I collagen, a protein most effective in resisting tensile forces, and DMEM+ constructs were unable to sustain the compressive peak stress and subsequently underwent a rapid relaxation. In contrast, CDM+ samples equilibrated at a stress closer to their peak stress, indicating an ability to better withstand and carry loads. This property is particularly important for the nucleus pulposus which is under almost constant load due to gravity and

other physiological forces. In agreement with trends observed in GAG and COL II quantification, E_y values were largest for CDM+ samples and significantly greater than all other groups.

Although untreated CDM constructs produced small, but quantifiable amounts of COL II by day 28, which was significantly greater than that produced by untreated DMEM samples, there was no difference in E_y between the untreated groups. This may be due to the fact that both DMEM and CDM constructs produced similar amounts of water-retaining GAGs, as evidenced by the DMMB assay, allowing the scaffold to resist comparable compressive forces through the generation of a hydrostatic swelling pressure. Although immunohistochemical staining indicated a better distributed, more intense CSPG-containing matrix in untreated CDM cultures (Figure 3.3 A, C), this staining technique employs an antibody specific to CSPG, whereas the DMMB assay detects all sulfated GAGs.

The temporal effect of TGF- β_3 delivery was also examined prior to completing this larger study. A subset of DMEM and CDM samples were supplemented with TGF- β_3 for the first two weeks of culture, at which time growth factor delivery was discontinued and constructs were maintained in their respective, untreated medium for an additional two weeks. Material and mechanical properties (Q_w and E_y , respectively) as well as biochemical content (GAGs and DNA) were greater for those specimens than for untreated constructs at 4 weeks, but values were less than those measured for samples with continuous TGF- β_3 supplementation, regardless of medium formulation. These data support the use of steady TGF- β_3 treatment employed in the present investigation but contradict the findings of Byers et al. who reported a superior maturation response of

chondrocyte-laden agarose gels cultured with a transient, two-week exposure to TGF- β_3 in serum-free medium⁹. However, given the differences in cell type and scaffold, it is difficult to make direct comparisons between these two studies.

While growth factor supplementation is commonly recognized as a required additive to stem cell differentiation medium, it is important to acknowledge its utility in the culture of native cells as well. Various growth factors have been shown to affect IVD cell matrix deposition. A systematic study by Alini et al. examined the effects of various combinations of growth factors on annulus fibrosus (AF) and NP cells cultured on a 3-D fibrous collagen-hyaluronan scaffold⁵³. The growth factors examined included TGF- β_1 , basic fibroblast growth factor (bFGF), and insulin-like growth factor (IGF)-1 in serum-free DMEM. This study found that although the combination of TGF- β_1 and bFGF produced the greatest increase in retained chondroitin sulfate, this value never exceeded 10% of the native NP, even after 60 days of culture. An investigation by Risbud et al. compared the effects of TGF- β_1 and TGF- β_3 on whole disc culture in DMEM with 10% fetal calf serum over one week and found that TGF- β_3 produced a differential increase in the expression of critical matrix genes and elevated proteoglycan synthesis¹¹. A study by Zhang et al. examined the effects of TGF- β_1 and IGF-1 on NP proliferation when grown in monolayer in F12 medium with 1% or 10% FBS⁵⁴. This work noted morphologic changes characteristic of nutrient deficiency when cultured in 1% FBS; however, cell morphology returned to normal when the low serum medium was supplemented with TGF- β_1 . Using a gene therapy approach, Lee and coworkers conducted an experiment examining the efficacy of pellet culture as an alternative to alginate bead culture, assessing matrix production by IVD cells transduced with a TGF- β_1 adenovirus⁵⁵. After

3 weeks *in vitro*, both culture systems experienced increased proteoglycan synthesis with the most pronounced increases observed in pellet culture. In our investigation, we utilized a serum-free, chemically-defined medium formulation supplemented with TGF- β_3 based on previous work in which articular chondrocytes encapsulated in agarose hydrogels exhibited improved matrix elaboration and mechanical properties under such conditions^{9, 12}. Further experiments may evaluate the response to additional growth factors, including IGF-1 and bFGF, by NP cells encapsulated in CMC hydrogels.

As with all experiments, there were potential limitations to this study. The effects of many growth factors on cells of the IVD, including bFGF, IGF-1, and TGF- β_1 , have been previously examined and are described above. Our study focused on the effect of just one growth factor, TGF- β_3 . However, this molecule was chosen because it has been shown to be highly effective in promoting a chondrogenic phenotype when delivered using serum-free medium^{9, 12}. Another limitation to this study is that matrix biosynthesis was not assessed, rather, only matrix accumulation. Quantifying matrix production through radiolabeling techniques and assaying the culture medium for GAG and collagen content would allow us to discern whether increased ECM biosynthesis or the ability of the scaffold to retain elaborated matrix molecules were responsible for the development of improved functional properties of CDM+ constructs. Additionally, examining gene expression would help determine if the differences observed in protein accumulation as a function of medium and growth factor supplementation are initiated at the transcriptional level.

Although many studies have described enhanced matrix deposition by IVD cells following growth factor supplementation, the effects of these cytokines on the functional

properties of the tissue-engineered constructs were not evaluated. Our study has shown a differential effect of both medium formulation and TGF- β_3 supplementation on cell-laden CMC hydrogel constructs, as the combination of serum-free medium and TGF- β_3 produced marked increases in GAG and COL II content and E_y , with the measured value of E_y comparable to that reported for the native NP⁵⁶. However, straight comparisons between studies are difficult due to the differences in medium formulation and scaffold selection. Future work will examine the effects of mechanical stimulation (i.e., hydrostatic pressurization)⁵⁷⁻⁶² to further increase GAG content in an attempt to match that of the native NP and enhance COL II distribution, as pressure has been shown to improve chondrogenic differentiation of mesenchymal stem cells when used in conjunction with TGF- β_3 supplemented, serum-free medium⁴⁷. Additional studies will assess matrix elaboration and functional properties of NP cell-laden CMC hydrogels following *in vivo* subcutaneous implantation⁶³, prior to use in a clinically relevant IVD degeneration model.

Taken together, these findings suggest that photocrosslinked CMC hydrogels support functional ECM assembly by encapsulated NP cells, which can be enhanced when cultured in serum-free, chemically-defined medium supplemented with TGF- β_3 . This system may eventually have application in intradiscal nucleus replacement therapy.

3.5. References

1. Buckwalter JA, Mow VC, Boden SD, Eyre DR and Weidenbaum M. 2000. "Intervertebral disk structure, composition, and mechanical function." In:

- Orthopaedic Basic Science. Edited by Buckwalter JA, Einhorn TA and Simon SR. 2nd ed. Rosemont, IL: American Academy of Orthopaedic Surgeons. p 547-556.
2. Hall SJ. 2003. In: Basic Biomechanics. Boston: McGraw-Hill. p 276-282.
 3. Urban JPG, Smith S and Fairbank JCT. 2004. Nutrition of the intervertebral disc. *Spine* **29(23)**: 2700-2709.
 4. Larson JW, Levicoff EA, Gilbertson LG and Kang JD. 2006. Biologic modification of animal models of intervertebral disc degeneration. *J Bone Joint Surg Am* **88 (Suppl 2)**: 83-87.
 5. Raj PP. 2008. Intervertebral disc: anatomy-physiology-pathophysiology-treatment. *Pain Pract* **8(1)**: 18-44.
 6. Buckwalter J. 1998. Do intervertebral discs deserve their bad reputation? *Iowa Orthop J* **18**: 1-11.
 7. Trout JJ, Buckwalter JA and Moore KC. 1982. Ultrastructure of the human intervertebral disc: II. Cells of the nucleus pulposus. *Anat Rec* **204(4)**: 307-314.
 8. Buckwalter JA, Boden SD, Eyre DR, Mow VC and Weidenbaum M. 2000. "Intervertebral disk aging, degeneration, and herniation." In: Orthopaedic Basic Science. Edited by Buckwalter JA, Einhorn TA and Simon SR. 2nd ed. Rosemont, IL: American Academy of Orthopaedic Surgeons. p 557-566.
 9. Byers BA, Mauck RL, Chiang IE and Tuan RS. 2008. Transient exposure to transforming growth factor beta 3 under serum-free conditions enhances the biomechanical and biochemical maturation of tissue-engineered cartilage. *Tissue Eng Part A* **14(11)**: 1821-1834.

10. Roberts AB. 1998. Molecular and cell biology of TGF-beta. *Miner Electrolyte Metab* **24(2-3)**: 111-119.
11. Risbud MV, Di Martino A, Guttapalli A, Seghatoleslami R, Denaro V, Vaccaro AR, Albert TJ and Shapiro IM. 2006. Toward an optimum system for intervertebral disc organ culture: TGF-beta 3 enhances nucleus pulposus and annulus fibrosus survival and function through modulation of TGF-beta-R expression and ERK signaling. *Spine* **31(8)**: 884-890.
12. Lima EG, Bian L, Ng KW, Mauck RL, Byers BA, Tuan RS, Ateshian GA and Hung CT. 2007. The beneficial effect of delayed compressive loading on tissue-engineered cartilage constructs cultured with TGF-beta3. *Osteoarthritis Cartilage* **15(9)**: 1025-1033.
13. Chou AI and Nicoll SB. 2009. Characterization of photocrosslinked alginate hydrogels for nucleus pulposus cell encapsulation. *J Biomed Mater Res A* **91A(1)**: 187-194.
14. Gan JC, Ducheyne P, Vresilovic EJ and Shapiro IM. 2003. Intervertebral disc tissue engineering II: cultures of nucleus pulposus cells. *Clin Orthop Relat Res* **411**: 315-324.
15. Korecki CL, Kuo CK, Tuan RS and Iatridis JC. 2008. Intervertebral disc cell response to dynamic compression is age and frequency dependent. *J Orthop Res* **27(6)**: 800-806.
16. Miyamoto K, An HS, Sah RL, Akeda K, Okuma M, Otten L, Thonar EJ and Masuda K. 2005. Exposure to pulsed low intensity ultrasound stimulates

- extracellular matrix metabolism of bovine intervertebral disc cells cultured in alginate beads. *Spine* **30(21)**: 2398-2405.
17. Mizuno H, Roy AK, Zaporozjan V, Vacanti CA, Ueda M and Bonassar LJ. 2006. Biomechanical and biochemical characterization of composite tissue-engineered intervertebral discs. *Biomaterials* **27(3)**: 362-370.
 18. Séguin CA, Gryn timer MD, Pilliar RM, Waldman SD and Kandel RA. 2004. Tissue engineered nucleus pulposus tissue formed on a porous calcium polyphosphate substrate. *Spine* **29(12)**: 1299-1306.
 19. Price PJ and Gregory EA. 1982. Relationship between *in vitro* growth promotion and biophysical and biochemical properties of the serum supplement. *In Vitro* **18(6)**: 576-584.
 20. Honn KV, Singley JA and Chavin W. 1975. Fetal bovine serum: a multivariate standard. *Proc Soc Exp Biol Med* **149(2)**: 344-347.
 21. Kisiday JD, Kurz B, DiMicco MA and Grodzinsky AJ. 2005. Evaluation of medium supplemented with insulin-transferrin-selenium for culture of primary bovine calf chondrocytes in three-dimensional hydrogel scaffolds. *Tissue Eng* **11(1-2)**: 141-151.
 22. Baer AE, Wang JY, Kraus VB and Setton LA. 2001. Collagen gene expression and mechanical properties of intervertebral disc cell-alginate cultures. *J Orthop Res* **19(1)**: 2-10.
 23. Gruber HE, Fisher EC, Desai B, Stasky AA, Hoelscher G and Hanley EN. 1997. Human intervertebral disc cells from the annulus: three-dimensional culture in agarose or alginate and responsiveness to TGF- β_1 . *Exp Cell Res* **235(1)**: 13-21.

24. Maldonado BA and Oegema TRJ. 1992. Initial characterization of the metabolism of intervertebral disc cells encapsulated in microspheres. *J Orthop Res* **10(5)**: 677-690.
25. Melrose J, Smith S, Ghosh P and Taylor TKF. 2001. Differential expression of proteoglycan epitopes and growth characteristics of intervertebral disc cells grown in alginate bead culture. *Cells Tissues Organs* **168(3)**: 137-146.
26. Wang JY, Baer AE, Kraus VB and Setton LA. 2001. Intervertebral disc cells exhibit differences in gene expression in alginate and monolayer culture. *Spine* **26(16)**: 1747-1751.
27. Orive G, Ponce S, Hernández RM, Gascón AR, Igartua M and Pedraz JL. 2002. Biocompatibility of microcapsules for cell immobilization elaborated with different type of alginates. *Biomaterials* **23(18)**: 3825-3831.
28. Smeds KA, Pfister-Serres A, Miki D, Dastgheib K, Inoue M, Hatchell DL and Grinstaff MW. 2001. Photocrosslinkable polysaccharides for *in situ* hydrogel formation. *J Biomed Mater Res* **54(1)**: 115-121.
29. Burdick JA, Chung C, Jia X, Randolph MA and Langer R. 2005. Controlled degradation and mechanical behavior of photopolymerized hyaluronic acid networks. *Biomacromolecules* **6(1)**: 386 -391.
30. Nettles DL, Vail TP, Morgan MT, Grinstaff MW and Setton LA. 2004. Photocrosslinkable hyaluronan as a scaffold for articular cartilage repair. *Ann Biomed Eng* **32(3)**: 391-397.

31. Chung C, Mesa J, Miller GJ, Randolph MA, Gill TJ and Burdick JA. 2006. Effects of auricular chondrocyte expansion on neocartilage formation in photocrosslinked hyaluronic acid networks. *Tissue Eng* **12(9)**: 2665-2673.
32. Roughley P, Hoemann C, DesRosiers E, Mwale F, Antoniou J and Alini M. 2006. The potential of chitosan-based gels containing intervertebral disc cells for nucleus pulposus supplementation. *Biomaterials* **27(3)**: 388-396.
33. Di Martino A, Sittinger M and Risbud MV. 2005. Chitosan: a versatile biopolymer for orthopaedic tissue-engineering. *Biomaterials* **26(30)**: 5983-5990.
34. Liu Y, Shu XZ and Prestwich GD. 2006. Osteochondral defect repair with autologous bone marrow-derived mesenchymal stem cells in an injectable, *in situ*, cross-linked synthetic extracellular matrix. *Tissue Eng* **12(12)**: 3405-3416.
35. Li Q, Williams CG, Sun DDN, Wang J, Leong K and Elisseeff JH. 2004. Photocrosslinkable polysaccharides based on chondroitin sulfate. *J Biomed Mater Res A* **68(1)**: 28-33.
36. Ogushi Y, Sakai S and Kawakami K. 2007. Synthesis of enzymatically-gellable carboxymethylcellulose for biomedical applications. *J Biosci Bioeng* **104(1)**: 30-33.
37. Reza AT and Nicoll SB. 2009. Characterization of novel photocrosslinked carboxymethylcellulose hydrogels for encapsulation of nucleus pulposus cells. *Acta Biomater* doi:10.1016/j.actbio.2009.1006.1004.
38. Chou AI, Bansal A, Miller GJ and Nicoll SB. 2006. The effect of serial monolayer passaging on the collagen expression profile of outer and inner annulus fibrosus cells. *Spine* **31(17)**: 1875-1881.

39. Chou AI, Reza AT and Nicoll SB. 2008. Distinct intervertebral disc cell populations adopt similar phenotypes in three-dimensional culture. *Tissue Eng Part A* **14(12)**: 2079-2087.
40. Iwasa J, Ochi M, Uchio Y, Katsube K, Adachi N and Kawasaki K. 2003. Effects of cell density on proliferation and matrix synthesis of chondrocytes embedded in atelocollagen gel. *Artif Organs* **27(3)**: 249-255.
41. Mauck RL, Seyhan SL, Ateshian GA and Hung CT. 2002. Influence of seeding density and dynamic deformational loading on the developing structure/function relationships of chondrocyte-seeded agarose hydrogels. *Ann Biomed Eng* **30(8)**: 1046-1056.
42. Chang SCN, Rowley JA, Tobias G, Genes NG, Roy AK, Mooney DJ, Vacanti CA and Bonassar LJ. 2001. Injection molding of chondrocyte/alginate constructs in the shape of facial implants. *J Biomed Mater Res* **55(4)**: 503-511.
43. Puelacher WC, Kim SW, Vacanti JP, Schloo B, Mooney D and Vacanti CA. 1994. Tissue-engineered growth of cartilage: the effect of varying the concentration of chondrocytes seeded onto synthetic polymer matrices. *Int J Oral Maxillofac Surg* **23(1)**: 49-53.
44. Vunjak-Novakovic G, Obradovic B, Martin I, Bursac PM, Langer R and Freed LE. 1998. Dynamic cell seeding of polymer scaffolds for cartilage tissue engineering. *Biotechnol Prog* **14(2)**: 193-202.
45. Hung CT, Mauck RL, Wang CC, Lima EG and Ateshian GA. 2004. A paradigm for functional tissue engineering of articular cartilage via applied physiologic deformational loading. *Ann Biomed Eng* **32(1)**: 35-49.

46. Mackay AM, Beck SC, Murphy JM, Barry FP, Chichester CO and Pittenger MF. 1998. Chondrogenic differentiation of cultured human mesenchymal stem cells from marrow. *Tissue Eng* **4(4)**: 415-428.
47. Miyanishi K, Trindade MCD, Lindsey DP, Beaupré GS, Carter DR, Goodman SB, Schurman DJ and Smith RL. 2006. Effects of hydrostatic pressure and transforming growth factor-beta 3 on adult human mesenchymal stem cell chondrogenesis *in vitro*. *Tissue Eng* **12(6)**: 1419-1428.
48. Singer VL, Jones LJ, Yue ST and Haugland RP. 1997. Characterization of PicoGreen reagent and development of a fluorescence-based solution assay for double-stranded DNA quantitation. *Anal Biochem* **249(2)**: 228-238.
49. Farndale RW, Sayers CA and Barrett AJ. 1982. A direct spectrophotometric microassay for sulfated glycosaminoglycans in cartilage cultures. *Connect Tissue Res* **9(4)**: 247-248.
50. Enobakhare BO, Bader DL and Lee DA. 1996. Quantification of sulfated glycosaminoglycans in chondrocyte/alginate cultures, by use of 1,9-dimethylmethylene blue. *Anal Biochem* **243(1)**: 189-191.
51. Soltz MA and Ateshian GA. 1998. Experimental verification and theoretical prediction of cartilage interstitial fluid pressurization at an impermeable contact interface in confined compression. *J Biomech* **31(10)**: 927-934.
52. Antoniou J, Steffen T, Nelson F, Winterbottom N, Hollander AP, Poole RA, Aebi M and Alini M. 1996. The human lumbar intervertebral disc: evidence for changes in the biosynthesis and denaturation of the extracellular matrix with growth, maturation, ageing, and degeneration. *J Clin Invest* **98(4)**: 996-1003.

53. Alini M, Li W, Markovic P, Aebi M, Spiro RC and Roughley PJ. 2003. The potential and limitations of a cell-seeded collagen/hyaluronan scaffold to engineer an intervertebral disc-like matrix. *Spine* **28(5)**: 446-454.
54. Zhang R, Ruan D and Zhang C. 2006. Effects of TGF-beta1 and IGF-1 on proliferation of human nucleus pulposus cells in medium with different serum concentrations. *J Orthop Surg Res* **1**: 9.
55. Lee JY, Hall R, Pelinkovic D, Cassinelli E, Usas A, Gilbertson L, Huard J and Kang J. 2001. New use of a three-dimensional pellet culture system for human intervertebral disc cells: initial characterization and potential use for tissue engineering. *Spine* **26(21)**: 2316-2322.
56. Cloyd JM, Malhotra NR, Weng L, Chen W, Mauck RL and Elliott DM. 2007. Material properties in unconfined compression of human nucleus pulposus, injectable hyaluronic acid-based hydrogels and tissue engineering scaffolds. *Eur Spine J* **16(11)**: 1892-1898.
57. Reza AT and Nicoll SB. 2008. Hydrostatic pressure differentially regulates outer and inner annulus fibrosus cell matrix production in 3D scaffolds. *Ann Biomed Eng* **36(2)**: 204-213.
58. Hutton WC, Elmer WA, Boden SD, Hyon S, Toribatake Y, Tomita K and Hair GA. 1999. The effect of hydrostatic pressure on intervertebral disc metabolism. *Spine* **24(15)**: 1507-1515.
59. Hutton WC, Elmer WA, Bryce LM, Kozlowska EE, Boden SD and Kozlowski M. 2001. Do the intervertebral disc cells respond to different levels of hydrostatic pressure? *Clin Biomech* **16(9)**: 728-734.

60. Kasra M, Goel V, Martin J, Wang S-T, Choi W and Buckwalter J. 2003. Effect of dynamic hydrostatic pressure on rabbit intervertebral disc cells. *J Orthop Res* **21(4)**: 597-603.
61. Neidlinger-Wilke C, Würtz K, Liedert A, Schmidt C, Börm W, Ignatius A, Wilke H-J and Claes L. 2005. A three-dimensional collagen matrix as a suitable culture system for the comparison of cyclic strain and hydrostatic pressure effects on intervertebral disc cells. *J Neurosurg Spine* **2(4)**: 457-465.
62. Neidlinger-Wilke C, Würtz K, Urban JPG, Börm W, Arand M, Ignatius A, Wilke H-J and Claes LE. 2006. Regulation of gene expression in intervertebral disc cells by low and high hydrostatic pressure. *Eur Spine J* **15 (Suppl 3)**: S372-378.
63. Chou AI, Akintoye SO and Nicoll SB. 2009. Photo-crosslinked alginate hydrogels support enhanced matrix accumulation by nucleus pulposus cells *in vivo*. *Osteoarthritis Cartilage* **17(10)**: 1377-1384.

Chapter 4: Hydrostatic Pressure Modulates Collagen Production but Does Not Affect the Functional Properties of Nucleus Pulposus Cell-laden Carboxymethylcellulose Hydrogel Constructs

4.1. Introduction

The intervertebral disc (IVD) is a fibrocartilaginous tissue located between the vertebrae of the spine, which functions to permit motion and flexibility. The IVD is a heterogeneous tissue comprised of the collagenous, lamellar annulus fibrosus, and the central gel-like nucleus pulposus (NP). The NP is primarily composed of negatively charged, water-retaining proteoglycans, such as aggrecan, and type II collagen, resulting in a highly hydrated tissue that allows the IVD to support and distribute loads through the generation of a hydrostatic swelling pressure¹.

IVD degeneration, a pathological condition frequently associated with back pain, often results from traumatic injury or occurs naturally with aging and is characterized by a decrease in aggregating proteoglycans². This alteration in the biochemical composition of the disc results in a decreased ability to retain water, which thus renders the disc more fibrous in structure and content³ and may hinder the ability to sustain loads placed upon the body⁴. Similar to articular cartilage, the IVD is a largely avascular, aneural tissue, dependent upon bulk diffusion for nutrient transport⁵. However, a fibrotic, degenerated

IVD impedes nutrient diffusion and waste removal, which further compromises the overall health of the tissue and additionally limits the capacity for self-repair.

Tissue engineering strategies may provide a biologic alternative capable of restoring both the structure and mechanical function of the IVD. Growth factor supplementation can affect the maturation of such tissue engineered constructs, as has been shown utilizing transforming growth factor-beta 3 (TGF- β_3)⁶⁻⁸. TGF- β_3 is known to improve the functional properties of tissue engineered cartilage constructs, increasing the compressive moduli and proteoglycan content of chondrocyte-seeded agarose hydrogels to values comparable to native tissue levels^{7, 8}. Additionally, work in our lab has shown that serum-free, chemically-defined medium supplemented with TGF- β_3 resulted in increased glycosaminoglycan (GAG) and type II collagen accumulation and enhanced functional properties by NP cells encapsulated in photocrosslinked carboxymethylcellulose (CMC) hydrogels⁶.

NP construct development may also be modulated through the application of mechanical loads to mimic those experienced *in vivo*. Deformational loading applied at physiologic magnitudes and frequencies has been reported to have beneficial effects, increasing production of extracellular matrix (ECM) macromolecules, including type II collagen and GAGs, and decreasing production of catabolic factors in the NP^{9, 10}. Hydrostatic pressurization has similarly been shown to affect matrix production by NP tissue. An early study by Ishihara et al. found a stimulatory effect of a short term (20s) application of 1 MPa hydrostatic pressure, while pressurization at 10 MPa inhibited sulfate incorporation of NP tissue fractions¹¹. A subsequent investigation by Handa et al. determined that physiologic levels of hydrostatic pressure stimulated proteoglycan

synthesis in NP tissue fractions while inhibiting production of matrix metalloproteinases (MMPs)¹². Pressures applied outside of the physiologic range of 0.1-3 MPa reduced proteoglycan synthesis and increased the production of catabolic factors.

Hydrostatic pressure has also been shown to enhance the development of IVD tissue engineered constructs when applied *in vitro*. NP cells encapsulated in collagen or polysaccharide-based hydrogel scaffolds have been reported to respond to hydrostatic pressurization with increased production of collagen and GAGs when subjected to physiologic ranges of mechanical stimulation (0.1 – 3.0 MPa)¹³⁻¹⁶. For example, a study by Neidlinger-Wilke et al. found that NP cells encapsulated in collagen gels increased aggrecan gene expression and decreased expression of MMPs in response to 0.25 MPa hydrostatic pressure applied at a frequency of 0.1 Hz¹⁵.

Recent studies have also examined the effect of combining growth factor supplementation and mechanical stimulation on the matrix production and functional properties of engineered constructs for various orthopaedic tissues. Mauck et al. investigated the effects of dynamic deformational loading and supplementation with TGF- β_1 or insulin-like growth factor-1 on the development of articular chondrocytes seeded in agarose and showed a synergistic effect, as proteoglycan and collagen content and mechanical properties all increased over controls when subjected to mechanical stimulation in the presence of growth factors¹⁷. Elder and Athanasiou also found a synergistic effect between static hydrostatic pressure and TGF- β_1 supplementation on GAG accumulation, collagen content, and functional properties of articular chondrocytes encapsulated in agarose hydrogels¹⁸. Gunjaa et al. similarly reported increased collagen and GAG deposition and enhanced compressive properties of meniscus cell-seeded

poly(L-lactic acid) scaffolds that were subjected to static hydrostatic pressure and cultured with TGF- β_1 ¹⁹.

Therefore, the objective of this study was to examine the effects of hydrostatic pressurization and TGF- β_3 supplementation on the matrix production and functional properties of NP cells encapsulated in photocrosslinked CMC hydrogels. We hypothesized that the application of dynamic hydrostatic pressure would increase the matrix accumulation (GAGs, type II collagen) and functional properties of NP cell-laden constructs and that these values would be further enhanced by TGF- β_3 supplementation.

4.2. Materials and Methods

4.2.1. Macromer Synthesis

Methacrylated carboxymethylcellulose was synthesized through esterification of hydroxyl groups based on previously described protocols²⁰⁻²³. Briefly, a 20-fold excess of methacrylic anhydride (Sigma, St. Louis, MO) was reacted with a 1 wt% solution of 250 kDa CMC (Sigma) in RNase/DNase-free water over 24 hours at 4°C. The pH was periodically adjusted to 8.0 using 3N NaOH to modify hydroxyl groups of the polymer with functional methacrylate groups. The modified CMC solution was purified via dialysis for 96 hours against RNase/DNase-free water (Spectra/Por1, MW 5-8 kDa, Rancho Dominguez, CA) to remove excess, unreacted methacrylic anhydride. Purified methacrylated CMC was recovered by lyophilization and stored at -20°C. The degree of substitution was confirmed using ¹H-NMR (360 MHz, DMX360, Bruker, Madison, WI) following acid hydrolysis of purified methacrylated CMC²². Molar percent of

methacrylation was determined by the relative integrations of methacrylate proton peaks (methylene, $\delta = 6.2$ ppm and 5.8 ppm and the methyl peak, $\delta = 2.0$ ppm) to carbohydrate protons.

4.2.2. *Primary Cell Culture and Isolation*

All cell culture supplies, including media, antibiotics, and buffering agents, were purchased from Invitrogen (Carlsbad, CA) unless otherwise noted. Discs C2-C4 were isolated from bovine caudal IVDs obtained from a local abattoir, and the NP was separated through gross visual inspection based on previous protocols^{24, 25}. Tissue was maintained in Dulbecco's Modified Eagle Medium (DMEM) supplemented with 20% fetal bovine serum (FBS) (Hyclone, Logan, UT), 0.075% sodium bicarbonate, 100 U/mL penicillin, 100 $\mu\text{g}/\text{mL}$ streptomycin, and 0.25 $\mu\text{g}/\text{mL}$ Fungizone reagent at 37°C, 5% CO₂ for two days prior to digestion to ensure no contamination occurred during harvesting. A single serum lot was used for all experiments to reduce potential variability in the cellular response.

Tissue was diced and NP cells were released by collagenase (Type IV, Sigma) digestion at an activity of 7000 U collagenase per gram of tissue. Following incubation in collagenase, undigested tissue was removed using a 40 μm mesh filter. Cells from multiple levels (C2-C4) were pooled and rinsed in sterile Dulbecco's Phosphate Buffered Saline (DPBS). These primary cells were plated onto tissue culture flasks, designated as passage 0, and maintained in DMEM with 10% FBS, 0.075% sodium bicarbonate, 100 U/mL penicillin, and 100 $\mu\text{g}/\text{mL}$ streptomycin (growth medium). Cells were subcultured twice to obtain the necessary number of cells, and passage 2 cells²⁴ were used in all

experiments, as these cells have been shown to retain phenotypic differences observed *in vivo* up to the second passage²⁵. Medium was changed three times per week.

4.2.3. Cell Encapsulation in Photocrosslinked Hydrogels

Lyophilized methacrylated CMC was sterilized by a 30-minute exposure to germicidal UV light. The sterilized product was then dissolved to 2.75% in filter-sterilized 0.05 wt% photoinitiator, 2-hydroxy-1-[4-(2-hydroxyethoxy)phenyl]-2-methyl-1-propanone (Irgacure 2959, I2959, Ciba Specialty Chemicals, Basel, Switzerland), in sterile DPBS at 4°C. Passage 2 NP cells were resuspended in a small volume of 0.05% I2959 and then homogeneously mixed with dissolved methacrylated CMC at 30×10^6 cells/mL for a final concentration of 2.5%. The seeding density was selected based on previous studies using cell-seeded constructs for engineering of cartilaginous tissues²⁶⁻³⁰. The 2.5% CMC solution was cast in a custom-made glass casting device and exposed to long-wave UV light (EIKO, Shawnee, KS, peak 368 nm, 1.2W) for 10 minutes to produce covalently photocrosslinked hydrogel disks of 5-mm diameter x 2-mm thickness. Each hydrogel was incubated in 1.5 mL of growth medium at 37°C, 5% CO₂. At day 1, growth medium was fully exchanged with chemically defined medium (CDM-), which was comprised of DMEM with 1% insulin-transferrin-selenium + universal culture supplement (BD Biosciences, San Jose, CA), 100 U/mL penicillin, 100 µg/mL streptomycin, 40 µg/mL L-proline (Sigma), 1 mM sodium pyruvate (Mediatech, Inc., Manassas, VA), 50 µg/mL ascorbic acid 2-phosphate (Sigma), and 100 nM dexamethasone (Sigma)³¹. CDM- was further supplemented with 10 ng/mL rhTGF-β₃ (R&D Systems, Minneapolis, MN) (CDM+). The TGF-β₃ concentration utilized was

chosen based on previous IVD and cartilage tissue engineering studies^{7, 8, 31-33}. Media were changed three times per week.

4.2.4. Dynamic Hydrostatic Pressurization

Constructs cultured in CDM- or CDM+ were subjected to dynamic hydrostatic pressure at a magnitude of 2 or 5 MPa and a frequency of 0.5 Hz for four hours a day, five days a week, based on prior studies³⁴⁻³⁶ and were designated as Dyn- or Dyn+. Loading began at day 3 and continued through day 28. Scaffolds were transferred to UV-sterilized, heat-sealed bags (Daigger, Vernon Hills, IL) filled with 10 mL of CDM- during the four hour loading period, and were placed in a water-filled pressure chamber housed at 37°C. Unloaded bagged control (BC) specimens for each condition (i.e., BC- and BC+) were similarly placed in UV-sterilized, heat-sealed bags and maintained in a vessel filled with warmed distilled water in the incubator that contained the pressure device, but were not subjected to mechanical stimulation. After 4 hours, all samples (BC-, BC+, Dyn-, and Dyn+) were removed from the heat-sealed bags, returned to their respective medium formulations, and cultured in tissue culture polystyrene dishes under standard culture conditions (37°C, 5% CO₂).

A custom-designed, stainless steel hydrostatic pressure device based on a prior design was used to apply the specified dynamic loading conditions³⁷. The device consists of a stainless steel pressure chamber filled with distilled water, connected to a stainless steel piston. The piston rod is driven via an air cylinder controlled by double acting solenoid valves in line with a compressed air source (SilentAire Technology, Houston, TX). The device was purged of air bubbles through the repeated advancement of the piston against the chamber medium. Experimental samples were placed in the chamber

medium; the chamber was then filled completely and sealed. Pressure magnitude was specified by the user and feedback-controlled by a LabVIEW program (National Instruments, Austin, TX) custom-written for this application. Frequency was controlled by varying the inlet pressure of air to the device.

Magnitude and frequency were verified using a custom-written MATLAB program. Average maximum and minimum pressures for the 2 MPa study were 2.05 ± 0.17 MPa and 0.12 ± 0.02 MPa, respectively, while the average frequency was 0.55 ± 0.09 Hz. The average maximum and minimum pressures for the 5 MPa study were 4.98 ± 0.05 MPa and 0.21 ± 0.03 MPa, respectively, with an average frequency of 0.49 ± 0.02 Hz. The hydrostatic pressure chamber and bagged control samples were housed in an incubator at 37°C . The hydrostatic pressure device and representative dynamic loading cycles at 2 and 5 MPa are shown in Figure 4.1.

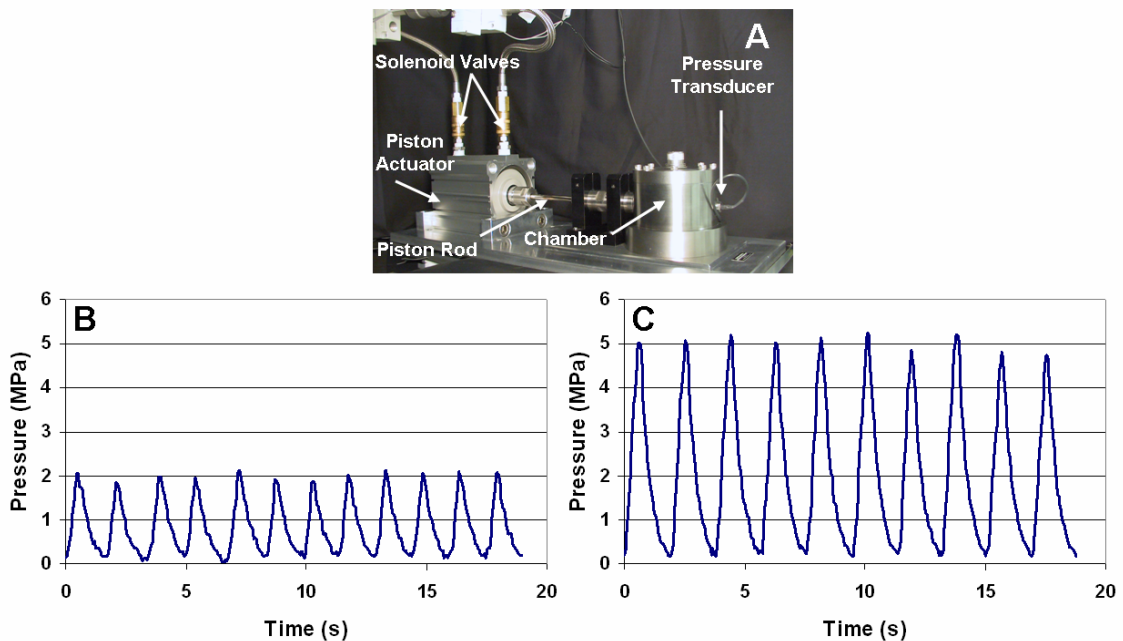


Figure 4.1. Hydrostatic pressure device (A) and representative 2 MPa (B) and 5 MPa (C) dynamic loading cycles.

4.2.5. Swelling Ratio

The equilibrium weight swelling ratio, Q_w , was calculated at day 3 (prior to the start of loading) and day 28 (n=4). Constructs were weighed to determine the wet weight (W_s), lyophilized, and then weighed again to measure the dry weight (W_d). Q_w was calculated using the following equation:

$$Q_w = W_s/W_d$$

4.2.6. Biochemistry

Following lyophilization, total protein and DNA (n=4) were extracted at days 3 and 28 by pepsin digestion based on previous studies²⁵. Briefly, lyophilized samples were homogenized and treated with pepsin (Sigma) in 0.05N acetic acid (1.9 mg/mL) for 48 hrs at 4°C. Afterwards, pepsin was neutralized by the addition of 10X tris buffered saline. Cell-free hydrogels (n=3) were maintained for all groups to serve as negative controls. Total DNA content was measured using the PicoGreen DNA assay³⁸ (Molecular Probes, Eugene, OR) with calf thymus DNA (Sigma) as the standard²⁵. Samples were analyzed at 480 nm excitation and 520 nm emission using a Bio-Tek Instruments microplate reader (Synergy HT™, Winooski, VT).

Total sulfated GAG content was measured at day 3 and day 28 using the 1,9 dimethylmethylene blue (DMMB) assay³⁹. The DMMB dye was reduced to pH 1.5 to minimize the formation of CMC carboxyl group-DMMB dye complexes⁴⁰ and absorbance was determined at 595 nm using a chondroitin-6 sulfate standard curve (Sigma).

Collagen production was quantified at days 3 and 28 via an indirect enzyme-linked immunosorbent assay using monoclonal antibodies to type I collagen (COL I, Sigma) and type II collagen (COL II) (II-II6B3, Developmental Studies Hybridoma Bank, University of Iowa, Iowa City, IA) based on previous protocols²⁵. Protein values for each sample were determined using a standard curve generated from bovine COL I and COL II (Rockland Immunochemicals, Gilbertsville, PA). Absorbance was measured at 450 nm. DNA, GAG, and collagen content are presented normalized to wet weight.

4.2.7. Histology and Immunohistochemistry

Constructs were fixed for 45 minutes in acid formalin at room temperature and processed for paraffin embedding after graded serial ethanol dehydration. Samples were sectioned at a thickness of 8 μm using a Leica microtome (Model 2030, Nussloch, Germany), and hematoxylin and eosin staining was conducted to visualize cellular distribution throughout the hydrogel. Immunohistochemical analyses were performed to assess ECM accumulation according to previous studies²⁵. Briefly, monoclonal antibodies to COL I (1:200 dilution in blocking solution, comprised of 10% horse serum diluted in DPBS), COL II (1:3 dilution in blocking solution, composed of 10% horse serum diluted in DPBS), and chondroitin sulfate proteoglycan (1:100 dilution in blocking solution, consisting of 10% goat serum diluted in DPBS) (CSPG, Sigma) were used, followed by incubation in biotinylated horse/anti-mouse IgG/anti-rabbit IgG (H+L) (COL I, COL II) or biotinylated goat/anti-mouse IgM (CSPG) secondary antibody (1:50 dilution in blocking solution) (Vector Labs, Burlingame, CA). A peroxidase-based detection system (Vectastain Elite ABC, Vector Labs) and 3,3' diaminobenzidine (Vector Labs) were employed to visualize ECM localization. Non-immune controls were

processed in blocking solution without primary antibody. Samples were viewed with a Zeiss Axioskop 40 optical microscope and images were captured using AxioVision software (Carl Zeiss, Inc., Thornwood, NY).

4.2.8. Mechanical Testing

Unconfined compression testing was conducted on CMC hydrogels (n=5) isolated at day 3, prior to the start of loading, and at day 28 using a custom-built apparatus, as previously described^{21, 22, 41}. Briefly, the unconfined compression testing protocol was comprised of a creep test followed by a multi-ramp stress-relaxation test. The creep test consisted of a 1 g tare load applied at a 10 $\mu\text{m/s}$ ramp velocity for 1800 seconds until equilibrium was reached (equilibrium criteria: <10 μm change in 10 minutes). The multi-ramp stress-relaxation test consisted of three 5% strain ramps at a 10 $\mu\text{m/s}$ ramp velocity, each followed by a 2000 second relaxation period (equilibrium criteria: <0.5 g change in 10 minutes). Equilibrium stress was calculated at each ramp using surface area measurements and plotted against the applied strain. An average equilibrium Young's modulus, E_y , was calculated from the slope of the stress versus strain curves and reported for each sample.

4.2.9. Statistical Analysis

A three-way ANOVA was used to determine the effects of time, TGF- β_3 , and hydrostatic pressure on wet weight, dry weight, Q_w , DNA content, GAG and collagen accumulation (n=4), and E_y (n=5). A Tukey's post-hoc test was performed on the three-factor interaction. A two-way ANOVA was used to determine the effects of TGF- β_3 and pressure magnitude (2 MPa vs. 5 MPa) on DNA, GAG, and collagen content (n=4) and

E_y (n=5) at day 28. A Tukey's post-hoc test was performed on the two-factor interaction. Significance was set at $p < 0.05$. Data represent the mean \pm standard deviation. All statistical analyses were performed using JMP software (SAS Institute, Cary, NC). The correlation (r) between GAG or COL II content and E_y was determined in EXCEL using day 3 and day 28 measurements for all groups. The coefficient of determination (R^2) was calculated using a least-squares fitting process for a linear trend line.

4.3. Results

250 kDa CMC was methacrylated at a 5.63% modification, as verified by $^1\text{H-NMR}$. Cell-laden constructs were subjected to dynamic hydrostatic pressure at a magnitude of 2 MPa. Samples were isolated at day 3, prior to beginning pressurization, and at day 28, following the completion of the experiment. All groups (BC-, BC+, Dyn-, and Dyn+) experienced a significant increase in wet weight over time; however, only TGF- β_3 -treated samples exhibited a corresponding increase in dry weight (Table 4.1). Wet weights and dry weights were highest in growth factor-treated samples in comparison to their respective controls. A significant temporal decrease in Q_w was measured for BC+ and Dyn+ groups, whereas the swelling ratio of corresponding untreated controls stayed constant and markedly higher. DNA content significantly decreased in BC- constructs but remained unchanged in Dyn- samples, while DNA content increased in both TGF- β_3 -supplemented groups and was highest in Dyn+ samples.

		Wet Weight (mg)	Dry Weight (mg)	Q _w	DNA/Wet Weight (ng/mg)
BC-	D3	64.52 ± 1.63 + #	1.81 ± 0.16	35.94 ± 2.92	82.27 ± 7.05 +
	D28	69.74 ± 2.10 *	1.97 ± 0.07 *	35.37 ± 0.87 *	61.07 ± 5.34 *
BC+	D3	67.81 ± 2.22 +	1.96 ± 0.07 +	34.62 ± 1.42 +	74.04 ± 4.05 +
	D28	117.32 ± 1.79 #	5.83 ± 0.41	20.18 ± 1.17	128.16 ± 9.98 #
Dyn-	D3	59.70 ± 2.18 * +	1.51 ± 0.17	39.90 ± 5.17	70.75 ± 3.40 *
	D28	67.65 ± 2.02 *	1.64 ± 0.12 *	41.37 ± 3.58 *	73.93 ± 9.13 *
Dyn+	D3	69.32 ± 1.39 +	1.98 ± 0.34 +	35.70 ± 5.41 +	103.32 ± 7.54 +
	D28	122.79 ± 1.18	5.96 ± 0.13	20.61 ± 0.48	151.59 ± 12.26

Table 4.1. Material properties and DNA content of 2 MPa constructs. +: significant effect of time within group. *: significant vs. corresponding TGF- β_3 -treated group within time point (i.e., BC- vs. BC+). #: significant vs. corresponding loaded group within time point (i.e., BC- vs. Dyn-).

GAG content in BC- and Dyn- samples remained unchanged from day 3 measurements, while BC+ and Dyn+ constructs experienced a significant increase in accumulation over time, indicating a marked effect of growth factor treatment (Figure 4.2A). However, there was no effect of mechanical stimulation detected in either group. Immunohistochemical analyses of CSPG conducted at day 28 revealed uniform interterritorial staining in both BC+ and Dyn+ samples (Figure 4.2 D, E). BC- and Dyn- constructs also exhibited some interterritorial staining; however, CSPG deposition in these samples remained strongly localized pericellularly in lacunae (Figure 4.2 B, C).

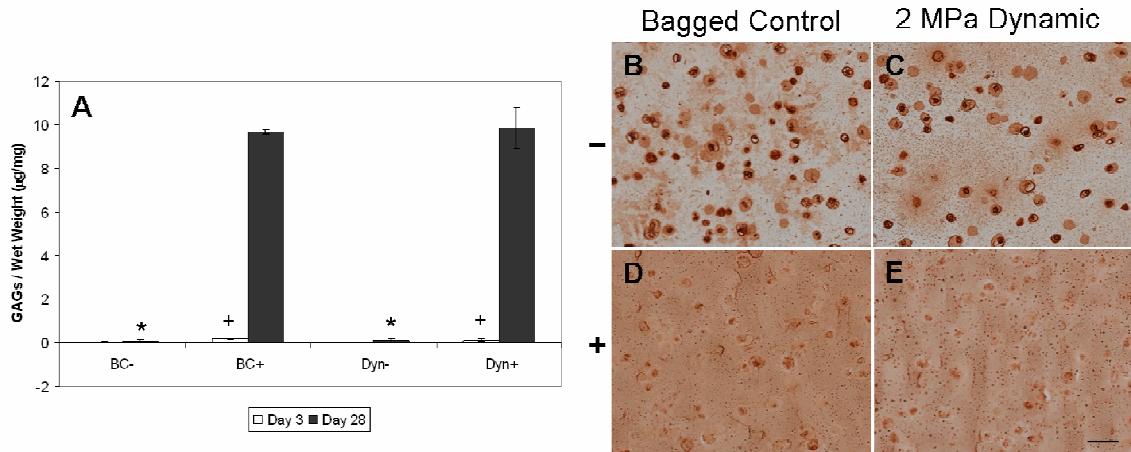


Figure 4.2. GAG quantification (A) and day 28 CSPG deposition of unloaded controls (B, D) and constructs pressurized at 2 MPa (C, E) with (D, E) and without (B, C) TGF- β_3 . Bar = 50 μm . +: significant effect of time within group. *: significant vs. corresponding TGF- β_3 -treated group within time point (i.e., BC- vs. BC+).

There was no detectable COL I in any group throughout the study. COL II content increased over time for all groups, with the highest normalized values observed in BC- samples (Figure 4.3A). There was no effect of loading within TGF- β_3 -treated groups. Immunohistochemical analyses of samples at day 28 verified punctate, intracellular COL II deposition in both BC- and Dyn- samples (Figure 4.3 B, C), while staining in TGF- β_3 -treated groups displayed slightly enhanced distribution into the pericellular matrix (Figure 4.3 D, E).

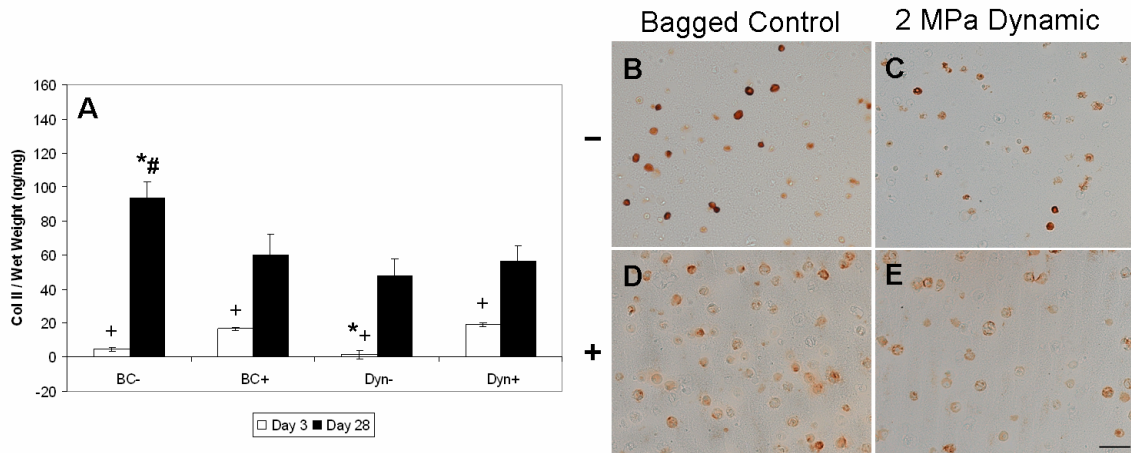


Figure 4.3. COL II quantification (A) and day 28 deposition of unloaded controls (B, D) and constructs pressurized at 2 MPa (C, E) with (D, E) and without (B, C) TGF- β_3 . Bar = 50 μm . +: significant effect of time within group. *: significant vs. corresponding TGF- β_3 -treated group within time point (i.e., BC- vs. BC+). #: significant vs. corresponding loaded group within time point (i.e., BC- vs. Dyn-).

Constructs were tested in unconfined compression to determine the mechanical properties. Hydrogel diameter and thickness measurements at day 28 remained unchanged from day 3 values in BC- and Dyn- samples, with no significant effect of pressurization (5.85 ± 0.13 mm and 2.48 ± 0.06 mm, respectively). By day 28, BC+ and Dyn+ samples displayed increases in both diameter and thickness which were significant in comparison to untreated counterparts (i.e., BC- and Dyn-); however, there was no significant effect of pressurization (6.96 ± 0.20 mm and 3.30 ± 0.09 mm, respectively). BC- and Dyn- constructs maintained initial mechanical properties over the 28-day study, with no significant increase in E_y over time (Figure 4.4). BC+ and Dyn+ samples exhibited a four-fold increase in E_y by day 28, which was significantly greater than their corresponding untreated controls.

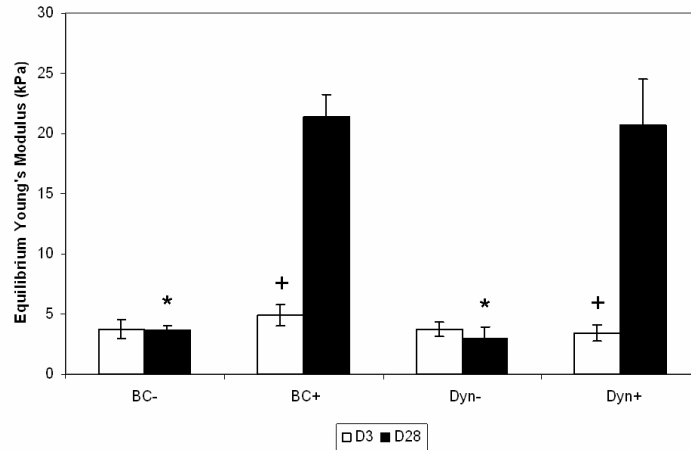


Figure 4.4. Equilibrium Young's modulus of unloaded controls and constructs pressurized at 2 MPa. +: significant effect of time within group. *: significant vs. corresponding TGF- β_3 -treated group within time point (i.e., BC- vs. BC+).

There was no effect of pressurization on the mechanical properties of either untreated or TGF- β_3 -treated scaffolds. Overall, there was a significant positive, linear correlation (r) between GAG content and E_y ($r = 0.98$, $R^2 = 0.96$), while the correlation between COL II deposition and E_y was not as pronounced ($r = 0.68$, $R^2 = 0.46$) (Figure 4.5).

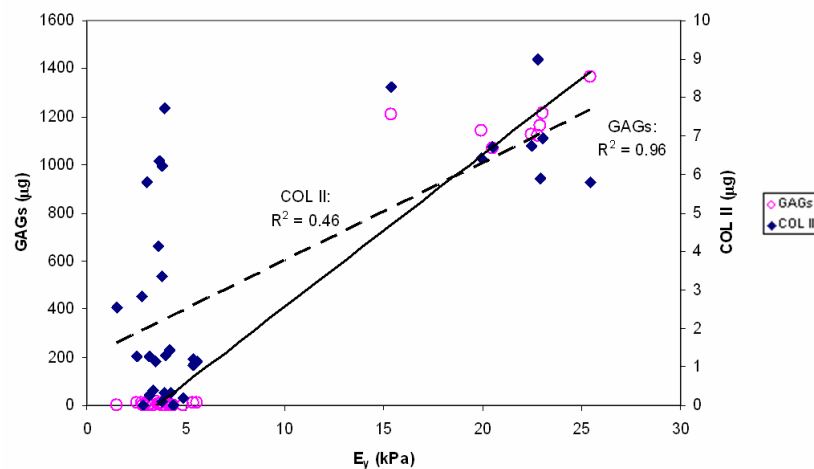


Figure 4.5. Correlation analyses of matrix content and the functional properties of 2 MPa constructs.

Given that hydrostatic pressure applied within the physiologic range (2 MPa) had no effect, the study was repeated at a hyperphysiologic magnitude of 5 MPa. All groups in the 5 MPa experiment experienced a significant increase in wet weight over time, while only TGF- β_3 -treated groups experienced a corresponding temporal increase in dry weight (Table 4.2). Wet weight and dry weight values at day 28 were highest in BC+ and Dyn+ samples, indicating a significant effect of growth factor treatment, with no effect of loading observed. BC+ and Dyn+ constructs also exhibited a significant decrease in Q_w over time, while Q_w stayed at initial values and was significantly higher in BC- and Dyn- samples, with no effect of pressurization for either group. DNA content decreased over time in untreated groups but increased in both BC+ and Dyn+ constructs and was markedly higher than untreated counterparts at day 28, with no effect of pressurization observed between loaded samples and controls.

		Wet Weight (mg)	Dry Weight (mg)	Q_w	DNA/Wet Weight (ng/mg)
BC-	D3	65.00 ± 1.17 +	1.73 ± 0.26	38.14 ± 6.09	90.82 ± 3.90 +
	D28	75.94 ± 4.16 *	1.98 ± 0.12 *	38.47 ± 3.21 *	50.32 ± 8.90 *
BC+	D3	65.26 ± 2.87 +	1.75 ± 0.15 +	37.35 ± 1.83 +	99.72 ± 12.34 +
	D28	118.29 ± 1.47	5.31 ± 0.33	22.34 ± 1.47	132.53 ± 2.81
Dyn-	D3	63.55 ± 0.63 +	1.77 ± 0.09	36.03 ± 2.08	94.17 ± 3.21 +
	D28	75.27 ± 3.31 *	1.80 ± 0.08 *	41.93 ± 2.48 *	49.41 ± 6.16 *
Dyn+	D3	64.34 ± 3.54 +	1.83 ± 0.16 +	35.40 ± 3.60 +	104.72 ± 8.66 +
	D28	123.62 ± 3.87	5.59 ± 0.35	22.17 ± 1.10	123.75 ± 3.90

Table 4.2. Material properties and DNA content of unloaded controls and constructs. pressurized at 5 MPa +: significant effect of time within group. *: significant vs. corresponding TGF- β_3 -treated group within time point (i.e., BC- vs. BC+).

GAG content increased in both TGF- β_3 -treated groups but remained at day 3 values and significantly lower in BC- and Dyn- constructs, with no effect of pressurization at 5 MPa for any group (Figure 4.6A). CSPG immunohistochemical analyses at day 28 revealed interterritorial deposition in both untreated groups with strong pericellular localization in lacunae (Figure 4.6 B, C), while BC+ and Dyn+ samples exhibited uniform interterritorial accumulation throughout the construct (Figure 4.6 D, E).

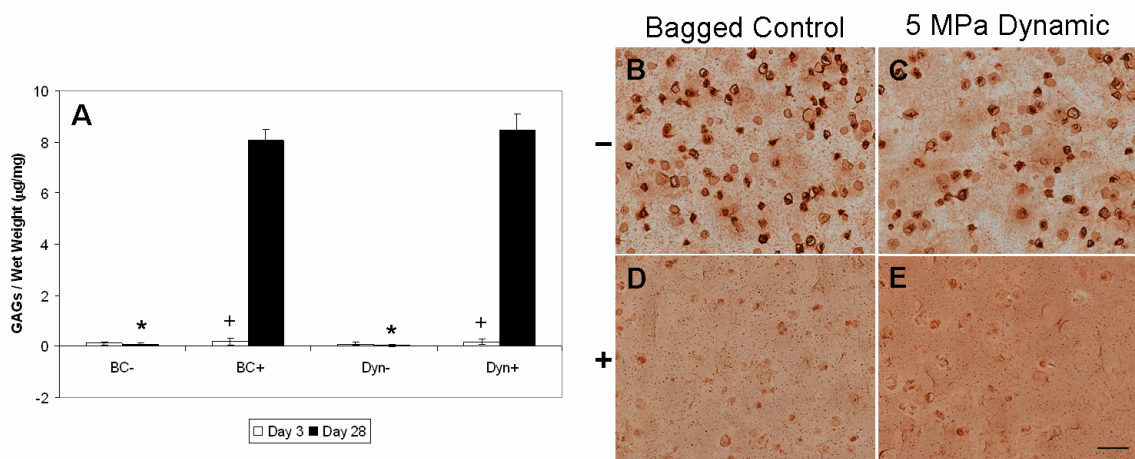


Figure 4.6. GAG quantification (A) and day 28 CSPG deposition of unloaded controls (B, D) and constructs pressurized at 5 MPa (C, E) with (D, E) and without (B, C) TGF- β_3 . Bar = 50 μm . +: significant effect of time within group. *: significant vs. corresponding TGF- β_3 -treated group within time point (i.e., BC- vs. BC+).

All samples were negative for COL I accumulation. Normalized COL II accumulation increased over time for all groups, and was highest in Dyn- samples (Figure 4.7A). COL II content in Dyn- constructs was significantly higher than in corresponding BC- controls, indicating an effect of pressurization; however, there was no effect of load

in TGF- β_3 -treated constructs (BC+ vs. Dyn+). COL II immunohistochemical analyses showed localized intracellular deposition in untreated samples (Figure 4.7 B, C) with improved, though limited, pericellular accumulation in BC+ and Dyn+ constructs (Figure 4.7 D, E).

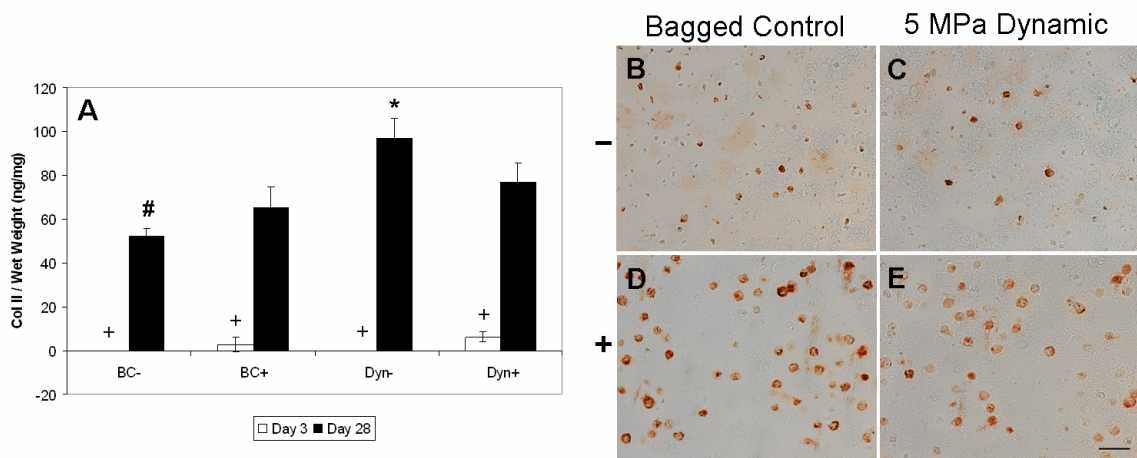


Figure 4.7. COL II quantification (A) and day 28 deposition of unloaded controls (B, D) and constructs pressurized at 5 MPa (C, E) with (D, E) and without (B, C) TGF- β_3 . Bar = 50 μm . +: significant effect of time within group. *: significant vs. corresponding TGF- β_3 -treated group within time point (i.e., BC- vs. BC+). #: significant vs. corresponding loaded group within time point (i.e., BC- vs. Dyn-).

Constructs from the 5 MPa loading experiment were also tested in unconfined compression. All groups experienced a significant increase in diameter over time, with the largest values seen in BC+ and Dyn+ samples, indicating an effect of growth factor treatment. There was, however, no effect of pressurization. The average diameter for untreated constructs at day 28 was 5.81 ± 0.14 mm, while the average diameter of TGF- β_3 -treated samples was 6.78 ± 0.11 mm. Hydrogel thickness increased over time in all groups except Dyn-, and was largest in both TGF- β_3 -treated groups, with no effect of

pressure. The average thickness for untreated constructs at day 28 was 2.50 ± 0.04 mm, while the average thickness in treated samples was 3.32 ± 0.10 . BC- and Dyn- samples exhibited no change from day 3 values for E_y (Figure 4.8). BC+ and Dyn+ samples both experienced a significant increase in E_y by day 28, indicating a marked effect of growth factor treatment, although there was no effect of mechanical stimulation for any group. As seen in the 2 MPa study, overall, there was a strong positive and linear correlation between GAG content and E_y at 5 MPa ($r = 0.95$, $R^2 = 0.91$), while COL II accumulation and E_y were not as directly related ($r = 0.68$, $R^2 = 0.46$) (Figure 4.9).

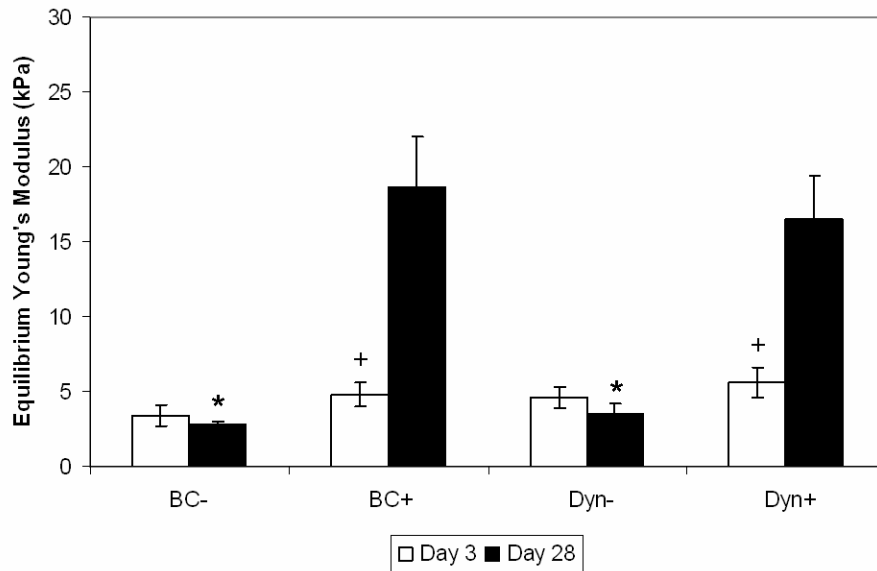


Figure 4.8. Equilibrium Young's modulus of unloaded controls and constructs pressurized at 5 MPa. +: significant effect of time within group. *: significant vs. corresponding TGF- β_3 -treated group within time point (i.e., BC- vs. BC+).

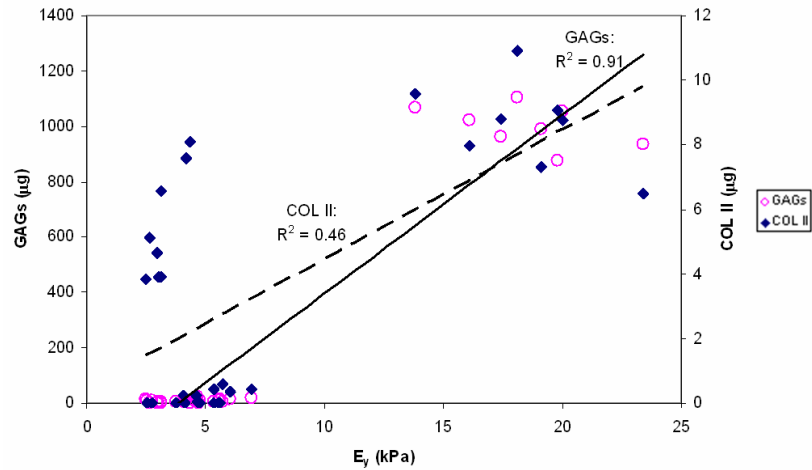


Figure 4.9. Correlation analyses of matrix content and the functional properties of 5 MPa constructs.

The effect of pressure magnitude was also examined to compare the 2 MPa and 5 MPa studies (Table 4.3). Pressurization to 5 MPa resulted in significantly decreased DNA content in Dyn- and Dyn+ groups at day 28, though these values did not differ from corresponding unloaded controls, as well as a slight but significant decrease in GAG content in Dyn+ constructs. However, there was no effect of pressure magnitude on GAG content in Dyn- samples and no effect on the functional properties (E_y) of any group. Pressurization to 5 MPa significantly increased COL II content in both Dyn- and Dyn+ samples.

		2 MPa	5 MPa	5 MPa vs. 2 MPa
DNA/Wet Weight (ng/mg)	Dyn-	73.93 ± 9.13	49.41 ± 6.16	↓
	Dyn+	151.59 ± 12.26	123.75 ± 3.90	↓
GAGs/Wet weight (μg/mg)	Dyn-	0.09 ± 0.08	0.03 ± 0.07	↔
	Dyn+	9.87 ± 0.97	8.48 ± 0.64	↓
Col II/Wet Weight (ng/mg)	Dyn-	47.47 ± 10.08	96.76 ± 9.17	↑
	Dyn+	56.50 ± 8.80	76.96 ± 8.51	↑
E _y (kPa)	Dyn-	3.07 ± 0.95	3.50 ± 0.68	↔
	Dyn+	20.68 ± 3.84	16.53 ± 2.88	↔

Table 4.3. Day 28 pressure magnitude comparison for mechanically stimulated constructs. Significance ($p < 0.05$) vs. 2 MPa indicated by ↓ and ↑ arrows. No significant difference indicated by ↔.

4.4. Discussion

To the best of our knowledge, this is the first study to compare the combinatorial effect of dynamic hydrostatic pressure and TGF- β_3 supplementation on the matrix deposition and functional properties of NP tissue-engineered constructs. Although previous IVD studies examining the effects of hydrostatic pressure on the NP have found a beneficial effect of mechanical stimulation applied within the physiologic range (0.1 – 3 MPa)¹³⁻¹⁶, we saw no effect of pressure when applied at 2 MPa. Instead, TGF- β_3 supplementation was the only variable shown to affect NP construct development, as it gave rise to an increase in dry weight and DNA content and a decrease in Q_w that approached native values ($Q_{w \text{ native}} = 19.94 \pm 3.09$, unpublished data). Additionally, TGF- β_3 supplementation resulted in significant increases in matrix accumulation, as demonstrated by GAG and COL II quantification and immunohistochemistry, and

marked improvements in mechanical properties, in support of our previous study⁶. However, no significant differences in E_y were observed between untreated or TGF- β_3 -treated pressurized samples and corresponding unloaded controls (Dyn- vs. BC- and Dyn+ vs. BC+, respectively), indicating that the structure-function relationships were not positively impacted by pressurization.

Earlier work from our laboratory examined the effect of pressure on outer and inner annulus fibrosus cells seeded on a fibrous poly(L-lactic acid) reinforced poly(glycolic acid) mesh and found significantly increased COL II deposition and improved matrix distribution when pressure was increased to the hyperphysiologic level of 5 MPa, with no effects observed at 2 MPa⁴². Although there is an obvious difference in cell type and scaffold selection, this served as the motivation to repeat the current study at the higher pressure magnitude of 5 MPa.

As with the 2 MPa study, growth factor supplementation had a significant impact on NP construct development at the higher magnitude. TGF- β_3 treatment (Dyn+, BC+) again resulted in a significant increase in dry weight, a marked decrease in Q_w to near native measurements, as well as an increase in DNA content in comparison to untreated pressurized (Dyn-) and control (BC-) groups, which experienced significant decreases in DNA over time. There was, however, no effect of pressure on any of these measurements. Additionally, TGF- β_3 supplementation produced marked improvements in GAG accumulation for both pressurized samples (Dyn+) and unloaded controls (BC+). Nonetheless, there was no effect of 5 MPa dynamic hydrostatic pressure on GAG deposition or distribution.

Interestingly, mechanical stimulation at 5 MPa did give rise to a significant increase in normalized COL II accumulation in untreated constructs (Dyn-). This measurement (96.76 ± 9.17 ng/mg) was nearly double that of untreated, unloaded controls (51.97 ± 3.81 ng/mg), and also exceeded normalized COL II accumulation by TGF- β_3 -treated samples. Pressure did not result in a corresponding increase in accumulation for mechanically stimulated TGF- β_3 -treated scaffolds (Dyn+), indicating that the effects of pressure were muted, rather than additive or synergistic, when accompanied by growth factor supplementation.

Although the application of 5 MPa hydrostatic pressure increased normalized COL II deposition in untreated constructs (Dyn-) over both unloaded controls (BC-) and TGF- β_3 -treated, pressurized samples (Dyn+), this was not accompanied by a pressure-driven increase in mechanical properties (E_y) for Dyn- samples, which remained unchanged from day 3 measurements and indistinguishable from unloaded controls. Furthermore, although normalized COL II measurements were greater in Dyn- specimens in comparison to Dyn+ or BC+ constructs, the growth factor-treated scaffolds retained markedly greater amounts of GAGs and possessed mechanical properties over three-times higher than corresponding untreated controls (Dyn-, BC-). GAG content was found to have a very strong positive correlation with E_y ($r = 0.95$), as the increased amount of water-retaining proteoglycans allowed the constructs to better resist compressive loads, while COL II accumulation did not have as direct an effect ($r = 0.68$).

Even though hydrostatic pressure applied at 5 MPa did not result in any substantial improvements in NP construct development, it is also important to note that mechanical loading at this magnitude did not have any deleterious effects on the cells, as

there was no significant reduction in any of the material, biochemical, or mechanical outcome measures when compared to unloaded controls. Moreover, the application of 5 MPa hydrostatic pressure produced a beneficial response by significantly increasing COL II accumulation in comparison to samples subjected to a pressure at 2 MPa.

Hydrostatic pressure has been previously shown to have an anabolic effect on NP matrix metabolism and may suppress expression of some catabolic factors^{12, 15, 16}; however, there is no clear consensus on the most effective loading regimen. Recent work has examined a variety of magnitudes (0.25-6 MPa) and frequencies (0-20 Hz), duty cycles (30 min/day to 12 hr/day) and loading durations (1 day to 4 weeks)^{13-16, 43-47}. In addition, multiple cell sources (human, bovine, rabbit, porcine, and canine), seeding densities (0.15×10^6 to 20×10^6 cells/mL), and biomaterial scaffolds (alginate, collagen I gel, agarose)^{13-16, 43-47} have been employed, which results in a considerable number of variables that may impact experimental outcomes (Table 4.4).

Many IVD pressure studies have examined the effect of a short term application of hydrostatic pressure on the gene expression or synthesis of relevant matrix macromolecules. A study by Kasra et al. compared the effects of pressure magnitude (0.75, 1.5, and 3 MPa) and frequency (1, 10, and 20 HZ) when applied for 30 minutes/day for 3 days to rabbit NP cells encapsulated in alginate. They found that a high magnitude, high frequency (3 MPa, 20 Hz) load resulted in the greatest increase in collagen production and decreased collagen degradation, despite the fact that a 20 Hz frequency greatly exceeds the physiologic range⁴³. A subsequent experiment by Kasra et al. examined the effect of 1 MPa pressure applied at lower frequencies which spanned the natural frequency of the disc (4-6 Hz)⁴⁴. They reported maximum protein degradation

Table 4.4. The effects of hydrostatic pressure on nucleus pulposus tissue engineered constructs

Author (Year)	NP Cell Source	Scaffold	Seeding Density (cells/mL)	Magnitude (MPa)	Frequency (Hz)	Duty Cycle/Duration	Effect
Hutton (1999) ¹³	Canine	Alginate beads	3x10 ⁶	1	0	continuously for 9 days	↑ collagen and proteoglycan synthesis ↑ aggrecan, COL I, and COL II gene expression No difference in DNA content vs. controls
Hutton (2001) ¹⁴	Canine	Alginate beads	3x10 ⁶	0.35	0	continuously for 9 days	↑ collagen synthesis, ↓ proteoglycan synthesis ↑ COL I, slight ↑ in COL II, ↓ in aggrecan gene expression No difference in DNA content vs. controls Compared to 1999 study at 1 MPa, ↑ proteoglycan synthesis at 1 MPa, but slight ↓ in collagen synthesis
Kasra (2003) ⁴³	Rabbit	Alginate beads	1.5x10 ⁶	0.75, 1.5, and 3	1, 10, 20	30 min/day for 3 days	3 MPa, 20Hz ↑ collagen production, ↓ degradation
Kasra (2006) ⁴⁴	Porcine	Alginate beads	1.5x10 ⁶	1	1, 3, 5, 8, 10	30 min/day for 3 days	↓ DNA at all frequencies Worst synthesis at 3-5 Hz, most degradation at 5 Hz
Neidinger-Wilke (2005) ¹⁵	herniated human	COL I gel	0.15x10 ⁶	0.25	0.1	30 min/day for 4 weeks	Trend for ↑ COL I and aggrecan gene expression ↓ MMP-2 and -3 No effect on COL II
Neidinger-Wilke (2006) ¹⁶	herniated human, Bovine	COL I gel	0.3x10 ⁶	0.25 and 2.5	0.1	30 minutes, once	Trend for ↑ COL I and aggrecan gene expression at 0.25 MPa 2.5 MPa ↓ aggrecan and COL II, ↑ MMP-3 in bovine NP No difference in DNA content vs. controls at either magnitude
Gokorsch (2004) ⁴⁵	Porcine	Agarose	20x10 ⁶	0.4, 3.4, and 6	ON/OFF; 3min/27min 10s/10s	12 hrs/day for 1 week	↑ GAG and collagen accumulation at 0.4 and 3.4 MPa at low frequency ↓ GAG and collagen at 6 MPa at both low and high frequency
Wuertz (2007) ⁴⁶	herniated human	COL I gel	0.3x10 ⁶	0.25	0.1	30 minutes, once	Pressure significantly ↑ aggrecan with trend to ↑ COL II gene expression but only under hypo-osmotic conditions (NP <i>in vivo</i> is hyperosmotic) HP under iso- and hyperosmotic conditions had trend to ↓ aggrecan and COL II
Le Maitre (2008) ⁴⁷	Healthy & degenerate human	Alginate	1x10 ⁶	1.7	0.5	2 hrs, once	Healthy NP ↑ c-fos and aggrecan gene expression, trend for ↑ Sox-9 and COL II No effect on MMP-3 No effect of pressure on degenerate NP cells

and minimum protein synthesis when constructs were pressurized at 3-5 Hz, indicating that loading near the natural frequency of the disc is most destructive. Neidlinger-Wilke et al. examined the effects of low magnitude, low frequency pressure (0.25 MPa, 0.1 Hz) on human NP cells seeded within a type I collagen gel and found little influence of low magnitude pressure, although there was a trend for increased aggrecan and COL I gene expression along with a significant decrease in expression of the matrix degrading enzymes MMP-2 and MMP-3¹⁵. A later investigation by this group compared the effects of pressure magnitude (0.25 vs. 2.5 MPa at 0.1 Hz) when applied once for 30 minutes, and again found minimal impact of low magnitude pressure. However, there was a significant decrease in aggrecan and COL II gene expression and increased MMP-3 expression at 2.5 MPa, indicating a harmful effect on cellular transcriptional activity by the short-term application of a higher magnitude load¹⁶.

In contrast, earlier studies by Hutton et al. comparing the effects 0.35 and 1 MPa pressure applied statically and continuously for 9 days to canine NP cells encapsulated in alginate beads showed enhanced proteoglycan synthesis at the higher magnitude, although there was a slight decrease in collagen synthesis. Nevertheless, it is important to note that this effect was observed after 9 days of continuous loading with no significant decrease in DNA content versus controls^{13, 14}. While many of the studies described above concluded a beneficial effect of hydrostatic pressurization, these experiments were largely short-term and only examined gene expression or protein biosynthesis. The investigators did not determine whether the effects of pressure were effectively translated into differences in protein accumulation or altered the functional mechanical properties of the tissue engineered constructs.

The duty cycle (4 hrs/day for 5 days/week) and loading duration (4 weeks) utilized in our study differ greatly from those described in current NP tissue engineering literature. Nevertheless, they are quite similar to parameters utilized in cartilage tissue engineering and were chosen to allow investigation of the long-term effect of mechanical stimulation on the functional properties of NP constructs. A study by Smith et al. showed that increasing the application of intermittent hydrostatic pressurization (10 MPa, 1 Hz) from four hours per day for one day to four hours per day for four days increased gene expression of both COL II and aggrecan in high density chondrocyte monolayers³⁴. A later study by Ikenoue et al. (5 and 10 MPa, 1 Hz) only observed increases in COL II gene expression when utilizing the longer, four day loading regimen³⁶. Similarly, Hu and Athanasiou measured significant increases in collagen synthesis and a prevention of GAG loss when pressure (10 MPa, 1 Hz) was applied for 4 hours/day, 5 days/week, for up to 8 weeks using self-assembled articular cartilage constructs³⁵. Nonetheless, as our current studies did not show a significant effect of pressure in modulating the functional properties of NP constructs, future work may employ loading parameters that more closely match those shown to be effective in cartilage and IVD tissue engineering (i.e., higher magnitude and frequency).

One potential limitation of this study is that the temporal effect of growth factor delivery was not examined in conjunction with mechanical stimulation. Lima et al. reported a decrease in mechanical properties when dynamic deformational loading was applied concurrently with TGF- β_3 supplementation of chondrocyte-seeded agarose hydrogels over 8 weeks⁷. However, mechanical properties significantly increased when loading was applied following transient growth factor delivery over the first 14 days.

Our study utilized continuous growth factor delivery throughout the experiment as this was previously shown to vastly improve NP construct development when used in conjunction with chemically-defined, serum-free medium⁶.

Deformational mechanical stimulation via dynamic compressive loading may also be investigated in subsequent investigations. This form of loading has been applied via an *in vivo* rat tail model and has been shown to elicit a frequency-dependent response when magnitude was maintained⁹, and a magnitude-dependent response when frequency was held constant⁴⁸. More recently, dynamic compression was applied *in vitro* by Korecki et al. to NP cell-laden alginate hydrogels to compare the effects of frequency (0.1, 1, and 3 Hz) and donor age. They found that maturation was a significant factor in the cellular response to mechanical loading, though the impact of loading frequency was minimal⁴⁹.

While integrins play a principal role in the mechanotransduction of biomechanical signals from the ECM to the cell nucleus in response to deformational loading, hydrostatic pressurization results in a state of stress without appreciable strain, and thereby bypasses known integrin signaling pathways. Rather, it has been hypothesized that the mechanotransduction pathway for hydrostatic pressure involves cell membrane ion channels, since these transmembrane proteins may alter conformation in response to load. Specifically, a study by Hall implicated the sodium/potassium (Na^+/K^+) pump and the $\text{Na}^+/\text{K}^+/\text{Cl}^-$ transporter, as these were significantly inhibited with increasing magnitude when bovine chondrocytes were subjected to static hydrostatic pressure⁵⁰. Another possible conduit involves G-protein coupled receptor activation of phospholipase C, which results in subsequent activation of the membrane phospholipid

cleavage product, IP₃, and mobilization of intracellular calcium stores. When combined with calmodulin, the calcium complex acts as a second messenger to initiate a wide range of downstream responses. Browning et al. showed that the intracellular calcium concentration of chondrocytes increased when subjected to hydrostatic pressurization. This effect was due in large part to a release of intracellular Ca²⁺ stores, as the response was inhibited when phospholipase C activation was blocked⁵¹. Future studies may investigate putative pressure-mediated mechanotransduction pathways in NP cell-laden CMC constructs.

Although others have shown an additive or synergistic effect of mechanical stimulation and growth factor supplementation on the development of constructs for orthopaedic tissue engineering¹⁷⁻¹⁹, TGF-β₃ supplementation was the only variable found to have a significant impact on NP construct maturation using this particular system. Hydrostatic pressure modulated COL II production in untreated samples at hyperphysiologic levels (5 MPa) but did not enhance the functional properties of these constructs, which remained significantly lower than those for unloaded and pressurized TGF-β₃-treated samples. As such, TGF-β₃ supplementation alone is most effective for enhancing the functional development of NP-seeded CMC constructs.

4.5. References

1. Buckwalter JA, Mow VC, Boden SD, Eyre DR and Weidenbaum M. 2000. "Intervertebral disk structure, composition, and mechanical function." In: Orthopaedic Basic Science. Edited by Buckwalter JA, Einhorn TA and Simon SR. 2nd ed. Rosemont, IL: American Academy of Orthopaedic Surgeons. p 547-556.

2. Larson JW, Levicoff EA, Gilbertson LG and Kang JD. 2006. Biologic modification of animal models of intervertebral disc degeneration. *J Bone Joint Surg Am* **88 (Suppl 2)**: 83-87.
3. Raj PP. 2008. Intervertebral disc: anatomy-physiology-pathophysiology-treatment. *Pain Pract* **8(1)**: 18-44.
4. Buckwalter JA, Boden SD, Eyre DR, Mow VC and Weidenbaum M. 2000. "Intervertebral disk aging, degeneration, and herniation." In: Orthopaedic Basic Science. Edited by Buckwalter JA, Einhorn TA and Simon SR. 2nd ed. Rosemont, IL: American Academy of Orthopaedic Surgeons. p 557-566.
5. Urban JPG, Smith S and Fairbank JCT. 2004. Nutrition of the intervertebral disc. *Spine* **29(23)**: 2700-2709.
6. Reza AT and Nicoll SB. 2009. Serum-free, chemically defined medium with TGF- β_3 enhances functional properties of nucleus pulposus cell-laden carboxymethylcellulose hydrogel constructs. *Biotechnol and Bioeng* doi:10.1002/bit.22545.
7. Lima EG, Bian L, Ng KW, Mauck RL, Byers BA, Tuan RS, Ateshian GA and Hung CT. 2007. The beneficial effect of delayed compressive loading on tissue-engineered cartilage constructs cultured with TGF-beta3. *Osteoarthritis Cartilage* **15(9)**: 1025-1033.
8. Byers BA, Mauck RL, Chiang IE and Tuan RS. 2008. Transient exposure to transforming growth factor beta 3 under serum-free conditions enhances the biomechanical and biochemical maturation of tissue-engineered cartilage. *Tissue Eng Part A* **14(11)**: 1821-1834.

9. MacLean JJ, Lee CR, Alini M and Iatridis JC. 2004. Anabolic and catabolic mRNA levels of the intervertebral disc vary with the magnitude and frequency of *in vivo* dynamic compression. *J Orthop Res* **22**: 1193-1200.
10. Walsh AJL and Lotz JC. 2004. Biological response of the intervertebral disc to dynamic loading. *J Biomech* **37(3)**: 329-337.
11. Ishihara H, McNally DS, Urban JPG and Hall AC. 1996. Effects of hydrostatic pressure on matrix synthesis in different regions of the intervertebral disk. *J Appl Physiol* **80**: 839-846.
12. Handa T, Ishihara H, Ohshima H, Osada R, Tsuji H and Obata Ki. 1997. Effects of hydrostatic pressure on matrix synthesis and matrix metalloproteinase production in the human lumbar intervertebral disc. *Spine* **22**: 1085-1091.
13. Hutton WC, Elmer WA, Boden SD, Hyon S, Toribatake Y, Tomita K and Hair GA. 1999. The effect of hydrostatic pressure on intervertebral disc metabolism. *Spine* **24(15)**: 1507-1515.
14. Hutton WC, Elmer WA, Bryce LM, Kozlowska EE, Boden SD and Kozlowski M. 2001. Do the intervertebral disc cells respond to different levels of hydrostatic pressure? *Clin Biomech* **16(9)**: 728-734.
15. Neidlinger-Wilke C, Würtz K, Liedert A, Schmidt C, Börm W, Ignatius A, Wilke H-J and Claes L. 2005. A three-dimensional collagen matrix as a suitable culture system for the comparison of cyclic strain and hydrostatic pressure effects on intervertebral disc cells. *J Neurosurg Spine* **2(4)**: 457-465.

16. Neidlinger-Wilke C, Würtz K, Urban JPG, Börm W, Arand M, Ignatius A, Wilke H-J and Claes LE. 2006. Regulation of gene expression in intervertebral disc cells by low and high hydrostatic pressure. *Eur Spine J* **15 (Suppl 3)**: S372-378.
17. Mauck RL, Nicoll SB, Seyhan SL, Ateshian GA and Hung CT. 2003. Synergistic action of growth factors and dynamic loading for articular cartilage tissue engineering. *Tissue Eng* **9(4)**: 597-611.
18. Elder BD and Athanasiou KA. 2008. Synergistic and additive effects of hydrostatic pressure and growth factors on tissue formation. *PLoS One* **3(6)**: e2341.
19. Gunjaa NJ, Uthamanthila RK and Athanasiou KA. 2009. Effects of TGF- β_1 and hydrostatic pressure on meniscus cell-seeded scaffolds. *Biomaterials* **30(4)**: 565-573.
20. Burdick JA, Chung C, Jia X, Randolph MA and Langer R. 2005. Controlled degradation and mechanical behavior of photopolymerized hyaluronic acid networks. *Biomacromolecules* **6(1)**: 386 -391.
21. Chou AI and Nicoll SB. 2009. Characterization of photocrosslinked alginate hydrogels for nucleus pulposus cell encapsulation. *J Biomed Mater Res A* **91A(1)**: 187-194.
22. Reza AT and Nicoll SB. 2009. Characterization of novel photocrosslinked carboxymethylcellulose hydrogels for encapsulation of nucleus pulposus cells. *Acta Biomater* doi:10.1016/j.actbio.2009.1006.1004.

23. Smeds KA, Pfister-Serres A, Miki D, Dastgheib K, Inoue M, Hatchell DL and Grinstaff MW. 2001. Photocrosslinkable polysaccharides for *in situ* hydrogel formation. *J Biomed Mater Res* **54(1)**: 115-121.
24. Chou AI, Bansal A, Miller GJ and Nicoll SB. 2006. The effect of serial monolayer passaging on the collagen expression profile of outer and inner annulus fibrosus cells. *Spine* **31(17)**: 1875-1881.
25. Chou AI, Reza AT and Nicoll SB. 2008. Distinct intervertebral disc cell populations adopt similar phenotypes in three-dimensional culture. *Tissue Eng Part A* **14(12)**: 2079-2087.
26. Chang SCN, Rowley JA, Tobias G, Genes NG, Roy AK, Mooney DJ, Vacanti CA and Bonassar LJ. 2001. Injection molding of chondrocyte/alginate constructs in the shape of facial implants. *J Biomed Mater Res* **55(4)**: 503-511.
27. Hung CT, Mauck RL, Wang CC, Lima EG and Ateshian GA. 2004. A paradigm for functional tissue engineering of articular cartilage via applied physiologic deformational loading. *Ann Biomed Eng* **32(1)**: 35-49.
28. Mauck RL, Seyhan SL, Ateshian GA and Hung CT. 2002. Influence of seeding density and dynamic deformational loading on the developing structure/function relationships of chondrocyte-seeded agarose hydrogels. *Ann Biomed Eng* **30(8)**: 1046-1056.
29. Puelacher WC, Kim SW, Vacanti JP, Schloo B, Mooney D and Vacanti CA. 1994. Tissue-engineered growth of cartilage: the effect of varying the concentration of chondrocytes seeded onto synthetic polymer matrices. *Int J Oral Maxillofac Surg* **23(1)**: 49-53.

30. Vunjak-Novakovic G, Obradovic B, Martin I, Bursac PM, Langer R and Freed LE. 1998. Dynamic cell seeding of polymer scaffolds for cartilage tissue engineering. *Biotechnol Prog* **14(2)**: 193-202.
31. Mackay AM, Beck SC, Murphy JM, Barry FP, Chichester CO and Pittenger MF. 1998. Chondrogenic differentiation of cultured human mesenchymal stem cells from marrow. *Tissue Eng* **4(4)**: 415-428.
32. Miyanishi K, Trindade MCD, Lindsey DP, Beaupré GS, Carter DR, Goodman SB, Schurman DJ and Smith RL. 2006. Effects of hydrostatic pressure and transforming growth factor-beta 3 on adult human mesenchymal stem cell chondrogenesis *in vitro*. *Tissue Eng* **12(6)**: 1419-1428.
33. Risbud MV, Di Martino A, Guttapalli A, Seghatoleslami R, Denaro V, Vaccaro AR, Albert TJ and Shapiro IM. 2006. Toward an optimum system for intervertebral disc organ culture: TGF-beta 3 enhances nucleus pulposus and annulus fibrosus survival and function through modulation of TGF-beta-R expression and ERK signaling. *Spine* **31(8)**: 884-890.
34. Smith RL, Lin J, Trindade MCD, Shida J, Kajiyama G, Vu T, Hoffman AR, Van der Meulen MCH, Goodman SB, Schurman DJ and Carter DR. 2000. Time-dependent effects of intermittent hydrostatic pressure on articular chondrocyte type II collagen and aggrecan mRNA expression. *J Rehabil Res Dev* **37(2)**: 153-161.
35. Hu JC and Athanasiou KA. 2006. The effects of intermittent hydrostatic pressure on self-assembled articular cartilage constructs. *Tissue Eng* **12(5)**: 1337-1344.

36. Ikenoue T, Trindade MCD, Lee MS, Lin EY, Schurman DJ, Goodman SB and Smith RL. 2003. Mechanoregulation of human articular chondrocyte aggrecan and type II collagen expression by intermittent hydrostatic pressure *in vitro*. *J Orthop Res* **21(1)**: 110-116.
37. Takai E, Mauck RL, Hung CT and Guo XE. 2004. Osteocyte viability and regulation of osteoblast function in a 3D trabecular bone explant under dynamic hydrostatic pressure. *J. Bone Miner Res* **19**: 1403-1410.
38. Singer VL, Jones LJ, Yue ST and Haugland RP. 1997. Characterization of PicoGreen reagent and development of a fluorescence-based solution assay for double-stranded DNA quantitation. *Anal Biochem* **249(2)**: 228-238.
39. Farndale RW, Sayers CA and Barrett AJ. 1982. A direct spectrophotometric microassay for sulfated glycosaminoglycans in cartilage cultures. *Connect Tissue Res* **9(4)**: 247-248.
40. Enobakhare BO, Bader DL and Lee DA. 1996. Quantification of sulfated glycosaminoglycans in chondrocyte/alginate cultures, by use of 1,9-dimethylmethylene blue. *Anal Biochem* **243(1)**: 189-191.
41. Soltz MA and Ateshian GA. 1998. Experimental verification and theoretical prediction of cartilage interstitial fluid pressurization at an impermeable contact interface in confined compression. *J Biomech* **31(10)**: 927-934.
42. Reza AT and Nicoll SB. 2008. Hydrostatic pressure differentially regulates outer and inner annulus fibrosus cell matrix production in 3D scaffolds. *Ann Biomed Eng* **36(2)**: 204-213.

43. Kasra M, Goel V, Martin J, Wang ST, Choi W and Buckwalter J. 2003. Effect of dynamic hydrostatic pressure on rabbit intervertebral disc cells. *J Orthop Res* **21(4)**: 597-603.
44. Kasra M, Merryman WD, Loveless KN, Goel VK, Martin JD and Buckwalter JA. 2006. Frequency response of pig intervertebral disc cells subjected to dynamic hydrostatic pressure. *J Orthop Res* **24**: 1967-1973.
45. Gokorsch S, Nehringm D, Grottke C and Czermak P. 2004. Hydrodynamic stimulation and long term cultivation of nucleus pulposus cells: a new bioreactor system to induce extracellular matrix synthesis by nucleus pulposus cells dependent on intermittent hydrostatic pressure. *Int J Artif Organs* **27(11)**: 962-970.
46. Wuertz K, Urban JPG, Klasen J, Ignatius A, Wilke H-J, Claes L and Neidlinger-Wilke C. 2007. Influence of extracellular osmolarity and mechanical stimulation on gene expression of intervertebral disc cells. *J Orthop Res* **25(11)**: 1513-1522.
47. Le Maitre CL, Frain J, Fotheringham AP, Freemont AJ and Hoyland JA. 2008. Human cells derived from degenerate intervertebral discs respond differently to those derived from non-degenerate intervertebral discs following application of dynamic hydrostatic pressure. *Biorheology* **45(5)**: 563-575.
48. Korecki CL, MacLean JJ and Iatridis JC. 2008. Dynamic compression effects on intervertebral disc mechanics and biology. *Spine* **33(13)**: 1403-1409.
49. Korecki CL, Kuo CK, Tuan RS and Iatridis JC. 2009. Intervertebral disc cell response to dynamic compression is age and frequency dependent. *J Orthop Res* **27(6)**: 800-806.

50. Hall AC. 1999. Differential effects of hydrostatic pressure on cation transport pathways of isolated articular chondrocytes. *J Cell Physiol* **178(2)**: 197-204.
51. Browning JA, Saunders K, Urban JPG and Wilkins RJ. 2004. The influence and interactions of hydrostatic and osmotic pressures on the intracellular milieu of chondrocytes. *Biorheology* **41(3-4)**: 299-308.

Chapter 5: Response of Nucleus Pulposus Cells Encapsulated in Photocrosslinked Carboxymethylcellulose Hydrogels Following Pretreatment with TGF- β_3 : Differential Maturation *in vitro* and *in vivo*

5.1. Introduction

The intervertebral disc (IVD) is a complex, fibrocartilaginous tissue, comprised of the collagenous annulus fibrosus, located at the periphery of the disc, and the gelatinous nucleus pulposus (NP) which is located at the center of the disc. The NP is predominantly composed of type II collagen and negatively charged proteoglycans, such as aggrecan, which permit the tissue to retain water¹. The high water content of the NP allows the IVD to resist compressive loads placed upon the spine through the generation of a hydrostatic swelling pressure². Nevertheless, a decrease in proteoglycan content occurs in conjunction with age¹ or the onset of disc degeneration, which then renders the disc more fibrous in content and structure and may hinder the ability of the IVD to sustain applied loads³. In addition, the IVD is the largest avascular, aneural tissue in the body and is dependent upon bulk fluid flow and diffusion for nutrient transport and waste removal^{4,5}. As the disc becomes more fibrotic, these processes are impeded, and the IVD must rely on anaerobic metabolism to survive. However, this results in the accumulation of lactic acid waste products, which decrease the local pH and may result in cell death⁶ and the activation of matrix degrading enzymes, which further compromises the health of the tissue¹.

Tissue engineering strategies may present an alternative to current surgical treatments for disc degeneration. Hydrogels mimic the highly hydrated nature of the NP and encapsulation of cells within these scaffolds retains the phenotypic rounded morphology observed *in vivo*⁷⁻¹⁰. A wide variety of starting materials have been used to form hydrogels for NP tissue engineering applications, including hyaluronic acid¹¹⁻¹³, collagen¹⁴⁻¹⁷, agarose¹⁸, and chitosan¹⁹⁻²¹. However, ionically crosslinked alginate, derived from brown algae, has been the most prevalent material utilized in NP tissue engineering^{9, 22-31}. While alginate has been well-established for use in short-term studies examining gene expression or extracellular matrix (ECM) accumulation, cell-laden alginate scaffolds have been shown to lose mechanical integrity over time when used in long-term investigations, possibly due to a loss of crosslinking calcium ions via diffusion or depletion by encapsulated cells^{24, 32}. This has motivated the examination of additional crosslinking techniques and materials for tissue engineering investigations.

Photopolymerization is a covalent crosslinking method that utilizes biocompatible photoinitiators to create a 3-D network via radical polymerization upon exposure to light. Elisseff et al. first described this technique using methacrylated poly(ethylene oxide) for cartilage tissue engineering applications^{33, 34}. Smeds et al. similarly created photocrosslinkable polysaccharide-based hydrogels from methacrylated alginate and hyaluronic acid, indicating the potential of similar photocrosslinkable polysaccharides for use in tissue engineering applications³⁵.

Carboxymethylcellulose (CMC) is a polysaccharide derived from cellulose, the main component of plant cell walls. This water-soluble polymer contains a carboxylic acid moiety within the carboxymethyl group which becomes deprotonated at

physiological pH, resulting in a negatively charged network, similar to that provided by the glycosaminoglycans (GAGs) in the native NP matrix. Photocrosslinked, methacrylated CMC has been recently shown to produce stable hydrogels, support NP cell viability, and promote phenotypic matrix deposition capable of maintaining initial mechanical properties *in vitro*³⁶. The functional properties of these constructs were later shown to be enhanced through the use of a serum-free, chemically-defined medium supplemented with transforming growth factor- β_3 (TGF- β_3), resulting in a five-fold increase in the equilibrium Young's modulus over untreated controls along with concomitant increases in GAG and type II collagen accumulation³⁷. However, continuous exogenous growth factor delivery is not a cost effective or clinically relevant method of construct modulation due to the short half life of these proteins, and it is unclear whether the effects of TGF- β_3 are retained once growth factor supplementation is discontinued.

Therefore, the objective of this study was to examine the long-term effects of TGF- β_3 pre-conditioning under both *in vitro* and subcutaneous *in vivo* culture conditions. We hypothesized that TGF- β_3 -treated constructs would exhibit greater matrix accumulation and higher mechanical properties in comparison to untreated controls, and that these properties would be maintained both *in vitro* and *in vivo* following the cessation of growth factor supplementation.

5.2. Materials and Methods

5.2.1. Macromer Synthesis

Methacrylated carboxymethylcellulose was synthesized through esterification of hydroxyl groups based on previously described protocols^{23, 35, 36, 38}. Briefly, a 20-fold excess of methacrylic anhydride (Sigma, St. Louis, MO) was reacted with a 1 wt% solution of 250 kDa CMC (Sigma) in RNase/DNase-free water over 24 hours at 4°C. The pH was periodically adjusted to 8.0 using 3N NaOH to modify hydroxyl groups of the polymer with functional methacrylate groups. The modified CMC solution was purified via dialysis for 96 hours against RNase/DNase-free water (Spectra/Por1, MW 5-8 kDa, Rancho Dominguez, CA) to remove excess, unreacted methacrylic anhydride. Purified methacrylated CMC was recovered by lyophilization and stored at -20°C. The degree of substitution was confirmed using ¹H-NMR (360 MHz, DMX360, Bruker, Madison, WI) following acid hydrolysis of purified methacrylated CMC³⁶. Molar percent of methacrylation was determined by the relative integrations of methacrylate proton peaks (methylene, $\delta = 6.2$ ppm and 5.8 ppm and the methyl peak, $\delta = 2.0$ ppm) to carbohydrate protons.

5.2.2. Primary Cell Culture and Isolation

All cell culture supplies, including media, antibiotics, and buffering agents, were purchased from Invitrogen (Carlsbad, CA) unless otherwise noted. Discs C2-C4 were isolated from bovine caudal IVDs obtained from a local abattoir, and the NP was separated through gross visual inspection based on previous protocols^{22, 26}. Tissue was maintained in Dulbecco's Modified Eagle Medium (DMEM) supplemented with 20%

fetal bovine serum (FBS) (Hyclone, Logan, UT), 0.075% sodium bicarbonate, 100 U/mL penicillin, 100 µg/mL streptomycin, and 0.25 µg/mL Fungizone reagent at 37°C, 5% CO₂ for two days prior to digestion to ensure no contamination occurred during harvesting. A single serum lot was used for all experiments to reduce potential variability in the cellular response.

Tissue was diced and NP cells were released by collagenase (Type IV, Sigma) digestion at an activity of 7000 U collagenase per gram of tissue. Following incubation in collagenase, undigested tissue was removed using a 40 µm mesh filter. Cells from multiple levels (C2-C4) were pooled and rinsed in sterile Dulbecco's Phosphate Buffered Saline (DPBS). These primary cells were plated onto tissue culture flasks, designated as passage 0, and maintained in DMEM with 10% FBS, 0.075% sodium bicarbonate, 100 U/mL penicillin, and 100 µg/mL streptomycin (growth medium). Cells were subcultured twice to obtain the necessary number of cells, and passage 2 cells²⁶ were used in all experiments, as these cells have been shown to retain phenotypic differences observed *in vivo* up to the second passage²². Medium was changed three times per week.

5.2.3. Cell Encapsulation in Photocrosslinked Hydrogels

Lyophilized methacrylated CMC was sterilized by a 30-minute exposure to germicidal UV light. The sterilized product was then dissolved to 2.5% in filter-sterilized 0.05 wt% photoinitiator, 2-hydroxy-1-[4-(2-hydroxyethoxy)phenyl]-2-methyl-1-propanone (Irgacure 2959, I2959, Ciba Specialty Chemicals, Basel, Switzerland), in sterile DPBS at 4°C. Passage 2 NP cells were resuspended in a small volume of 0.05% I2959 and then homogeneously mixed with dissolved methacrylated CMC at 30×10^6 cells/mL for a final concentration of 2.25%. The seeding density was selected based on

previous studies using cell-seeded constructs for engineering of cartilaginous tissues³⁹⁻⁴³. The 2.25% CMC solution was cast in a custom-made glass casting device and exposed to long-wave UV light (EIKO, Shawnee, KS, peak 368 nm, 1.2W) for 10 minutes to produce covalently photocrosslinked hydrogel disks of 5-mm diameter x 2-mm thickness. Each hydrogel was incubated in 1.5 mL of growth medium at 37°C, 5% CO₂. At day 1, growth medium was fully exchanged with chemically-defined medium (Cells-), which was comprised of DMEM with 1% insulin-transferrin-selenium + universal culture supplement (BD Biosciences, San Jose, CA), 100 U/mL penicillin, 100 µg/mL streptomycin, 40 µg/mL L-proline (Sigma), 1 mM sodium pyruvate (Mediatech, Inc., Manassas, VA), 50 µg/mL ascorbic acid 2-phosphate (Sigma), and 100 nM dexamethasone (Sigma)⁴⁴. This medium was further supplemented with 10 ng/mL rhTGF-β₃ (R&D Systems, Minneapolis, MN) (Cells+). The TGF-β₃ concentration utilized was chosen based on previous IVD and cartilage tissue engineering studies⁴⁴⁻⁴⁸. Media were changed three times per week. Cell-free control gels cast at 2.25% were maintained for all groups (Ctrl-, Ctrl+).

5.2.4. *in vivo* Subcutaneous Pouch Model

After 14 days of *in vitro* pre-culture, growth factor supplementation was discontinued, and cell-laden (Cells-, Cells+) and cell-free constructs (Ctrl-, Ctrl+) were subcutaneously implanted (Cells- *in vivo*, Cells+ *in vivo*, Ctrl- *in vivo*, Ctrl+ *in vivo*) in immunocompromised nude mice (4-6 week old female mice, Strain: NIH-III-NU, Charles River Laboratories, Wilimington, MA) in accordance with University of Pennsylvania guidelines for the use of vertebrate animals for research (Animal Protocol #800209). Surgery was performed aseptically under anesthesia induced by injection of 140 mg/kg

body weight of ketamine (Fort Dodge, Animal Health, Fort Dodge, IA), 7 mg/kg xylazine (Phoenix Pharmaceuticals, St. Joseph, MO), and 1 mg/kg acepromazine (Burns Veterinary Supply, Farmers Branch, TX). A mid-longitudinal sagittal skin incision on the dorsum of each mouse was expanded by blunt dissection to create a subcutaneous pocket into which six implants were placed. Each group (4 groups total: cell-free control gels with and without TGF- β_3 ; cell-laden gels with and without TGF- β_3) consisted of a total of 18 constructs implanted in 3 animals per time point. Subcutaneous constructs were harvested at 4 and 8 weeks following implantation. The animals were euthanized by CO₂ asphyxiation in accordance with the guidelines established by the American Veterinary Medical Association Panel on Euthanasia. Corresponding controls were maintained *in vitro* throughout the course of the study (Cells- *in vitro*, Cells+ *in vitro*, Ctrl- *in vitro*, Ctrl+ *in vitro*). A schematic detailing the timeline of this investigation is shown below (Figure 5.1).

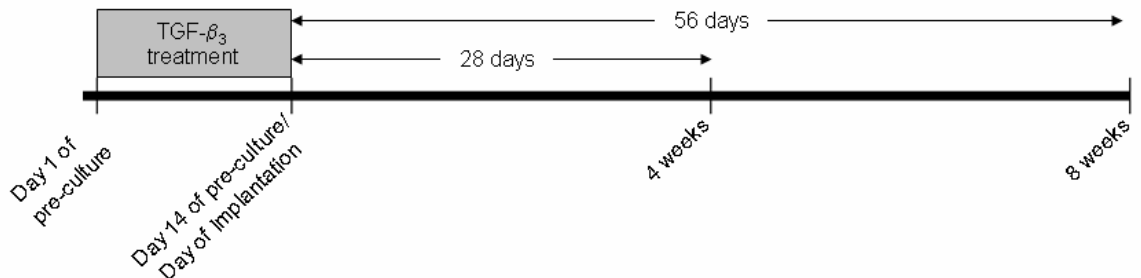


Figure 5.1. Timeline for the investigation of the long-term effects of TGF- β_3 pre-treatment. Constructs were cultured with or without TGF- β_3 through 14 days of *in vitro* pre-culture, at which time a subset of constructs was implanted subcutaneously, while others remained *in vitro* without TGF- β_3 .

5.2.5. Swelling Ratio

The equilibrium weight swelling ratio, Q_w , was calculated after 14 days of *in vitro* pre-culture (prior to subcutaneous implantation) and after 4 and 8 weeks of subcutaneous implantation (n=5). Constructs were weighed to determine the wet weight (W_s), lyophilized, and then weighed again to measure the dry weight (W_d). Q_w was calculated using the following equation:

$$Q_w = W_s/W_d$$

5.2.6. Biochemistry

Following lyophilization, total protein and DNA (n=5) were extracted at day 14 of *in vitro* pre-culture, 4 weeks, and 8 weeks by pepsin digestion based on previous studies²². Briefly, lyophilized samples were homogenized and treated with pepsin (Sigma) in 0.05N acetic acid (1.9 mg/mL) for 48 hrs at 4°C. Afterwards, pepsin was neutralized by the addition of 10X tris buffered saline. Cell-free hydrogels (n=4) were maintained for all groups and served as negative controls. Total DNA content was measured using the PicoGreen DNA assay⁴⁹ (Molecular Probes, Eugene, OR) with calf thymus DNA (Sigma) as the standard²². Samples were analyzed at 480 nm excitation and 520 nm emission using a Bio-Tek Instruments microplate reader (Synergy HTTM, Winooski, VT).

Total sulfated GAG content was measured at day 14 of pre-culture, 4 weeks, and 8 weeks using the 1,9 dimethylmethylene blue (DMMB) assay⁵⁰. The DMMB dye was reduced to pH 1.5 to minimize the formation of CMC carboxyl group-DMMB dye complexes⁵¹ and absorbance was determined at 595 nm using a chondroitin-6 sulfate standard curve (Sigma).

Collagen production was quantified at day 14 of pre-culture, 4 weeks, and 8 weeks via an indirect enzyme-linked immunosorbent assay using polyclonal antibodies to type I collagen (COL I) (rabbit anti-bovine, 1:2000, AbD Serotec, Raleigh, NC) and type II collagen (COL II) (rabbit anti-bovine, 1:2000, Millipore, Billerica, MA) based on previous protocols^{22, 24}. A biotinylated secondary antibody (goat anti-rabbit IgG (H+L), Vector Labs, Burlingame, CA) and a streptavidin-horseradish peroxidase enzyme conjugate (R&D Systems, Minneapolis, MN) were employed. Protein values for each sample were determined using a standard curve generated from bovine COL I and COL II (Rockland Immunochemicals, Gilbertsville, PA). Absorbance was measured at 450 nm. DNA, GAG, and collagen content are presented normalized to wet weight.

5.2.7. Histology and Immunohistochemistry

Constructs were fixed for 45 minutes in acid formalin at room temperature and processed for paraffin embedding after graded serial ethanol dehydration. Samples were sectioned at a thickness of 8 μm using a Leica microtome (Model 2030, Nussloch, Germany), and hematoxylin and eosin staining was conducted to visualize cellular distribution throughout the hydrogel. Immunohistochemical analyses were performed to assess ECM accumulation according to previous studies²⁴. Briefly, polyclonal antibodies to COL I (1:1000 dilution in blocking solution, comprised of 10% goat serum diluted in DPBS) and COL II (1:40 dilution in blocking solution, composed of 10% goat serum diluted in DPBS), and a monoclonal antibody to chondroitin sulfate proteoglycan (1:100 dilution in blocking solution, consisting of 10% goat serum, 10% evaporated milk, and 1% Goat Anti-Mouse IgG+A+M (H+L) (Invitrogen) diluted in DPBS) (CSPG, Sigma) were used, followed by incubation in biotinylated goat/anti-rabbit IgG (H+L) (COL I,

COL II) or biotinylated goat/anti-mouse IgM (CSPG) secondary antibody (1:50 dilution in blocking solution) (Vector Labs). A peroxidase-based detection system (Vectastain Elite ABC, Vector Labs) and 3,3' diaminobenzidine (Vector Labs) were employed to visualize ECM localization. Non-immune controls were processed in blocking solution without primary antibody. Samples were viewed with a Zeiss Axioskop 40 optical microscope and images were captured using AxioVision software (Carl Zeiss, Inc., Thornwood, NY). Fibrous capsule thickness was measured using AxioVision software.

5.2.8. Mechanical Testing

Unconfined compression testing was conducted on CMC hydrogels (n=5) isolated at day 1 of pre-culture, prior to TGF- β_3 treatment, and day 14 of pre-culture, prior to implantation. Additionally, excised *in vivo* and corresponding *in vitro* samples were tested at 4 and 8 weeks of implantation using a custom-built apparatus, as previously described^{23, 36, 52}. Briefly, the unconfined compression testing protocol was comprised of a creep test followed by a multi-ramp stress-relaxation test. The creep test consisted of a 1 g tare load applied at a 10 $\mu\text{m/s}$ ramp velocity for 1800 seconds until equilibrium was reached (equilibrium criteria: <10 μm change in 10 minutes). The multi-ramp stress-relaxation test consisted of three 5% strain ramps applied at 10 $\mu\text{m/s}$, each followed by a 2000 second relaxation period (equilibrium criteria: <0.5 g change in 10 minutes). Equilibrium stress was calculated at each ramp using surface area measurements and plotted against the applied strain. An average equilibrium Young's modulus, E_y , was calculated from the slope of the stress versus strain curves and reported for each sample.

5.2.9. Statistical Analysis

A three-way ANOVA was used to determine the effects of time, TGF- β_3 , and culture condition (*in vivo* vs. *in vitro*) on DNA content, GAG and collagen accumulation (n=5). A three-way ANOVA was also used to determine the effects of time, cells (cell-laden vs. cell-free gels), and TGF- β_3 on Q_w and mechanical properties (n=5) for *in vitro* and *in vivo* samples analyzed separately. A Tukey's post-hoc test was performed on the three-factor interactions. A four-way ANOVA was used to determine the effects of time, cells, TGF- β_3 , and culture condition on Q_w and mechanical properties (n=5) at 4 and 8 weeks. A Tukey's post-hoc test was performed on the four-factor interaction. Significance was set at $p < 0.05$. Data represent the mean \pm standard deviation. All statistical analyses were performed using JMP software (SAS Institute, Cary, NC).

5.3. Results

CMC was methacrylated at an 8.15% modification, as verified by $^1\text{H-NMR}$. Cell-laden and cell-free constructs were initially cultured *in vitro* for 14 days with or without TGF- β_3 , at which time samples were implanted subcutaneously in nude mice or were maintained *in vitro* without growth factor supplementation for an additional 4 or 8 weeks (Figure 5.1). Q_w remained consistent over time in all Ctrl- and Cells+ (Figure 5.2). Q_w was similarly stable over time across all *in vitro* Ctrl+ samples; however, Q_w was significantly greater at 8 weeks in Ctrl+ *in vivo* samples in comparison to the corresponding group at 4 weeks. There was no effect of the presence of cells in

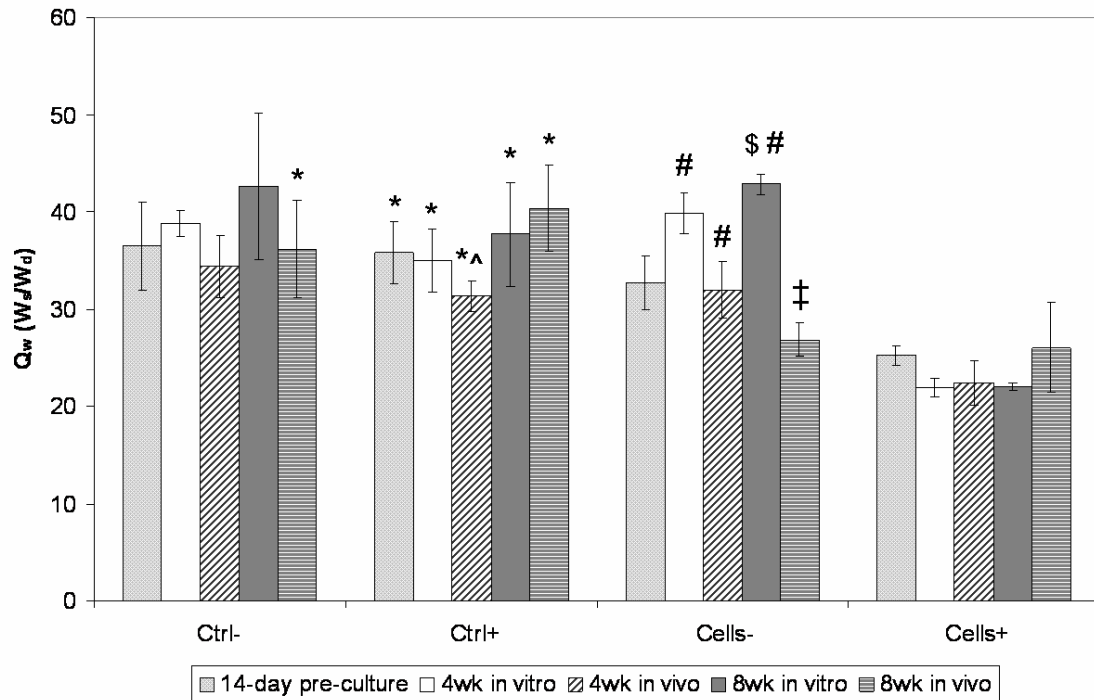


Figure 5.2. Equilibrium weight swelling ratio (Q_w) for cell-laden and cell-free CMC constructs with and without TGF- β_3 maintained under *in vitro* or *in vivo* culture conditions. \$ significant vs. 14-day pre-culture time point. ^ significant vs. 8wk within group. * Significant vs. cell-laden gel within group (Ctrl- vs. Cells-). # significant vs. corresponding TGF- β_3 -treated constructs within group (Cells- vs. Cells+). ‡ significant effect of culture condition (*in vitro* vs. *in vivo*).

comparing untreated constructs (Cells- vs. Ctrl-), while Cells+ scaffolds exhibited a significantly lower Q_w in comparison to Ctrl+ samples in both *in vitro* and *in vivo* culture. TGF- β_3 treatment resulted in a significantly lower Q_w at 4 and 8 weeks when comparing Cells+ *in vitro* to Cells- *in vitro* samples, while this comparison was only significant at 4 weeks for Cells+ *in vivo* versus Cells- *in vivo* specimens. Subcutaneous culture resulted in a marked decrease in Q_w for Cells- samples at 8 weeks in comparison to the corresponding *in vitro* group (Cells- *in vivo* vs. Cells- *in vitro*).

Hematoxylin and eosin (H&E) staining of *in vitro* and *in vivo* cell-laden constructs revealed more prevalent formation of lacunae in untreated (Cells-) *in vivo* samples (Figure 5.3 C, E) in comparison to corresponding *in vitro* constructs (Figure 5.3 B, D). Cells+ samples cultured *in vitro* (Figure 5.3 F, G, I arrows) exhibited signs of clonal cell expansion, while Cells+ *in vivo* constructs (Figure 5.3 H, J) demonstrated lacunae formation similar to that seen in Cells- *in vivo* scaffolds. The fibrous capsule surrounding cell-free and cell-laden hydrogels ranged from ~30-75 μm in thickness at 4 and 8 weeks of implantation, with no observed cellular infiltration into the scaffold (Figure 5.4).

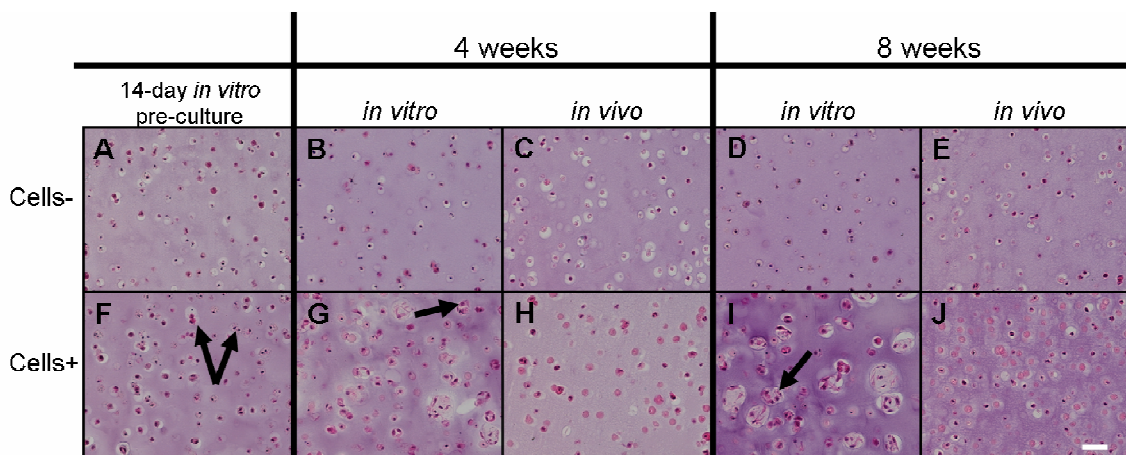


Figure 5.3. Hematoxylin and eosin staining of cell-laden CMC constructs cultured *in vitro* (A, B, D, F, G, I) and *in vivo* (C, E, H, J) with (F-J) and without (A-E) TGF- β_3 . Arrows indicate the presence of cell clusters. Bar = 50 μm .

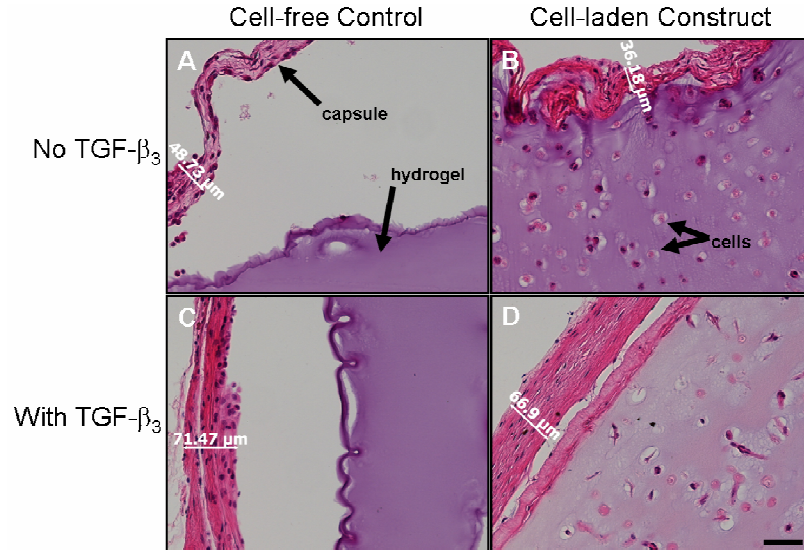


Figure 5.4. Hematoxylin and eosin staining of fibrous capsule formation for cell-free (A, C) and cell-laden (B, D) CMC constructs at 8 weeks of *in vivo* culture. Fibrous capsule thickness measurements are indicated in each panel. Bar = 50 μm .

Immunohistochemical analyses indicated interterritorial deposition and localized pericellular accumulation of CSPG in Cells- constructs after 14 days of *in vitro* pre-culture (Figure 5.5A). In contrast, Cells+ constructs exhibited a more even distribution of CSPG accompanied by more intense interterritorial deposition (Figure 5.5F). At 4 and 8 weeks, Cells- *in vivo* samples (Figure 5.5 C, E, respectively) demonstrated enhanced interterritorial staining in comparison to *in vitro* constructs (Figure 5.5 B, D, respectively). Conversely, there was no differential effect of culture condition observed histologically in Cells+ constructs at 4 weeks (Figure 5.5 G, H), and CSPG accumulation was reduced in 8 week *in vivo* samples in comparison to Cells+ scaffolds cultured *in vitro*. GAG accumulation, quantified using the DMMB assay, indicated a significant effect of TGF- β_3 treatment for both *in vitro* and *in vivo* samples prior to implantation (14-day pre-culture) and at 4 weeks (Cells+ vs. Cells-); however, no significant difference was detected between Cells+ and Cells- *in vivo* samples at the 8-week time point (Figure

5.5K). GAG accumulation in Cells+ *in vivo* constructs decreased markedly at each time point but remained constant over time in Cells- samples regardless of culture condition (*in vitro* vs. *in vivo*). GAG accumulation in Cells+ samples was also significantly affected by culture condition, as *in vitro* constructs retained greater amounts of GAGs at both 4 and 8 weeks.

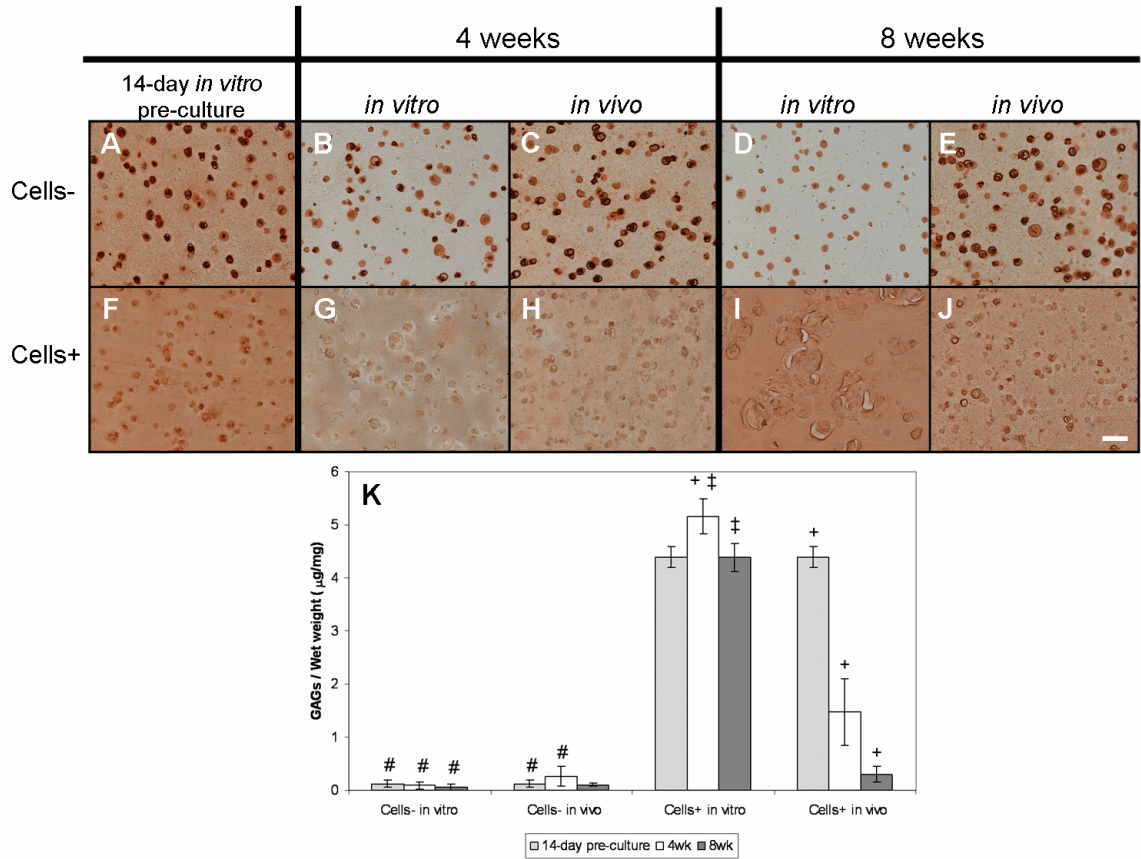


Figure 5.5. Immunohistochemical analyses of chondroitin sulfate proteoglycan localization in cell-laden CMC constructs cultured *in vitro* (A, B, D, F, G, I) and *in vivo* (C, E, H, J) with (F-J) and without (A-E) TGF- β_3 . Biochemical quantification of GAG accumulation (K) in constructs under various culture conditions. Bar = 50 μm . + significant vs. all other time points within group. # significant vs. corresponding TGF- β_3 -treated constructs within group (Cells- vs. Cells+). ‡ significant effect of culture condition (*in vitro* vs. *in vivo*).

COL II immunohistochemical analyses indicated a significant effect of TGF- β_3 treatment at all time points in all groups, as Cells+ constructs (Figure 5.6, F-J) displayed more intense staining than corresponding Cells- samples (Figure 5.6, A-E). COL II quantification (Figure 5.6K) verified a significant effect of growth factor treatment at the 8-week time point (Cells+ *in vitro* and *in vivo* vs. Cells- *in vitro* and *in vivo*), and accumulation in Cells+ constructs increased significantly over time. All groups demonstrated minimal staining for COL I at all time points and quantification of COL I content did not exceed 20 pg/mg (Figure 5.7).

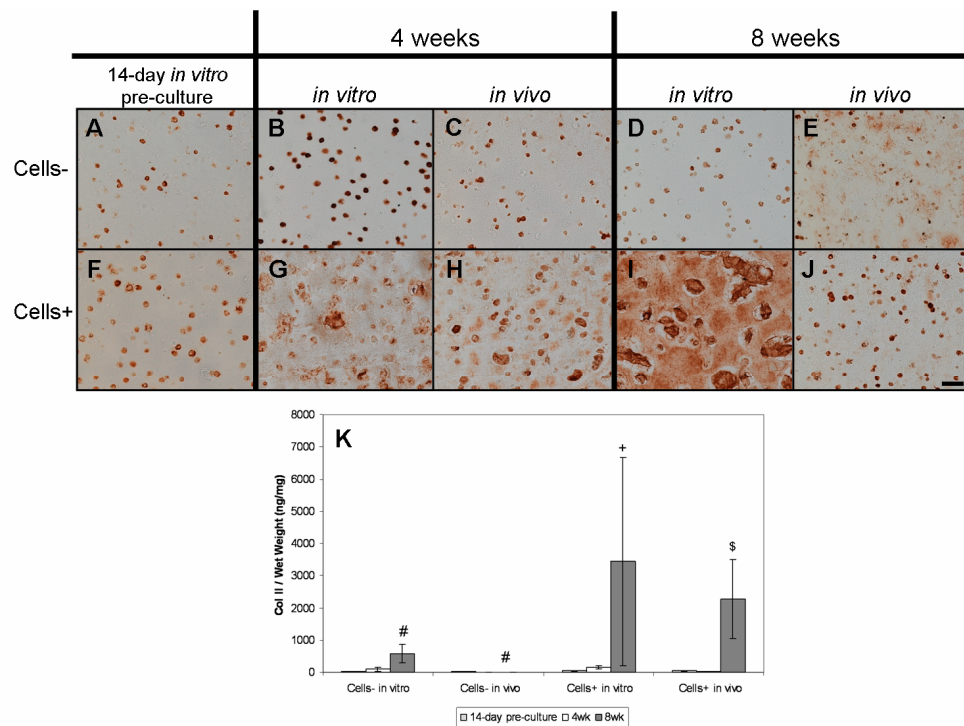


Figure 5.6. Immunohistochemical analyses of type II collagen (COL II) localization in cell-laden CMC constructs cultured *in vitro* (A, B, D, F, G, I) and *in vivo* (C, E, H, J) with (F-J) and without (A-E) TGF- β_3 . Biochemical quantification of COL II accumulation (K) in constructs. Bar = 50 μ m. + significant vs. all other time points within group. \$ significant vs. 14-day pre-culture. # significant vs. corresponding TGF- β_3 -treated constructs within group (Cells- vs. Cells+). ‡ significant effect of culture condition (*in vitro* vs. *in vivo*).

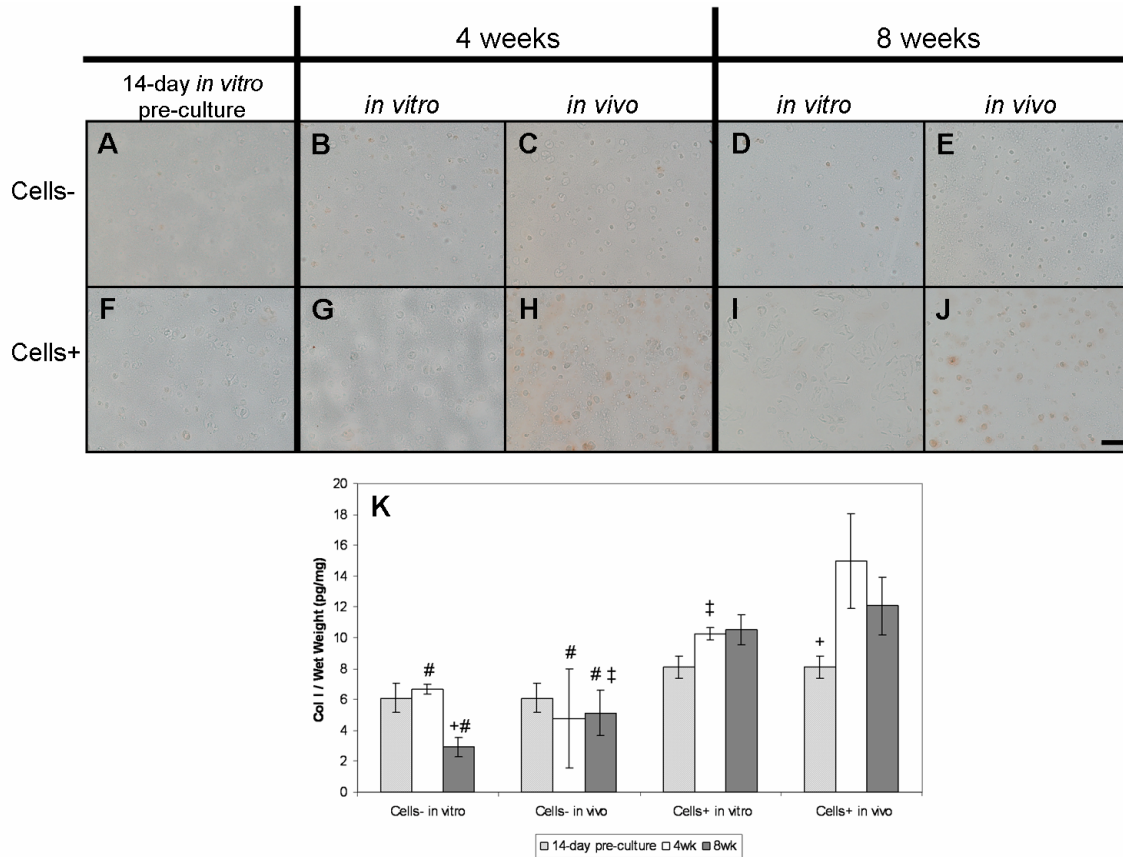


Figure 5.7. Immunohistochemical analyses of type I collagen (COL I) localization in cell-laden CMC constructs cultured *in vitro* (A, B, D, F, G, I) and *in vivo* (C, E, H, J) with (F-J) and without (A-E) TGF- β_3 . Biochemical quantification of COL I accumulation (K) in constructs under various culture conditions. Bar = 50 μ m. + significant vs. all other time points within group. # significant vs. corresponding TGF- β_3 -treated constructs within group (Cells- vs. Cells+). ‡ significant effect of culture condition (*in vitro* vs. *in vivo*).

TGF- β_3 treatment significantly increased DNA content in Cells+ constructs at the 14-day pre-culture time point and at 4 weeks in both *in vitro* and *in vivo* samples (Figure 5.8). However, by 8 weeks, the DNA content of the Cells+ *in vivo* group experienced a significant temporal decrease in comparison to Cells+ *in vitro* measurements at this time

point. Furthermore, at 8 weeks, Cells+ *in vivo* constructs were not significantly different from untreated Cells- *in vivo* samples.

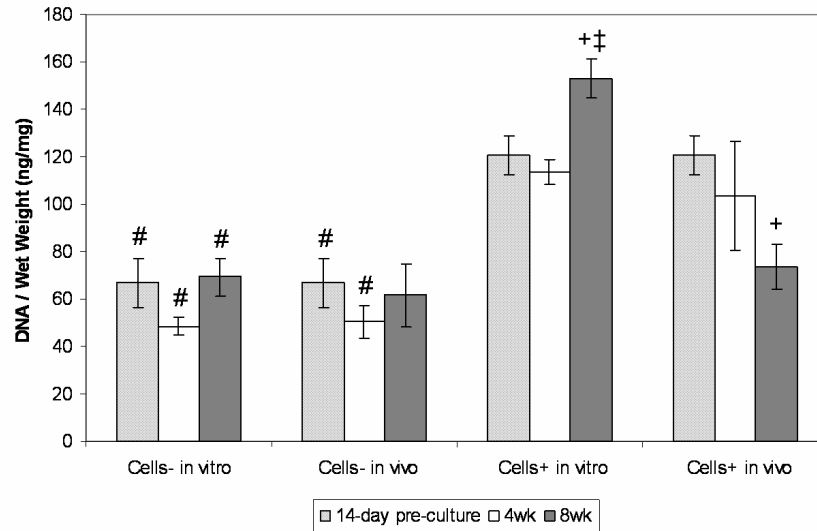


Figure 5.8. DNA content of constructs cultured *in vitro* and *in vivo* with and without TGF- β_3 . + significant vs. all other time points within group. # significant vs. corresponding TGF- β_3 -treated constructs within group (Cells- vs. Cells+). ‡ significant effect of culture condition (*in vitro* vs. *in vivo*).

Gross observation of both *in vitro* and *in vivo* samples (following excision and capsule removal) at 8 weeks indicated increased opacity in cell-laden TGF- β_3 -treated constructs (Figure 5.9 G, H). In addition, subcutaneously implanted cell-free hydrogels, with and without TGF- β_3 treatment (Figure 5.9 B, F), did not demonstrate any cellular infiltration into the scaffold, consistent with H&E staining shown in Figure 5.4, as samples remained transparent upon excision and removal of the fibrous capsule.

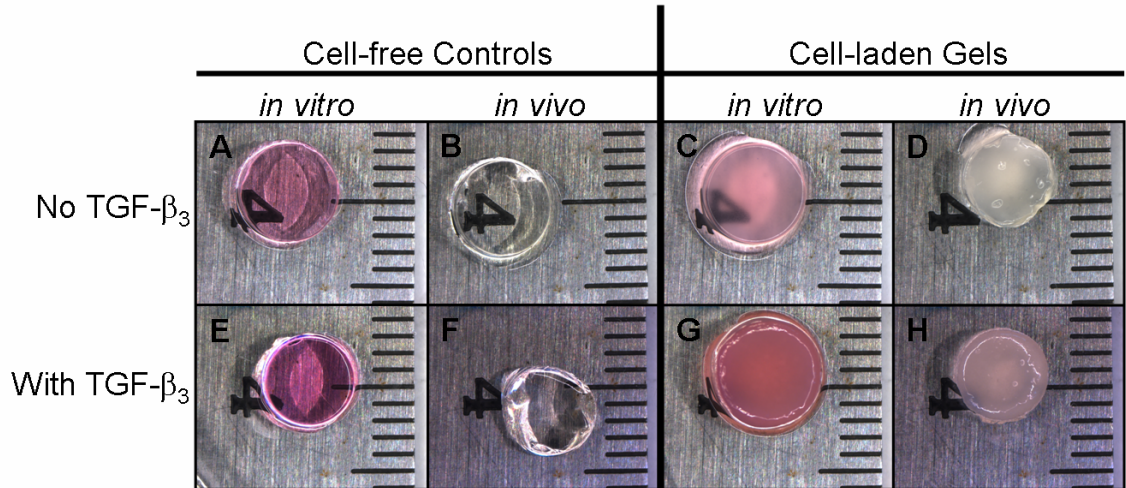


Figure 5.9. Gross images of constructs cultured *in vitro* (A, C, E, G) and *in vivo* (following excision and fibrous capsule removal) (B, D, F, H), with (E-H) and without (A-D) TGF- β_3 at 8 weeks following the *in vitro* pre-culture period. Scale in millimeters.

Construct diameter and thickness were measured prior to mechanical testing (Table 5.1). By 14 days of pre-culture, Cells+ samples were significantly larger than Cells- specimens and corresponding cell-free controls (Ctrl+). In contrast, there were no differences in diameter or thickness when comparing untreated Cells- gels to cell-free Ctrl- samples in any culture condition, at any time point throughout the study, indicating no effect of the presence of cells when cultured without TGF- β_3 . At 4 weeks, Cells+ samples remained significantly larger than Cells- gels, both *in vitro* and *in vivo*, as TGF- β_3 treatment had a marked effect on construct dimensions. However, the diameter of Cells+ *in vivo* samples at 4 weeks was significantly lower in comparison to the 14-day time point, indicating a temporal loss following subcutaneous implantation which was not seen in Cells+ *in vitro* constructs. In addition, the culture condition markedly affected scaffold dimensions at 4 weeks, as both Cells- and Cells+ *in vitro* constructs were

significantly larger than corresponding *in vivo* samples. Furthermore, the diameter of Cells+ *in vivo* constructs was not significantly different than that for cell-free *in vivo* controls (Ctrl+) at 4 weeks. By 8 weeks, the diameter and thickness measurements of Cells+ *in vivo* constructs were not significantly different from those of Cells- *in vivo* or Ctrl+ *in vivo* scaffolds, demonstrating a loss in the effect of TGF- β_3 treatment and the presence of cells by this later time point. In contrast, Cells+ *in vitro* samples were significantly larger than Cells- and Ctrl+ *in vitro* scaffolds at 8 weeks. Overall, *in vivo* conditions resulted in a significant decrease in diameter for both Cells- and Cells+ constructs in comparison to scaffolds cultured *in vitro*.

Constructs were tested in unconfined compression to determine the mechanical properties (Figure 5.10). Cell-free control gels, with and without TGF- β_3 (Ctrl+, Ctrl-), maintained initial mechanical properties throughout the study, regardless of culture condition (*in vitro* vs. *in vivo*). TGF- β_3 treatment of cell-laden constructs (Cells+) resulted in a significant increase in E_y from day 1 to day 14 of the *in vitro* pre-culture period, markedly increasing E_y over Cells- and Ctrl+ samples at 14 days. Cells+ *in vitro* constructs maintained these mechanical properties over the remainder of the experiment. In contrast, E_y for Cells+ *in vivo* samples decreased following subcutaneous implantation, and by 8 weeks, E_y was not significantly different when compared to Cells- or Ctrl+ *in vivo* scaffolds or versus Cells+ measurements recorded at the 1-day pre-culture time point. The presence of cells did not affect the mechanical properties of untreated constructs, as there were no significant differences detected between Ctrl- or Cells- samples at any time point, regardless of culture condition. In addition, at 8 weeks, E_y decreased below 1-day pre-culture values in both Cells- *in vivo* and *in vitro* scaffolds.

		Diameter (mm)	Thickness (mm)
Ctrl-	1-day pre-culture	5.33 ± 0.08	2.21 ± 0.04
	14-day pre-culture	5.54 ± 0.10	2.30 ± 0.04
	4wk <i>in vitro</i>	5.59 ± 0.17	2.25 ± 0.05
	4 wk <i>in vivo</i>	5.48 ± 0.15	2.29 ± 0.08
	8wk <i>in vitro</i>	5.39 ± 0.15	2.26 ± 0.12
	8wk <i>in vivo</i>	5.57 ± 0.08	2.24 ± 0.16
Ctrl+	1-day pre-culture	5.32 ± 0.14	2.23 ± 0.01
	14-day pre-culture	5.45 ± 0.09 *	2.30 ± 0.02 *
	4wk <i>in vitro</i>	5.73 ± 0.10 - *	2.35 ± 0.10 *
	4 wk <i>in vivo</i>	5.54 ± 0.07	2.31 ± 0.08 *
	8wk <i>in vitro</i>	5.52 ± 0.19 *	2.27 ± 0.07 *
	8wk <i>in vivo</i>	5.20 ± 0.17	2.22 ± 0.09
Cells-	1-day pre-culture	5.35 ± 0.06	2.24 ± 0.02
	14-day pre-culture	5.47 ± 0.10 #	2.25 ± 0.03 #
	4wk <i>in vitro</i>	5.65 ± 0.13 # ‡	2.36 ± 0.07 #
	4 wk <i>in vivo</i>	5.24 ± 0.23 #	2.26 ± 0.08 #
	8wk <i>in vitro</i>	5.67 ± 0.10 - # ‡	2.32 ± 0.05 #
	8wk <i>in vivo</i>	5.31 ± 0.16	2.22 ± 0.08
Cells+	1-day pre-culture	5.34 ± 0.14 +	2.21 ± 0.05 +
	14-day pre-culture	6.32 ± 0.23	2.88 ± 0.12 +
	4wk <i>in vitro</i>	6.47 ± 0.08 ‡	3.19 ± 0.14
	4 wk <i>in vivo</i>	5.64 ± 0.15 \$	2.98 ± 0.48 ^ -
	8wk <i>in vitro</i>	6.36 ± 0.19 ‡	3.34 ± 0.18 ‡
	8wk <i>in vivo</i>	5.50 ± 0.06 \$	2.36 ± 0.06 \$

Table 5.1. Diameter and thickness measurements of *in vitro* and *in vivo* constructs cultured with and without TGF- β_3 . + significant vs. all other *in vitro* time points within group. ^ significant vs. 8wk within group. - significant vs. 1-day pre-culture within group. \$ significant vs. 14-day pre-culture within group. * significant vs. cell-laden gel within group. # significant vs. corresponding TGF- β_3 -treated constructs within group. ‡ significant effect of culture condition (*in vitro* vs. *in vivo*).

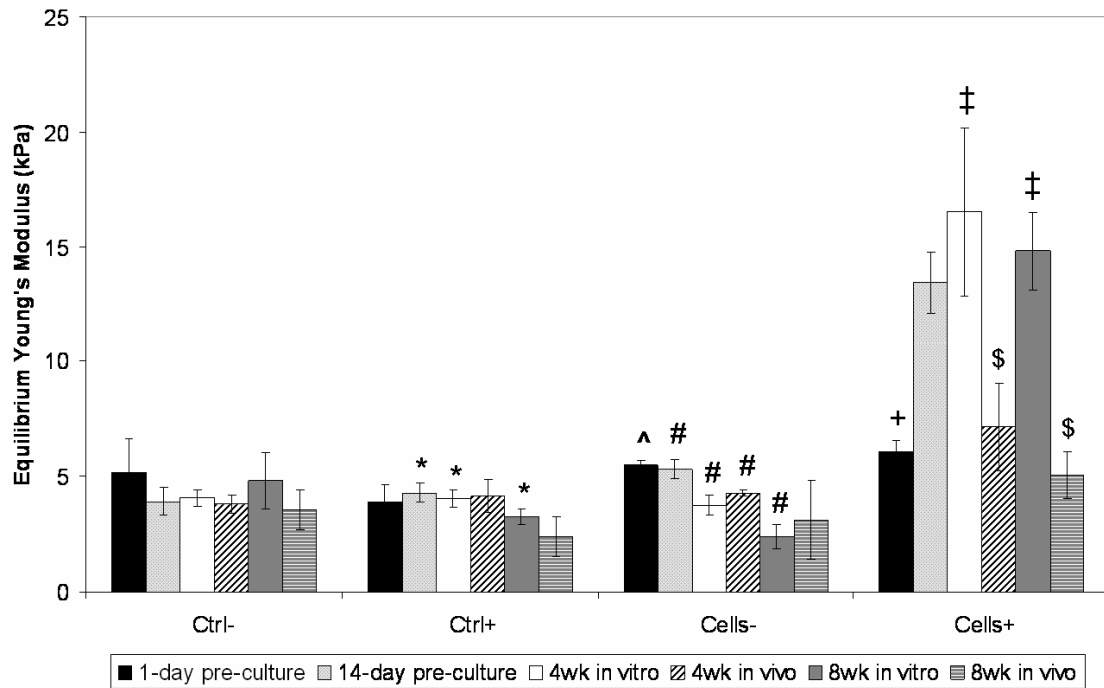


Figure 5.10. Equilibrium Young's modulus of *in vitro* and *in vivo* constructs cultured with and without TGF- β_3 . + significant vs. all other *in vitro* time points within group. ^ significant vs. 8wk *in vitro* and *in vivo* within group. \$ significant vs. 14-day pre-culture within group. * significant vs. cell-laden gel within group (Ctrl- vs. Cells-). # significant vs. corresponding TGF- β_3 -treated constructs within group (Cells- vs. Cells+). ‡ significant effect of culture condition (*in vitro* vs. *in vivo*).

5.4. Discussion

This is the first study to compare the long-term effect of *in vitro* TGF- β_3 pre-conditioning prior to *in vitro* and *in vivo* culture using photocrosslinked CMC hydrogels encapsulated with NP cells. Consistent with our original hypothesis, a 14-day pre-culture period in the presence of TGF- β_3 produced significant increases in matrix accumulation (GAGs, COL II) and mechanical properties, which were maintained for up to 8 weeks *in*

vitro following the cessation of growth factor supplementation. However, samples which were exposed to TGF- β_3 and subsequently implanted *in vivo* experienced a significant decrease in retained GAGs, a loss of DNA content, and a reduction in mechanical properties over time, contrary to our hypothesis. These results indicate a differential effect on construct maturation in response to TGF- β_3 supplementation, which is dependent upon culture condition (*in vitro* vs. *in vivo*).

Q_w remained constant in all groups throughout the study, except for 4wk Ctrl+ *in vivo* and 8wk Cells- *in vitro* samples. A stable swelling ratio is an important characteristic of any potential intradiscal material in that this will decrease the likelihood of extrusion into the annulus. Furthermore, the addition of TGF- β_3 produced a significant decrease in Q_w in cell-laden samples (Cells+) in comparison to untreated constructs (Cells-) and treated, cell-free controls (Ctrl+), indicating a pronounced accumulation of ECM proteins within Cells+ gels. Q_w for Cells- was similar to that for cell-free controls (Ctrl-), as the presence of cells had no effect when cultured in the absence of TGF- β_3 . Q_w for Cells+ samples was 23.53 ± 2.81 , which closely approximates the Q_w measured for native NP tissue (19.94 ± 3.09 , unpublished data).

The mechanical and material properties of untreated (Cells-) scaffolds remained indistinguishable from Ctrl- samples throughout the study, indicating that, although these cells remained viable both *in vitro* and *in vivo*, they had entered a basal, senescent-like state in comparison to Cells+ scaffolds. As such, the minimal amount of accumulated ECM in Cells- constructs was insufficient to affect the overall properties of these hydrogels. Nonetheless, Cells- *in vivo* samples exhibited prevalent lacuna formation and enhanced interterritorial CSPG accumulation in comparison to Cells- *in vitro* constructs.

Cellular localization within lacunae is characteristic of cartilaginous tissues, such as the NP^{53, 54}. While subcutaneous implantation does not replicate a load-bearing environment, *in vivo* samples were exposed to various mechanical stimuli which were not present in static, free-swelling, *in vitro* culture, including tension from the skin and forces produced in response to locomotion of the mice. These loads may have stimulated matrix deposition and lacuna formation by untreated cells cultured *in vivo*; however, this was not sufficient to impact mechanical properties, as Cells- *in vivo* constructs remained similar to Cells- *in vitro* scaffolds and cell-free Ctrl- samples.

TGF- β_3 supplementation significantly enhanced matrix accumulation in cell-laden samples (Cells+) in comparison to untreated controls (Cells-). Cells+ constructs demonstrated uniform interterritorial accumulation of CSPG at later time points, while CSPG remained highly localized within the pericellular matrix of Cells- scaffolds. In addition, at 8 weeks after the cessation of TGF- β_3 treatment, Cells+ *in vitro* samples contained ~70 times greater GAG content than the corresponding Cells- *in vitro* group. Furthermore, E_y measured for Cells+ *in vitro* constructs at 8 weeks was six-fold greater than that for Cells- *in vitro* specimens at that time point, indicating a significant and long-term improvement in the maturation of these construct resulting from a two-week exposure to TGF- β_3 . These data support a similar study conducted by our group which examined the effect of continuous treatment with TGF- β_3 over 28 days of *in vitro* culture³⁷. While the absolute values observed at 8 weeks for *in vitro* GAG content and E_y in this current 14-day TGF- β_3 -treatment study are less than those observed after 28 days of continuous growth factor treatment (GAGs: 4.39 ± 0.26 vs. 9.46 ± 1.51 $\mu\text{g}/\text{mg}$, respectively; E_y : 14.82 ± 1.68 vs. 18.84 ± 1.63 kPa, respectively), a decrease in the

period of TGF- β_3 treatment and increase in the overall duration of the experiment represents a study design that is more relevant to a clinically-applicable tissue engineering therapy.

Although TGF- β_3 supplementation resulted in significant improvements after 14 days of *in vitro* pre-culture, immunohistochemical and biochemical analyses of Cells+ *in vivo* scaffolds implanted after this period indicated a decrease in CSPG and GAG accumulation. A similar trend was observed via COL II immunohistochemistry (IHC), as interterritorial staining for Cells+ *in vivo* constructs decreased from 4 to 8 weeks and reverted to localized intracellular staining similar to, though more intense than, that seen after the 14-day pre-culture period. Cells+ *in vivo* constructs experienced a concomitant loss in mechanical properties, and by 4 weeks, these samples were significantly weaker than Cells+ *in vitro* constructs. In contrast, CSPG accumulation in Cells+ *in vitro* samples was similar at 8 weeks to that observed at the time of implantation, while COL II IHC depicted more intense staining and greater interterritorial deposition at 8 weeks in comparison to earlier time points. As such, culture condition was shown to significantly affect the matrix retention and mechanical properties of TGF- β_3 -treated scaffolds.

Measurements of E_y for cell-free controls (Ctrl-, Ctrl+) indicated that these covalently photocrosslinked CMC scaffolds experienced no significant degradation over the course of the study, as constructs did not exhibit a loss in mechanical properties *in vitro* or *in vivo*. Given the load bearing function of the NP, a biomaterial scaffold utilized as an intradiscal replacement material must provide immediate and sustained structural support to withstand the stresses to which the native tissue is subjected. However, biomaterials that serve as cell-laden scaffolds for tissue engineering applications must

balance mechanical demands with construct degradation in order to allow for nutrient and waste diffusion and provide void space for ECM deposition and tissue formation over time. Bryant and Anseth incorporated hydrolyzable lactic acid units into a non-degrading, photocrosslinkable poly(glycolic acid) (PEG) hydrogel used in cartilage tissue engineering applications⁵⁵. As the concentration of incorporated lactic acid units increased, DNA, GAG, and total collagen content increased as well over 6 weeks of *in vitro* culture. PEG constructs with the lowest concentration of degradable units exhibited localized pericellular deposition of COL II, while more rapidly degrading hydrogels demonstrated diffusion of COL II into the extracellular, interterritorial space, illustrating the importance of scaffold degradation in proper matrix assembly. Sahoo et al. similarly incorporated degradable lactic acid units into a methacrylated hyaluronic acid hydrogel used to encapsulate mesenchymal stem cells cultured in chondrogenic medium and observed increased chondroitin sulfate distribution throughout the scaffold with increased lactic acid concentration after 2 weeks of *in vitro* culture⁵⁶.

Cell proliferation, as measured by DNA content, and matrix accumulation in Cells+ constructs significantly exceeded that in Cells- constructs *in vitro*. Free-swelling *in vitro* culture provided sufficient nutrient diffusion through the scaffold and opportunity for the hydrolysis of ester crosslinks. As a result, void space was created over time, allowing for cell proliferation and ECM assembly *in vitro*, which is a known anabolic effect of TGF- β_3 . Histological analyses of Cells+ scaffolds revealed clonal expansion, as evidenced by cell clusters, and increased deposition of COL II, which is a large matrix protein that may require increased void space for proper assembly. Mauck et al. observed a similar phenomenon of clonal expansion when examining the effect of TGF- β_1

supplementation on chondrocyte-seeded agarose gels over 5 weeks of free-swelling *in vitro* culture. A peripheral mass composed of multiple cell layers located on the outer surface of the scaffold was also identified and these occurrences were attributed to the known proliferative effect⁵⁷ of TGF- β ⁵⁸.

H&E staining of *in vivo* constructs showed the formation of a fibrous capsule surrounding hydrogels from all groups. While *in vitro* diffusion conditions may have provided adequate ester hydrolysis to create void space for cell expansion and matrix deposition, the fibrous capsule observed *in vivo* may have impaired nutrient transport and constricted the hydrogel, resulting in a stiffer, less hospitable environment for the encapsulated cells. When combined with the limited hydrolytically-labile nature of the CMC scaffold, these conditions may have caused the metabolic and biosynthetic activity of *in vivo* TGF- β ₃-treated cells to plummet to basal levels seen in Cells- constructs. The remaining cells may have subsequently entered a senescent state similar to that seen in Cells- constructs, decreasing the production of matrix components and thereby increasing matrix turnover. As a result, by 8 weeks, GAG accumulation and E_y for *in vivo* TGF- β ₃-treated scaffolds fell to baseline levels comparable to that of untreated, cell-laden controls.

One limitation to the *in vivo* portion of this study is that it was conducted using nude mice, which prevents the full characterization of the foreign body response to construct implantation. However, as these constructs contained encapsulated xenogeneic bovine NP cells, an immunocompromised animal model was necessary in order to form an initial assessment of *in vivo* tissue development. A similar photocrosslinkable methylcellulose hydrogel platform was recently developed and cell-free constructs were

implanted in normal CD-1 mice⁵⁹. After 80 days of implantation, samples were circumscribed by a thin (~50 μm), translucent fibrous capsule with no inflammatory exudates observed, indicating a mild inflammatory response and supporting the use of the CMC constructs described here.

Early studies examining photocrosslinked CMC for NP cell encapsulation utilized a formulation with an initial E_y of ~1.5 kPa³⁶. However, cell-laden constructs weakened as the hydrolytic degradation rate exceeded the rate of matrix production by the encapsulated cells. A stiffer hydrogel was subsequently selected (E_y ~4.5 kPa) and the mechanical properties of cell-laden constructs were shown to remain stable over the 14-day study; however, it should be noted that these investigations were conducted without growth factor supplementation. As such, future studies will examine a less stiff CMC hydrogel, which can be formulated by decreasing the macromer concentration (weight percent), degree of methacrylation (% modification), or molecular weight^{38, 60}. Over time, this less rigid gel will provide more void space for matrix accumulation, and this will be studied in conjunction with TGF- β_3 supplementation in order to assess functional matrix deposition by encapsulated cells. These upcoming studies will assess the cellular metabolic activity and matrix turnover processes (i.e., matrix metalloproteinase function) in NP construct development.

Taken together, this study has demonstrated a long-term enhancement in the matrix accumulation and mechanical properties of constructs maintained *in vitro* in response to a two-week period of TGF- β_3 supplementation. However, in order to improve the clinical application of this tissue engineering therapy, the CMC scaffold formulation must be optimized for *in vivo* conditions.

5.5. References

1. Roughley PJ. 2004. Biology of intervertebral disc aging and degeneration: involvement of the extracellular matrix. *Spine* **29(23)**: 2691-2699.
2. Buckwalter JA, Mow VC, Boden SD, Eyre DR and Weidenbaum M. 2000. "Intervertebral disk structure, composition, and mechanical function." In: Orthopaedic Basic Science. Edited by Buckwalter JA, Einhorn TA and Simon SR. 2nd ed. Rosemont, IL: American Academy of Orthopaedic Surgeons. p 547-556.
3. Raj PP. 2008. Intervertebral disc: anatomy-physiology-pathophysiology-treatment. *Pain Pract* **8(1)**: 18-44.
4. Selard E, Shirazi-Adl A and Urban JPG. 2003. Finite element study of nutrient diffusion in the human intervertebral disc. *Spine* **28(17)**: 1945-1953.
5. Taylor JR. 1975. Growth of human intervertebral discs and vertebral bodies. *J Anat* **120(1)**: 49-68.
6. Trout JJ, Buckwalter JA and Moore KC. 1982. Ultrastructure of the human intervertebral disc: II. Cells of the nucleus pulposus. *Anat Rec* **204(4)**: 307-314.
7. Maldonado BA and Oegema TRJ. 1992. Initial characterization of the metabolism of intervertebral disc cells encapsulated in microspheres. *J Orthop Res* **10(5)**: 677-690.
8. Wang JY, Baer AE, Kraus VB and Setton LA. 2001. Intervertebral disc cells exhibit differences in gene expression in alginate and monolayer culture. *Spine* **26(16)**: 1747-1751.

9. Chiba K, Andersson GBJ, Masuda K, Momohara S, Williams JM and Thonar EJ-MA. 1998. A new culture system to study the metabolism of the intervertebral disc *in vitro*. *Spine* **23(17)**: 1821-1827.
10. Gruber HE and Hanley Jr. EN. 2000. Human disc cells in monolayer vs 3D culture: cell shape, division and matrix formation. *BMC Musculoskelet Disord* **1(1)**: EPub.
11. Nesti LJ, Li W-J, Shanti RM, Jiang YJ, Jackson W, Freedman BA, Kuklo TR, Giuliani JR and Tuan RS. 2008. Intervertebral disc tissue engineering using a novel hyaluronic acid-nanofibrous scaffold (HANFS) amalgam. *Tissue Eng Part A* **14(9)**: 1527-1537.
12. Cloyd JM, Malhotra NR, Weng L, Chen W, Mauck RL and Elliott DM. 2007. Material properties in unconfined compression of human nucleus pulposus, injectable hyaluronic acid-based hydrogels and tissue engineering scaffolds. *Eur Spine J* **16(11)**: 1892-1898.
13. Crevensten G, Walsh AJL, Ananthakrishnan D, Page P, Wahba GM, Lotz JC and Berven S. 2004. Intervertebral disc cell therapy for regeneration: mesenchymal stem cell implantation in rat intervertebral discs. *Ann Biomed Eng* **32(3)**: 430-434.
14. Neidlinger-Wilke C, Würtz K, Liedert A, Schmidt C, Börm W, Ignatius A, Wilke H-J and Claes L. 2005. A three-dimensional collagen matrix as a suitable culture system for the comparison of cyclic strain and hydrostatic pressure effects on intervertebral disc cells. *J Neurosurg Spine* **2(4)**: 457-465.

15. Neidlinger-Wilke C, Würtz K, Urban JPG, Börm W, Arand M, Ignatius A, Wilke H-J and Claes LE. 2006. Regulation of gene expression in intervertebral disc cells by low and high hydrostatic pressure. *Eur Spine J* **15 (Suppl 3)**: S372-378.
16. Sakai D, Mochida J, Iwashina T, Watanabe T, Nakai T, Ando K and Hotta T. 2005. Differentiation of mesenchymal stem cells transplanted to a rabbit degenerative disc model: potential and limitations for stem cell therapy in disc regeneration. *Spine* **30(21)**: 2379-2387.
17. Sakai D, Mochida J, Iwashina T, Hiyama A, Omi H, Imai M, Nakai T, Ando K and Hotta T. 2006. Regenerative effects of transplanting mesenchymal stem cells embedded in atelocollagen to the degenerated intervertebral disc. *Biomaterials* **27(3)**: 335-345.
18. Gokorsch S, Nehringm D, Grottke C and Czermak P. 2004. Hydrodynamic stimulation and long term cultivation of nucleus pulposus cells: a new bioreactor system to induce extracellular matrix synthesis by nucleus pulposus cells dependent on intermittent hydrostatic pressure. *Int J Artif Organs* **27(11)**: 962-970.
19. Alini M, Roughley PJ, Antoniou J, Stoll T and Aebi M. 2002. A biological approach to treating disc degeneration: not for today, but maybe for tomorrow. *Eur Spine J* **11(Suppl 2)**: S215-S220.
20. Roughley P, Hoemann C, DesRosiers E, Mwale F, Antoniou J and Alini M. 2006. The potential of chitosan-based gels containing intervertebral disc cells for nucleus pulposus supplementation. *Biomaterials* **27(3)**: 388-396.

21. Cheng Y-H, Lin F-H and Yang KC. 2009. Thermosensitive chitosan-gelatin-glycerol phosphate hydrogels as a cell carrier for nucleus pulposus regeneration: an *in-vitro* study. *Tissue Eng Part A* doi:10.1089/ten.TEA.2009.0229.
22. Chou AI, Reza AT and Nicoll SB. 2008. Distinct intervertebral disc cell populations adopt similar phenotypes in three-dimensional culture. *Tissue Eng Part A* **14(12)**: 2079-2087.
23. Chou AI and Nicoll SB. 2009. Characterization of photocrosslinked alginate hydrogels for nucleus pulposus cell encapsulation. *J Biomed Mater Res A* **91A(1)**: 187-194.
24. Chou AI, Akintoye SO and Nicoll SB. 2009. Photo-crosslinked alginate hydrogels support enhanced matrix accumulation by nucleus pulposus cells *in vivo*. *Osteoarthritis Cartilage* **17(10)**: 1377-1384.
25. Kasra M, Goel V, Martin J, Wang ST, Choi W and Buckwalter J. 2003. Effect of dynamic hydrostatic pressure on rabbit intervertebral disc cells. *J Orthop Res* **21(4)**: 597-603.
26. Chou AI, Bansal A, Miller GJ and Nicoll SB. 2006. The effect of serial monolayer passaging on the collagen expression profile of outer and inner annulus fibrosus cells. *Spine* **31(17)**: 1875-1881.
27. Hutton WC, Elmer WA, Boden SD, Hyon S, Toribatake Y, Tomita K and Hair GA. 1999. The effect of hydrostatic pressure on intervertebral disc metabolism. *Spine* **24(15)**: 1507-1515.

28. Hutton WC, Elmer WA, Bryce LM, Kozlowska EE, Boden SD and Kozlowski M. 2001. Do the intervertebral disc cells respond to different levels of hydrostatic pressure? *Clin Biomech* **16(9)**: 728-734.
29. Kasra M, Merryman WD, Loveless KN, Goel VK, Martin JD and Buckwalter JA. 2006. Frequency response of pig intervertebral disc cells subjected to dynamic hydrostatic pressure. *J Orthop Res* **24(10)**: 1967-1973.
30. Gruber HE, Stasky AA and Hanley Jr EN. 1997. Characterization and phenotypic stability of human disc cells *in vitro*. *Matrix Biol* **16(5)**: 285-288.
31. Thonar E, An H and Masuda K. 2002. Compartmentalization of the matrix formed by nucleus pulposus and annulus fibrosus cells in alginate gel. *Biochem Soc Trans* **30(6)**: 874-888.
32. Baer AE, Wang JY, Kraus VB and Setton LA. 2001. Collagen gene expression and mechanical properties of intervertebral disc cell-alginate cultures. *J Orthop Res* **19**: 2-10.
33. Elisseeff JH, Anseth K, Sims D, McIntosh W, Randolph M and Langer R. 1999. Transdermal photopolymerization for minimally invasive implantation. *Proc Natl Acad Sci USA* **96(6)**: 3104–3107.
34. Elisseeff J, Anseth K, Sims D, McIntosh W, Randolph M, Yaremchuk M and Langer R. 1999. Transdermal photopolymerization of poly(ethylene oxide)-based injectable hydrogels for tissue-engineered cartilage. *Plast Reconstr Surg* **104(4)**: 1014-1022.

35. Smeds KA, Pfister-Serres A, Miki D, Dastgheib K, Inoue M, Hatchell DL and Grinstaff MW. 2001. Photocrosslinkable polysaccharides for *in situ* hydrogel formation. *J Biomed Mater Res* **54(1)**: 115-121.
36. Reza AT and Nicoll SB. 2009. Characterization of novel photocrosslinked carboxymethylcellulose hydrogels for encapsulation of nucleus pulposus cells. *Acta Biomater* doi:10.1016/j.actbio.2009.1006.1004.
37. Reza AT and Nicoll SB. 2009. Serum-free, chemically defined medium with TGF-beta(3) enhances functional properties of nucleus pulposus cell-laden carboxymethylcellulose hydrogel constructs. *Biotechnol Bioeng* doi: 10.1002/bit.22545.
38. Burdick JA, Chung C, Jia X, Randolph MA and Langer R. 2005. Controlled degradation and mechanical behavior of photopolymerized hyaluronic acid networks. *Biomacromolecules* **6(1)**: 386 -391.
39. Chang SCN, Rowley JA, Tobias G, Genes NG, Roy AK, Mooney DJ, Vacanti CA and Bonassar LJ. 2001. Injection molding of chondrocyte/alginate constructs in the shape of facial implants. *J Biomed Mater Res* **55(4)**: 503-511.
40. Hung CT, Mauck RL, Wang CC, Lima EG and Ateshian GA. 2004. A paradigm for functional tissue engineering of articular cartilage via applied physiologic deformational loading. *Ann Biomed Eng* **32(1)**: 35-49.
41. Mauck RL, Seyhan SL, Ateshian GA and Hung CT. 2002. Influence of seeding density and dynamic deformational loading on the developing structure/function relationships of chondrocyte-seeded agarose hydrogels. *Ann Biomed Eng* **30(8)**: 1046-1056.

42. Puelacher WC, Kim SW, Vacanti JP, Schloo B, Mooney D and Vacanti CA. 1994. Tissue-engineered growth of cartilage: the effect of varying the concentration of chondrocytes seeded onto synthetic polymer matrices. *Int J Oral Maxillofac Surg* **23(1)**: 49-53.
43. Vunjak-Novakovic G, Obradovic B, Martin I, Bursac PM, Langer R and Freed LE. 1998. Dynamic cell seeding of polymer scaffolds for cartilage tissue engineering. *Biotechnol Prog* **14(2)**: 193-202.
44. Mackay AM, Beck SC, Murphy JM, Barry FP, Chichester CO and Pittenger MF. 1998. Chondrogenic differentiation of cultured human mesenchymal stem cells from marrow. *Tissue Eng* **4(4)**: 415-428.
45. Lima EG, Bian L, Ng KW, Mauck RL, Byers BA, Tuan RS, Ateshian GA and Hung CT. 2007. The beneficial effect of delayed compressive loading on tissue-engineered cartilage constructs cultured with TGF-beta3. *Osteoarthritis Cartilage* **15(9)**: 1025-1033.
46. Byers BA, Mauck RL, Chiang IE and Tuan RS. 2008. Transient exposure to transforming growth factor beta 3 under serum-free conditions enhances the biomechanical and biochemical maturation of tissue-engineered cartilage. *Tissue Eng Part A* **14(11)**: 1821-1834.
47. Miyanishi K, Trindade MCD, Lindsey DP, Beaupré GS, Carter DR, Goodman SB, Schurman DJ and Smith RL. 2006. Effects of hydrostatic pressure and transforming growth factor-beta 3 on adult human mesenchymal stem cell chondrogenesis *in vitro*. *Tissue Eng* **12(6)**: 1419-1428.

48. Risbud MV, Di Martino A, Guttapalli A, Seghatoleslami R, Denaro V, Vaccaro AR, Albert TJ and Shapiro IM. 2006. Toward an optimum system for intervertebral disc organ culture: TGF-beta 3 enhances nucleus pulposus and annulus fibrosus survival and function through modulation of TGF-beta-R expression and ERK signaling. *Spine* **31(8)**: 884-890.
49. Singer VL, Jones LJ, Yue ST and Haugland RP. 1997. Characterization of PicoGreen reagent and development of a fluorescence-based solution assay for double-stranded DNA quantitation. *Anal Biochem* **249(2)**: 228-238.
50. Farndale RW, Sayers CA and Barrett AJ. 1982. A direct spectrophotometric microassay for sulfated glycosaminoglycans in cartilage cultures. *Connect Tissue Res* **9(4)**: 247-248.
51. Enobakhare BO, Bader DL and Lee DA. 1996. Quantification of sulfated glycosaminoglycans in chondrocyte/alginate cultures, by use of 1,9-dimethylmethylene blue. *Anal Biochem* **243(1)**: 189-191.
52. Soltz MA and Ateshian GA. 1998. Experimental verification and theoretical prediction of cartilage interstitial fluid pressurization at an impermeable contact interface in confined compression. *J Biomech* **31(10)**: 927-934.
53. Minns RJ and Stevens FS. 1977. The collagen fibril organization in human articular cartilage. *J Anat* **123(2)**: 437-457.
54. Stockwell RA. 1979. "Biology of cartilage cells." In: Biological Structure and Function. Edited by Harrison RJ and McMinn RMH. 1st ed. London/New York/Melbourne: Cambridge University Press. p 25-27, 67, 74-79.

55. Bryant SJ and Anseth KS. 2003. Controlling the spatial distribution of ECM components in degradable PEG hydrogels for tissue engineering cartilage. *J Biomed Mater Res A* **64(1)**: 70-79.
56. Sahoo S, Chung C, Khetan S and Burdick JA. 2008. Hydrolytically degradable hyaluronic acid hydrogels with controlled temporal structures. *Biomacromolecules* **9(4)**: 1088-1092.
57. Roberts AB. 1998. Molecular and cell biology of TGF-beta. *Miner Electrolyte Metab* **24(2-3)**: 111-119.
58. Mauck RL, Nicoll SB, Seyhan SL, Ateshian GA and Hung CT. 2003. Synergistic action of growth factors and dynamic loading for articular cartilage tissue engineering. *Tissue Eng* **9(4)**: 597-611.
59. Stalling SS, Akintoye SO and Nicoll SB. 2009. Development of photocrosslinked methylcellulose hydrogels for soft tissue reconstruction. *Acta Biomater* **5(6)**: 1911-1918.
60. Anseth KS, Bowman CN and Brannon-Peppas L. 1996. Mechanical properties of hydrogels and their experimental determination. *Biomaterials* **17(17)**: 1647-1657.

Chapter 6: Conclusions, Limitations, and Future Directions

6.1. Overview

Carboxymethylcellulose (CMC) was characterized and developed for potential use as a tissue engineering scaffold for the replacement of the nucleus pulposus (NP) of the intervertebral disc (IVD). Covalently photocrosslinked CMC hydrogels were produced by modifying CMC hydroxyl groups with functional methacrylate moieties, which were able to undergo radical polymerization, creating a three-dimensional crosslinked network. The material properties of these hydrogels were controlled by varying the macromer concentration and molecular weight in order to identify a formulation capable of supporting encapsulated NP cells (Chapter 2). Upon selection of a suitable CMC scaffold, medium formulation and transforming growth factor- β_3 (TGF- β_3) supplementation were examined as a method to enhance the development of cell-seeded constructs (Chapter 3). Mechanical stimulation via hydrostatic pressurization, applied in the presence and absence of TGF- β_3 , was explored as a technique to increase the matrix deposition and functional properties of cell-laden CMC scaffolds (Chapter 4). Finally, the long-term effects of *in vitro* pre-conditioning with TGF- β_3 were examined *in vitro* and *in vivo* using a subcutaneous murine pouch model to characterize functional matrix elaboration (Chapter 5). The major findings and limitations of these studies, as well as future directions for this work, are presented in this chapter.

6.2. Characterization of Photocrosslinked CMC for NP Cell Encapsulation (Chapter 2)

Although ionically crosslinked alginate has been the prevalent biomaterial scaffold choice for NP tissue engineering applications¹⁻¹¹, this hydrogel has been shown to lose mechanical integrity over time, as crosslinking calcium ions diffuse out of the gel or are depleted by encapsulated cells^{5, 12}. This study sought to establish a covalently photocrosslinked CMC hydrogel with tunable properties that was capable of supporting encapsulated NP cells and promoting phenotypic matrix deposition. We hypothesized that an increase in CMC macromer concentration and molecular weight would result in an increase in hydrogel mechanical properties and a decrease in the swelling ratio.

In a series of initial studies, we evaluated photocrosslinked hydrogels composed of 90 kDa and 250 kDa CMC cast at a variety of weight percents and subsequently characterized these scaffolds by quantifying the elastic modulus and cell viability over seven days of *in vitro* culture. Gross observations revealed a decrease in structural stability with decreasing macromer concentration, as indicated by the amorphous composition of 1% 250 kDa CMC constructs. This assessment was verified quantitatively by determining the elastic modulus of these scaffolds under compression, and, in agreement with our hypothesis and results shown by others^{4, 13}, increasing macromer concentration resulted in an increase in mechanical properties. Cells remained viable in all groups over the 7-day study.

From these early investigations, we chose a 4% 90 kDa and 2% 250 kDa CMC formulation for further examination, in which we quantified the swelling ratio (Q_w) and equilibrium mechanical properties (E_y). Although Q_w remained stable in all groups over

the 14-day study, cell-laden and cell-free constructs experienced a significant decrease in E_y over time, indicating that hydrolysis of the ester crosslinks was occurring more rapidly than the elaboration of extracellular matrix (ECM) components. As such, a 3% 250 kDa CMC was chosen in order to provide a stiffer initial environment for a subsequent study. Q_w for 3% 250 kDa CMC constructs remained constant over time and significantly lower in cell-laden samples in comparison to cell-free gels, indicating that the presence of cells resulted in an increase in the overall dry weight due to matrix production. This was confirmed by mechanical testing which demonstrated a significant loss in the mechanical properties of cell-free constructs, while cell-laden samples were able to maintain the initial E_y . Histological and immunohistochemical analyses showed the formation of lacunae and pericellular deposition of chondroitin sulfate proteoglycan (CSPG), a phenotypic matrix component. Overall, these findings identified a suitable CMC formulation for NP tissue engineering applications.

6.3. Biochemical Stimulation of Cell-laden CMC Constructs (Chapter 3)

Growth factor supplementation has been shown to enhance matrix deposition of cartilage and IVD tissue-engineered constructs¹⁴⁻¹⁷, and studies have demonstrated the importance of medium formulation in modulating the effectiveness of such biochemical signaling molecules. Although it was demonstrated in Chapter 2 that cell-laden CMC constructs were able to maintain their initial mechanical properties over time, we sought to investigate TGF- β_3 supplementation and medium composition as a means to increase functional properties. This study compared a standard serum-containing medium formulation, which was utilized in the experiments detailed in Chapter 2, to a chemically-

defined, serum-free medium commonly used in cartilage tissue engineering. We hypothesized that a chemically-defined, serum-free medium would support the stability of the NP cellular phenotype, as evidenced by phenotypic GAG and type II collagen (COL II) accumulation, and TGF- β_3 supplementation would further improve matrix deposition and functional material properties.

TGF- β_3 significantly decreased Q_w to near native values and increased DNA content, GAG accumulation, and COL II deposition, in agreement with our hypothesis. There was no detectable type I collagen (COL I) accumulation in constructs cultured in chemically-defined, serum-free medium. However, scaffolds maintained in TGF- β_3 -supplemented, serum-containing medium were circumscribed by a ring of fibroblast-like cells which stained positive for COL I, consistent with fibrous tissue rather than the native NP phenotype. The effects of TGF- β_3 were most pronounced in serum-free, chemically-defined medium, as these constructs exhibited the largest E_y while maintaining phenotypic matrix deposition. Therefore, serum-free, chemically-defined medium supplemented with TGF- β_3 was selected for use in all future NP tissue engineering studies.

6.4. Biomechanical and Biochemical Stimulation of Cell-laden CMC Constructs (Chapter 4)

Hydrostatic pressurization of tissue engineered IVD constructs has been shown to stimulate matrix production when applied at magnitudes within the physiologic range (0.1 – 3 MPa) to mimic the loads experienced *in vivo*^{7, 8, 18, 19}. Although TGF- β_3 supplementation of chemically-defined, serum-free medium produced a five-fold increase

in mechanical properties in comparison to untreated constructs, GAG accumulation (210 $\mu\text{g}/\text{mg}$ dry weight) remained ~40% of that seen in the native NP (~550 $\mu\text{g}/\text{mg}$)²⁰. We sought to examine the effects of hydrostatic pressurization and growth factor supplementation on the matrix production and functional properties of cell-laden CMC scaffolds in an effort to further enhance construct development. We hypothesized that the application of hydrostatic pressure would increase the matrix accumulation (GAGs, COL II) and functional properties of cell-laden constructs and that these values would be further augmented by TGF- β_3 supplementation.

Hydrostatic pressure was applied at 2 MPa and 0.5 Hz from day 3 to day 28 of *in vitro* culture. Constructs were loaded for 4 hrs/day, 5 days/week for 4 weeks. In support of the findings from Chapter 3, TGF- β_3 supplementation resulted in significant increases in GAG and COL II accumulation and produced a marked increase in E_y in comparison to untreated constructs. However, there was no significant difference between TGF- β_3 -treated unloaded controls and TGF- β_3 -treated pressurized constructs, or untreated, unloaded controls and the corresponding pressurized scaffolds, which was in contrast to our hypothesis.

Earlier work from our laboratory examined the effect of pressure on outer and inner annulus fibrosus cells seeded on a fibrous poly(L-lactic acid) reinforced poly(glycolic acid) mesh and found significantly increased COL II deposition and improved matrix distribution when pressure was elevated to the hyperphysiologic level of 5 MPa, with no effects observed at 2 MPa²¹. As such, an additional study was conducted applying a pressure of 5 MPa.

TGF- β_3 supplementation again produced significant increases in GAG and COL II accumulation and a marked increase in E_y in comparison to untreated constructs. However, as with the 2 MPa study, there was no significant difference between TGF- β_3 -treated unloaded controls and TGF- β_3 -treated constructs pressurized at 5 MPa, indicating no significant effect of pressurization at this magnitude in TGF- β_3 -treated constructs. In contrast, scaffolds cultured without TGF- β_3 and subjected to 5 MPa hydrostatic pressure exhibited a significant increase in COL II accumulation in comparison to unloaded, untreated controls, in agreement with our hypothesis. Still, GAG accumulation, which was shown to have a more direct relationship with E_y than COL II, was comparable between these two groups. Not surprisingly, there was no detectable difference in the functional properties of untreated, pressurized constructs and untreated, unloaded controls. E_y for all untreated groups (3.14 ± 0.62 kPa) was over five-fold lower in comparison to TGF- β_3 -treated samples (17.56 ± 3.18 kPa).

Hydrostatic pressure applied within the physiologic range experienced within the IVD (2 MPa) did not have any significant effect on construct properties. Although increasing the load to the hyperphysiologic magnitude of 5 MPa resulted in a slight modulation, increasing COL II deposition in untreated, pressurized constructs, this had no effect on overall functional properties. It is important to note that the application of hydrostatic pressure at this elevated magnitude did not affect cell viability, as the DNA content of unloaded controls and pressurized samples were similar in groups maintained both with and without TGF- β_3 . While the goal of this study was to recapitulate the primary form of mechanical loading experienced *in vivo* within the disc, our bioreactor system nevertheless represented a highly artificial, engineered environment, as many

variables (i.e., annular confinement) found in the native tissue were not recreated in our *in vitro* loading paradigm. Since dynamic hydrostatic pressure applied at 5 MPa exhibited a marginal impact on cell-seeded constructs, future studies may employ higher magnitudes, similar to those utilized in cartilage tissue engineering (10 MPa)²²⁻²⁴, to examine the effect on construct development, monitoring the expression of both anabolic (COL II, GAGs) and catabolic (matrix metalloproteinases – MMPs) factors to ensure that these hyperphysiologic forces do not produce negative effects.

Taken together, these data indicate that while pressure applied at 5 MPa in the absence of TGF- β_3 modulated COL II production, this did not impact the overall functional properties of cell-laden constructs. Instead, TGF- β_3 supplementation utilized alone rather than in conjunction with hydrostatic pressure was shown to be effective in enhancing the development of NP tissue engineered CMC constructs.

6.5. Long-term Assessment of *in vitro* Pre-Conditioning with TGF- β_3 (Chapter 5)

Although TGF- β_3 supplementation to serum-free, chemically-defined medium was shown to be an effective means of modulating NP cell-laden CMC construct development, continuous delivery of exogenous growth factors is not a cost-effective or clinically relevant method due to the short half-life of these proteins. In addition, it is not clear whether the beneficial effects of TGF- β_3 treatment are retained once growth factor supplementation is discontinued. Therefore, we investigated the long-term effects of a two-week *in vitro* pre-culture period in the presence of TGF- β_3 . This response was characterized *in vitro* and *in vivo* using a subcutaneous murine pouch model. We hypothesized that TGF- β_3 -treated constructs would exhibit greater matrix accumulation

and higher mechanical properties in comparison to untreated controls, and that these properties would be maintained both *in vitro* and *in vivo* following the cessation of growth factor supplementation.

TGF- β_3 supplementation resulted in a significant decrease in Q_w by the end of the 14-day *in vitro* pre-culture period in comparison to treated, cell-free controls, while Q_w for untreated cell-laden constructs was similar to that for untreated, cell-free controls. TGF- β_3 additionally produced increased GAG and COL II accumulation with a concomitant increase in E_y in comparison to untreated cell-laden gels after 14 days, in support of our hypothesis. At the 14-day time point, growth factor supplementation was discontinued and both cell-laden and cell-free constructs cultured with and without TGF- β_3 were subcutaneously implanted in nude mice, while a subset of these groups was maintained *in vitro* in the absence of TGF- β_3 .

UNTREATED CONSTRUCTS – *in vitro* and *in vivo*: Constructs cultured without TGF- β_3 were mechanically indistinguishable from corresponding cell-free controls, indicating that although the encapsulated cells remained viable both *in vitro* and *in vivo*, they were not metabolically active and did not deposit sufficient ECM to impact the overall mechanical function of the scaffold. Untreated cells remained in a basal, senescent-like state in comparison to TGF- β_3 -treated cells. However, untreated cells cultured *in vivo* exhibited more prevalent lacuna formation, an increase in interterritorial accumulation of CSPG, and a slight increase in interterritorial COL II deposition in comparison to corresponding *in vitro* scaffolds. While subcutaneous implantation does not recapitulate the native loading environment of the NP, this form of *in vivo* culture does expose constructs to various forms of mechanical loading, and this may have

stimulated matrix deposition by the encapsulated cells. Nonetheless, the mechanical properties of *in vivo* scaffolds were not significantly affected by this culture condition, as untreated *in vivo* constructs exhibited a similar E_y as corresponding *in vitro* scaffolds.

TGF- β_3 -TREATED CONSTRUCTS – *in vitro*: TGF- β_3 -treated constructs cultured *in vitro* were able to maintain the gains in GAG and COL II accumulation and E_y that resulted from the pre-culture period, in support of our hypothesis. Specifically, TGF- β_3 -treated scaffolds exhibited an E_y approximately six-fold greater than corresponding untreated samples up to 8 weeks after growth factor supplementation was ceased. The *in vitro*, free-swelling culture conditions provided adequate nutrient diffusion through the scaffold and opportunity for the hydrolysis of ester crosslinks. As such, void space was created over time, allowing for cell proliferation, which is a known anabolic effect of TGF- β_3 supplementation. Histological analyses of TGF- β_3 -treated scaffolds revealed clonal expansion, as evidenced by cell clusters, and increased deposition of COL II, which is a large matrix protein that may require increased void space for proper assembly.

TGF- β_3 -TREATED CONSTRUCTS – *in vivo*: Samples which were exposed to TGF- β_3 and subsequently implanted *in vivo* experienced a significant decrease in the retention of GAGs, a loss of DNA content, and a reduction in mechanical properties over time. This was contrary to our hypothesis and indicated that such conditions were less favorable than *in vitro* culture. Given the increased number of cells and greater matrix accumulation in comparison to untreated constructs upon implantation, TGF- β_3 -treated constructs required an ample nutrient supply to maintain homeostasis. While free-swelling *in vitro* conditions may have provided adequate diffusion for ester hydrolysis to

create void space for matrix deposition, *in vivo* constructs were surrounded by a fibrous capsule which may have impaired nutrient transport and constricted the hydrogel. The extracellular matrix that had been established during the TGF- β_3 pre-culture period may have also contracted, resulting in a more stiff, locally confined pericellular environment that was consequently less hospitable. In addition, as indicated by mechanical testing data for cell-free constructs, photocrosslinked CMC hydrogels did not undergo significant degradation over time, which may have further hindered matrix accumulation while promoting the expression of matrix degrading enzymes. Therefore, even though the subcutaneous pouch model is an accepted model to assess *in vivo* tissue formation, the overall combination of conditions may have caused *in vivo* TGF- β_3 -treated cells to enter a senescent state similar to that seen in untreated constructs. Values of GAG accumulation and E_y for treated scaffolds fell to baseline levels comparable to those of untreated, cell-laden controls, with the cells likely undergoing programmed cell death in the absence of stimulatory signals (giving rise to decreased DNA content). One technique to address this issue would be to utilize a less stiff hydrogel with a lower initial modulus and crosslinking density. Such gels would allow for more rapid hydrolytic degradation of the network structure during the *in vitro* pre-culture period. This would create void space for future matrix accumulation, while TGF- β_3 treatment would promote matrix deposition that would overcome the loss in material properties. Future studies will monitor MMP activity to better assess matrix turnover under *in vitro* and *in vivo* conditions.

This study demonstrated a long-term enhancement in the matrix accumulation and mechanical properties of constructs maintained *in vitro* in response to a short-term TGF-

β_3 treatment. However, in order to improve the clinical application of this tissue engineering therapy, the CMC scaffold formulation must be optimized for *in vivo* conditions.

6.6. Limitations and Future Directions

Although this dissertation has characterized and developed a novel CMC hydrogel scaffold for use in NP tissue engineering, there are several limitations which must be considered when interpreting this work. Because the IVD is less characterized at the cellular and tissue levels in comparison to other orthopaedic tissues, such as cartilage, primary bovine NP cells were utilized throughout this study in order to gain a better understanding of native cell behavior under *in vitro* conditions. However, primary NP cells are not a clinically feasible cell source, and autologous mesenchymal stem cells (MSCs) represent a more clinically relevant option. These multipotent progenitor cells have been identified in various adult tissues, including bone marrow, trabecular bone, cartilage, muscle, and adipose tissue²⁵. MSCs have been shown to be capable of undergoing chondrogenesis when cultured in a 3-D environment in the presence of growth factors, such as TGF- β ²⁶⁻²⁸. In addition, recent work has shown that MSCs can be induced along an NP-like differentiation pathway when cultured under hypoxic conditions in the presence of TGF- β_1 ²⁹. Steck et al. reported IVD-like differentiation when MSCs in spheroid culture were maintained in the presence of TGF- β_3 , dexamethasone, and ascorbate³⁰. As such, future studies should employ MSCs for encapsulation in CMC scaffolds. Matrix production and functional properties could then

be compared to those measurements described in this work, using primary NP cells as a benchmark for construct development.

As growth factor delivery has been shown to aid in MSC differentiation, gene therapy is an alternative approach to exogenous supplementation in which cells are genetically modified in order to induce sustained growth factor synthesis endogenously. Cells can be transduced *ex vivo* using viral (i.e., adenoviral, retroviral, baculoviral) vectors and then incorporated into tissue engineered scaffolds or delivered *in vivo*. However, although viral vectors have high transfection efficiency, they also present certain safety concerns, such as induction of viral protein production that may stimulate a host immune reaction. Still, this technique has been safely implemented in IVD cell culture, as primary IVD cells have been successfully transduced using adenoviral BMP-12 and TGF- β_1 , resulting in increased matrix synthesis^{17, 31}. Other methods of growth factor delivery include encapsulation within microspheres³², covalent tethers³³, and affinity ligands³⁴.

Another limitation to covalently photocrosslinked CMC hydrogels is the slow degradation of the scaffold (as introduced in Chapter 5). Although any biomaterial scaffold intended for use within a load-bearing tissue, such as the NP, must provide immediate structural support, the degradation properties of this material should coincide with ECM accumulation within the scaffold, eventually leaving behind a biologically functional tissue replacement. To achieve more rapid ester hydrolysis, a softer CMC hydrogel may be formulated by decreasing the macromer concentration (weight percent), degree of methacrylation (% modification), or molecular weight^{13, 35}. Another alternative is incorporating degradable units onto the CMC backbone to alter the degradation profile.

Bryant and Anseth incorporated rapidly degradable lactic acid units into a non-degrading, inert poly(ethylene glycol) (PEG) hydrogel³⁶, while Sahoo et al. similarly incorporated hydrolyzable lactic acid units into an enzymatically degradable hyaluronic acid construct³⁷. MMP-sensitive peptides have also been used to crosslink PEG hydrogels encapsulated with bovine chondrocytes, resulting in scaffold degradation in concert with matrix turnover³⁸.

While the photopolymerizable CMC system described in this dissertation could be effectively incorporated into a tissue engineered IVD composite, such as those described by Mizuno et al.^{39, 40} and Bowles et al.⁴¹, this platform may not be suitable for use as an intradiscal therapy in the early stages of degeneration, as polymerization cannot be performed uniformly through the fibrous annular tissue where light penetration is limited. Instead, an injectable, *in situ*-curing redox-initiated system may provide a minimally-invasive, clinically-relevant option. Redox initiators utilize two reagents which, when mixed, generate free radicals capable of initiating polymerization. Oxidizing agents which have been studied include sodium persulfate and ammonium persulfate, and reducing agents include ascorbic acid, ascorbate, and ascorbate-2-phosphate⁴². One commonly used oxidizing/reducing agent combination is ammonium persulfate (APS)/ N, N, N', N'-tetramethylethylenediamine (TEMED), which is a cytocompatible, water-soluble redox initiation system⁴³⁻⁴⁶ which has been shown to be non-cytotoxic at low initiator concentrations⁴⁴.

We recently conducted a pilot study examining APS/TEMED redox-initiated crosslinking of methacrylated CMC. Certain factors to consider when designing an injectable system include viscosity of the solution in order to maintain injectability and

the rate of polymerization, as the solution should not crosslink too rapidly which would prevent any clinical manipulation, but polymerization should also not progress too slowly, which would allow the solution to diffuse from the injection site. Similar to the photoinitiated CMC system described in this dissertation, redox polymerization rate is affected by initiator concentration and macromer concentration, whereby increasing these values will decrease the amount of time required for polymerization.

Cell-free CMC hydrogels were cast at 2% and 2.5% using APS and TEMED initiators, each at a 10 mM concentration. Constructs were maintained in sterile DPBS for 24 hrs at 37°C, 5% CO₂, at which time they were isolated to assess the compressive elastic modulus using the DMA apparatus described in Chapter 2. Similar to the results from Chapter 2, an increase in macromer concentration (weight percent) resulted in an increase in construct stiffness, although this trend was not statistically significant ($p=0.565$) (Figure 6.1). Bovine NP cells were encapsulated in 2.5% 10 mM CMC hydrogels at 30×10^6 cells/mL and viability was determined at day 1 using the Live/Dead stain (Figure 6.2). Viable cells were evenly distributed throughout the construct. However, a larger population of dead cells was present in comparison to similar photocrosslinked gels described in Chapter 2. Therefore, additional formulations should be examined by varying the initiator concentration and/or macromer concentration in order to improve this potential injectable intradiscal therapy.

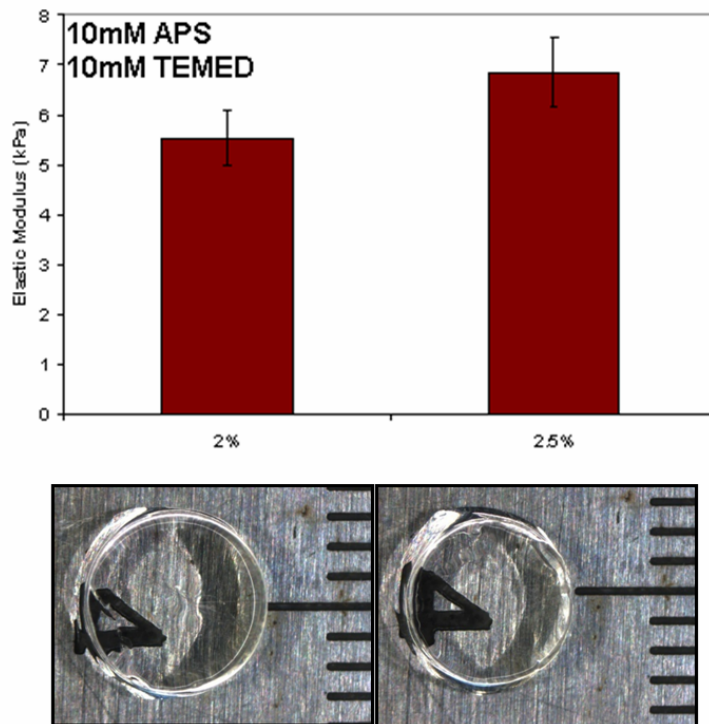


Figure 6.1. Day 1 compressive elastic modulus of 2% and 2.5% cell-free CMC hydrogels formed via redox-initiated polymerization, with corresponding representative stereo micrograph images below (scale in mm).

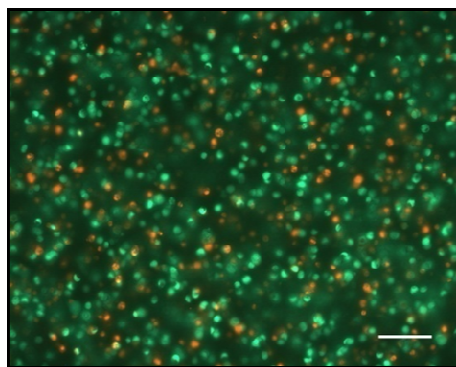


Figure 6.2. Live/Dead image of 2.5% 10 mM CMC hydrogels at day 1, with live cells stained green and dead cells shown in red (Bar = 100 μ m).

One major goal of this dissertation was to examine the effect of mechanical stimulation on matrix production by encapsulated NP cells. We investigated the effects of hydrostatic pressure and found that, although pressure increased COL II accumulation in untreated constructs, it did not enhance mechanical properties, and had no impact on TGF- β_3 -treated scaffolds. A number of variables exist that can affect the cellular response to mechanical stimulation. Previous IVD tissue engineering studies have examined mechanical stimulation via hydrostatic pressurization applied at a variety of magnitudes (0.25-6 MPa) and frequencies (0-20 Hz), duty cycles (30 min/day to 12 hr/day) and loading durations (1 day to 4 weeks)^{7-10, 18, 19, 47-49}. While these investigations have mainly examined the short-term response to pressure, they provide a starting point for various loading regimens that may be incorporated into future work examining the long-term effect of pressure on the functional properties of tissue engineered constructs. Additionally, as pressure applied at the hyperphysiologic magnitude of 5 MPa in this artificial environment resulted in a slight modulation of NP matrix production, future studies may examine loading protocols utilized in cartilage tissue engineering which routinely pressurize samples to a magnitude of 10 MPa²²⁻²⁴.

Deformational mechanical loading via dynamic compression may also serve as an effective stimulus for matrix production. While compressive load has been traditionally utilized *in vivo* using a rat tail model, it has recently been applied *in vitro* by Korecki et al. who used NP cell-laden alginate hydrogels to compare the effects of compression frequency (0.1, 1, and 3 Hz) and donor age⁵⁰. As such, this form of mechanical stimulation may also be investigated in future studies as a method to augment the functional properties of tissue engineered constructs.

Finally, once a CMC platform has been developed, constructs should be assessed in an animal model of disc degeneration. Although Chapter 5 has detailed the effects of subcutaneous implantation in nude mice in an effort to characterize and develop CMC constructs, this system does not replicate the load-bearing environment of the NP. The effects of disc degeneration are wide-ranging, impacting mechanical integrity and biochemical composition. Various *in vivo* animal models have been created to mimic these conditions and evaluate potential therapies. Although naturally-occurring animal models, such as those established in rats, dogs, and primates, allow for thorough examination of the broad effects of degeneration, the underlying cause of this species-specific condition and the potential interaction with therapeutic interventions remain unclear⁵¹. Experimentally-induced disc degeneration allows for greater control and reproducibility. Masuda et al. have developed a rabbit model of mild disc degeneration using the annulus needle puncture technique⁵², while Boxberger et al. have developed a chemically-controlled rat lumbar model that results in reduced GAG content following NP injection with chondroitinase ABC⁵³. Therefore, the efficacy of the cell-CMC hydrogel system at restoring mechanical integrity and biochemical composition of degenerated discs should be evaluated using an appropriate animal model in order to assess the clinical applications of this potential therapy.

6.7. Final Conclusions

Taken together, this thesis work has established a photocrosslinkable CMC scaffold with tunable material properties that may be utilized for the encapsulation of NP cells. The functional properties of these cell-laden constructs may be modulated via

TGF- β_3 supplementation, as this growth factor was shown to produce long-term enhancements in matrix accumulation and mechanical properties *in vitro* after a two-week pre-culture period. However, the degradative profile of the CMC scaffold must be optimized for *in vivo* conditions prior to any clinical applications.

6.8. References

1. Chiba K, Andersson GBJ, Masuda K, Momohara S, Williams JM and Thonar EJ-MA. 1998. A new culture system to study the metabolism of the intervertebral disc *in vitro*. *Spine* **23(17)**: 1821-1827.
2. Chou AI, Bansal A, Miller GJ and Nicoll SB. 2006. The effect of serial monolayer passaging on the collagen expression profile of outer and inner annulus fibrosus cells. *Spine* **31(17)**: 1875-1881.
3. Chou AI, Reza AT and Nicoll SB. 2008. Distinct intervertebral disc cell populations adopt similar phenotypes in three-dimensional culture. *Tissue Eng Part A* **14(12)**: 2079-2087.
4. Chou AI and Nicoll SB. 2009. Characterization of photocrosslinked alginate hydrogels for nucleus pulposus cell encapsulation. *J Biomed Mater Res A* **91A(1)**: 187-194.
5. Chou AI, Akintoye SO and Nicoll SB. 2009. Photo-crosslinked alginate hydrogels support enhanced matrix accumulation by nucleus pulposus cells *in vivo*. *Osteoarthritis Cartilage* **17(10)**: 1377-1384.

6. Gruber HE, Stasky AA and Hanley Jr EN. 1997. Characterization and phenotypic stability of human disc cells *in vitro*. *Matrix Biol* **16(5)**: 285-288.
7. Hutton WC, Elmer WA, Boden SD, Hyon S, Toribatake Y, Tomita K and Hair GA. 1999. The effect of hydrostatic pressure on intervertebral disc metabolism. *Spine* **24(15)**: 1507-1515.
8. Hutton WC, Elmer WA, Bryce LM, Kozlowska EE, Boden SD and Kozlowski M. 2001. Do the intervertebral disc cells respond to different levels of hydrostatic pressure? *Clin Biomech* **16(9)**: 728-734.
9. Kasra M, Goel V, Martin J, Wang ST, Choi W and Buckwalter J. 2003. Effect of dynamic hydrostatic pressure on rabbit intervertebral disc cells. *J Orthop Res* **21(4)**: 597-603.
10. Kasra M, Merryman WD, Loveless KN, Goel VK, Martin JD and Buckwalter JA. 2006. Frequency response of pig intervertebral disc cells subjected to dynamic hydrostatic pressure. *J Orthop Res* **24(10)**: 1967-1973.
11. Thonar E, An H and Masuda K. 2002. Compartmentalization of the matrix formed by nucleus pulposus and annulus fibrosus cells in alginate gel. *Biochem Soc Trans* **30(6)**: 874-888.
12. Baer AE, Wang JY, Kraus VB and Setton LA. 2001. Collagen gene expression and mechanical properties of intervertebral disc cell-alginate cultures. *J Orthop Res* **19**: 2-10.
13. Burdick JA, Chung C, Jia X, Randolph MA and Langer R. 2005. Controlled degradation and mechanical behavior of photopolymerized hyaluronic acid networks. *Biomacromolecules* **6(1)**: 386 -391.

14. Byers BA, Mauck RL, Chiang IE and Tuan RS. 2008. Transient exposure to transforming growth factor beta 3 under serum-free conditions enhances the biomechanical and biochemical maturation of tissue-engineered cartilage. *Tissue Eng Part A* **14(11)**: 1821-1834.
15. Lima EG, Bian L, Ng KW, Mauck RL, Byers BA, Tuan RS, Ateshian GA and Hung CT. 2007. The beneficial effect of delayed compressive loading on tissue-engineered cartilage constructs cultured with TGF-beta3. *Osteoarthritis Cartilage* **15(9)**: 1025-1033.
16. Alini M, Li W, Markovic P, Aebi M, Spiro RC and Roughley PJ. 2003. The potential and limitations of a cell-seeded collagen/hyaluronan scaffold to engineer an intervertebral disc-like matrix. *Spine* **28(5)**: 446-454.
17. Lee JY, Hall R, Pelinkovic D, Cassinelli E, Usas A, Gilbertson L, Huard J and Kang J. 2001. New use of a three-dimensional pellet culture system for human intervertebral disc cells: initial characterization and potential use for tissue engineering. *Spine* **26(21)**: 2316-2322.
18. Neidlinger-Wilke C, Würtz K, Liedert A, Schmidt C, Börm W, Ignatius A, Wilke H-J and Claes L. 2005. A three-dimensional collagen matrix as a suitable culture system for the comparison of cyclic strain and hydrostatic pressure effects on intervertebral disc cells. *J Neurosurg Spine* **2(4)**: 457-465.
19. Neidlinger-Wilke C, Würtz K, Urban JPG, Börm W, Arand M, Ignatius A, Wilke H-J and Claes LE. 2006. Regulation of gene expression in intervertebral disc cells by low and high hydrostatic pressure. *Eur Spine J* **15 (Suppl 3)**: S372-378.

20. Antoniou J, Steffen T, Nelson F, Winterbottom N, Hollander AP, Poole RA, Aebi M and Alini M. 1996. The human lumbar intervertebral disc: evidence for changes in the biosynthesis and denaturation of the extracellular matrix with growth, maturation, ageing, and degeneration. *J Clin Invest* **98(4)**: 996-1003.
21. Reza AT and Nicoll SB. 2008. Hydrostatic pressure differentially regulates outer and inner annulus fibrosus cell matrix production in 3D scaffolds. *Ann Biomed Eng* **36(2)**: 204-213.
22. Ikenoue T, Trindade MCD, Lee MS, Lin EY, Schurman DJ, Goodman SB and Smith RL. 2003. Mechanoregulation of human articular chondrocyte aggrecan and type II collagen expression by intermittent hydrostatic pressure *in vitro*. *J Orthop Res* **21(1)**: 110-116.
23. Hu JC and Athanasiou KA. 2006. The effects of intermittent hydrostatic pressure on self-assembled articular cartilage constructs. *Tissue Eng* **12(5)**: 1337-1344.
24. Smith RL, Lin J, Trindade MCD, Shida J, Kajiyama G, Vu T, Hoffman AR, Van der Meulen MCH, Goodman SB, Schurman DJ and Carter DR. 2000. Time-dependent effects of intermittent hydrostatic pressure on articular chondrocyte type II collagen and aggrecan mRNA expression. *J Rehabil Res Dev* **37(2)**: 153-161.
25. Chen FH and Tuan RS. 2008. Mesenchymal stem cells in arthritic diseases. *Arthritis Res Ther* **10(5)**: 223-234.
26. Mackay AM, Beck SC, Murphy JM, Barry FP, Chichester CO and Pittenger MF. 1998. Chondrogenic differentiation of cultured human mesenchymal stem cells from marrow. *Tissue Eng* **4(4)**: 415-428.

27. Yoo JU, Barthel TS, Nishimura K, Solchaga L, Caplan AI, Goldberg VM and Johnstone B. 1998. The chondrogenic potential of human bone-marrow-derived mesenchymal progenitor cells. *J Bone Joint Surg Am* **80(12)**: 1745-1757.
28. Chung C and Burdick JA. 2009. Influence of three-dimensional hyaluronic acid microenvironments on mesenchymal stem cell chondrogenesis. *Tissue Eng Part A* **15(2)**: 243-254.
29. Risbud MV, Albert TJ, Guttapalli A, Vresilovic EJ, Hillibrand AS, Vaccaro AR and Shapiro IM. 2004. Differentiation of mesenchymal stem cells towards a nucleus pulposus-like phenotype *in vitro*: implications for cell-based transplantation therapy. *Spine* **29(23)**: 2627-2632.
30. Steck E, Bertram H, Abel R, Chen B, Winter A and Richter W. 2005. Induction of intervertebral disc-like cells from adult mesenchymal stem cells. *Stem Cells* **23(3)**: 403-411.
31. Gilbertson L, Ahn S-H, Teng P-N, Studer RK, Niyibizi C and Kang JD. 2008. The effects of recombinant human bone morphogenetic protein-2, recombinant human bone morphogenetic protein-12, and adenoviral bone morphogenetic protein-12 on matrix synthesis in human annulus fibrosis and nucleus pulposus cells. *Spine J* **8(3)**: 449-456.
32. Park H, Temenoff JS, Holland TA, Tabata Y and Mikos AG. 2005. Delivery of TGF-beta1 and chondrocytes via injectable, biodegradable hydrogels for cartilage tissue engineering applications. *Biomaterials* **26(34)**: 7095-7103.

33. Mann BK, Schmedlen RH and West JL. 2001. Tethered-TGF-beta increases extracellular matrix production of vascular smooth muscle cells. *Biomaterials* **22(5)**: 439-444.
34. Park JS, Woo DG, Yang HN, Na K and Park K-H. 2009. Transforming growth factor beta-3 bound with sulfate polysaccharide in synthetic extracellular matrix enhanced the biological activities for neocartilage formation *in vivo*. *J Biomed Mater Res A* **91(2)**: 408-415.
35. Anseth KS, Bowman CN and Brannon-Peppas L. 1996. Mechanical properties of hydrogels and their experimental determination. *Biomaterials* **17(17)**: 1647-1657.
36. Bryant SJ, Durand KL and Anseth KS. 2003. Manipulations in hydrogel chemistry control photoencapsulated chondrocyte behavior and their extracellular matrix production. *J Biomed Mater Res A* **67(4)**: 1430-1436.
37. Sahoo S, Chung C, Khetan S and Burdick JA. 2008. Hydrolytically degradable hyaluronic acid hydrogels with controlled temporal structures. *Biomacromolecules* **9(4)**: 1088-1092.
38. Park Y, Lutolf MP, Hubbell JA, Hunziker EB and Wong M. 2004. Bovine primary chondrocyte culture in synthetic matrix metalloproteinase-sensitive poly(ethylene glycol)-based hydrogels as a scaffold for cartilage repair. *Tissue Eng* **10(3-4)**: 515-522.
39. Mizuno H, Roy AK, Zaporozhan V, Vacanti CA, Ueda M and Bonassar LJ. 2006. Biomechanical and biochemical characterization of composite tissue-engineered intervertebral discs. *Biomaterials* **27(3)**: 362-370.

40. Mizuno H, Roy AK, Vacanti CA, Kojima K, Ueda M and Bonassar LJ. 2004. Tissue-engineered composites of annulus fibrosus and nucleus pulposus for intervertebral disc replacement. *Spine* **29(12)**: 1290-1297.
41. Bowles RD, Williams R, Zipfel W and Bonassar LJ. 2009. Self-assembly of aligned tissue engineered annulus fibrosus and IVD composite via collagen gel contraction. *Tissue Eng Part A* doi:10.1089/ten.TEA.2009.0442.
42. Temenoff JS, Shin H, Conway DE, Engel PS and Mikos AG. 2003. *In vitro* cytotoxicity of redox radical initiators for cross-linking of oligo(poly(ethylene glycol) fumarate) macromers. *Biomacromolecules* **4(6)**: 1605-1613.
43. Hong Y, Song H, Gong Y, Mao Z, Gao C and Shen J. 2007. Covalently crosslinked chitosan hydrogel: properties of *in vitro* degradation and chondrocyte encapsulation. *Acta Biomater* **3(1)**: 23-31.
44. Hong Y, Mao Z, Wang H, Gao C and Shen J. 2006. Covalently crosslinked chitosan hydrogel formed at neutral pH and body temperature. *J Biomed Mater Res A* **79(4)**: 913-922.
45. Temenoff JS, Park H, Jabbari E, Conway DE, Sheffield TL, Ambrose CG and Mikos AG. 2004. Thermally cross-linked oligo(poly(ethylene glycol) fumarate) hydrogels support osteogenic differentiation of encapsulated marrow stromal cells *in vitro*. *Biomacromolecules* **5(1)**: 5-10.
46. Temenoff JS, Park H, Jabbari E, Sheffield TL, LeBaron RG, Ambrose CG and Mikos AG. 2004. *In vitro* osteogenic differentiation of marrow stromal cells encapsulated in biodegradable hydrogels. *J Biomed Mater Res A* **70(2)**: 235-244.

47. Wuertz K, Urban JPG, Klasen J, Ignatius A, Wilke H-J, Claes L and Neidlinger-Wilke C. 2007. Influence of extracellular osmolarity and mechanical stimulation on gene expression of intervertebral disc cells. *J Orthop Res* **25(11)**: 1513-1522.
48. Le Maitre CL, Frain J, Fotheringham AP, Freemont AJ and Hoyland JA. 2008. Human cells derived from degenerate intervertebral discs respond differently to those derived from non-degenerate intervertebral discs following application of dynamic hydrostatic pressure. *Biorheology* **45(5)**: 563-575.
49. Gokorsch S, Nehringm D, Grottke C and Czermak P. 2004. Hydrodynamic stimulation and long term cultivation of nucleus pulposus cells: a new bioreactor system to induce extracellular matrix synthesis by nucleus pulposus cells dependent on intermittent hydrostatic pressure. *Int J Artif Organs* **27(11)**: 962-970.
50. Korecki CL, Kuo CK, Tuan RS and Iatridis JC. 2009. Intervertebral disc cell response to dynamic compression is age and frequency dependent. *J Orthop Res* **27(6)**: 800-806.
51. An HS and Masuda K. 2006. Relevance of *in vitro* and *in vivo* models for intervertebral disc degeneration. *J Bone Joint Surg Am* **88(Suppl 2)**: 88-94.
52. Masuda K, Aota Y, Muehleman C, Imai Y, Okuma M, Thonar EJ, Andersson GB and An HS. 2005. A novel rabbit model of mild, reproducible disc degeneration by an anulus needle puncture: correlation between the degree of disc injury and radiological and histological appearances of disc degeneration. *Spine* **30(1)**: 5-14.

53. Boxberger JI, Auerbach JD, Sen S and Elliott DM. 2008. An *in vivo* model of reduced nucleus pulposus glycosaminoglycan content in the rat lumbar intervertebral disc. *Spine* **33**(2): 146-154.